



UNIVERSITY OF  
LIVERPOOL

**The efficacy of dmrFABP5 on suppressing the malignant progression of prostate cancer cells either singly or in combination with drugs in use and relevant molecular mechanisms**

THESIS SUBMITTED IN ACCORDANCE WITH THE REQUIREMENTS OF  
THE UNIVERSITY OF LIVERPOOL  
FOR THE DEGREE OF DOCTOR IN PHILOSOPHY

By:

**Saud Abdulsamad Mohammad Abdulsamad**

February 2023

**Department of Molecular and Clinical Cancer Medicine  
(Molecular Cancer Biology)**

## **Dedication**

To my father, the great man who support me during my journey

My great mother, for her endless love, and support.

My great wife, son and daughter for making my life so happy and  
easy.

My brothers and sister, for the endless support.

## **Acknowledgement**

### **First of all, thanks and praise are due to God**

I would like to express my deep appreciation to my primary supervisor, Professor Youqiang Ke, for providing me with the valuable opportunity to pursue my PhD studies in the Department of Molecular and Clinical Cancer Medicine and for his unwavering support, guidance, encouragement, and insightful critiques.

Furthermore, I would like to thank my secondary supervisor, Professor Philip Rudland, for his support and encouragement. I am also grateful to Doctor Gang He for his valuable information, insightful discussions, and advice on the experimental skills required for this research.

I am eternally grateful to my parents for their love and support, which enabled me to overcome the difficulties and obstacles that I faced during my PhD journey. I would like to express my sincere gratitude to my wife Nouf, son Abdulaziz, and daughter Sarah for their unwavering support, kindness, and understanding. I would also like to deeply appreciate my brothers Sultan, Mohammad, Ahmed, Khalid, and sister Al Anoud for their constant love and support. Special thanks to my colleagues in my research team, Dr Asmaa Al-Bayati, Dr Bander Alenezi, and Mr Abdulghani Naeem for their support, encouragement, and friendship.

I would also like to thank the Head of the Department and all the staff members in the Department of Molecular and Clinical Cancer Medicine, University of Liverpool, for their support in providing and maintaining laboratory space and facilities.

Finally, I would like to express my deep and sincere gratitude to my sponsor, King Saud bin Abdulaziz University for Health Sciences, College of Science and Health Professions, for providing me a scholarship.

## **Declaration**

I completed this thesis during my PhD program in the Department of Molecular and Clinical Cancer Medicine, University of Liverpool. All of the experiments included in the result sections were conducted by me, under the guidance and supervision of Professor Youqiang Ke.



## Publications

1. **Saud A. Abdulsamad**, Abdulghani A.A. Naeem, Philip S. Rudland Mohammed I. Malki and Youqiang Ke. FABP5-related signal transduction pathway in castration-resistant prostate cancer: A possible therapeutic target. *Precision Clinical Medicine* 2019, **2**:192-196.
2. **Saud A. Abdulsamad**, Abdulghani A. Naeem, Gang He, Xi Jin, Jiachen Zhang, Qiang Wei, and Youqiang Ke. Epidemiology of Prostate Cancer in Saudi Arabia (2021). A systematic review in e-Book: *New Frontiers in Medicine and Medical Research* (Chapter 3), Vol 14: published by BP International Publisher on August 23, 2021; Pages18-36. <https://doi.org/10.9734/bpi/nfmnr/v14/12894D>
3. **Saud A Abdulsamad**, Abdulghani A Naeem, Asmaa Al-Bayati, Jiacheng Zhang, Mohammed I Malki, Hongwen Ma, and Youqiang Ke. Prostate Cell Lines. *Open Acc J Oncol Med* 2021. 05- 000208. Published online on February 25, 2022. **DOI**: 10.32474/OAJOM.2021.05.000208.
4. Zhang, Jiacheng, Gang He, Xi Jin, Bandar T. Alenezi, Abdulghani A. Naeem, **Saud A. Abdulsamad**, and Youqiang Ke. "Molecular mechanisms on how FABP5 inhibitors promote apoptosis-induction sensitivity of prostate cancer cells." *Cell Biology International* (2023).

## Abstract

Standard prostate cancer (PCa) treatment options, including chemotherapy and androgen deprivation therapy (ADT) with drugs like docetaxel and enzalutamide, eventually become ineffective, necessitating the exploration of new therapeutic strategies, such as the recently proposed Anti-FABP5 therapy with its bio-inhibitor dmrFABP5. This study is aimed to assess the synergistic effects of combining dmrFABP5 with either docetaxel or enzalutamide in experimental PCa treatment. We found that the treatment of dmrFABP5 combined with docetaxel in androgen-independent Du145 and androgen-responsive 22RV1 cells exhibited a synergistic effect as determined by the Combination Index (CI) assessed with CompuSyn software and resulted in a significant reduction in the malignant characteristics of the cells. The treatment of 22RV1 cells with dmrFABP5 combined with enzalutamide produced a synergistic suppression effect on the malignant characteristics of the cells. To study the molecular mechanisms behind the synergistic interactions, we investigated the changes in expression levels of a number of proteins related to FABP5-initiated signal transduction pathways and those related to tumorigenicity, apoptosis, and angiogenesis in DU145 and 22RV1 cells. The results showed that the combination treatment of dmrFABP5 with docetaxel promoted apoptosis with disrupted some apoptosis factors, decreased angiogenesis factor, suppressed fatty acid receptor and reduced the level of Sp1. In 22RV1 cells, apart from similar aforementioned enhancement effect, a synergistic suppression on the expression of AR and AR-V7 was also observed. Furthermore, the combination of dmrFABP5 with enzalutamide significantly suppressed not only the same pathways, except apoptosis, as those in 22RV1 cells, but also the expression of AR and AR-V7. RNA profiling of DU145 treated with dmrFABP5 revealed the most enriched pathways and differential gene expression, providing insight into the underlying mechanisms of dmrFABP5 action. These findings provided a theoretical basis for a therapy to combine dmrFABP5 with either docetaxel or enzalutamide as a treatment strategy for prostate cancer.

## Table of Contents

<b>Cover Page</b> .....	<b>1</b>
<b>Dedication</b> .....	<b>2</b>
<b>Acknowledgement</b> .....	<b>3</b>
<b>Declaration</b> .....	<b>4</b>
<b>Publications</b> .....	<b>5</b>
<b>Abstract</b> .....	<b>6</b>
<b>Chapter 1</b> .....	<b>18</b>
1.1 Prostate Cancer Epidemiology .....	19
1.1.1 Cancer Epidemiology.....	19
1.1.2 Prostate cancer mortality.....	21
1.1.3 Prostate cancer survival.....	22
1.1.4 Prostate cancer risk factors.....	24
1.2 Prostate cancer pathology .....	26
1.2.1 Prostate gland anatomy.....	26
1.2.2 Prostate gland epithelial cells .....	28
1.2.3 Prostate cancer pathogenesis.....	29
1.2.4 Prostate cancer cell lines.....	32
1.3 Prostate cancer androgens and treatments .....	34
1.3.1 Androgen role in prostate cancer .....	34
1.3.2 AR mutations, overexpression and amplifications in CRPC and GCPR .....	35
1.3.3 Prostate cancer treatments .....	37
1.3.4 Androgen- independent prostate cancer.....	38
1.3.5 Molecular mechanism involved in CRPC progression.....	38
1.3.6 CRPC AR-dependent signalling pathway.....	39
1.3.7 CRPC and drug resistance .....	40
1.3.8 Other CRPC related pathways.....	41
1.4 Fatty acid binding proteins .....	42
1.4.1 FABP family members .....	42
1.4.2 FABPs' general functions.....	45

1.4.3 FABP structure .....	47
1.5 FABP5 role in prostate cancer.....	49
1.6 Specificity Protein (Sp1) in FABP5.....	51
1.7 Apoptosis and FABP5 in prostate cancer .....	51
1.8 Prostate cancer and targeting FABP5 .....	51
1.9 Drug combination roles.....	53
1.10 Hypothesis.....	54
1.11 Aim .....	55
1.12 The specific Aims in different phases of the work .....	55
<b>Chapter 2 .....</b>	<b>56</b>
<b>Materials and Methods.....</b>	<b>56</b>
2.1 Cell culture .....	57
2.1.1 Routine cell culture .....	57
2.1.2 Sub-culture.....	57
2.1.3 Thawing of the cells .....	58
2.1.4 Counting of the cells .....	58
2.1.5 Freezing of the cells .....	58
2.2 Expression and purification of dmrFABP5 and wtFABP5 .....	59
2.2.1 E. coli cell growth and protein induction .....	59
2.2.2 Recombinant protein purification.....	59
2.2.3 Dialysis for recombinant protein cleaning .....	61
2.2.4 Bradford assay for protein measurement.....	61
2.2.5 Sodium dodecyl sulphate- polyacrylamide protein gel electrophoresis.....	63
2.2.6 Transferring protein from SDS gel into PVDF membrane .....	63
2.2.7 Protein detection by immunoblotting .....	64
2.2.8 Western blot for molecular mechanism .....	65
2.3 Drug preparations and IC <sub>50</sub> determinations.....	68
2.3.1 Docetaxel preparation and storing .....	68
2.3.2 Enzalutamide preparation and storing .....	68
2.3.3 Half maximum inhibitory concentration (IC <sub>50</sub> ) of dmrFABP5, docetaxel and enzalutamide .....	68
2.3.4 The combination treatment of dmrFABP5 with docetaxel or enzalutamide.....	69
2.4 <i>In vitro</i> assays for testing malignant characteristics cells .....	70
2.4.1 Assay to test cell viability .....	70
2.4.2 Cell motility assay.....	70
2.4.3 Cell invasion assay.....	71

2.4.4 Anchorage independent cell growth (soft agar assay) .....	72
2.5 RNA- profile analysis .....	73
2.5.1 Cell preparation.....	73
2.5.2 RNA extraction .....	73
2.5.3 RNA library preparation .....	74
2.5.4 RNA sequence data analysis .....	75
2.6 Data analysis .....	78
<b>Chapter 3 .....</b>	<b>79</b>
<b>Result-1: Treatment with dmrFABP5 in combination with docetaxel or enzalutamide produced synergistic suppressive effect in prostate cancer cells .....</b>	<b>79</b>
3.1 Introduction .....	80
3.2 Aim of the study.....	81
3.3 IC <sub>50</sub> of dmrFABP5, docetaxel or enzalutamide in cell viability assays with prostate cancer cells .....	82
3.3.1 The suppressive effect of dmrFABP5 on the cell viability of prostate cancer cells ...	83
3.3.2 The effect of docetaxel on prostate cancer cells growth.....	84
3.3.3 The effect of enzalutamide on DU145, 22RV1 and LNCaP growth .....	85
3.4 The assessment of the synergistic effect produced by dmrFABP5 on docetaxel .....	86
3.4.1 DmrFABP5 enhanced the suppressive effect of docetaxel on DU145.....	86
3.4.2 DmrFABP5 enhanced the suppressive effect of docetaxel on 22RV1 .....	89
3.4.3 The combination effect of dmrFABP5 with docetaxel on LNCaP.....	92
3.5 The assessment of the synergistic effect produced by dmrFABP5 on enzalutamide.....	95
3.5.1 The effect of dmrFABP5 with enzalutamide on DU145 .....	95
3.5.2 The synergistic effect of DmrFABP5 with enzalutamide on 22RV1 .....	98
3.5.3 The effect of dmrFABP5 with enzalutamide on LNCaP.....	101
3.6 Discussion.....	104
<b>Chapter 4 .....</b>	<b>106</b>
<b>Result-2: The effect of combination treatments on malignant characteristics of the prostate cancer cells .....</b>	<b>106</b>
4.1 Introduction .....	107
4.2 Aim of the study.....	108
4.3 Synergistic action of dmrFABP5 to the treatment drug effect on motility of prostate cancer cells.....	109
4.3.1 Synergistic action of dmrFABP5 to the effect of docetaxel on motility of DU145 cells .....	109
4.3.2 Synergistic action of dmrFABP5 to the effect of docetaxel on motility of 22RV1 cells .....	111

4.3.3	The effect of dmrFABP5 combined with docetaxel in motility on LNCaP.....	114
4.3.4	The action of dmrFABP5 to the effect of enzalutamide on motility of DU145 cells	116
4.3.5	Synergistic action of dmrFABP5 to the effect of enzalutamide on motility of 22RV1 cells .....	118
4.3.6	The effect of dmrFABP5 combined with enzalutamide in motility on LNCaP .....	120
4.4	Invasion assay .....	122
4.4.1	The enhancement effect of dmrFABP5 to docetaxel on DU145 invasion .....	122
4.4.2	The enhancement effect of dmrFABP5 to docetaxel on invasion of 22RV1.....	125
4.4.3	The activity of dmrFABP5 to the effect of docetaxel on the invasion of LNCaP.....	128
4.5	The effect of dmrFABP5 on the suppressive activity of enzalutamide to DU145 invasion .....	131
4.5.1	The enhancement activity of dmrFABP5 to the effect of enzalutamide on the invasiveness of 22RV1 cells.....	134
4.5.2	The treatment effect of dmrFABP5 to enzalutamide on the invasion of LNCaP .....	137
4.6	Anchorage independent cell growth (soft agar assay) .....	141
4.6.1	The effect of dmrFABP5 combined with docetaxel on the colony formation of DU145 .....	141
4.6.2	The activity of dmrFABP5 to the effect of docetaxel on the colony formation by 22RV1 .....	144
4.6.3	The effect of dmrFABP5 alone, or combined with docetaxel on the colony formation of LNCaP cell.....	147
4.6.4	The activity of dmrFABP5 combined with enzalutamide on the colony formation of DU145 .....	150
4.6.5	The treatment action of dmrFABP5 to enzalutamide on the colony formation abilities of 22RV1 .....	153
4.6.6	The effect of dmrFABP5 to the suppressive effect of enzalutamide on the colony formation of LNCaP .....	156
4.7	Discussion.....	159
<b>Chapter 5</b>	.....	<b>161</b>
<b>Result-3: The molecular mechanism involved in the interactions of the compounds in prostate cancer cells</b>	.....	<b>161</b>
5.1	Introduction .....	162
5.2	Aim of the study.....	163
5.3	Investigating the molecular mechanism involved in the biological activity of dmrFABP5 on the effect of docetaxel on DU145.....	164
5.3.1	The effect of dmrFABP5 alone, or combined with docetaxel on PPAR $\gamma$ and p-PPAR $\gamma$ levels on DU145 .....	164
5.3.2	The enhancement effect of dmrFABP5 to docetaxel on suppressing VEGFA expression in DU145 .....	167

5.3.3 The effect of dmrFABP5 combined with docetaxel on Sp1 expression in DU145 ...	169
5.3.4 The effect of dmrFABP5 alone, or combined with docetaxel on Bcl-2 expression in DU145 cells .....	171
5.3.5 The effect of dmrFABP5 and docetaxel on BAX expression in DU145 cells.....	172
5.4 Investigating the molecular mechanism involved in the biological activity of dmrFABP5 to the effect of docetaxel on 22RV1 cells .....	174
5.5 The effect of dmrFABP5 alone, or in combination with docetaxel on AR or AR-V7 expression in 22RV1 cells.....	174
5.5.1 The effect of treatments with dmrFABP5 alone, or in combination with docetaxel on levels of PPAR $\gamma$ and p-PPAR $\gamma$ expressed in 22RV1 cells.....	176
5.5.2 The effect of dmrFABP5 alone, or combined with docetaxel on VEGFA expression in 22RV1 cells.....	179
5.5.3 The action of dmrFABP5 alone, or in combination with docetaxel on Sp1 expression in 22RV1 cells .....	180
5.5.4 The action of dmrFABP5 singly or in combined with docetaxel on Bcl-2 expression in 22RV1 cells.....	182
5.5.5 The effect of dmrFABP5 alone, or combined with docetaxel on BAX expression in 22RV1 .....	184
5.6 Investigating the molecular mechanism of the biological activity of dmrFABP5 to the effect of enzalutamide on 22RV1 cells .....	186
5.6.1 The effect of dmrFABP5 alone, or combined with enzalutamide on AR or AR-V7 expression in 22RV1 cells.....	186
5.6.2 The effect of treatments with dmrFABP5 alone, combined with enzalutamide on levels of PPAR $\gamma$ and p-PPAR $\gamma$ in 22RV1 cells.....	188
5.6.3 The action of dmrFABP5 singly or combined with enzalutamide on VEGFA expression in 22RV1 cells .....	190
5.6.4 The effect of the treatment of dmrFABP5 combined with enzalutamide on Sp1 level in 22RV1 cells .....	192
5.7 Further molecular mechanism investigations.....	193
5.7.1 The effect of enzalutamide on AR and AR-V7 expression in 22RV1-FABP5- KO cells .....	193
5.7.2 The effect of wtFABP5 treatment on levels of AR and AR-V7 in 22RV1 cells .....	195
5.7.3 The effect of wtFABP5 on Sp1 expression in 22RV1 cells .....	196
5.7.4 Sp1 expression in 22RV1-FABP5-KO.....	197
5.7.5 The effect of Sp1 inhibitor (Plicamycin) on AR and AR-V7 expression in 22RV1 cells .....	199
5.7.6 The effect of Plicamycin on FABP5 expression in 22RV1 cells .....	200
5.7.7 The effect of Plicamycin on PPAR $\gamma$ expression in 22RV1 cells .....	201
5.7.8 The effect of Plicamycin on p- PPAR $\gamma$ in 22RV1 cells .....	202

5.7.9 The effect of Sp1 expression in DU145-FABP5-KO cells.....	203
5.7.10 The effect of Plicamycin on FABP5 expression in DU145 cells .....	204
5.7.11 The effect of Plicamycin on PPAR $\gamma$ expression in DU145 cells .....	206
5.7.12 The effect of Plicamycin on p-PPAR $\gamma$ expression in DU145 cells .....	207
5.8 Discussion.....	209
<b>Chapter 6 .....</b>	<b>211</b>
6.1 Introduction .....	212
6.2 Identification of the DEGs between DU145 cells treated and untreated with dmrFABP5. .....	213
6.3 The effect of dmrFABP5 on Gene Ontology (GO) of biological processes Enriched in DEGs by comparing untreated and treated Du145 cells.....	219
6.4 The effect of dmrFABP5 on expression of FABP5, GRPR, CAV1, EGR1, CRIP2, and BMF	223
6.5 Discussion.....	225
<b>Chapter 7 .....</b>	<b>226</b>
<b>General Discussion, Conclusion and Future Work.....</b>	<b>226</b>
7.1 General discussion .....	227
7.2 Half inhibitory concentration or IC <sub>50</sub> of different compounds in PCa cells .....	229
7.3 The effect of dmrFABP5 treatment combined with docetaxel in PCa cells .....	230
7.4 The effect of dmrFABP5 treatment combined with enzalutamide in PCa cells .....	230
7.5 The action of dmrFABP5 to the effect of docetaxel or enzalutamide on PCa cell motility .....	231
7.6 The action of dmrFABP5 to the suppression effect of docetaxel or enzalutamide on invasiveness of PCa cells.....	232
7.7 The effect of dmrFABP5 in combination with docetaxel or enzalutamide on PCa cell anchorage-independent growth.....	233
7.8 The molecular mechanisms underlying the synergistic action of dmrFABP5 to the suppression effect of docetaxel or enzalutamide on the malignant characteristics of PCa cells .....	234
7.9 Highlighted the possible interactions between dmrFABP5 and differentially expressed genes identified by comparing expression profile in DU145 cells.....	238
7.10 Six most pronounced DEGs between dmrFABP5- treated and untreated DU145 cells.	239
7.10.1 FABP5 .....	239
7.10.2 GRPR.....	240
7.10.3 CAV1.....	240
7.10.4 EGR1.....	241
7.10.5 CRIP2 .....	242
7.10.6 BMF .....	242
7.11 Future Perspectives and Clinical Implications.....	243



7.12 Conclusion.....	244
7.13 Future work.....	245
A Reagents .....	273
C. Western blot .....	278
<b>References.....</b>	<b>230</b>
<b>Appendices .</b> .....	<b>255</b>
<b>A. Reagents</b> .....	<b>256</b>
<b>A1. Cell culture and treatment reagents</b> .....	<b>256</b>
<b>A2. Routine cell culture medium</b> .....	<b>256</b>
<b>A3. Freezing medium</b> .....	<b>257</b>
<b>A4. Reagents for molecular biology</b> .....	<b>257</b>
<b>A5. Reagents for western blot</b> .....	<b>257</b>
<b>A6. Reagents for drug combinations</b> .....	<b>258</b>
<b>A7. Reagents for cell viability detection</b> .....	<b>258</b>
<b>A8. Reagents for invasion assay</b> .....	<b>258</b>
<b>A9. Reagents for soft agar assay</b> .....	<b>259</b>
<b>B. Buffers</b> .....	<b>259</b>
<b>B1. Bacterial culture</b> .....	<b>259</b>
<b>B2. Bacterial Stock medium</b> .....	<b>259</b>
<b>B3. IPTG 100mM</b> .....	<b>260</b>
<b>B4. Ampicillin stock solution</b> .....	<b>260</b>
<b>C. Western blot</b> .....	<b>261</b>

**D. Equipment .....262**

**E. Cell authentication and publications .....265**

## List of Abbreviations

<b>Abbreviation</b>	<b>Full name</b>
ADT	Androgen deprivation therapy
AR	Androgen receptor
AR-Vs	Androgen splice variants
AR-V7	Androgen splice variants 7
Bax	Bcl-2-associated X protein
BCL-2	B-cell lymphoma 2
BPH	Benign Prostatic Hyperplasia
BMF	Bcl-2-modifying factor
CAV1	Caveolin-1
cDNA	Complementary DNA
CL	Cell lysate
CRIP2	Cysteine-rich intestinal protein 2
CRPC	Castration-resistant prostate cancer
CZ	Central zone
DBD	DNA-binding domain
dmrFABP5	Double mutant recombinant FABP5
DMSO	Dimethyl sulfoxide
DOC	Docetaxel
E coli	Escherichia coli
EDTA	Ethylene diaminetetraacetic acid
EGR 1	Early growth response 1
ENZ	Enzalutamide
FABPs	Fatty acid binding proteins

<b>Abbreviation</b>	<b>Full name</b>
FABP5	Fatty acid binding protein 5
FABP5-KO	FABP5 knockout
FASN	Fatty acid Synthase
FBS	Fetal bovine serum
FL	Flow-through
FOSB	FosB Proto-Oncogene
GRPR	Gastrin releasing peptide receptor
GS	Gleason scores
IPTG	Isopropylthiogalactoside
kDa	kilo Dalton
LB medium	Lysogeny broth medium
LBD	Ligand-binding domain
mRNA	Messenger RNA
MTT bromide	3-(4, 5-dimethylthiazol-2-yl)-2, 5-diphenylterazolium
OD	Optical density
PBS	Phosphate buffered saline
PIN	Prostatic Intraepithelial Neoplasia
PPAR	Peroxisome proliferator-activated receptors
p-PPAR $\gamma$	Phosphorylated- PPAR $\gamma$
PSA	Prostate-Specific Antigen
PZ	Peripheral Zone
SBFI26	$\alpha$ -truxillic acid 1-naphthyl mono-ester
SDS-PAGE electrophoresis	Sodium dodecyl sulphate polyacrylamide gel
TBE buffer	Tris-Borate-EDTA buffer
Sp1	Specificity protein 1

TBS-T	Tris Base Salt-Tween
<b>Abbreviation</b>	<b>Full name</b>
TZ	Transitional Zone
VEGF	Vascular endothelial growth factor
wtrFABP5	Wild type recombinant FABP5

## **Chapter 1**

### **Introduction**

## 1.1 Prostate Cancer Epidemiology

### 1.1.1 Cancer Epidemiology

Worldwide, cancers are a major causal factor in mortality, forming a significant impediment to extending life expectancy (1). Of these, prostate cancer in males is the second most commonly-diagnosed disease, and there are estimated to be 1.4 million new diagnoses globally (1) (Figure 1.1).

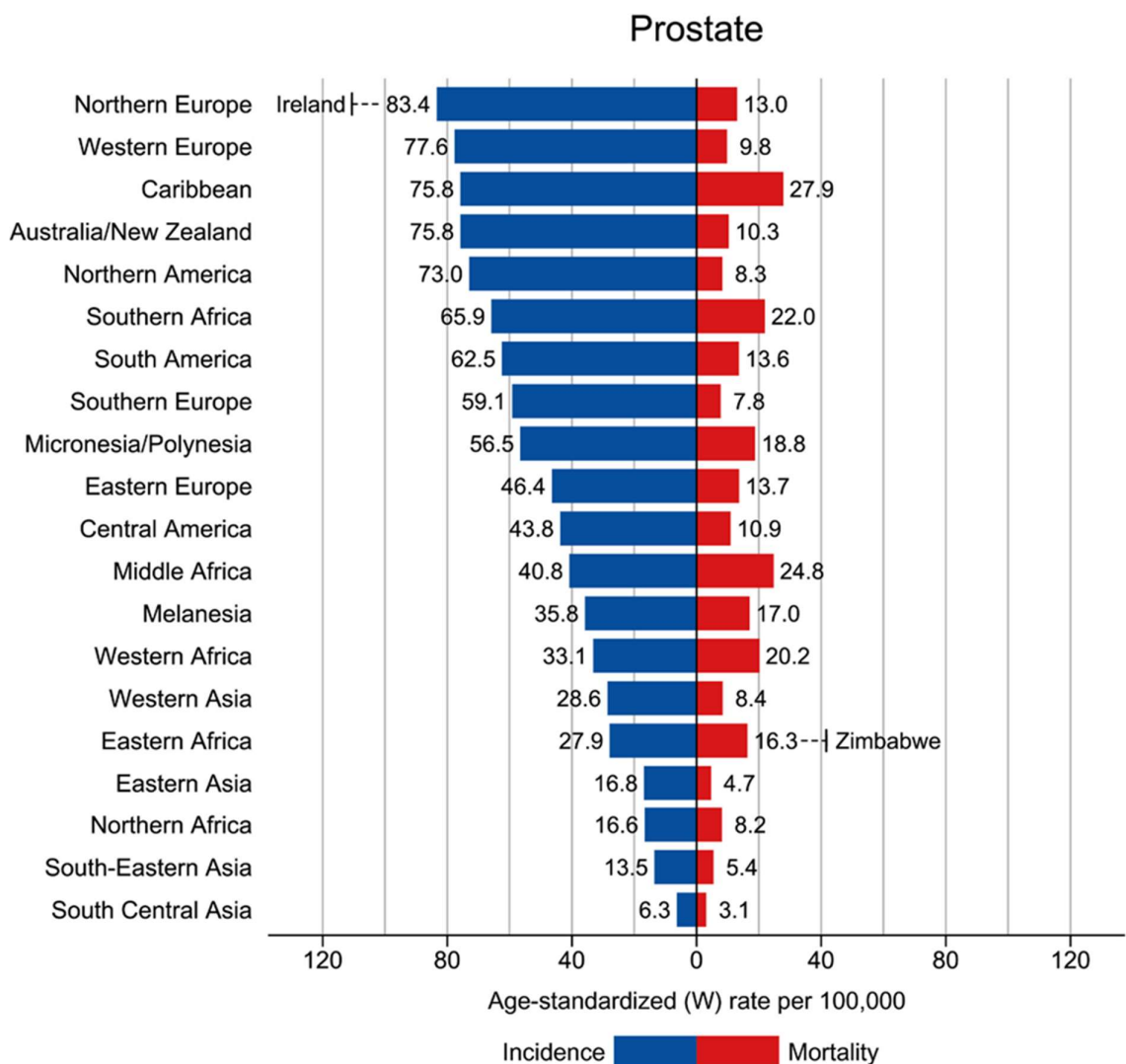


**Figure 1.1 Prostate cancer incidence rates worldwide (GLOBOCAN 2020)**

It is concerning that if the current numbers of cases continue to grow, diagnosed new cases each year are expected to reach 29.5 million, equal to 62% more cases by 2040 (1,

2). In the UK, these cancers accounted for approximately 53% of all new cancer cases in 2017. The cancer incidence in the UK is ranked higher than two-thirds of Europe's countries, and higher by 90% than world case rates (2). Prostate cancer (PCa) incidence in the UK is expected to rise between 2014 and 2035 by 12%, to reach around 233 cases per 100,000 males (3).

As shown in Fig 1.2, in 2017, breast cancer in the female and prostate cancer in the male were the two most common cancers in England (4).

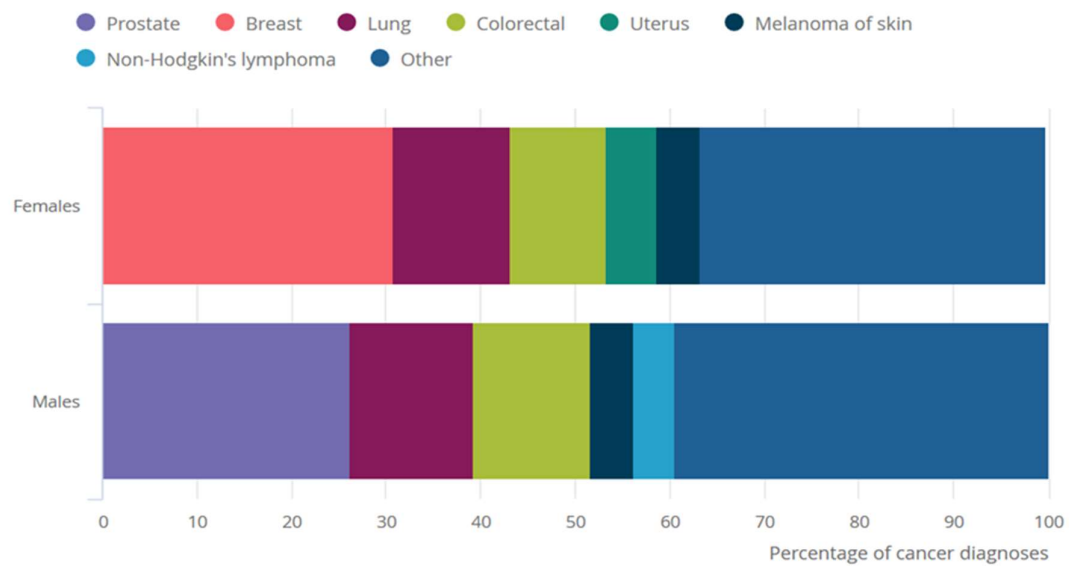


**Figure 1.2.** Illustration in 2017 showing that breast and prostate cancers are the two most common cancers in England in the male and female population respectively (4).



### 1.1.2 Prostate cancer mortality

In the UK, each year, over 11,900 men die due to prostate cancer: approximately 32 each day (2016-2018) (3). Statistics show that the age-related incidence of prostate cancer grew from age 50 to 54 and peaked at 75-79, then somewhat decreased from 80-84, before increasing again after that (5) (Figure 1.3).

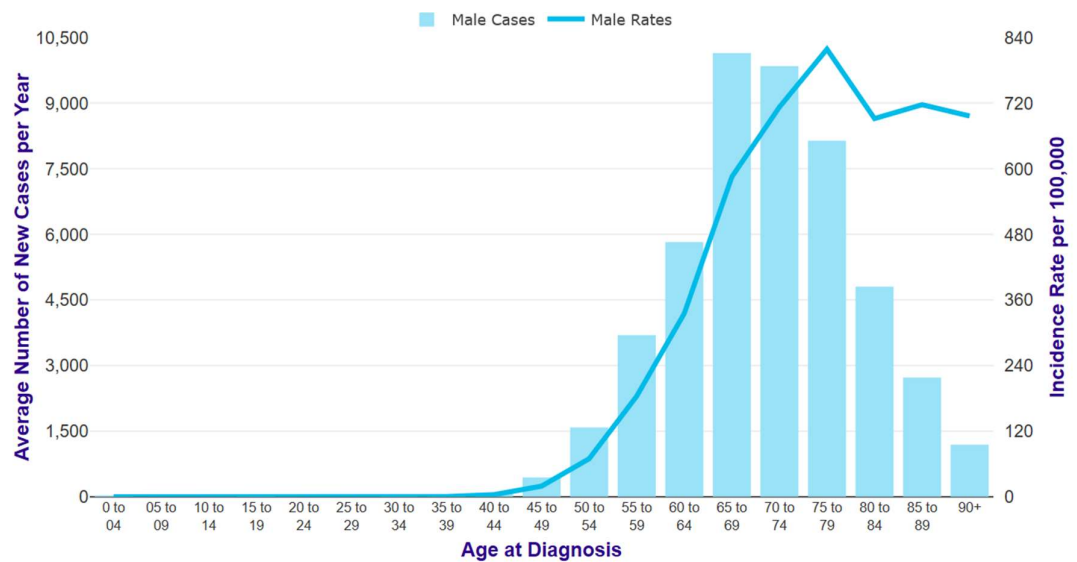


**Figure 1.3.** Mean annual new cases of prostate cancer with incidence by age per 100,000 in males in the United Kingdom between 2015 and 2017 (5).

Further, statistical analysis showed that people aged 90 and above had the highest prostate cancer mortality rate, as seen in Figure 1.4 (5,6).

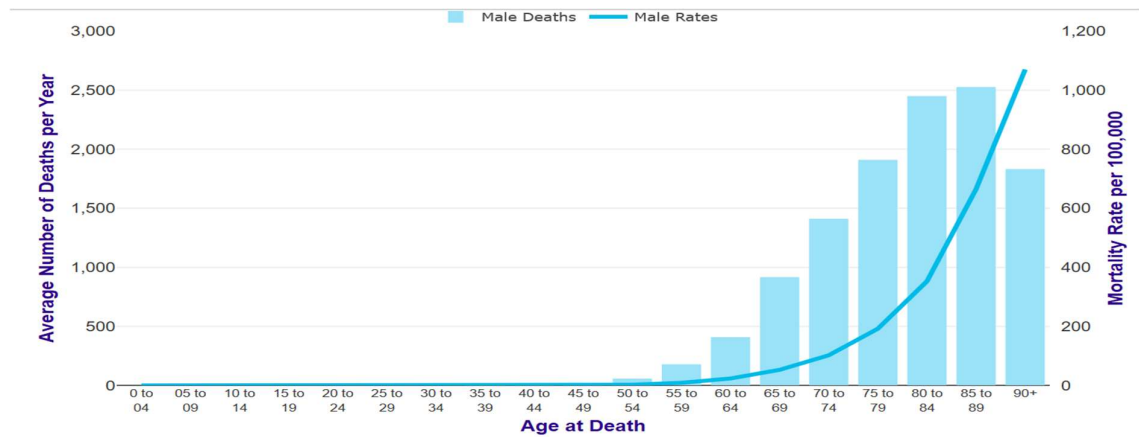


**Figure 1.4.** Males in the UK dying from prostate cancer each year (average) by age. The age-related death rate was highest between 2015 and 2017 (5).

### 1.1.3 Prostate cancer survival

It was reported in 2010 that the ten-year survival rate for patients with PCa was 84 percent. Since 1970, the ten-year survival percentage for this illness has grown, as seen in Figure 1.5. The rate of survival at 10 years rose by 59 percent over a 40-year span, from 1971 to 2010. In England, more than 80% of males are expected to survive for at least ten years after being diagnosed with PCa. Early diagnostic tests, including transurethral resection of prostate (TURP), as well as measuring the level of prostate-specific antigen (PSA), may have contributed to this (3,7-9).

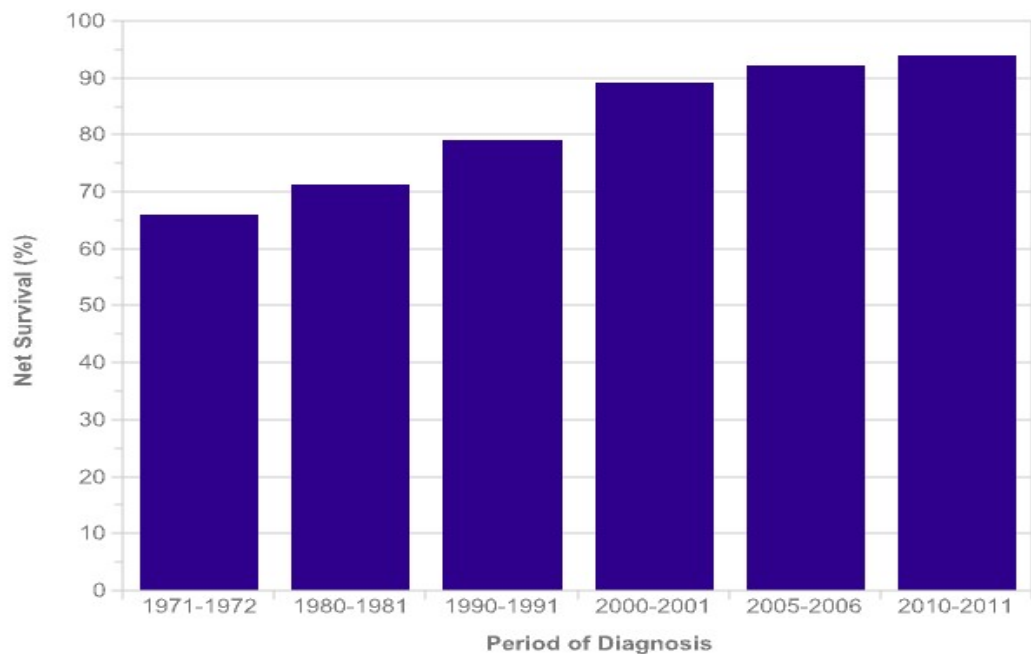


**Figure 1.5.** Ten-year prostate cancer patient survival (9). The bar graphs showed the 15–99-year survival rate for men with prostate cancer in Britain. This data provides valuable insights into the long-term prognosis and overall survival of individuals affected by this prevalent form of cancer. The x-axis of the graph represents age groups ranging from 15 to 99 years, allowing for a comprehensive analysis across various stages of life. Meanwhile, the y-axis depicts the survival rate, which indicates the percentage of patients who successfully survived ten years after their prostate cancer diagnosis.

## **1.1.4 Prostate cancer risk factors**

### **1.1.4.1 Age risk**

PCa is infrequently diagnosed in males younger than 40, according to research. However, as people get older, they are more likely to get prostate cancer: 60-79 year olds accounted for 13.7 percent of cases, 40-59 year olds 2.2 percent, and those less than 39 years old accounted for less than 0.005 percent of prostate cancer cases (10).

### **1.1.4.2 Ethnicity and prostate cancer**

Black men have a larger risk of PCa than white men, according to research around the world. Prostate cancer is the most common disease among African Americans (275.3 per 100,000 males) (11), and this represents a risk factor that is almost 60% higher than Caucasians or Asian/Pacific Islanders. Furthermore, African Americans have a mortality rate that is around twice that of Caucasians. Despite this, it is uncertain whether race or ethnicity has an impact on either incidence or mortality for this disease. Variations in the level of socioeconomic factors, diagnosis stages, genetic influences, and environmental factors or their interactions explain the difference in incidence and mortality (12-14).

### **1.1.4.2 Family history risk and prostate cancer**

PCa diagnosis of a first-degree relative raises cancer risks 120-150 percent (15-17). A man's risk increases by 120-140 percent if his father is affected, and by 187-230 percent if his brother is affected. When many first-degree relatives are affected, the risk increases. A 90-150 percent increase in risk was also documented in men with a second-degree

afflicted relative (15-17). Men with breast cancer-affected mothers are at an increased risk of 19-24%: however, men with breast cancer-affected sisters are not at an increased risk. Men with a germ line mutation within the breast cancer gene (BRCA2) have a five-fold greater PCa risk, whereas males under 65 have a seven-fold potential higher risk. Prostate cancer cases are thought to be linked to genes and family history in roughly 5-9 percent of cases (18-20).

#### **1.1.4.3 Diet/ lifestyle and prostate cancer**

A significant number of epidemiological studies have suggested that correct dietary supplements and a healthy lifestyle are important in lowering the risk of prostate cancer (21,22). Red meat and fat consumption at high levels shows links to an elevated risk factor in PCa. Consumption of fatty fish, on the other hand, is linked to a low risk factor for heart disease (21-23). The exact mechanism through which obesity raises the chances of prostate cancer is unknown at this time. Nonetheless, high insulin-like growth factor 1 (IGF-1) levels circulating are associated with prostate cancer induction (21,24). The most significant types of fatty acid are polyunsaturated fatty acids (PUFAs), such as omega-3, and ALA (alpha-linoleic acid) such as omega 6 which can only be obtained through dietary sources. An elevated omega-6 (polyunsaturated fatty acid) level has been shown to contribute to an elevation of prostate cancer. High levels of omega 3 (eicosapentaenoic acid) (EPA), a PUFA, are linked with lower PCa risk (25,26). Cruciferous, Vegetables, tomatoes, green tea, and phytoestrogens from soya are all considered to reduce prostate cancer risk (27). PCa may also be linked to alcohol intake, tobacco, vasectomies, sexually transmitted infectious disease (e.g. chlamydia), and an inflamed prostate gland (28).

## 1.2 Prostate cancer pathology

### 1.2.1 Prostate gland anatomy

The prostate gland is considered the largest accessory gland in the reproductive system of the male, and it surrounds the urethra's proximal section. Unstriated muscle, minor amounts of striped muscle and fibrous, connective and elastic tissues, as well as glandular, nerve, vascular, and lymphatic tissues make up this structure (29), which is located within the sub-peritoneal compartment, separating the pelvic diaphragm from the peritoneal cavity positioned posteriorly to the lower symphysis pubis, anteriorly to the rectal, and inferiorly to the bladder. The prostate gland of a healthy male adult is around the size of a walnut. The average weight of an adult man's typical prostate gland is roughly 11 grams (30). The gland's blood supply comes from the internal iliac artery, and lymphatic drainage is mostly provided by the internal iliac nodes, while the supply of nerves is provided by the prostatic plexus (29,30) (Figure 1.7).

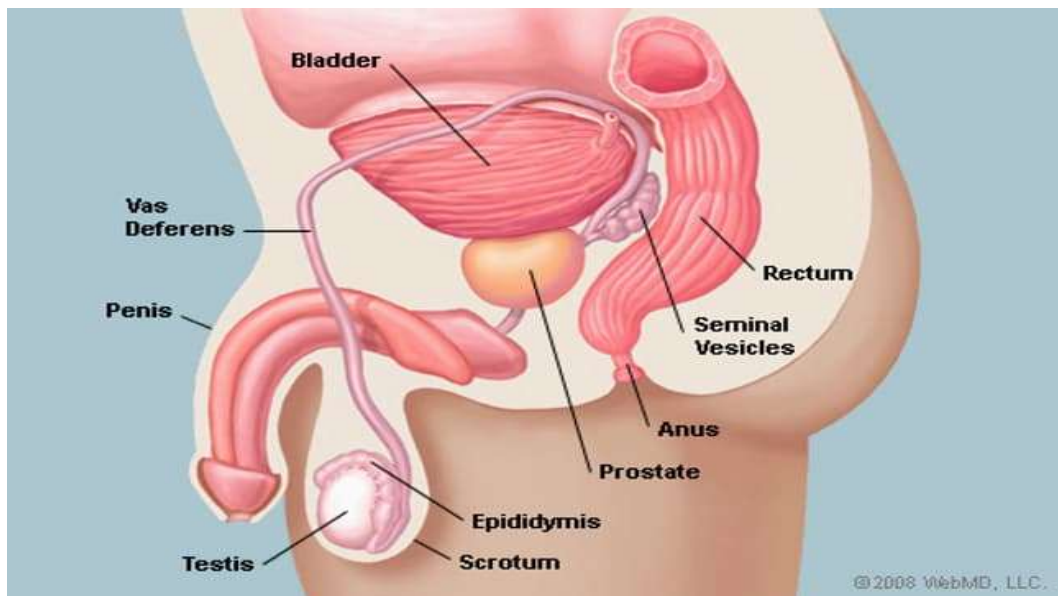


**Figure 1.6.** The prostate gland's location (31).

The prostate gland contains three areas, according to zonal anatomy. The periphery zone (PZ) is the biggest zone, accounting for seven tenths of the gland's overall volume. The distal urethra near the apex of the prostate is surrounded by the peripheral zone, and is felt as part of digital rectal examinations. Prostate cancer starts in the peripheral zone in more than 64% of cases. The central zone (CZ) covers the ejaculatory channels and takes up around twenty five percent of the total prostate gland. Only around 2.5 percent of prostate tumours occur in this zone: however these tumours show high aggressiveness (32). The prostate's middle region is termed the transition zone (TZ), accounting for about five percent of the gland's total area. This zone is modest in younger males. The enlargement of the transition zone in the prostate gland is known as benign prostatic hyperplasia (BPH) and occurs in older males (33-35) (Figure 1.7).

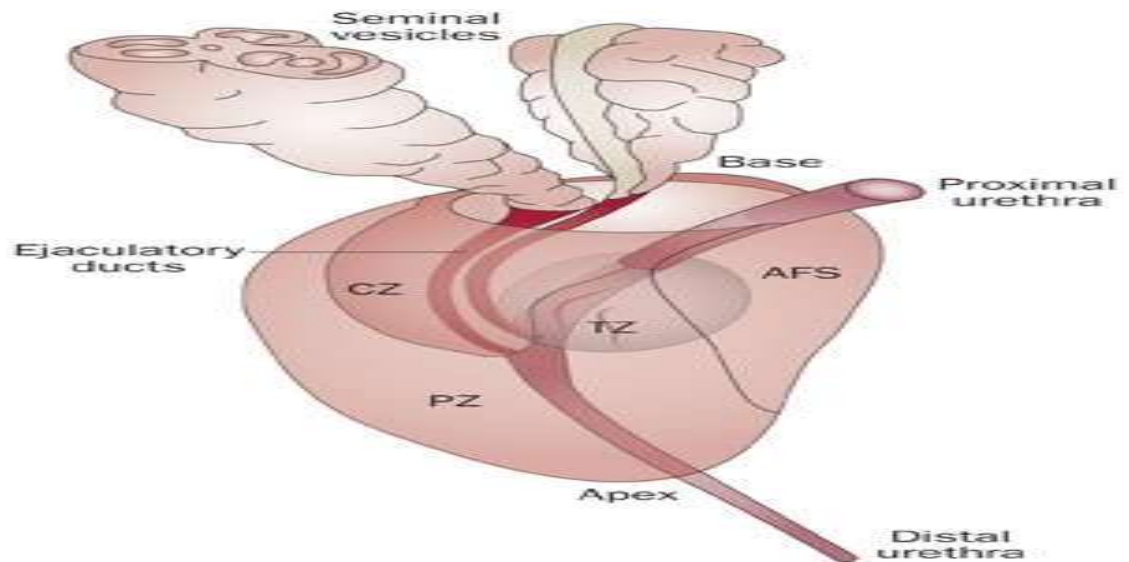


**Figure 1.7.** The prostate gland and the urethra from the front, obliquely (36).

The prostate gland functions as one of the accessory sex organs, and contributes to the overall semen ejaculated during orgasm. The prostate gland naturally tends to grow during adolescence and produces the fluid portion of sperm volume under the influence of the testosterone hormone. The secretions of the prostate are milky white,, slightly

alkaline and in simple sugars (glucose and fructose) that serve to feed the sperm while entering the female and traveling to fertilise the ovum. Also, they contain enzymes and prostate-specific antigen (PSA), and these cause protein breakdown, freeing sperm viscous fluids. In addition, prostatic fluids contain alkaline chemical and mineral components (including zinc and citrate) which help in maintaining pH and neutralise acids secreted in the vagina in order to promote sperms' chance of surviving (37).

### 1.2.2 Prostate gland epithelial cells

In the prostatic epithelium, three different cell entities have been identified, each with its unique structure, function, and relationship to cancer development. The predominant type is secretory luminal cells, which release prostatic proteins and are androgen dependent, as seen in Fig. 1.8. Therefore, androgen receptors are produced by secretory luminal cells (38).

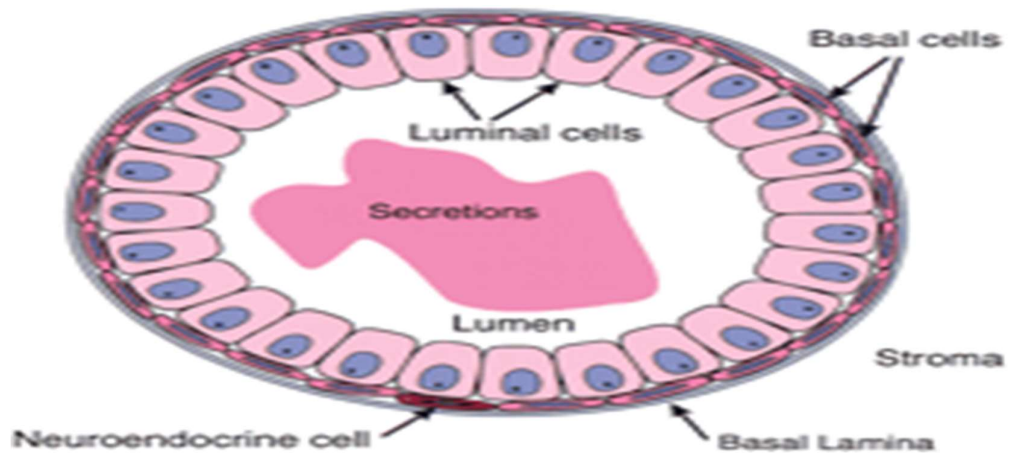


**Figure 1.8.** Classification of cell types in prostate duct (38).

Another prostate cell type is basal cell, which form a continuous sheet between luminal cells and the basement membrane. Neuroendocrine cells are a less common form of cell,



and may help luminal cell proliferation via signalling due to their uncertain embryology origin. They are androgen-independent, generally present in small clusters in the basal layer, and produce neuropeptides like serotonin. Regardless of their small numbers, neuroendocrine cells are a unique trait of aggressive forms of cancer when they congregate or acquire their characteristics (38).

### **1.2.3 Prostate cancer pathogenesis**

#### **1.2.3.1 Benign prostatic hyperplasia**

Benign prostatic hyperplasia is a non-cancerous increase in the size of the prostate gland that affects many older men. BPH develops as smooth muscle and gland epithelium, particularly in the transition zone (39). It is known as a condition that affects nearly all males as they become older. For males in their 30s, the histologic incidence of BPH is around 10%, 20% in their 40s, 50-60% in their 60s, and 80-90% in their 80s, according to various studies conducted in different regions (40,41). Clear correlation is found linking BPH and PCa, with each sharing striking characteristics in terms of ageing and androgen needs: therefore they are frequently encountered together. Despite this, no causal connection between the two issues has been identified (42). Researchers have proposed that androgen/androgen receptor (AR) signalling plays a critical role in benign prostatic hyperplasia: moreover suggesting that blocking of AR signalling may present an important treatment option. However, the exact mechanisms, and particularly the pathogenic effects of AR in BPH, remain unknown. Men with BPH are treated with androgen deprivation therapy (ADT) with 5-reductase inhibitors (5ARIs): these impede testosterone from being converted to form dihydrotestosterone (DHT) (43,44).

### **1.2.3.2 Prostatic Intraepithelial Neoplasia**

Prostatic intraepithelial neoplasia (PIN) forms a subphase or pre-cancer phase of change at cell level in which the prostatic epithelium, previously healthy, becomes malignant prostatic epithelium, as the epithelial cells proliferate abnormally but with no invasion of the surrounding stroma (45). It is distinguished from cancer through various traits in its cytology and architecture, which result in modest alterations: meaning that it is not always distinguishable from cancer (46). Two categories are identified in PIN, which are low and high grades of the condition. Low-grade PIN shows clear differentiation as an, early-stage invasive tumour which has primarily a basal cell makeup (47). In contrast, tumours which show poor differentiation and have secretory luminal cells are referred to as high grade PIN (48,49). At this grade, PIN occurs in 4 main classes, which are tufting (which is the most known type), cribriform, micropapillary, and flat (50). High-grade PIN is demonstrated to be a key marker, forming the only identified precursor to PCa (51).

### **1.2.3.3 Grading system and Gleason scale**

The development by Gleason in 1966 of a histology-based grading system (the Gleason scale, or GS) aimed to allow assessment of the aggressiveness of prostate cancer. The Gleason scale goes from 1 to 5, with 1 being the lowest and 5 being the highest. This PCa assessment It is a prostate cancer assessment system functions by measuring subjectively how far the architectural features of healthy gland tissue have been lost when viewed with a microscope. For example, the pattern with lowest aggressiveness is grade 1 while the highest aggressiveness is grade 5 (52) (Figure 1.9).

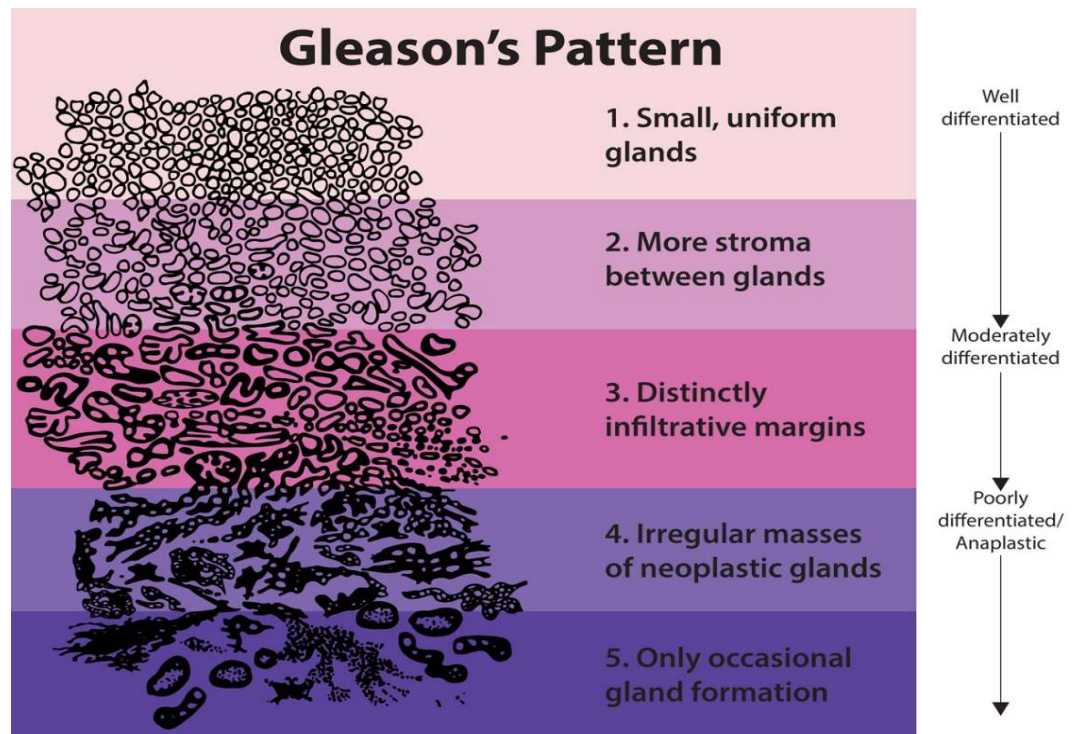


**Figure 1.9.** Gleason grading system Illustration summarizing the Gleason grading system for prostate cancer. The Gleason grading system, depicted here, provides a standardized method for assessing the histological patterns of prostate cancer. The system categorizes cancerous tissue based on architectural patterns, with grades ranging from 1 to 5. Low-grade cancers (Gleason scores 2-4) display well-formed glandular structures, while higher-grade cancers (Gleason scores 4-5) exhibit disorganized and infiltrative growth patterns. The combined Gleason score, determined by adding the primary and secondary grades, helps predict the aggressiveness of the tumor and guides treatment decisions. This figure serves as a visual aid to understand the Gleason grading system and its implications in prostate cancer diagnosis and management. (53).

Each case is given two grades (primary and secondary) based on diversity in histology in distinct lesions within tumours. Overall grades can range from 2 to 10, depending on how

each grade pattern is combined to produce the combined GS (54). This score is the sum of primary (>50% of total observed pattern, which indicates >50% of the tumour) and secondary grades (with 5-50% of the overall observed pattern, which indicates less than half of the tumour). Scoring is divided across 3 classes by this system: well-differentiated (GS 6), moderately differentiated (GS 6-7), and poorly differentiated (GS 7-8) (GS 8-10) (55-57). The primary lesion and secondary lesion scores are added to create the combined Gleason score. The highest combined Gleason scores are 10 and the lowest are 2, as each lesion is evaluated using five different scores. By grouping the scores into three categories, with good differentiation (GS 6), moderate differentiation (GS 6-7), and poor differentiation (GS 8-10), meaning that the Gleason grading system has been made simpler. In prostate carcinomas, the combined Gleason score has been frequently utilised for prognostic purposes and are correlated with significant pathologic parameters and clinical outcomes (58).

#### **1.2.4 Prostate cancer cell lines**

Researchers exploring molecular aetiology, proliferative activity, tumorigenicity, apoptosis and metastasis of prostate cancer have established various cell models. Frequently used PCa lines for laboratory work include PNT2, LNCaP, 22RV1, DU145, PC3 and PC3-M.

##### **1.2.4.1 PNT2**

PNT2 is a human cell lineage originally taken from prostate gland tissue in a deceased male aged 33 years. To establish an immortalised epithelial cell line, a plasmid harbouring the genome of Simian virus 40 with defective replicative origin (SV40 ori-) was

transfected into these cells (59). They express high T-protein levels as well as cytokeratins 8, 18, and 19, with these being indicators of luminal prostate cell differentiation. They are also slightly positive for PSA and negative for an epithelial basal cell marker (cytokeratin 14). Moreover, in nude mice, these cells do not cause tumours (60,61).

#### **1.2.4.2 LNCaP**

Researchers were limited in developing novel therapies treatments due to lacking cell lineages to explore pre-clinical prostate cancer. There were previously no lines which accurately represented human PCa's clinical progression (59). LNCaP is considered a weakly malignant cell line, and originated in a metastasis in the left supraclavicular lymph node which started from primary PCa in a 50-year-old Caucasian male in 1980. The cells were removed from the metastasis first using a needle aspiration biopsy. Because this cell line expresses AR and PSA, it can be classified as an androgen-responsive cell line (62). The LNCaP cell line can be used as a model for androgen research when cultured in culture media supplemented with foetal bovine serum which contains testosterone. However, it has been found that in the absence of androgen (for example, when charcoal-stripped foetal bovine serum was utilised instead of serum albumin), these cells will proliferate (63-65).

#### **1.2.4.3 22RV1**

In 1999, a xenograft taken from a patient with a bone cancer metastasized from the original prostate cancer was used to create the moderately malignant PCa cell line 22RV1. PSA and AR are both expressed in these cells (65,66). The line is derived from a CWR22

xenograft castrated and relapsed in mice and then subject to serial replication, again using mice (59).

#### **1.2.4.4 DU145**

A brain lesion from a white man of 69 years who had metastatic prostate malignancy yielded the DU145 cell line. These cells are androgen-independent and lack the expression of PSA or AR as prostate-specific markers (67). The DU145 line shows moderate ability to spread and morphologically, cells are epithelial (68). Subcutaneous implantation of this cell line into nude mice gave a resulting tumour which retained both genotypic and phenotypic characteristics of prostate cancer (67,69).

#### **1.2.4.5 PC3 and PC3-M**

PC3 cells, a lineage with poor differentiation, were isolated from human prostate cancer rib bone metastases of a Caucasian aged 62 years (59,70). These cells are androgen-independent and grow properly in androgen-free medium. Furthermore, PC3 xenograft tumours grow rapidly in nude mice, with a greater incidence of tumorigenicity and metastasis (71). The PC3-M metastatic subline of PC3 was isolated from nude mice with a liver cancer by intrasplenic injection of PC3 cells. The line shows similarities to PC3: however, it is more malignant, with greater aggression (69,72).

### **1.3 Prostate cancer androgens and treatments**

#### **1.3.1 Androgen role in prostate cancer**

The prostate gland's development, growth, maintenance, and function are all influenced by androgen. Testosterone circulates more abundantly in males than any other androgen,

with more than 95 percent synthesised in the testes. The adrenal glands are responsible for the remaining 5% of testosterone (73). In men, androgen secretions are regulated in the hypothalamus. When blood androgen levels (mostly comprising testosterone) fall, a pulse of luteinizing hormone-releasing hormone (LHRH) is released by the hypothalamus and binds to a target receptor within the pituitary gland and causes luteinizing hormone (LH) to be produced (73). Progression of steroidogenesis in Leydig cells is aided by the release of LH in the peripheral circulation (74). When the 5  $\alpha$  - reductase enzyme within the prostate gland is stimulated, this converts into a more potent metabolite, dihydrotestosterone (DHT). DHT binds AR, which is a ligand-controlling transcription factor belonging to the nuclear hormone superfamily. DHT-AR binds and activates androgen response elements (AREs) within downstream genes' promoter regions within the cell's nucleus, and this may regulate prostate cells' differentiation, proliferation and survival (73-80).

### **1.3.2 AR mutations, overexpression and amplifications in CRPC and GCPR**

With more than 1110 distinct mutations, AR has the most mutations among hormone receptors, and 168 of these have been linked to prostate cancer, according to a report from the Androgen Receptor Gene Mutations Database (81). In the early stages of prostate cancer, AR mutations are extremely uncommon, but they were present in 10–30% of CRPC patients who received ADT. Some arguments propose a selective pressure role of ADT increasing mutation rate for the androgen-receptor gene. (82-84). A majority of mutations occurred in LBD (94%) or NTD (40%), DBD (7%) and less common in the hinge area, occurring at 2%. Even with very low levels of androgen, CRPC cell growth and survival may be supported due to AR gene mutations (85). Due to various mutations in the LBD, AR is capable of binding to activation ligands usually found in the body,

such as oestrogens, corticosteroids, progesterone, and also in flutamide, and antiandrogen. This enables prostate cells to proliferate without the need for androgen (86,87).

Another potent mechanism that makes CRPC cells more responsive to a decrease in circulating androgen and promotes CRPC progression is AR gene amplification. ADT was shown to enhance the chances of AR gene amplification in CRPC patients by 20–30%: however, only a small number of cases of untreated primary prostate cancer were observed. ADT may cause an increase in AR in the CRPC cells' cytoplasm, allowing tumour cells response to occur at low androgen levels and allowing continued growth of PCa in an androgen-dependent manner despite castration (88,89). In CRPC tissues, amplification of the AR gene was linked to a significantly increased level of both protein and mRNA. Additionally, studies have shown that patients who originally responded well to ADT were more likely to experience AR sensitivity amplification, while patients who did not respond to ADT were far less likely to experience it (88,90). Moreover, certain AR mutations can lead to conformational changes in the receptor protein, affecting its interaction with co-regulatory proteins or its binding to DNA, thereby altering gene transcription and downstream signalling pathways. These changes can promote cell proliferation, survival, and the development of resistance to therapy (90).

Understanding the specific AR mutations present in prostate cancer and their downstream impact is crucial for personalized treatment approaches. Targeting the altered AR signalling pathways, such as using next-generation anti-androgens or other novel therapeutic strategies, can help overcome resistance and improve patient outcomes in the management of prostate cancer.



The regulatory role of G protein-coupled receptors (GPCRs) in various physiological processes is well established. In the context of prostate cancer, the influence of androgen and androgen receptor (AR) signalling has been extensively investigated. Androgens and the activation of AR signalling pathways play a significant role in the regulation of prostate cancer development and progression. Consequently, there has been considerable research focused on blocking AR signalling using AR antagonists and steroidogenic enzyme inhibitors as potential therapeutic strategies. The comprehensive studies conducted on the regulation of prostate cancer by androgens and AR signalling, as well as the exploration of AR-targeted interventions, have contributed to our understanding of the underlying mechanisms and potential treatment approaches for this disease (91).

### **1.3.3 Prostate cancer treatments**

In the early stages of PCa, frequent treatment approaches include radical prostatectomy and external radiation therapy(92). Androgen deprivation therapy has been used to treat PCa since the 1940s, when Charles Huggins demonstrated that the changes generated by surgical testes removal had a significant impact on the disease. According to this research, PCa growth and expansion are influenced by the availability of androgen in the peripheral blood circulation. Following this finding, androgen deprivation became a routine treatment for PCa, either through surgical castration or medication. These treatments improved the prognosis and survival of PCa patients (93). Suppressing androgen

signalling forms a significant strategy in treating advanced or metastasised PCa, and ADT using medication, surgical castration, anti-androgen therapies and combination androgen blockade have become frequent approaches (94). ADT, being the most effective therapy, can provide a primary response in 80 percent to 90 percent of patients. Nonetheless, ADT response expires fourteen to twenty months subsequently, and androgen-independent PCa then develops and is unresponsive to androgen deprivation (95). Enzalutamide (ENZ) is a second generation anti-androgen treatment which can treat prostate cancer in its early stages, and is one of the ADT options (96,97). Chemotherapy such as docetaxel (DOC) is also one of the standard treatment strategies for prostate cancer (98,99). It was designed to disrupt cell cycle division and trigger apoptosis by targeting microtubules (100).

#### **1.3.4 Androgen- independent prostate cancer**

CRPC is another name for androgen-independent prostate cancer disease. In comparison to other stages of PCa, CRPC is linked with poorer prognoses, reduced length of survival, and is resistant to castration (74). There is a significant drive within PCa research to identify pathways contributing to transformation of prostate cancer cells from androgen-dependence to androgen-independence and this presents a critical challenge or prerequisite to developing new CRPC therapy strategies (82,97,101).

#### **1.3.5 Molecular mechanism involved in CRPC progression**

Molecular mechanisms by which progression of androgen-dependent PCa to CRPC occurs is a significant topic that has been studied by numerous laboratories. Currently, androgen deprivation therapy is the main approach to treating PCa (102). Despite this, in most cases, individuals undergoing ADT later relapse, progressing to CRPC. AR is expressed by some CRPC cells. The AR-negative CRPC cell is unresponsive to ADT

treatment, whereas AR-positive CRPC cells respond to androgen, expressing. Despite this, these cells do not subsequently depend upon androgen to develop and grow, meaning that ADT in CRPC cells then becomes ineffective (101-103). It is unclear how the PCa cell progresses from androgen-dependence to CRPC cell status (101-103). Several theories have been proposed regarding a mechanism for this critical change (104). However, these theories each address merely a portion of the problem, with no unified hypothesis currently which satisfactorily explains the process.

### **1.3.6 CRPC AR-dependent signalling pathway**

The transcription factor androgen receptor is ligand-dependent and belongs within the family of steroid hormone receptors. AR has several functional domains, namely, a ligand-binding domain (LBD), a DNA-binding domain (DBD), a hinge region and a large N-terminal domain (NTD) (105). Continual AR activation is suggested as a significant mechanism in CRPC growth (106). While ADT reduces androgen levels within peripheral blood, effects on DHT levels are not seen. As a result, DHT can continue to stimulate AR (107). It has been proposed that several molecular and cellular changes, such as AR amplification, mutation and ligand signalling, as well as abnormal co-regulating factors and splice- biomarkers for AR, are significant in PCa (108,109). The androgen receptor (AR) function plays a vital role in various physiological processes, particularly in the development and maintenance of male reproductive organs and secondary sexual characteristics. The AR is a protein that binds to androgens, such as testosterone and dihydrotestosterone, and upon activation, translocate to the cell nucleus where it regulates gene expression.

In target tissues, the binding of androgens to the AR triggers a series of intracellular events, leading to the modulation of gene transcription and subsequent protein synthesis. This signalling pathway is essential for normal sexual development, sperm production, muscle growth, bone density maintenance, and other androgen-dependent functions.

Furthermore, the AR is crucial in the context of prostate cancer. In normal prostate tissue, the AR plays a role in regulating cellular growth, differentiation, and apoptosis. However, in prostate cancer, aberrant AR signalling can contribute to tumor initiation and progression. Understanding the intricate mechanisms of AR function is critical for developing targeted therapies and interventions for prostate cancer management.

Overall, normal AR function is vital for the proper functioning of male reproductive tissues and is involved in various physiological processes. Its role in prostate cancer highlights the significance of studying and modulating AR signalling for both normal development and disease management (81).

### **1.3.7 CRPC and drug resistance**

In CRPC cells, xenografts, and tissues, various AR splice variants (AR-Vs) are recognised (110,111). Studies have demonstrated that truncation of AR-Vs to lack LBD, which is targeted in androgen therapies, constitutively activates AR in a ligand-independent manner and leads CRPC to develop (112). Mechanisms that cause these AR-Vs to express more frequently in CRPC cells are currently unknown. Splicing may be caused by genomic rearrangements or/as well as intragenic deletions in the AR gene locus (113). The most common variants found is AR-V7, and high expression of this variant has been linked to a poor outcome in CRPC patients (114). AR-V7 expression was shown to be high in CRPC cells and tissues sampled from individuals with CRPC (114,115). AR-V7 levels in mice cannot be inhibited, although ADT, such as abiraterone

acetate and enzalutamide, may give some improvement in treatment effect (116). Androgen receptor splice variants such as AR-V7 were recently related to enzalutamide resistance (84,113,115,117). Enzalutamide is unable to bind to AR-V7 due to the fact that AR-V7 lacked LBD, resulting in cell resistance (84,117-120). Researchers have proposed that AR-V7 could be targeted by CRPC therapies (121). The androgen responsive 22RV1 cell line is a well-established model of enzalutamide resistance prostate cancer cell, due to the expression of AR splice variants including AR-V7 (84,122-124). In terms of chemotherapy options, docetaxel is a first line therapy used to treat CRPC. Despite docetaxel's initial positive response, drug resistance is inevitable, however. The mechanisms of docetaxel resistance are not well understood (125).

### **1.3.8 Other CRPC related pathways**

CRPC progression has been linked to several pathways. Specific protein 1 (Sp1), also known as transcription factor, contributes significantly to promoting PCa and in the disease progressing (126). It promotes angiogenesis through VEGF through upregulating AR via Sp1 binding site in prostate cancer cells (127). Another pathway is that the Bcl-2 gene which act as Anti-apoptotic that inhibits apoptosis and may result in androgen independence (128,129). Various new hypotheses have been brought up in recent years in addition to the core hypothesis supporting an AR sensitivity-amplification perspective. The FABP5-related signalling pathway (FABP5- PPAR $\gamma$ - VEGF) hypothesis for example, proposes that it this and not AR-related pathway was crucial to increasing malignant growth in CRPC cells (130). Other markers that play a significant role in CRPC such as GFs, such as NGF, IGF, and EGF, play significant roles in prostate cancer. NGF, typically low in normal prostate tissue, is increased in prostate cancer and promotes tumor growth and nerve fiber formation. IGF-1 and IGF-2 are elevated in prostate cancer and stimulate cell proliferation, inhibit apoptosis, and enhance metastatic potential. EGF,

along with its receptor EGFR, is overexpressed in prostate cancer and promotes cell growth, invasion, and metastasis. Targeting these GFs and their associated pathways holds promise for developing effective therapeutic approaches against prostate cancer(131,132).

## **1.4 Fatty acid binding proteins**

### **1.4.1 FABP family members**

Fatty acids provide energy and can be used as cell fuel. Ester bonds contained inside fat or oil are hydrolysed to create fatty acids (133). According to research, fatty acids function as signalling molecules that are important for a number of metabolic processes in cells, including cell growth, gene regulation, and death (134-136). Fatty acids produced by adipocytes have the ability to flow from the cellular membrane, entering the cytoplasm. They may also be helped to travel to an adjacent cell through transporters or being passively diffused. Once fatty acids enter the cytoplasm, there are two possibilities for them: joining the metabolic pathway to be used as a fuel source; or binding to FABPs to be transported to different organelles (136). FABPs, or intracellular lipid chaperones, belong to the super lipid-binding protein (LBP) group (137). FABPs have been identified in twelve different species since 1972, but two of them are only found in fish (138,139). FABPs have been discovered or are frequently found within various organs, and their names reflect where they were discovered (**Table 1.1**). Yet FABPs' expression is not restricted to their respective organ- or cell-related names. Thus, FABP1 (liver FABP) expression occurs primarily in the liver, but is additionally found in pancreatic, intestinal, lung, stomach, and kidney tissues. Moreover, FABP5 (epidermal FABP) shows high expression in the brain, skin, lungs, tongue, adipocyte, intestinal tissue, macrophages, liver, kidneys, mammary glands, heart, skeletal muscle, testis, retina, lens, and spleen

(134,139). Fatty acids serve as common building blocks for the synthesis and storage of lipids wherever they are expressed. Generally, when higher levels of FABP are produced, this is accompanied by increased fatty acid levels entering the cell (140).

<b>Protein (FABPs)</b>	<b>Name</b>	<b>Alternate name</b>	<b>Tissue/cell expressed in</b>
FABP1	Liver FABP	L- FABP	Intestine, liver, stomach, lung, pancreas, kidney
FABP2	Intestinal FABP	I-FABP	Liver, intestine
FABP3	Muscle, heart FABP	H-FABP	skeletal, muscle, brain, kidney, lung, stomach, testis, aorta, adrenal gland, mammary gland, placenta, ovary, brown adipose tissue
FABP4	Adipocyte FABP	A-FABP	Macrophage, dendritic cell, adipocyte
FABP5	Epidermal FABP	E-FABP	Tongue, skin, adipocyte, skeletal macrophage, mammary gland, brain, liver, intestine, kidney, lunge testis, retina prostate, spleen
FABP6	Ileal FABP	II-FABP	Ileum, adrenal gland, ovary, stomach
FABP7	Brain FABP	B-FABP	Glia cells, brain, retina, mammary gland
FABP8	Myelin FABP	M-FABP	Peripheral nervous system



FABP9	Testis FABP	T-FABP	Salivary gland, testis, mammary gland
FABP10	Liver FABP	L-FABP	Teleost fish liver
FABP11	-	-	Intestine, liver, brain, heart, muscle, kidney, testis and ovary of teleost fish, skin, eye, swim bladder
FABP12	-	-	Testis, retinoblastoma cells from human retina, kidney, germ

**Table 1.1 Multigene family of fatty acid- binding proteins (141)**

#### **1.4.2 FABPs' general functions**

Fatty acid binding proteins are capable of active binding and transportation of lipids to particular cell organelles or sites in their capacity as lipid chaperones. Lipid droplets, which store lipids, are among these places or organelles, as is the endoplasmic reticulum, which is a signal transducer and functions in transportation as well as membrane formation (142). Fatty acids are transported to various sites in cells, including mitochondria or peroxisomes to be oxidised, the cytosol or various enzymes to regulate enzyme activities, and to cell nuclei for lipid-mediated transcription regulation. Also, fatty acid transport to extracellular signals can occur through the paracrine or autocrine pathway (142,143). Peroxisome proliferator-activated receptors (PPARs), for instance, are a family which can carry out their functions due to the ability of FABP to reach the

cell nucleus, transferring fatty acids to transcriptional regulators (144-146). It has been reported that FABPs may perform fatty acid transport from the cytoplasm to the PPAR nuclear receptor (142). Additionally, it has been found that the cytoplasm and nucleus of cancerous tumours express FABP (145,147). These studies have provided evidence of FABP involvement with particular signalling pathways within the nucleus responsible for regulation of gene expression. Figure 1.10 illustrates the method for fatty acid transport and the metabolic pathway within the cell.

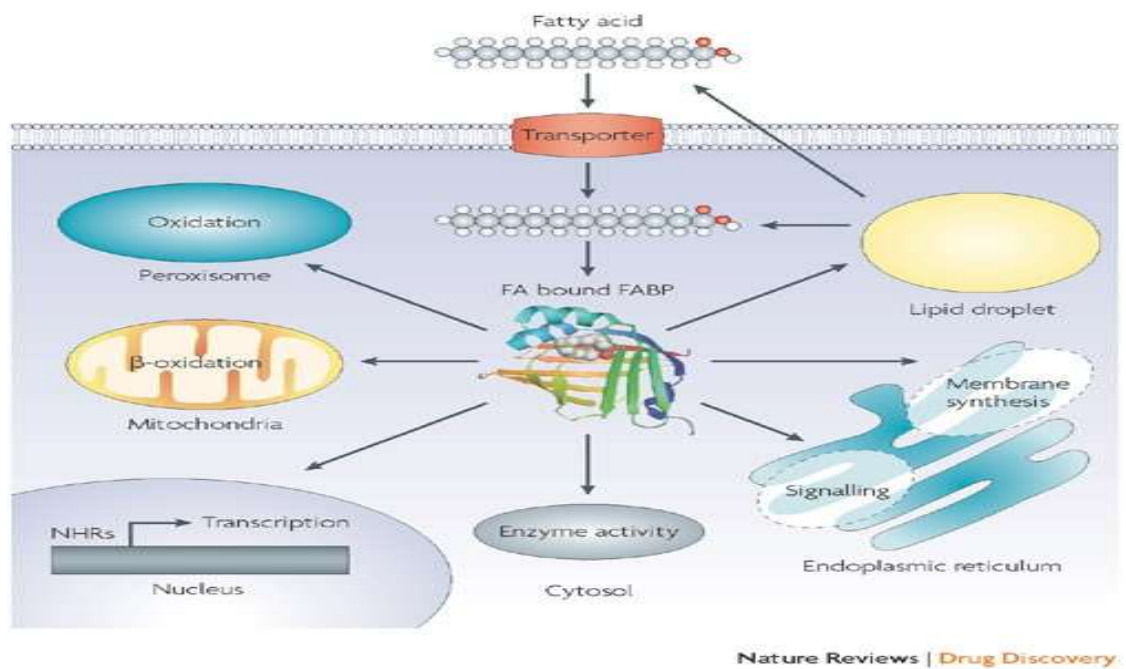


**Figure 1.10.** Different Fatty Acid Binding Proteins (FABPs) play distinct roles in cellular processes related to fatty acid metabolism and transport (134)

### 1.4.3 FABP structure

Nuclear magnetic resonance, X-ray crystallography, and various biological approaches were used to investigate FABP structure. FABPs presented with between 15% and 70% amino acid sequence homology (137), and were also shown to have tertiary structures that were quite comparable (148). FABP typically has an antiparallel 10-strand structure, with a binding pocket found within the  $\beta$ -barrel which has an N-terminal helix-loop-helix motif on one side. This motif is hypothesised as the primary site for binding to fatty acids (137). All FABPs have been found to exhibit three-element fingerprints (Figure 1.11). Due to minor structural variations across isoforms, all FABPs have ligand selectivity and bind long-chain fatty acids (148). Unsaturated fatty acids are an exception, and the ligands' binding affinity increases with increasing hydrophobicity (149). Affinity and selectivity for the main isotype forms at various sites may also be influenced by the necessity for target cells (137). For instance, the very long-chain fatty acid FABP7 is highly selective for docosahexaenoic acid. However, FABP1 is able to bind many ligands, including lysophospholipids and haemoglobin (149,150).

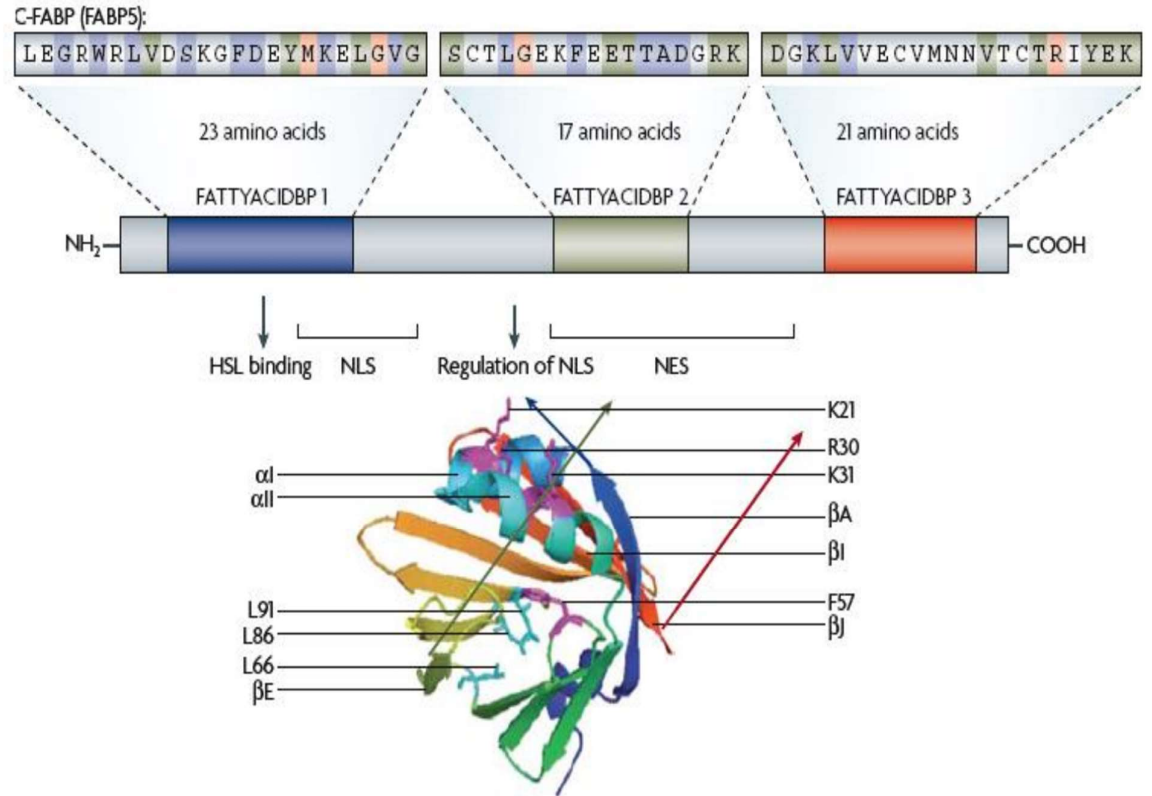


**Figure 1.11** The fingerprint of Fatty Acid Binding Proteins (FABPs) encompasses key structural and functional characteristics shared among these intracellular proteins. FABPs have a beta-barrel structure with a hydrophobic cavity that binds fatty acids. Conserved amino acid residues within the ligand-binding pocket determine fatty acid selectivity. Flexible loop regions enable conformational changes for ligand binding and release. FABPs are primarily located in the cytoplasm but can be found in other cellular compartments. Understanding the fingerprint of FABPs aids in their identification, characterization, and comprehension of their role in cellular lipid metabolism and transport. (134).

The ribbon diagram is provided together with an illustration of three largely conserved motifs. The blue ribbon FATTYACIDBP1 shows part of the first  $\beta$  strands ( $\beta$ A). Additionally, it has a hormone-sensitive lipase (HSL) and nuclear localization signal (NLS) binding sites. The green ribbon FATTYACIDBP2 contains the nuclear export signal (NES) domain that includes  $\beta$  sheet 4 and 5 ( $\beta$ E). Beta sheet 9 ( $\beta$ I) and 10 ( $\beta$ J) are encoded by the red ribbon FATTYACIDBP3. Blue, red and green are used to identify the key amino acids.

### **1.5FABP5 role in prostate cancer**

The 15 kDa cytosolic protein FABP5 is among the proteins that bind fatty acids and has a strong binding affinity for medium-chain and long-chain fatty acids (151,152). FABP5 is identified as having a crucial part in advancement in prostate and breast cancer disease. Studies showed that it could cause metastasis in vivo through upregulation of vascular endothelial growth factor (VEGF) production (153-155). Moreover, FABP5 is shown as a reliable indicator for prognosis and outcome prediction. It is also a target for therapeutic action. Inhibiting FABP5 with siRNA successfully suppressed prostate cancer in nude mice (153,156-158). FABP5 expression level is high for androgen-independent cells (DU145, PC3 and PC3-M) and modest in androgen-responsive lines (22RV1), while it is very low (hardly detectable) in androgen-dependent cell lines (LNCaP) and benign PNT-2 cells (153,159). High levels of intracellular fatty acids are carried to CRPC cell nuclei (DU145, PC3 and PC3-M), and there function as molecular signallers, activating nuclear receptor PPAR $\gamma$ . After activation, PPAR $\gamma$  modifies related downstream target regulatory gene expression, and ultimately leading to tumour development and aggression through upregulating cancer-promoting genes downstream, including VEGF, as well as downregulating tumour suppressor genes. It is also partially due to the disturbance of the balance in cell numbers regulated cell growth and apoptosis (130,158) (Figure.1.12).

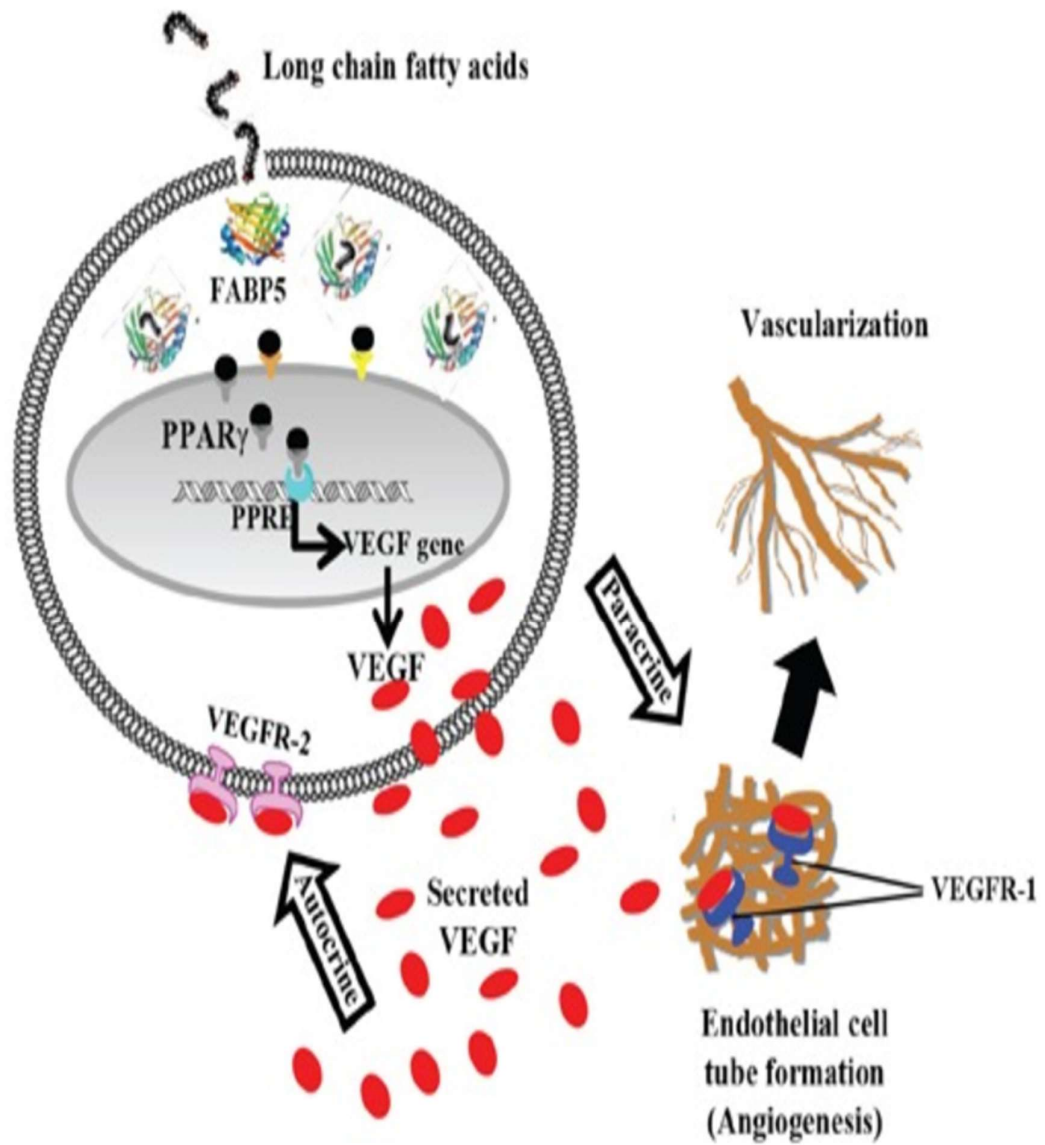


**Figure 1.12.** The role of fatty acids with FABP5 in PPAR $\gamma$  activation and downstream regulations (160).

## **1.6 Specificity Protein (Sp1) in FABP5**

FABP5 is significantly linked to poor overall survival in breast and prostate cancers. The transcription factor Sp1 is determined to be critical to the expression of FABP5. A CpG island was found around the promoter region of FABP5, and elevated levels of Sp1 and c-Myc were identified. Altogether, these processes lead to the transcriptional stimulation of FABP5 expression throughout the development of human prostate cancer (161).

## **1.7 Apoptosis and FABP5 in prostate cancer**

FABP5 are shown to have an influence on the apoptotic process in prostate cancer. An increase in FABP5 was shown to boost tumorigenic abilities and metastasis in prostate cancer cells. This effect may be partially mediated by a frequency decrease in apoptotic cells or a decrease in the sensitivity of the cells to apoptotic induction signals (130). Additionally, other investigations have demonstrated that FABP5 significantly influenced the suppression of apoptosis in the high-malignancy PC3-M and DU145 cell lines, as likely accomplished through upregulation of specific pro-apoptotic proteins (162,163). Strong data also demonstrated that prostate cancer cells were less likely to undergo apoptosis when the PPAR pathway was activated (164-170). Double mutant recombinant fatty acid binding protein 5 (dmrFABP5) was associated with inducing apoptosis. DmrFABP5 as a FABP5 inhibitor downregulated the Bcl-2 and upregulated the pro-apoptotic gene Bax in prostate cancer cells (171).

## **1.8 Prostate cancer and targeting FABP5**

On the basis of the extensive research available, FABP5 (as well as the fatty acids transported by it) can be reasonably considered to form a significant therapeutic target. Previously, knockdown of FABP5 gene encoding was performed through RNA interference in the high-malignancy PC3-M cell line and subline (Si-clone-2) was created which showed significant reductions in FABP5 expression, in order to evaluate whether

it was practical to target FABP5 in developing PCa treatment. The cells with FABP5 knockdown were orthotopically injected into the mouse prostate gland, which reduced mean tumour size by a factor of 63, with 7 times fewer occurrences of tumour, while metastasis was reduced by 100%. (156). These results show the particular effectiveness of the short FABP5 siRNA generated inside the cancerous cell in halting malignant development of the cancer in mice. On the other hand, siRNA molecules will quickly break down after being administered as external reagents because of their instability and limited life at body temperature. Therefore, siRNA is unsuitable as a standalone PCa therapy. Even on dissolving siRNA against FABP5 with a stabilising liquid (called Atolecollagen, a cow-skin extract) and the direct application of this within advanced PCa tumours in nude mice, the effect was merely slowing and stabilising the rate at which the tumour grew, without shrinking tumours or stopping malignant progression (157). Therefore, the primary challenge is to identify novel FABP5 inhibitors that are highly efficient, focused, and relatively stable so as to establish optimum PCa treatment through inhibiting FABP5's biological activities. FABP5 is responsible for binding and transporting fatty acids into cells from a variety of external and intracellular sources as part of its regular biological function. It has a fatty acid-binding motif comprising the three important amino acids Arg109, Arg129, and Tyr131, allowing FABP5 to bind to fatty acids through the carboxylate group (172). An earlier study found that fatty acid binding motifs' structurally stable characteristics totally controlled FABP5's ability to promote tumour growth in the PCa cell.

An earlier group investigated prospects for creating an inhibiting agent for wild-type FABP5 through altering its fatty acid-binding motif structure, as motivated by discovering the ability of tumour suppressor p53 to enhance tumorigenic characteristics (173). The production of cDNA coding to produce double-mutated FABP5 was



undertaken by using site-directed mutagenesis to modify 2 out of 3 fatty-acid binding motif amino acids, from Arginine109 to Alanine109 and Arg129 to Alanine129. This recombinant product was given the designation dmrFABP5 (130,174). While dmrFABP5 are incapable of binding fatty acids or boosting tumorigenic capacity, wild-type recombinant FABP5 (wtFABP5) shows complete capacity for fatty acid binding and dramatically promotes PCa cell tumorigenicity, with a 13-fold increase. The group's earlier findings demonstrated that altering two of the three essential amino acids in FABP5's fatty acid-binding motif nearly totally eliminated the protein's capacity to bind fatty acids (130). DmrFABP5, which has nearly lost the capacity for attaching to fatty acids, does not have its tumour-promoting and biological activities, making it a novel FABP5 inhibitor. It also now has the capacity to block wtFABP5's biological activities. Surprisingly, dmrFABP5 exhibited a decrease of over 14 times in the mass of original tumours, as well as inhibiting metastasis completely when administered as a treatment for PCa grown in nude mice (175). The results of the therapy test using dmrFABP5 in a nude mouse model *in vitro* and *in vivo* are extremely significant. Therefore, dmrFABP5 is a promising candidate molecule for the curing of prostate cancer disease.

## **1.9 Drug combination roles**

Drug combinations are considered the most common strategy to improve treatment results, and this strategy has been used in the treatment of severe diseases such as cancer and AIDS. Through combined applications of different drugs, clinicians aim to find synergistic treatment effects, possible reduction of toxicity, and suppression or postponement of the possible development of drug resistance (176). Drug combination treatment includes at least two or more drugs given in a single dosage form at a fixed dose. The treatment plan must take into account different physiological variations, pharmacokinetic profiles, and drug dosage regimens (177). In cancer treatment, even the

same tumour from different patients or the various cells within the same tumours exhibit intrinsic heterogeneity. The primary cause of rapid cancer relapse or incurability is frequently intrinsic or acquired resistance to a single chemotherapeutic agent due to multiple-drug resistance, apoptotic suppression, or enhanced DNA repair (178). Therefore, the application of combinational therapy within a therapeutic drug treatment regime has advantages because various medications can target various pathways or gene targets, significantly reducing the number of cancer cells that survive the treatment and significantly delaying or even eliminating cancer recurrence (179).

### **1.10 Hypothesis**

In this work, I hypothesise that dmrFABP5, in combination with the currently used prostate cancer drugs docetaxel or enzalutamide, may enhance the treatment efficiency through a synergic effect. I plan to produce and purify a large quantity of dmrFABP5 to use it alone or in combination with the chemotherapeutic agent docetaxel and the anti-androgen drug enzalutamide. Then, I will evaluate the impact of the combination on the tumorigenicity and metastatic abilities of prostate cancer cells DU145, 22RV1 and LNCaP by assaying their malignant characteristics in comparison to the treatment with each single agent alone. Next, I plan to evaluate the molecular mechanisms involved in the possible synergistic interactions by measuring the changes in expression levels of a number of the relevant signal transduction factors. To further study the molecular mechanism underlying the tumour suppressing activity of dmrFABP5, I intend to compare and to analyse the gene expression profiles between the dmrFABP5- treated DU145 cells and the untreated control to systematically assess the relevant signal transduction pathways induced by dmrFABP5 treatment.

## 1.11 Aim

This research endeavour is dedicated to addressing the pressing challenge of finding an effective treatment for castration-resistant prostate cancer (CRPC). Specifically, our main objective is to explore the potential of combination therapy involving dmrFABP5, docetaxel, or enzalutamide as a novel treatment strategy for CRPC.

## 1.12 The specific Aims in different phases of the work

- ❖ Producing and purifying sufficient quantity of dmrFABP5 and wtFABP5 with the E. coli system.
- ❖ Evaluation and determine the  $IC_{50}$  of dmrFABP5, docetaxel and enzalutamide on DU145, 22RV1 and LNCaP cell lines.
- ❖ Conducting experiments to test the suppression effect of dmrFABP5 alone, or in combination with docetaxel and enzalutamide respectively on DU145, 22RV1 and LNCaP cell lines.
- ❖ Evaluating whether the combined treatments of different reagents of DU145, 22RV1 and LNCaP cells have synergistic effects in suppressing tumorigenicity.
- ❖ Studying the molecular mechanism involved in the possible synergic interaction by combined treatments.
- ❖ Evaluation of relevant signal transduction pathways induced by dmrFABP5 stimulation in DU145 cells using RNA profiling.

## **Chapter 2**

### **Materials and Methods**

## **2.1 Cell culture**

### **2.1.1 Routine cell culture**

Cell lines were grown in flasks and incubated at 37°C in a humid environment with 5% (v/v) CO<sub>2</sub>. The culture medium was RPMI-1640 supplemented with 10% (v/v) foetal bovine serum (FBS), L-glutamine, and 100IU penicillin/streptomycin (PEN-STREP). In this work, 4 cell lines, LNCaP, 22RV1, DU145 and PC3-M were grown and used for the experimental work. All regular culture media were replaced every other day to ensure enough nutrient supply for the cells. Each cell line's authenticity was verified using DNA short tandem repeat (STR) profile analysis (both of which are shown in the Appendix). The cell culture was routinely checked for mycoplasma contamination by a department technician. The Northgene Company verified STR test, the validity of the cells, and the certificate for each cell line were supplied in the appendix.

### **2.1.2 Sub-culture**

Sub-culture of cells was carried out to split the culture into more other flasks when the cell density reached 60–80 percent confluence, allowing the cells to continue to grow and multiply. After the old medium was aspirated, the flask was washed twice with PBS before the sub-culture. A sufficient amount of TrypLE reagent was added to the culture flask, incubated for 3-5 minutes in the incubator. The effect of the TrypLE reagent was neutralised by the addition of complete medium containing double amount of FBS. After 3 minutes of centrifugation at 1000 rpm, the cell pellet was collected and re-suspended in fresh medium, distributed into 3 fresh flasks, and incubated at 37°C with 5 percent (v/v) CO<sub>2</sub> in an incubator.

### **2.1.3 Thawing of the cells**

Cells were collected from a storage tank of liquid nitrogen and defrosted in a 37°C water bath. The cells were then transferred to a universal tube containing 10 ml of fresh medium and centrifuged at 1000 rpm for 3 minutes. After the supernatant was discarded, the cell pellet was re-suspended in fresh medium in a cell culture flask, incubated in an incubator at 37°C with 5% (v/v) CO<sub>2</sub>.

### **2.1.4 Counting of the cells**

An improved Neuberg double counting chamber haemocytometer was used to count the number of cells. Using the procedure outlined in the earlier description, cells were removed from the culture flask. After a good mixture, 10µl of cell suspension was added to a haemocytometer. Then, under a microscope, cells were counted in squares with four corners. The hemocytometer comprises a gridded area with nine 1 x 1 mm (1 mm<sup>2</sup>) squares. Each square is further divided into smaller sections in three directions: 0.25 x 0.25 mm (0.0625 mm<sup>2</sup>), 0.25 x 0.20 mm (0.05 mm<sup>2</sup>), and 0.20 x 0.20 mm (0.04 mm<sup>2</sup>). Additionally, the central square is divided into even smaller 0.05 x 0.05 mm (0.0025 mm<sup>2</sup>) squares. The raised edges of the hemocytometer keep the coverslip 0.1 mm above the marked grid, ensuring that each square has a precisely defined volume. The following equation was used to get the total number of cells in suspension:

Total number of cells = Average cell count per square × Dilution factor × 10<sup>4</sup> × Total volume (ml).

### **2.1.5 Freezing of the cells**

When the culture reached 65-85% confluence, cells were washed and detached as described in section 2.1.3. The freezing medium, which is complete medium with 0.75 percent (v/v) DMSO, was used to resuspension the cell pellets. 1 ml of cell suspension

was added to each cryogenic vial before it was placed in a Nalgene cryo-preserved box with 250 ml of isopropyl alcohol. After spending the night in a -80°C freezer, the box was transferred to a liquid nitrogen tank for long-term storage.

## **2.2 Expression and purification of dmrFABP5 and wtFABP5**

### **2.2.1 E. coli cell growth and protein induction**

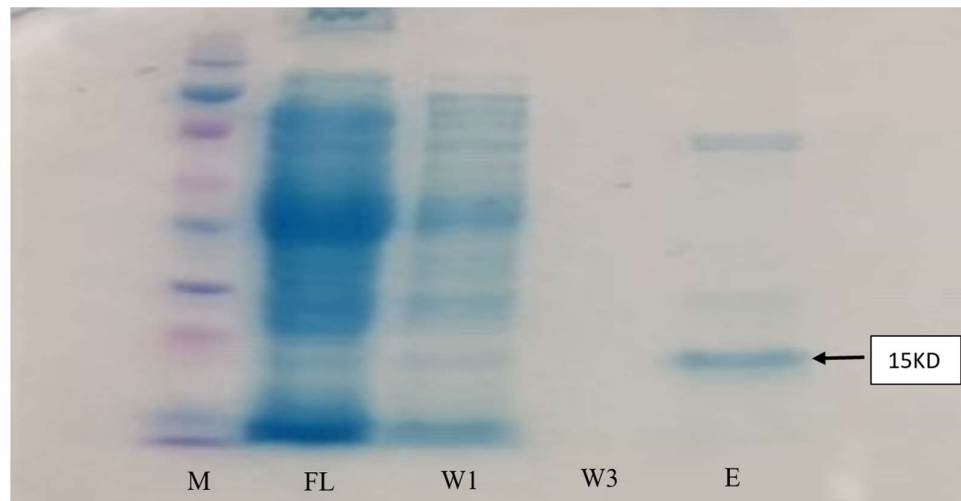
The transfection steps were previously described by Waseem et al (175). A single colony of E. coli cells harbouring the expression constructs pQE-32-wtrFABP5 or pQE-32-dmrFABP5 (InvivoGen, USA) was picked from a selective antibiotic LB agar plate and incubated at 37°C overnight in a 50ml flask with 10ml LB medium and 100g/ml ampicillin. On the following day, the overnight bacterial culture (10ml) was transferred into a 1-liter flask with 250ml of warmed LB broth containing 100g/ml ampicillin, and inoculated in an obiter incubator shaking at 200 rounds /hour at 37°C until OD600 reached 0.6 (usually 90-120 minutes). Isopropylthiogalactoside (IPTG) (Sigma, USA) was added at a concentration of 1 mM to induce a high level of protein expression. Centrifugation at 5000 g for 30 minutes was used to collect the cells, and the pellet was stored at -20 °C for the recombinant protein purification.

### **2.2.2 Recombinant protein purification**

The BL21 E. coli cells harbouring the expression plasmid (InvivoGen, USA) were purchased with the expression construct. The establishment of the expression construct was performed with the procedures described previously by Waseem et al (175). The Qiagen Ni-NTA Fast Start Kit was used to purify the recombinant FABP5s produced in E. coli cells. With a 6 His-tag antibody conjugated to Ni-NTA agarose in a column,

wtrFABP5 and dmrFABP5 (both fused with a 6 His-tag) were isolated from bacterial proteins by affinity chromatography. The clean cell lysate supernatant was collected following centrifugation at 14,000 g for 30 minutes at 4°C and native lysis buffer in 10 ml was added to the cell pellet for approximately an hour. In order to confirm the existence of relevant His-tag (conjugated with recombinant FABP5) bands, 5 of supernatant were collected for SDS-PAGE examination. After that, a Ni-NTA column was used to separate the supernatant, and 5 µl of the flow-through fraction were collected for additional SDS-PAGE analysis. After that, the column was washed three times with 4ml native wash buffer. Five µl was taken for each fraction for SDS-PAGE analysis. In the column, FABP5 proteins (either dmrFABP5 or wtrFABP5) conjugated to 6His-tagged antibody were eluted twice with 1ml native elution buffer. Finally, the presence of the band detected on the blot with antiFABP5 antibody confirmed the presence of the recombinant protein (dmrFABP5 or wtrFABP5) as shown in Figure 2.1 A and B

**A**





## B



**Figure 2.1** The production and purification of recombinant protein. A) SDS-PAGE analysis of the recombinant protein in *E. coli* cells. The protein marker (M), the whole bacterial protein flow through (FL), the protein wash steps 1 and 3 (W1 and W3), and the confirmation of recombinant FABP5 (6 His-tag bound protein) at the final protein purification stage as shown in elution section (E). B) Western blot analysis of purified recombinant FABP5 detected by monoclonal anti-human FABP5 antibody (HycultR Biotech, UK). As shown, E, represented the elution of the recombinant protein.

### 2.2.3 Dialysis for recombinant protein cleaning

Purified recombinant protein was dialyzed to remove the buffer using a D-Tube dialyzer (Merck). Deionized water was used to treat the D-Tube for five minutes. Protein in the elution buffer was then added to the tube after the water had been removed. Tube was inserted into pre cold PBS when it was floating on a beaker. The dialysis was carried out with gentle stirring in 4°C for 4 hours. Then, the proteins were collected from D- Tube and aliquot in Eppendorf. 5 µL of the purified proteins were taken and stored in -20 freezer for Bradford assay to measure the protein concentration. After that, the proteins were flashed with liquid nitrogen and stored immediately in -80 freezer.

### 2.2.4 Bradford assay for protein measurement

Protein concentration in each sample loaded for Western blot analysis was determined using the Bradford assay. Since Coomassie Blue G 250 dye can turn from brown to blue

when protein binds to it, the protein concentration is quantitatively related to the dye colour change which can be measured by the changes in light absorbance. Thus, a spectrometer (Biotech, UK) was used to measure the absorbance at 595 nm. Protein concentration was calculated by comparing absorbance to a standard curve of serial dilutions of a common protein known as bovine serum albumin (BSA) (180). Each protein (Figure 2.2) tube of the serial dilutions received 1 ml of Bradford dye after it had been filtered through a Whatman paper. Then, transfer the serial dilutions and triplicate samples of the cell proteins into a microplate reader. In order to determine unknown sample concentrations, a standard linear curve of protein concentration vs. corresponding absorbance values was plotted.

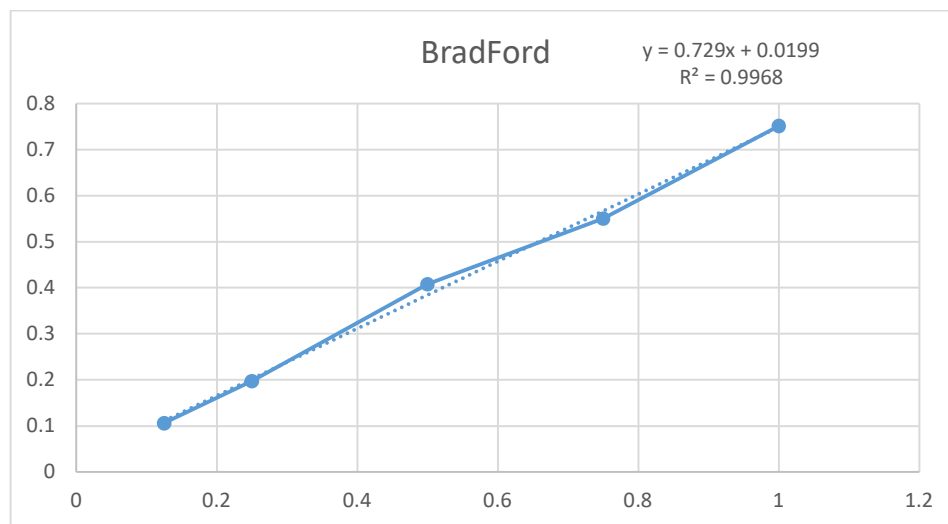


**Figure 2.2** Standard curves and different transfected cell lines.

Using linear regression analysis, Standard curves were established for protein.

plotting absorbance (OD at 570 nm) (Y-axis) against the concentration (X-axis).

### **2.2.5 Sodium dodecyl sulphate- polyacrylamide protein gel electrophoresis**

Proteins are typically separated based on their molecular weight using sodium dodecyl sulphate-polyacrylamide gel electrophoresis (SDS- PAGE). This method is based on the various rates at which proteins migrate across a gel when an electrical field is applied. SDS is used to denature the proteins. Protein samples were added to sample loading buffer (Laemmli buffer), containing  $\beta$ -mercaptoethanol to prevent the formation of disulphide bonds and hence prevent protein aggregation. The sample was heated at 95°C for 10 minutes, and then treated on ice for 2 minutes before being loaded onto a plate sandwich of ready gel supplied by Bio-Rad. The samples in the gel run at 150V for 40 to 60 minutes.

### **2.2.6 Transferring protein from SDS gel into PVDF membrane**

Following SDS-PAGE, proteins were transferred from gel to PolyVinylidene DiFluoride (PVDF) membrane (Immobilon -P, Millipore USA) using Bio- Rad Mini- Protein gel system (Bio-Rad, UK). The transfer of the polyacrylamide gel onto the PVDF membrane for immune detection, the polyacrylamide gel and PVDF membrane were placed together to form a sandwich and then wrapped by a cassette. Using the following order to create a cassette: sponge, filter paper, polyacrylamide gel, PVDF membrane, filter paper and sponge. The Bio- Rad filter papers were placed in 1x transfer buffer in cold for five minutes. Air bubbles were removed using a roller. The PVDF membrane was placed in methanol for two minutes to be activated. After that, it was rinsed in the cold transfer buffer before applied into the cassette with the sponge and filter papers. The transfer was

carried out in a 1x cold transfer buffer at 100V, for an hour and ice was used to avoid overheating or gel break.

### **2.2.7 Protein detection by immunoblotting**

The transferred proteins on membrane was incubated for an hour at room temperature with gentle shaking in 20 ml of 5% blocking solution (5 g skimmed milk in 100 ml TBST). The membrane then incubated with targeted primary anti-body in a milk-TBS-T mixture overnight at 4°C with gentle shaking (Table 2.1). To eliminate the unbound primary antibody, wash the membrane 10 minutes for 3 times 1x T-TBS. A secondary antibody conjugated with HRP in a milk- TBS-T mixture was applied to the washed membrane in the proper concentration (Table 2.1) and incubated at room temperature for one to two hours. Following the secondary anti-body incubation, the membrane was washed 10 minutes for 3 times with 1x T-TBS. An Immobilon ECL Ultra Western HRP Substrate (1ml of Reagent A combined with 1ml of solution B) was applied to the membrane to detect and to visualise the bound antibodies for five minutes at room temperature. Protein band intensities were measured by densitometry scanning using an image analysis device (ChemiDoc MP Imaging System, Bio-Rad, UK).

To correct any sample loading discrepancies, the PVDF membrane was incubated with anti- $\beta$ -actin. After being blocked by TBS-T milk for 1 hour, the membrane was incubated with the anti- $\beta$ -actin primary antibody in 20 ml milk for 45 minutes. The membrane then washed 10 minutes for 3 times with 1x TBS-T each, then incubated with the secondary antibody for another 45 minutes (Table 2.1). The membrane was washed three times with 1x TBS-T then visualised by ECL system as described above.

**Table 2.1 Antibodies used in detection of recombinant FABP5**

<b>Protein</b>	<b>Primary Antibody</b>	<b>Secondary Antibody</b>
FABP5	Rabbit Anti-human Monoclonal (1:500) (HycultR Biotech)	Swine Anti- Rabbit Polyclonal HRP (1:10,000) (DAKO)
6- His- tagged	Penta- his Mouse monoclonal (1:1000) Qiagen	Rabbit Anti-Mouse polyclonal HRP (1:10,000) (DAKO)
$\beta$ -actin	Mouse Monoclonal Anti- $\beta$ -Actin (1: 20,000) (Abcam)	Rabbit Anti-Mouse (#Polyclonal HRP (1: 20,000) (DAKO)

### **2.2.8 Western blot for molecular mechanism**

Western blot technique and ECL reagent were used to detect different proteins in prostate cancer cells after the treatments of dmrFABP5, docetaxel and enzalutamide whether singly or in combination between dmrFABP5 and docetaxel or enzalutamide at the IC<sub>50</sub> values. WtrFABP5, Sp1 inhibitor (Plicamycin) (MedChemExpress, UK) were used to study some molecular mechanism related to the experiments. Also, 22RV1- FABP5 KO and DU145- FABP5 KO cells were obtained from Abdulghani Naeem (Ph.D. candidate at the same group) for further molecular mechanism investigations.

Western blot was run as explained previously, primary antibody against AR (Santa Cruz Biotechnology) was diluted at 1: 400 and incubated overnight at 4 °C in a cold room with the blot with gentle shaking. Next day, the blot was incubated with the secondary Rabbit Anti- mouse antibody that was diluted at 1: 10,000 for 2 hours and Imaging analysis

system machine (ChemiDoc MP Imaging System Bio-Rad, UK) was used to scan the proteins bands. Primary antibodies against Bcl-2, BAX and PPAR $\gamma$  (Santa Cruz Biotechnology), Sp1, AR-V7 and BMF (Cell Signalling, UK), p-PPAR $\gamma$  (Ser 112) (Thermo Fisher Scientific, UK), VEGF, CAV1, GRPR, EGR1, CRIP2 (Abcam, UK), were diluted at different ranges from 1: 200 -1000 and incubated overnight. The primary antibody anti  $\beta$ -actin was used to correct possible loading discrepancies. The primary and second antibodies used against different proteins and their dilutions were shown in Table 2.2.

**Table 2. Antibodies and dilutions**

<b>Protein</b>	<b>Primary Antibody</b>	<b>Secondary Antibody</b>
AR	Mouse monoclonal (1: 400) (Santa Cruz)	Rabbit Anti-Mouse polyclonal HRP (1:10,000) (DAKO)
AR-V7	Rabbit polyclonal (1: 1000) (Cell Signalling)	Swine Anti- Rabbit Polyclonal HRP (1:10,000) (DAKO)
Sp1	Rabbit polyclonal (1: 1000) (Cell Signalling)	Swine Anti- Rabbit Polyclonal HRP (1:10,000) (DAKO)
Bcl-2	Mouse monoclonal (1: 250) (Santa Cruz)	Rabbit Anti-Mouse polyclonal HRP (1:10,000) (DAKO)

BAX	Mouse monoclonal (1: 500) (Santa Cruz)	Rabbit Anti-Mouse polyclonal HRP (1:10,000) (DAKO)
PPAR $\gamma$	Mouse monoclonal (1: 500) (Santa Cruz)	Rabbit Anti-Mouse polyclonal HRP (1:10,000) (DAKO)
p-PPAR $\gamma$ (Ser 112)	Rabbit polyclonal phospho- PPAR $\gamma$ (Ser112) (1: 250) (Thermo Fisher)	Swine Anti- Rabbit Polyclonal HRP (1:10,000) (DAKO)
VEGFA	Rabbit polyclonal (1: 1000) (Abcam)	Swine Anti- Rabbit Polyclonal HRP (1:10,000) (DAKO)
CAV1	Rabbit polyclonal (1:1000) (Abcam)	Swine Anti-Rabbit Polyclonal HRP (1:20,000) (DAKO)
GRPR	Rabbit polyclonal (1:1000) (Abcam)	Swine Anti-Rabbit Polyclonal HRP (1:20,000) (DAKO)
EGR1	Rabbit monoclonal (1:1000) (Abcam)	Swine Anti-Rabbit Polyclonal HRP (1:10,000) (DAKO)
CRIP2	Rabbit polyclonal (1:1000) (Abcam)	Swine Anti-Rabbit Polyclonal HRP (1:20,000) (DAKO)
BMF	Rabbit monoclonal (1:1000) (Cell Signalling)	Swine Anti-Rabbit Polyclonal HRP (1:20,000) (DAKO)
$\beta$ -actin	Mouse Monoclonal Anti- $\beta$ -Actin (1: 20,000) (Abcam)	Rabbit Anti-Mouse (Polyclonal) HRP (1: 20,000) (Abcam)

## **2.3 Drug preparations and IC<sub>50</sub> determinations**

### **2.3.1 Docetaxel preparation and storing**

Ten mg of docetaxel was purchased from (MedChemExpress, UK) in a powder form. DMSO was used as solvent. Stock solution was prepared by dissolving 10 mg of docetaxel in 1.2 mL of DMSO to obtain 10 mM of docetaxel according to the manufacturer's instructions. To avoid the repeated freezing cycle, the stock solution was aliquoted into an 1 ml Eppendorf which was wrapped with foil to protect the docetaxel from light and stored in -80°C freezer. At each experiment, one Eppendorf from -80°C freezer was thawed and was serially diluted in RPMI 1640 medium contained FBS and penicillin/streptomycin, to prepare a working solution with different concentrations. The DMSO concentration was considered to be 0.1% or less to minimise the side effect of DMSO.

### **2.3.2 Enzalutamide preparation and storing**

Enzalutamide was purchased from (MedChemExpress, UK) as 10 mg lot. It was dissolved in 2.1 mL of DMSO to get 10 mM stock solution. Working solution preparation and storing process same as that for docetaxel.

### **2.3.3 Half maximum inhibitory concentration (IC<sub>50</sub>) of dmrFABP5, docetaxel and enzalutamide**

Docetaxel, enzalutamide and dmrFABP5 were prepared in the way described above and were used at different concentrations to determine the IC<sub>50</sub> the viability of the cells. Docetaxel concentration was ranged from (0.001 nM to 200 nM); enzalutamide (0.001 μM to 100 μM); dmrFABP5 (0.05 μM to 20 μM). DU145, 22RV1 and LNCaP were plated in 96- well plate and cell numbers from each cell lines were accounted. The cell



lines were treated by each compound for 72h. IC<sub>50</sub> was calculated by Graphpad Prism software. All control groups were treated with 0.1% of DMSO.

### **2.3.4 The combination treatment of dmrFABP5 with docetaxel or enzalutamide**

To test the possible synergistic effect produced by dmrFABP5 to docetaxel or enzalutamide, all compounds were prepared as working solutions. DmrFABP5 was combined with docetaxel or enzalutamide with different non-constant concentration ratios as a fixed concentration of dmrFABP5 at the IC<sub>50</sub> value combined with different concentrations of docetaxel or enzalutamide. Fixed concentrations of docetaxel or enzalutamide at their IC<sub>50</sub> values of cell viability combined with different concentrations of dmrFABP5. Different concentrations of dmrFABP5, docetaxel and enzalutamide alone were prepared more or less than the IC<sub>50</sub> values. The combination index (CI) is a quantitative measure used to assess the interaction between two or more drugs in combination therapy. It provides insights into the synergistic, additive, or antagonistic effects of the drug combination. The CI value is calculated based on the dose-response relationship, combining different concentrations of the drugs, and comparing the observed effect with the expected effect based on individual drug responses. A CI value less than 1 indicates synergism, suggesting that the combined effect is greater than the sum of individual effects. A value of 1 indicates additivity, while values greater than 1 suggest antagonism, where the combined effect is less than expected. The synergistic interaction was assessed according to Chou- Talalay with CompuSyn software to calculate combination index (CI). Values of <1 were considered to be synergistic and >1 were antagonism (181).

## **2.4 *In vitro* assays for testing malignant characteristics cells**

### **2.4.1 Assay to test cell viability**

The viability test was performed to examine the effect of dmrFABP5 singly or in combination with docetaxel or enzalutamide on PCa cell viability. A cell viability reagent kit PrestoBlue® (Thermofisher, UK) was used to perform this assay. Presto Blue worked by measuring the cell metabolic activity to provide accurate data on cell viability in a short period of time. It contains Resazurin which is a blue, non-fluorescent molecule that chemically converted to red resorufin once this substance penetrates live cells. The changing colour indicated the live cells viability. This can be measured with fluorescence or absorbance plate readers to quantify cell viability.

DU145 was plated in 96 well plate, 5000 cells/ well; 10,000 cells/ well for 22RV1 and LNCaP. Cells were treated with dmrFABP5 alone or in combination with docetaxel or enzalutamide. The combination treatments were prepared according to each agent IC<sub>50</sub> values to examine whether the IC<sub>50</sub> combinations produced stronger effect compared to each single agent IC<sub>50</sub> alone. The control groups were treated with 0.1% DMSO. Medium only wells, were considered as the background level. After 72h, the absorbance was taken at 570 nm and 600 nm for background using spectrophotometer (Labtech, UK). The cell viability tests were performed in triplicate.

### **2.4.2 Cell motility assay**

This test is performed to determine the effect of the combination compared each single agent alone on the migration ability of the cells. Culture- insert 2 well  $\mu$ - Dish (ibidi, Germany) was used to assess the migration ability of the cells. The insert consists of two wells and there is a wall separated the wells. Cell suspensions were seeded in each well

at  $8 \times 10^5$  cells. After cells attached (24h), the insert was removed, leaving a space of 500  $\mu\text{M}$  in between.

Cell culture suspensions were prepared as described previously in the cell culture section. Seventy  $\mu\text{l}$  suspension was carefully added to each well. After that, the cells were incubated in a cell culture incubator under humidified conditions at  $37^\circ\text{C}$  and 5 %  $\text{CO}_2$ . After allowing the cells to form a complete monolayer and reach full confluence, the insert was carefully removed with sterile tweezers. DmrFABP5, docetaxel and enzalutamide were prepared at their  $\text{IC}_{50}$  concentrations singly or in combination with each of the other reagents which were also prepared at the  $\text{IC}_{50}$  concentrations. DMSO was used to treat the control group at the concentration of 0.1%. The plate was examined under a microscope (EVOS, Thermo Scientific, UK), and pictures were taken at different time points according to each cell aggressiveness to evaluate the gap closure. The photos were captured using a microscope, and Image J software was used to quantitatively analyse wound gaps. The motility assay was performed in triplicate. The duration of the assay was dependent on the cells. The closure of DU145 cells were achieved after 24h of the starting point of the experiment whereas 22RV1 and LNCaP cells were achieved after 72h.

### **2.4.3 Cell invasion assay**

The cell invasion assay was performed to test the ability of the cells to invade the extracellular matrix. The assay was conducted with an invasion assay reagent kit (Invasion Chamber with Corning Matrigel Matrix, Fisher Scientific, UK). The cell invasion kit inserts are pre-coated by extracellular matrix. DU145, 22RV1 and LNCaP cells were plated in the upper chamber. Matrigel pores (8  $\mu\text{M}$ ) enabled invasive cells to invade through the pores. Whereas the non-invaded cells were not able to invade through the pores. To start the experiment, warm medium was placed on the chambers and

incubated at 37°C for two hours. The medium was then removed carefully. RPMI1640 medium containing FBS and penicillin/streptomycin was added into the lower chamber. FBS acts as a chemoattractant for the cancer cells. Cells from DU145, 22RV1 and LNCaP were seeded and the  $2.5 \times 10^4$ / 500  $\mu$ L cells were used for each treatment group in serum-free medium prepared for the control group and all treatment groups. The cells were placed on the upper chamber. The control groups were treated with DMSO at the concentration of 0.1%. DmrFABP5, docetaxel and enzalutamide were prepared at the IC<sub>50</sub> concentrations singly. The combination groups were prepared by combining the IC<sub>50</sub> concentration of dmrFABP5 with that of docetaxel or that of enzalutamide, respectively. The next day, cells that did not pass through the membrane were gently scrubbed out of the top chamber using a cotton swab, and the invaded cells that had passed through the membrane were stained with crystal violet and counted under a microscope (EVOS, Thermo Scientific, UK). The invaded cells were counted from 9 magnified areas selected randomly. All cells were treated for 24h.

#### **2.4.4 Anchorage independent cell growth (soft agar assay)**

The soft agar assay experiment was performed to test the synergic effect of the dmrFABP5 to docetaxel or enzalutamide on the colony formation ability (as a sign of tumorigenicity). The experiment was conducted in 6-well plates that had been pre-coated with 2 ml of 1% (w/v) low melting agarose in regular culture media. The mixture was then refrigerated for 25 minutes to solidify before use. As described previously, cells from DU145, 22RV1 and LNCaP were grown in a culture flask to 60–80% confluence, and suspended in RPMI complete cell culture medium. Low melting agarose (0.5%) was prepared in regular culture medium and was used to seed and mixed with the treatment mixtures. The cells at  $5 \times 10^4$  for DU145, 22RV1 and LNCaP were mixed with a different treatment contents and mix it with the semi solid 0.5% agarose in complete medium.

The control groups treated with 0.1% of DMSO, each single agent alone at the IC<sub>50</sub> concentration and the combination groups. The plates were then placed in the refrigerator for 20 minutes until hardened. The plates were then incubated for 3 weeks at 37°C and 5% CO<sub>2</sub>. To prevent drying out and to make sure the cells had enough nutrients, 250 µl of the medium containing 0.1% of DMSO for the control groups or medium containing all treatment required were used. At the end of the experiment, the plates were stained and treated with MTT at a concentration of 0.5 mg/ml and incubated for 4 hours at 37°C with 5 percent CO<sub>2</sub>. DU145 and 22RV1 colonies larger than 250µm and colonies larger than 150 µm in LNCaP were counted using a GelCount (Oxford Optronix, UK). DU145, 22RV1 and LNCaP cells were incubated for 21 days.

## **2.5RNA- profile analysis**

### **2.5.1Cell preparation**

To study the molecular mechanisms on how dmrFABP5 works inside the cancer cells, RNA expression profiles were analysed and compared between the dmrFABP5 treated DU145 cells and the untreated control cells. The control cells and the dmrFABP5 treated cells at the IC<sub>50</sub> concentration were cultured in an incubator for 24h. Next day, the cells were collected in different Eppendorf vials, flashed in liquid nitrogen and stored immediately in dry ice. The cells were packaged and sent to Genewiz, Germany company for the RNA sequence analysis. When it is needed, quantification of the expression profiling and transcript quantification were performed with Poly(A)-seq-based technique.

### **2.5.2RNA extraction**

Total RNA was isolated from frozen cell pellets using the Qiagen RNeasy Mini kit (Qiagen, Hilden, Germany), following the manufacturer's instruction.

### **2.5.3 RNA library preparation**

Total RNA was isolated from frozen cell pellets using the Qiagen RNeasy Mini kit (Qiagen, Hilden, Germany), following the manufacturer's instruction.

Qubit 2.0 Fluorometer (ThermoFisher Scientific, Waltham, MA, USA) was used to measure the quantity of RNA in cell samples, and a 4200 TapeStation (Agilent Technologies, Palo Alto, CA, USA) was used to check the RNA integrity. The Qiagen FastSelect rRNA HMR kit (Qiagen, Hilden, Germany) was used to prepare the rRNA depletion sequencing library. The NEBNext Ultra II RNA library preparation kit (NEB, Ipswich, MA, USA) for Illumina was used for the RNA sequencing library preparation, following the manufacturer's instructions. In brief, enriched RNAs are fragmented at 94 °C for 15 minutes and then the first and the second strands of the cDNA were synthesized. At the 3'-end, end repairs and adenylation were carried out on cDNA fragments, followed by universal adapters ligated to fragments. Then, index addition and library enrichment were performed with limited PCR cycle figure 2.1. Agilent TapeStation 4200 (Agilent Technologies, Palo Alto, CA, USA) was used to validate sequencing of libraries, and Qubit 2.0 Fluorometer (ThermoFisher Scientific, Waltham, MA, USA) and quantitative PCR (KAPA Biosystem, Wilmington, MA, USA) were used for quantification. Following the Illumina NovaSeq 6000 instrument manufactures instructions, the flowcell was used for the sequencing libraries multiplexed and loaded, and 2x150 Pair-End (PE) configuration v1.5 was used to sequence all samples. Base calling and image analysis were performed using NovaSeq Control Software v1.7). The raw sequence data files generated by Illumina NovaSeq as bcl file then converted into fastq files and after that de-multiplexed by the 2.20 version of bcl2fasq program. Index sequence identification was only allowed one mismatch.

## 2.5.4 RNA sequence data analysis

After confirming the raw data quality, Trimmomatic v.36 was used to trim the sequence reads to eliminate possible adapter sequences as well as nucleotides with poor quality, then the trimmed reads were mapped to the Homo sapiens reference genome which is available on ENSEMBL by STAR aligner v.2.5.2b. The STAR aligner considers as a splice aligner which can detect splices junctions that can facilitate align whole reads sequences. As a result, BAM files produced. Feature Counts that in Subread package v.1.5.2 used to count the gene hits and the unique reads that take place within the exon were only counted. The downstream differential gene expression was analyzed using the gene hit counts table. DESeq2 was used to compare the different gene expression between all sample groups. *P*- Value and Log<sub>2</sub> fold changes were performed by the Wald test. For each comparison, *P*-value <0.05 and log<sub>2</sub> fold changes >1 were regarded as differentially expressed genes. GeneSCF software was used to analyze the statistically significance of gene ontology. Genes cluster based on their biological process and statistical significance were used for the go human GO list. PlotPCA function within DESeq2R package was used to perform PCA analysis. In a 2D plane that is spanned by their first two principal components, the plot displayed the samples. The plot was produced using the top 500 genes, ordered by highest row variance. STAR Fusion v.1.1.0 was used to analyze gene fusions and to find potential fusion transcripts. The procedures of RNA sequencing via rRNA depletion was illustrated in Figure 2.2 and Figure 2.3.

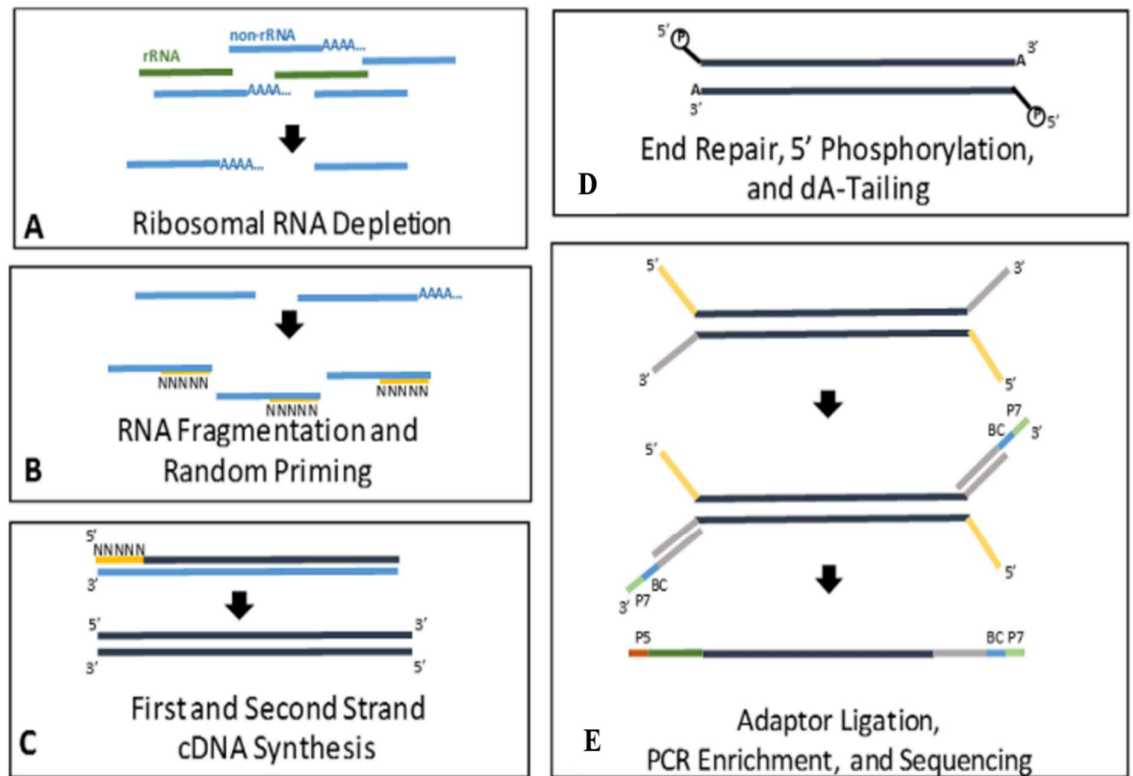


**Figure 2.2.** Illustration of the RNA sequencing via rRNA depletion (182)



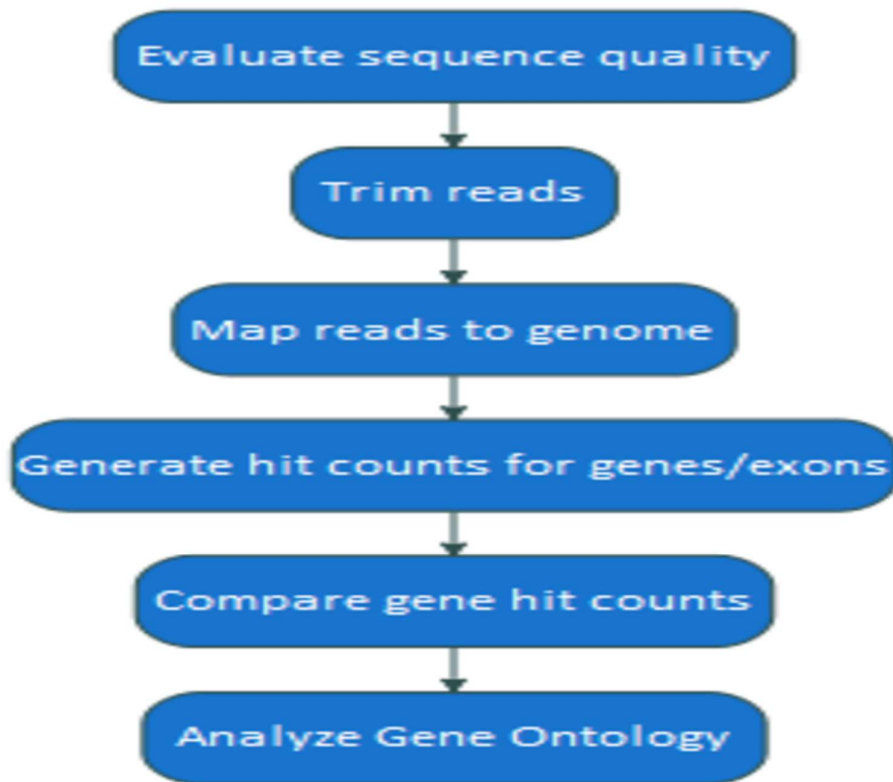


**Figure 2.3.** The steps of sequencing analysis, gene expression and gene ontology.

## **2.6 Data analysis**

In this research project, several software tools were utilized to analyze the collected data. These included CompuSyn, Microsoft Excel, Image J, and GraphPad Prism 9, which played crucial roles in processing and interpreting the experimental findings.

To assess and compare the results obtained from various experiments, such as cell viability, motility, invasion, soft agar, and western blot assays, a Student t-test and one way ANOVA were employed. This statistical analysis method enabled the researchers to evaluate the significance of observed differences between experimental groups.

For the comparison of RNA profiles, visually informative representations such as volcano plots and heatmap plots were employed. These visualization techniques allowed for a comprehensive examination of gene expression patterns and facilitated the identification of differentially expressed genes.

It is important to note that all experiments were conducted in triplicates, ensuring the reliability and reproducibility of the findings. This approach involved performing each experiment three times ( $n=3$ ), which helped to minimize the impact of random variations and improve the statistical robustness of the results.

Overall, the utilization of appropriate software tools, statistical analyses, and visualization techniques, combined with rigorous experimental design, strengthened the validity and accuracy of the research outcomes.

## **Chapter 3**

**Result-1: Treatment with dmrFABP5 in combination with docetaxel or enzalutamide produced synergistic suppressive effect in prostate cancer cells**

### 3.1 Introduction

Previous study in our lab established that FABP5 had a tumour-promoting effect on prostate cancer cells. This effect was dependent on FABP5's ability to bind to and to transfer fatty acids into cells from intracellular and extracellular sources in order to activate their nuclear receptor PPAR $\gamma$  (130,156). Through a binding motif made up of the amino acids Arg109, Arg129, and Tyr131, FABP5 binds to medium- and long-chain fatty acids with a high affinity. Previous research in our group showed that mutating 2 of the 3 key amino acids (Arg109 to Ala109 and Arg129 to Ala129) almost completely deprived of the FABP5's capability of binding to fatty acids. In fact, this 2 amino-acid-mutated recombinant protein dmrFABP5 is able to inhibit the biological activity of wtFABP5 (130,152,174,175). The bio-inhibitor dmrFABP5 which work as anti- FABP5, had a potent effect *in vitro* and *in vivo*. It has been shown that dmrFABP5 work by suppressing the signaling transduction pathway of FABP5- PPAR $\gamma$ - VEGF in the highly malignant prostate cancer cell PC3-M (160,175).

Docetaxel is a chemotherapeutic agent, extracted from a species of plant called *Taxus brevifolia* (183). The Food and Drug Administration of USA approved docetaxel as a drug for cancer treatment in 1996 (184). As an anti-cancer agent, it works by causing intracellular damage. Through preventing either the depolymerization or polymerization of tubulin dimers of already created dimmers, they disrupt the balance between the depolymerization or the polymerization of tubulin dimmers (185,186). Docetaxel is a clinically available drug, however prostate cancer usually develops resistance to it (99). The anti-androgen agent enzalutamide on the other hand, is a second-generation anti-androgen use to treat PCa (96,97). It can bind to AR in LNCaP prostate cancer cells with around five fold more affinity compared to another anti- androgen treatment bicalutamide (187). Enzalutamide blocks the binding of androgens to the AR , nuclear translocation of

the AR, and interaction of the AR with DNA (188). Although they are frequently used in clinical treatment, resistance is inevitable (116,189).

### **3.2 Aim of the study**

The aim of this chapter is to explore the potential of dmrFABP5 to enhance the effectiveness of two commonly used drugs, docetaxel and enzalutamide, in prostate cancer treatment. To achieve this, we will employ the COMPUSYN software, utilizing the Combination Index (CI) approach, to evaluate and confirm the synergistic effect generated by the combination of dmrFABP5 with the aforementioned drugs.

The investigation will involve conducting experiments on prostate cancer cell lines to assess the combined effects of dmrFABP5, docetaxel, and enzalutamide. By employing the CI method, we will determine the interaction between dmrFABP5 and each drug individually, as well as the interaction between dmrFABP5 and the drug combinations.

The COMPUSYN software will analyse the experimental data and generate CI values for each drug combination. The CI values provide a quantitative measure of the synergistic, additive, or antagonistic effect of the drug combinations. A CI value less than 1 indicates synergy, suggesting that the combined treatment produces a more potent effect than the sum of the individual treatments.

By evaluating the CI values, we will determine whether the addition of dmrFABP5 enhances the efficacy of docetaxel or enzalutamide in prostate cancer cell lines. The results will shed light on the potential synergistic interactions between dmrFABP5 and these drugs, providing valuable insights into the development of combination therapies for prostate cancer treatment.

This chapter will contribute to our understanding of how dmrFABP5 can augment the therapeutic outcomes of docetaxel or enzalutamide in prostate cancer, potentially leading to the identification of novel treatment strategies that improve patient outcomes.

### **3.3 IC<sub>50</sub> of dmrFABP5, docetaxel or enzalutamide in cell viability assays with prostate cancer cells**

The half maximal inhibitory concentration (IC<sub>50</sub>) is a parameter used to assess how effective a substance is at blocking a particular biological or metabolic process (190). To measure the cell viabilities, the androgen independent prostate cancer cell line DU145, androgen responsive cell line 22RV1 and androgen dependent cell line LNCaP were cultured to a confluence of 90% and sub-cultured in triplicate in 96 well plate. DU145 was plated and cultured at 5000 cells/ well; 22RV1 and LNCaP were plated 10,000 cells/ well and incubated for 24h in a cell culture incubator. Next day, the stock solution of dmrFABP5, docetaxel and enzalutamide were taken from -80 freezer and serially diluted at different concentrations in the freshly prepared culture medium. DMSO was prepared at a concentration of 0.1% and used for treatment in the control group and for dissolving solutions of reagents docetaxel and enzalutamide. Since dmrFABP5 was dissolved in PBS, PBS was used to treat its control group. DmrFABP5 concentrations were ranged from 0.05  $\mu$ M to 20  $\mu$ M for DU145, 22RV1 and ranged from 0.05  $\mu$ M to 40  $\mu$ M for LNCaP; docetaxel concentrations ranged from 0.001 nM to 200 nM; enzalutamide concentrations used for the treatment of DU145 and 22RV1 were ranged from 1  $\mu$ M to 100  $\mu$ M, but for LNCaP the concentrations were ranged from 0.001  $\mu$ M to 100  $\mu$ M. After all substances were ready to use, the old medium was aspirated from 96 well plates. The cells then were treated with each single agent alone with the different concentrations

prepared and incubated for 72h. The cell viabilities were evaluated by Presto Blue HS (Invitrogen). Presto Blue reagent was added to each well and incubated in cell culture for 1h, the absorbance reading was measured with a spectrophotometer as described in 2.4.1.

### 3.3.1 The suppressive effect of dmrFABP5 on the cell viability of prostate cancer cells

The FABP5 inhibitor dmrFABP5 had a potent suppression effect in DU145 and 22RV1 cells and did not produce any inhibition effect in FABP5 negative cell LNCaP. The  $IC_{50}$  assessed by GraphPad Prism 9 software. The results were analysed as log concentrations  $\mu\text{M}$  against the cell viability of control %. The potent inhibitory effect of the bio inhibitor dmrFABP5 in FABP5 positive cells, DU145 and 22RV1 produced an  $IC_{50}$  values of 5, 12  $\mu\text{M}$  respectively as shown in Figure 3.1.

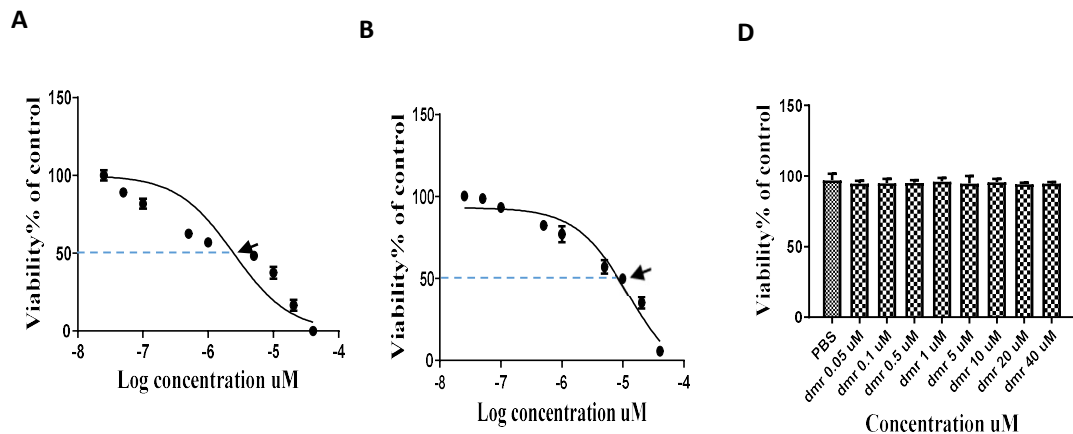


**Figure 3.1.** Determination of the  $IC_{50}$  values of dmrFABP5 in prostate cancer cells. (A) DU145 was treated with different concentrations of dmrFABP5 and the  $IC_{50}$  was 5  $\mu\text{M}$ , as pointed by the arrow head and blue scattered line. (B) 22RV1 was treated with dmrFABP5 at the same concentration range and the  $IC_{50}$  value was 12  $\mu\text{M}$ , as pointed by the arrow head. (C) The viabilities of LNCaP cells treated with different concentrations of DmrFABP5. No significant effect was observed with any concentrations used. Each

figure (Y axis ) control %, represented the cell viabilities of the treated control with DMOS against the log concentrations. Each experiments were performed in triplicate n=3.

### 3.3.2 The effect of docetaxel on prostate cancer cells growth

The chemotherapeutic agent docetaxel significantly suppressed the growth of DU145, 22RV1 and LNCaP. The results showed that the IC<sub>50</sub> values were 3, 4, 2.2 nM respectively in these cell lines. The IC<sub>50</sub> values were calculated by GraphPad Prism 9 software and analysed as log concentrations nM against the viability of control %. Figure 3.2

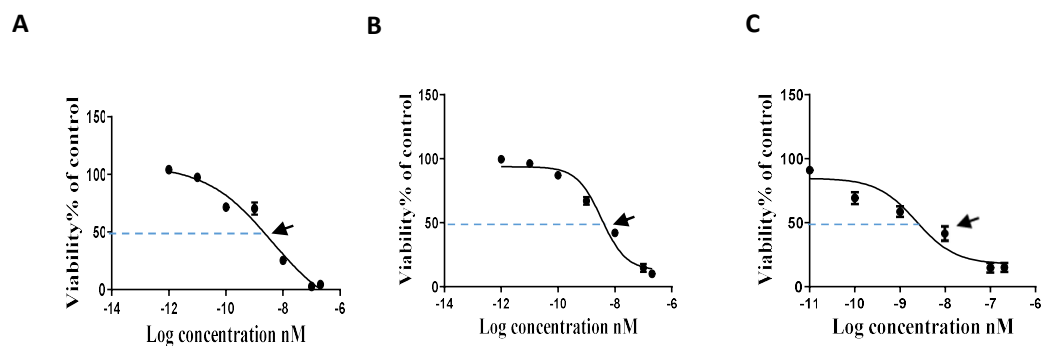


**Figure 3.2.** The cell viabilities and IC<sub>50</sub> of docetaxel treatment on the prostate cancer cells. (A) docetaxel inhibited DU145 growth with IC<sub>50</sub> value of 4 nM. (B) docetaxel inhibited 22RV1 growth with an IC<sub>50</sub> value of 3 nM. (C) docetaxel inhibited the growth of LNCaP with an IC<sub>50</sub> value of 2.2 nM. The arrow heads pointed to the IC<sub>50</sub> value. Each figure (Y axis ) control %, represented the cell viabilities of the treated control with DMOS against the log concentrations. Each experiments were performed in triplicate n=3.



### 3.3.3 The effect of enzalutamide on DU145, 22RV1 and LNCaP growth

As shown in Figure 3.3, the inhibitory effect of the anti- androgen agent enzalutamide was shown on the androgen sensitive prostate cancer cell line LNCaP with the  $IC_{50}$  value of 97 nM. Enzalutamide did not inhibit the growth of the androgen-independent prostate cancer cell DU145 and the androgen-responsive cell 22RV1. The  $IC_{50}$  result and inhibition were calculated by GraphPad Prism 9 software.

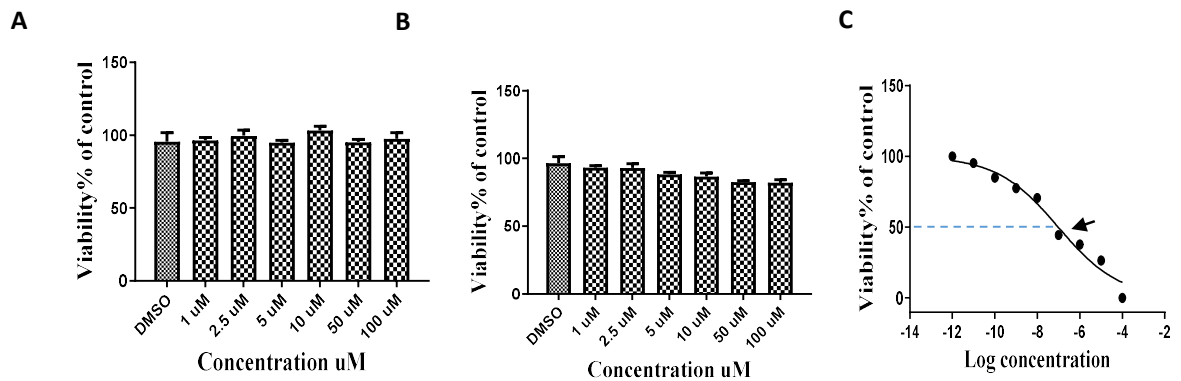


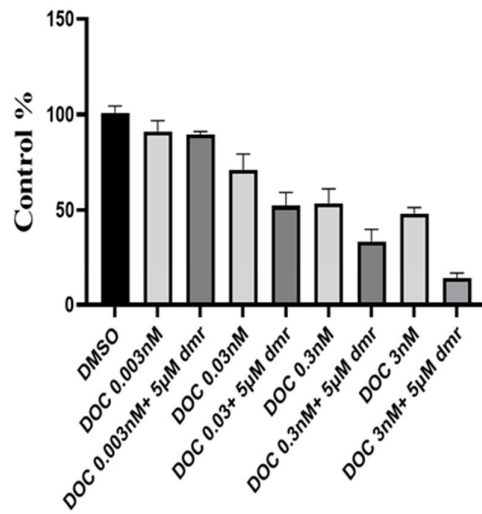
**Figure 3.3.** The effect of enzalutamide on prostate cancer cells. (A) The effect of enzalutamide on DU145 cells (B) The activity of enzalutamide on 22RV1 cells. (C) The effect of enzalutamide on LNCaP, with  $IC_{50}$  value of 97 nM, as pointed by the arrow head. Each figure (Y axis) control %, represented the cell viabilities of the treated control with DMSO against the log concentrations. Each experiment were performed in triplicate  $n=3$ .

### **3.4 The assessment of the synergistic effect produced by dmrFABP5 on docetaxel**

#### **3.4.1 DmrFABP5 enhanced the suppressive effect of docetaxel on DU145**

The cells were treated with 1 of the 2 reagents either alone, in a fixed  $IC_{50}$  concentration, or in combination with different concentrations of another reagent for 72h incubated in cell culture incubator, as shown in Table 3.1A and 1B. After 72h, the cells were treated with Presto Blue HS and the suppressive effect was assessed by calculating the Combination Index (CI) with the COMPUSYN software (191). As shown in figure 3.4, dmrFABP5 at 5  $\mu$ M combined with docetaxel at different concentrations of 3, 0.3, 0.03, 0.003 nM respectively, produced synergistic effect (Figure 3. 4A). When fixed concentration of dmrFABP5 at 5  $\mu$ M combined with 3, 0.3, 0.03 nM of docetaxel, the percentage of viable cells were 14%, 33%, 52% respectively, while 49%, 54%, 71% respectively for docetaxel alone. When docetaxel was used to treat the cells, a fixed docetaxel concentration at its  $IC_{50}$  (3 nM), combined with different concentrations of dmrFABP5 at 5, 1, 0.5  $\mu$ M respectively, produced a similar synergistic effect as that produced by dmrFABP5 (Figure 3 4B). As data analysis showed that the percentage of cell viabilities for fixed concentration of docetaxel at 3 nM combined with 5, 1, 0.1  $\mu$ M of dmrFABP5 were 19 %, 40%, 52% respectively while 48%, 62%, 70% respectively for dmrFABP5 alone. The maximum suppression significant effect was found when 5 $\mu$ M combined with docetaxel at 3 nM, with  $CI= 0.004$ . No synergistic effect was found in the combination of dmrFABP5 at 5  $\mu$ M and 0.003 nM of docetaxel, as shown in Table 3.1A. Same negative effect was found when combined dmrFABP5 at 0.1  $\mu$ M and 3 nM of docetaxel with no synergistic effect.

A



B

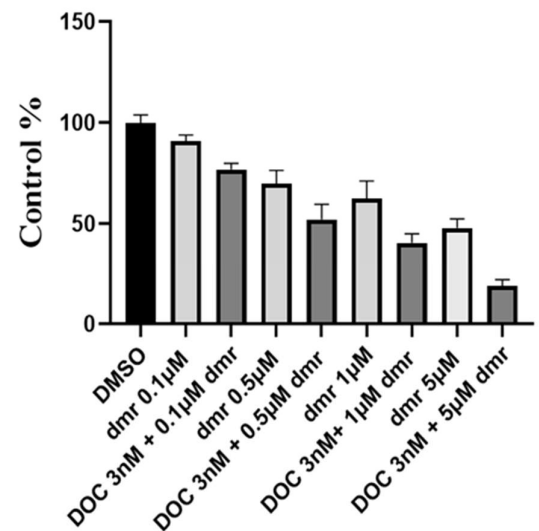


**Figure 3.4** Synergistic effects of dmrFABP5 and docetaxel in in suppression of DU145 cells. A). Fixed concentration of dmrFABP5 at 5µM combined with different concentrations of docetaxel. B). Fixed concentration of docetaxel at 3nM combined with different concentrations of dmrFABP5. Each experiment were performed in triplicate n=3.

**Table 3.1 Results of the synergistic tests on effect of suppressing DU145 cells by dmrFABP5 or by docetaxel\*.**

**(A)** Fixed concentration of dmrFABP5 combined with different concentrations of docetaxel

Cell line	Dmr, $\mu$ M	Docetaxel, nM	CI value	Relationship
DU145	5	3	0.007	Synergic
DU145	5	0.3	0.389	Synergic
DU145	5	0.03	0.658	Synergic
DU145	5	0.003	12.17	Antagonism

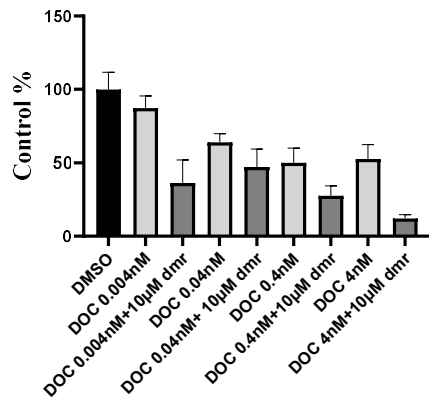
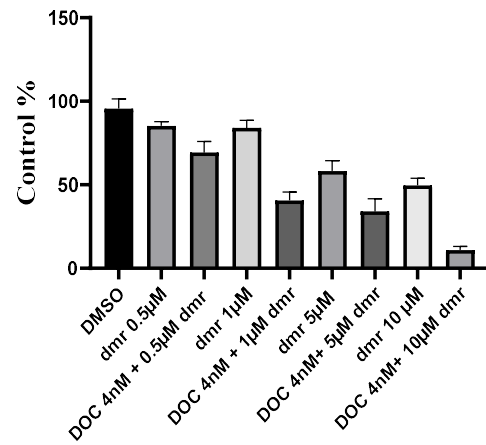
**(B)** Fixed concentration of docetaxel combined with different concentrations of dmrFABP5

Cell line	Dmr, $\mu$ M	Docetaxel, nM	CI value	Relationship
DU145	0.1	3	2.483	Antagonism
DU145	0.5	3	0.228	Synergistic
DU145	1	3	0.163	Synergistic
DU145	5	3	0.004	Synergistic

\*The synergistic interaction was assessed according to Chou- Talalay with CompuSyn software to calculate combination index (CI). Values of  $<1$  were considered to be synergistic and  $>1$  were antagonism (181).

### **3.4.2DmrFABP5 enhanced the suppressive effect of docetaxel on 22RV1**

The cells were treated with 1 of the 2 reagents either alone, in a fixed  $IC_{50}$  concentration, or in combination with different concentrations of another reagent for 72h incubated in cell culture incubator, as shown in Table 3.2A and B. After 72h, the cells were treated with Presto Blue HS and the suppressive effect was assess by calculating the Combination Index (CI) with the COMPUSYN software (191). As shown in figure 3.5, dmrFABP5 at 10  $\mu$ M combined with docetaxel at different concentrations of 4, 0.4, 0.04, 0.004 nM respectively, produced synergistic effect (Figure 3. 5A). When fixed concentration of dmrFABP5 at 10  $\mu$ M combined with 4, 0.4, 0.04, 0.004 nM of docetaxel, the percentage of viable cells were 12%, 28%, 47%, 48% respectively, while 53%, 49%, 64%, 88% respectively for docetaxel alone. When docetaxel was used to treat the cells, a fixed docetaxel concentration at its  $IC_{50}$  (4 nM), combined with different concentrations of dmrFABP5 at 10, 5, 1, 0.5  $\mu$ M respectively, produced a similar synergistic effect (Figure 3.5B). As data analysis showed that the percentage of cell viabilities for fixed concentration of docetaxel at 4 nM combined with 10, 5, 1,  $\mu$ M of dmrFABP5 were 11 %, 34%, 41% respectively while 50%, 58%, 84% respectively for dmrFABP5 alone. The significant maximum suppression effect was found when 10  $\mu$ M combined with docetaxel at 4 nM, with  $CI= 0.068$ . No synergistic effect was found in the combination of dmrFABP5 at 0.5  $\mu$ M and 4 nM of docetaxel, as shown in Table 3.2B.

**A****B**

**Figure 3.5** Reciprocal synergistic suppression effects of dmrFABP5 and docetaxel in 22RV1 cell. A). Fixed concentration of dmrFABP5 at 10µM combined with different concentrations of docetaxel. B). Fixed concentration of docetaxel at 4nM combined with different concentrations of dmrFABP5. Each experiment was performed in triplicate n=3. The synergistic effect was determined by CI values.

**Table 3.2 Recipical synergistic effects of dmrFABP5 and docetaxel on 22RV1 cells\*.**

**(A)** Fixed concentration of dmrFABP5 combined with different concentrations of docetaxel

Cell line	Dmr, $\mu\text{M}$	Docetaxel, nM	CI value	Relationship
22RV1	10	4	0.068	Synergic
22RV1	10	0.4	0.618	Synergic
22RV1	10	0.04	0.812	Synergic
22RV1	10	0.004	0.719	Synergic

**(B)** Fixed concentration of docetaxel combined with different concentrations of dmrFABP5

Cell line	Dmr, $\mu\text{M}$	Docetaxel, nM	CI value	Relationship
22RV1	0.5	4	7.434	Antagonism
22RV1	1	4	0.388	Synergic
22RV1	5	4	0.535	Synergic
22RV1	10	4	0.072	Synergic

\*The synergistic interaction was assessed according to Chou- Talalay with CompuSyn software to calculate combination index (CI). Values of  $<1$  were considered to be synergistic and  $>1$  were antagonism (181).

### 3.4.3 The combination effect of dmrFABP5 with docetaxel on LNCaP

The cells were treated with 1 of the 2 reagents either alone, in a fixed concentration, or in combination with different concentrations of another reagent for 72h incubated in cell culture incubator, as shown in Table 3.3 A and B. After 72h, the cells were treated with Presto Blue HS and the suppressive effect was assessed by calculating the Combination Index (CI) with the COMPUSYN software (191). As shown in figure 3.6, high concentration of dmrFABP5 at 20  $\mu$ M combined with docetaxel at different concentrations of 20, 2, 0.2, 0.02 nM respectively, did not produce synergistic effect (Figure 3.6A). When fixed concentration of dmrFABP5 at 20  $\mu$ M combined with 20, 2, 0.2, 0.02 nM of docetaxel, the percentage of viable cells were 39%, 53%, 68%, 85% respectively, while 37%, 49%, 67%, 86% respectively for docetaxel alone. When docetaxel was used to treat the cells, a fixed docetaxel concentration at its  $IC_{50}$  (2 nM), combined with different concentrations of dmrFABP5 at 20, 10, 5, 1  $\mu$ M respectively, did not produce synergistic effect (Figure 3.6B). As data analysis showed that the percentage of cell viabilities for fixed concentration of docetaxel at 2 nM combined with 20, 10, 5, 1  $\mu$ M of dmrFABP5 were 55 %, 52%, 56%, 53% respectively while 94%, 95%, 97%, 95 respectively for dmrFABP5 alone. Docetaxel alone suppressed LNCaP growth while dmrFABP5 did not produce any suppression effect of LNCaP. All CI values were shown  $>1$  which indicated no synergistic interaction as shown in Table 3.3 A and B.



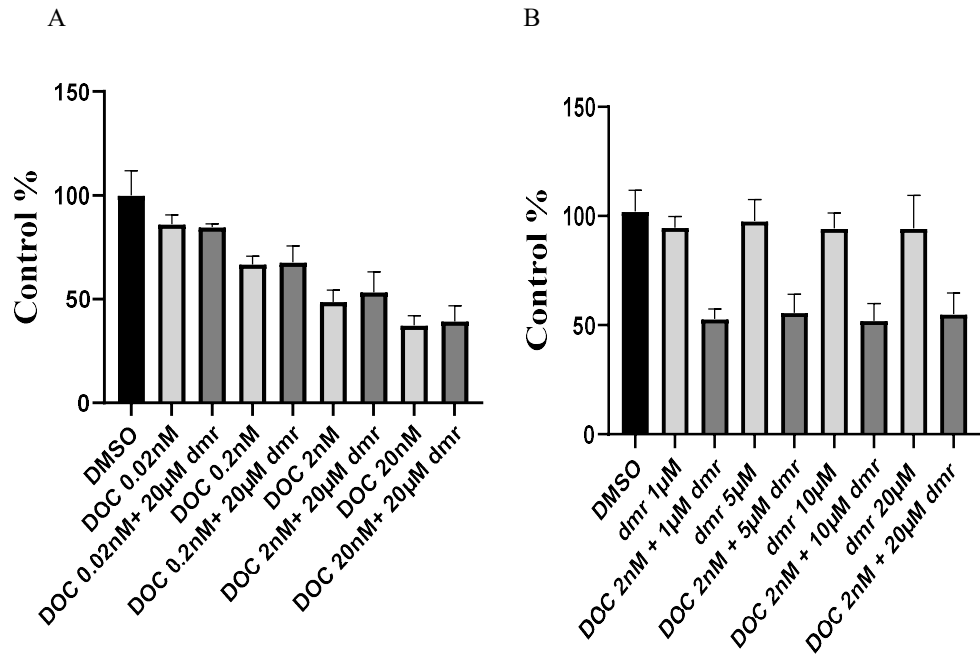


**Figure 3.6.** Combination treatment between dmrFABP5 and enzalutamide on LNCaP. **A.** Fixed concentration of dmrFABP5 at 20µM combined with different concentrations of enzalutamide. **B.** Fixed concentration of enzalutamide at 100nM combined with different concentrations of dmrFABP5. Each experiment were performed in triplicate n=3

**Table 3.3 Recipical effect of dmrFABP5 and enzalutamide on the growth of LNCaP cells\*.**

**(A)**Fixed concentarion of dmrFABP5 combined with different concentarions of docetaxel

Cell line	Dmr, $\mu$ M	Docetaxel, nM	CI value	Relationship
LNCaP	20	20	1.855	Antagonism
LNCaP	20	2	1.126	Antagonism
LNCaP	20	0.2	1.981	Antagonism
LNCaP	20	0.02	6.614	Antagonism

**(B)**Fixed concentraion of docetaxel combined with different concenations of dmrFABP5

Cell line	Dmr, $\mu$ M	Docetaxel, nM	CI value	Relationship
LNCaP	20	2	1.126	Antagonism
LNCaP	10	2	1.129	Antagonism
LNCaP	5	2	1.281	Antagonism
LNCaP	1	2	1.002	Antagonism

\*The synergistic interaction was assessed according to Chou- Talalay with CompuSyn software to calculate combination index (CI). Values of  $<1$  were considered to be synergistic and  $>1$  were antagonism (181).

### **3.5 The assessment of the synergistic effect produced by dmrFABP5 on enzalutamide**

#### **3.5.1 The effect of dmrFABP5 with enzalutamide on DU145**

The cells were treated with dmrFABP5 or enzalutamide alone, in a fixed concentration, or in combination with different concentrations of another reagent for 72h incubated in cell culture incubator, as shown in Table 3.4 A and B. After 72h, the cells were treated with Presto Blue HS and the suppressive effect was assessed by calculating the Combination Index (CI) with the COMPUSYN software (191). As shown in figure 3.7, dmrFABP5 at 5  $\mu\text{M}$  combined with enzalutamide at different concentrations of 100, 50, 10, 1  $\mu\text{M}$  respectively, did not produce synergistic effect (Figure 3.7A). The cell viability percentages for a fixed concentration of dmrFABP5 at 5  $\mu\text{M}$  combined with 100, 50, 10, 1  $\mu\text{M}$  of enzalutamide were 49%, 57%, 55%, 53% respectively, while 96%, 94%, 95%, 99% respectively for enzalutamide alone. When enzalutamide was used to treat the cells, a fixed enzalutamide at 100  $\mu\text{M}$ , combined with different concentrations of dmrFABP5 at 5, 1, 0.5, 0.1  $\mu\text{M}$  respectively, did not produce synergistic effect (Figure 3.7B). As data analysis showed that the percentage of cell viabilities for a fixed concentration of enzalutamide at 100  $\mu\text{M}$  combined with 5, 1, 0.5, 0.1  $\mu\text{M}$  of dmrFABP5 were 53%, 66%, 71%, 92% respectively while 49%, 63%, 69%, 91% respectively for dmrFABP5 alone. DmrFABP5 alone suppressed DU145 growth while enzalutamide did not produce any suppression effect of DU145. All CI values were shown  $>1$  which indicated no synergistic interaction as shown in Table 3.4 A and B.

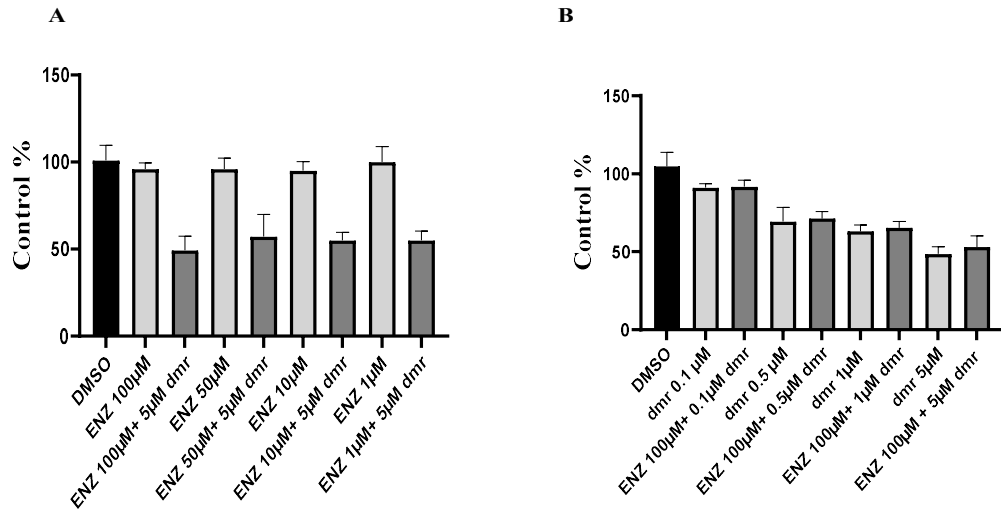


**Figure 3.7** The effect of dmrFABP5 and enzalutamide in suppression of DU145 cells. A). Fixed concentration of dmrFABP5 at 5  $\mu$ M combined with different concentrations of enzalutamide. B). Fixed concentration of enzalutamide at 100  $\mu$ M combined with different concentrations of dmrFABP5. Each experiment were performed in triplicate n=3

**Table 3.4 Recipical effect of dmrFABP5 and enzalutamide on the growth of DU145 cells\*.**

**(A)** Fixed concentration of dmrFABP5 combined with different concentrations of enzalutamide.

Cell line	Dmr, $\mu\text{M}$	Enzalutamide, $\mu\text{M}$	CI value	Relationship
DU145	5	100	1.499	Antagonism
DU145	5	50	1.693	Antagonism
DU145	5	10	2.503	Antagonism
DU145	5	1	1.989	Antagonism

**(B)** Fixed concentration of enzalutamide combined with different concentrations of dmrFABP5.

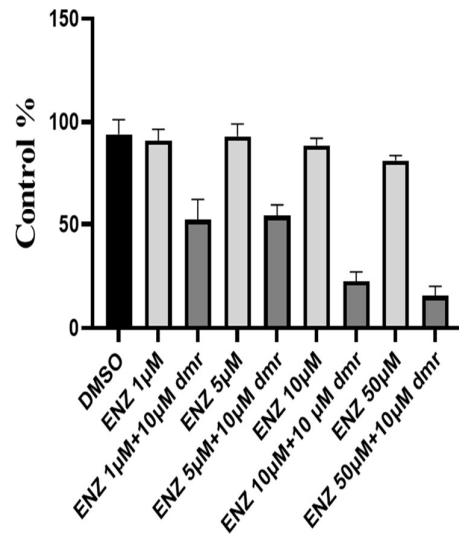
Cell line	Dmr, $\mu\text{M}$	Enzalutamide, $\mu\text{M}$	CI value	Relationship
DU145	5	100	1.369	Antagonism
DU145	1	100	1.767	Antagonism
DU145	0.5	100	1.903	Antagonism
DU145	0.1	100	1.454	Antagonism

\*The synergistic interaction was assessed according to Chou- Talalay with CompuSyn software to calculate combination index (CI). Values of  $<1$  were considered to be synergistic and  $>1$  were antagonism (181).

### 3.5.2 The synergistic effect of DmrFABP5 with enzalutamide on 22RV1

The cells were treated with either dmrFABP5 or enzalutamide alone, in a fixed concentration, or in combination with different concentrations of another reagent for 72h incubated in cell culture incubator, as shown in Table 3.5A and B. After 72h, the cells were treated with Presto Blue HS and the suppressive effect was assessed by calculating the Combination Index (CI) with the COMPUSYN software (191). As shown in figure 3.8, dmrFABP5 at 10  $\mu$ M combined with enzalutamide at different concentrations of 50, 10, and 5  $\mu$ M respectively, produced synergistic effect (Figure 3.8A). The percentage of cell viabilities of the combination were 16%, 23%, 55% respectively, while 83%, 89%, 93% respectively for enzalutamide alone. No synergistic effect when fixed dmrFABP5 at 10  $\mu$ M combined with 1  $\mu$ M of enzalutamide CI= 1.21405. When enzalutamide was used to treat the cells, a fixed enzalutamide concentration (10  $\mu$ M), combined with different concentrations of dmrFABP5 at 10, 5 and 1 $\mu$ M respectively, produced a similar synergistic effect as that produced by dmrFABP5 (Figure 3.8B). As data analysis showed that the percentage of cell viabilities for fixed concentration of enzalutamide at 10  $\mu$ M combined with 10, 5, 1,  $\mu$ M of dmrFABP5 were 20 %, 38%, 66% respectively while 42%, 54%, 74% respectively for dmrFABP5 alone. The maximum suppression effect was found when 10  $\mu$ M combined with enzalutamide at 10  $\mu$ M, with CI= 0.10383. No synergistic effect was found in the combination of dmrFABP5 at 0.5  $\mu$ M and 10  $\mu$ M of enzalutamide CI= 1.496, although dmrFABP5 alone slightly suppressed the viable cells, as shown in Table 3.5B.

A



B

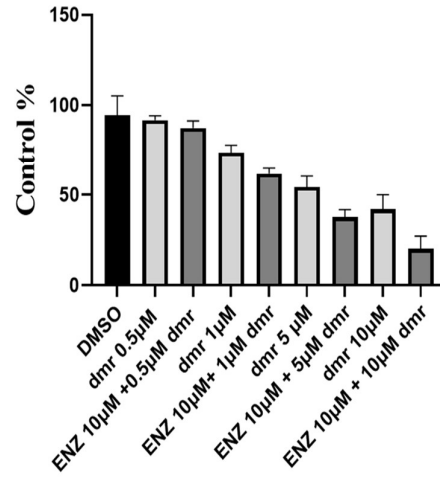


**Figure 3.8** Synergistic effects of dmrFABP5 and enzalutamide in suppression of 22RV1 cells.

A). Fixed concentration of dmrFABP5 at 10  $\mu\text{M}$  combined with different concentrations of enzalutamide. B). Fixed concentration of enzalutamide at 10  $\mu\text{M}$  combined with different concentrations of dmrFABP5. Each experiment were performed in triplicate  $n=3$

**Table 3.5 Results of the synergistic tests on effect of suppressing 22RV1 cells by dmrFABP5 or by enzalutamide\*.**

**(A)** Fixed concentration of dmrFABP5 combined with different concentrations of enzalutamide.

Cell line	Dmr, $\mu\text{M}$	Enzalutamide, $\mu\text{M}$	CI value	Relationship
22RV1	10	50	0.144	Synergistic
22RV1	10	10	0.108	Synergistic
22RV1	10	5	0.888	Synergistic
22RV1	10	1	1.214	Antagonism

**(B)** Fixed concentration of enzalutamide combined with different concentrations of dmrFABP5.

Cell line	Dmr, $\mu\text{M}$	Enzalutamide, $\mu\text{M}$	CI value	Relationship
22RV1	0.5	10	1.496	Antagonism
22RV1	1	10	0.861	Synergistic
22RV1	5	10	0.232	Synergistic
22RV1	10	10	0.113	Synergistic

\*The synergistic interaction was assessed according to Chou- Talalay with CompuSyn software to calculate combination index (CI). Values of  $<1$  were considered to be synergistic and  $>1$  were antagonism (181).



### 3.5.3 The effect of dmrFABP5 with enzalutamide on LNCaP

LNCaP cells were treated with 1 of the 2 reagents either alone, in a fixed concentration, or in combination with different concentrations of another reagent for 72h incubated in cell culture incubator, as shown in Table 3.6 A and B. After 72h, the cells were treated with Presto Blue HS and the suppressive effect was assessed by calculating the Combination Index (CI) with the COMPUSYN software. As shown in figure 3.9, high concentration of dmrFABP5 at 20  $\mu$ M combined with enzalutamide at different concentrations of 1000, 100, 10, 1 nM respectively, did not produce synergistic effect (Figure 3.9A). The percentage of viable cells for this combination were 20%, 51%, 68%, 94% respectively, while 21%, 52%, 66%, 93% respectively for enzalutamide alone. When enzalutamide was used to treat the cells, a fixed enzalutamide concentration at its  $IC_{50}$  (100 nM), combined with different concentrations of dmrFABP5 at 20, 10, 5, 1  $\mu$ M respectively, did not produce synergistic effect (Figure 3.9B). As data analysis showed that the percentage of cell viabilities for fixed concentration of docetaxel at 2 nM combined with 20, 10, 5, 1  $\mu$ M of dmrFABP5 were 55 %, 52%, 56%, 53% respectively while 94%, 95%, 97%, 95 respectively for dmrFABP5 alone. Docetaxel alone suppressed LNCaP growth while dmrFABP5 did not produce any suppression effect of LNCaP. All CI values were shown  $>1$  which indicated no synergistic interaction as shown in Table 3.6 A and B.

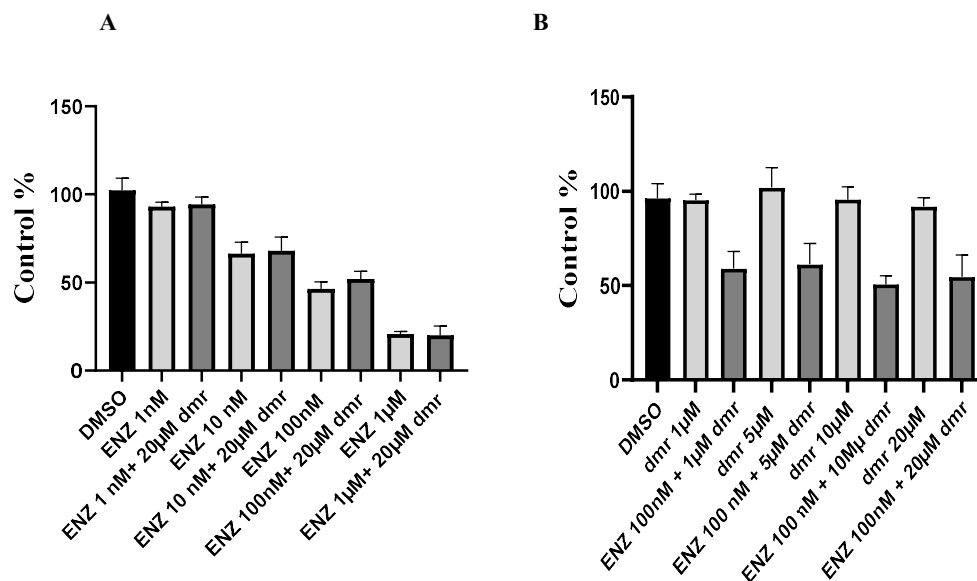


**Figure 3.9** Combination treatment between dmrFABP5 and enzalutamide on LNCaP. Fixed concentration of dmrFABP5 at 20µM combined with different concentrations of enzalutamide (A) Fixed concentration of enzalutamide at 100nM combined with different concentrations of dmrFABP5 (B). Each experiment were performed in triplicate n=3.

**Table 3.6 Results of the tests on effect of suppressing LNCaP cells by dmrFABP5 or by enzalutamide.**

**(A)** Fixed concentration of dmrFABP5 combined with different concentrations of enzalutamide.

Cell line	Dmr, $\mu$ M	Enzalutamide	CI value	Relationship
LNCaP	20	1 $\mu$ M	1.744	Antagonism
LNCaP	20	100nM	1.026	Antagonism
LNCaP	20	10nM	3.982	Antagonism
LNCaP	20	1nM	1.644	Antagonism

**(B)** Fixed concentration of enzalutamide combined with different concentrations of dmrFABP5

Cell line	Dmr, $\mu$ M	Enzalutamide, nM	CI value	Relationship
LNCaP	20	100	1.036	Antagonism
LNCaP	10	100	1.992	Antagonism
LNCaP	5	100	1.664	Antagonism
LNCaP	1	100	1.984	Antagonism

### 3.6 Discussion

The study aimed to determine the half inhibitory concentration (IC<sub>50</sub>) of different compounds, including dmrFABP5, docetaxel, and enzalutamide, in prostate cancer (PCa) cell lines (DU145, 22RV1, and LNCaP). IC<sub>50</sub> represents the concentration of a drug that inhibits 50% of the target biological process. The results revealed that dmrFABP5 had IC<sub>50</sub> values of 5 μM in DU145 cells and 12 μM in 22RV1 cells, but it had no significant effect on LNCaP cells. Docetaxel exhibited IC<sub>50</sub> values of 3 nM in DU145 cells, 4 nM in 22RV1 cells, and 2.2 nM in LNCaP cells. Enzalutamide did not achieve an IC<sub>50</sub> in DU145 and 22RV1 cells, indicating no significant inhibition, while its IC<sub>50</sub> value in LNCaP cells was 97 nM.

To evaluate the treatment effect of combining dmrFABP5 with docetaxel to enhance suppression activity in different prostate cancer cell lines. In DU145 cells, the combination of dmrFABP5 (5 μM) and docetaxel (3 nM) resulted in a maximum suppression of 89% with a very strong synergistic effect (CI = 0.00445). Similarly, in 22RV1 cells, a maximum suppression of 92% was achieved with a significant synergistic effect (CI = 0.06834) when suitable concentrations of dmrFABP5 and docetaxel were used. However, in LNCaP cells, the combination did not exhibit synergistic interactions (CI > 1), despite the significant suppression activity of docetaxel alone. This lack of synergy was expected as LNCaP cells do not express FABP5.

Then dmrFABP5 was used in combination with enzalutamide in different prostate cancer cell lines. In DU145 cells, no synergistic effect was observed with the combination, likely because DU145 cells were androgen-independent and did not express the androgen receptor (AR), which is the target of enzalutamide. Although dmrFABP5 significantly suppressed DU145 cell growth, enzalutamide had no significant effect.

In 22RV1 cells, a significant enhancement was observed when dmrFABP5 was combined with enzalutamide. The combination achieved a maximum suppression of 87% with a highly synergistic effect (CI = 0.14490). This suggests that the combination of dmrFABP5 and enzalutamide effectively suppressed cell growth in 22RV1 cells.

In LNCaP cells, no synergistic interaction was observed between dmrFABP5 and enzalutamide. While dmrFABP5 did not suppress LNCaP cell growth, enzalutamide exhibited significant suppression. This lack of dmrFABP5's action may be attributed to the FABP5-negative nature of LNCaP cells, but enzalutamide was able to suppress LNCaP cells independently due to their AR-positive status(62).

These findings suggest that dmrFABP5 specifically targets FABP5-positive cells and has no impact on FABP5-negative LNCaP cells. Docetaxel, a potent chemotherapy drug, effectively suppressed the growth of all PCa cells. In contrast, enzalutamide, an anti-androgen drug, failed to inhibit androgen-independent DU145 cells and androgen-responsive 22RV1 cells, even though the latter expressed androgen receptor (AR). The resistance of 22RV1 cells to enzalutamide might be due to the expression of AR-V7, lacking the ligand-binding domain (LBD). However, enzalutamide successfully suppressed the growth of LNCaP cells, which only expressed AR-FL and lacked AR-V7 (95,120,123).

## **Chapter 4**

**Result-2: The effect of combination treatments on malignant characteristics of the prostate cancer cells**

## 4.1 Introduction

Previously in our research group, it was confirmed that elevated FABP5 level can be associated with a tumour-promoting effect and malignancy of prostate cancer cells by the ability to deliver fatty acids whether from intracellular or extracellular to its nuclear receptor (130,156). The chemotherapeutic agent docetaxel is a second-generation which originates from the taxan family (192). The primary function of docetaxel is to bind to beta-tubulin and increase its proliferation and cause stabilisation of the cell cycle during G2/M. It prevents the normal assembly of microtubules into the mitotic spindle causing cell cycle arrest. Additionally, docetaxel lowers the expression of the BCL2 gene, an anti-apoptotic gene that cancer cells frequently overexpress in order to increase survival (192,193). Enzalutamide on the other hand is a second-generation androgen receptor inhibitor used to treat CRPC (either metastatic and non-metastatic prostate cancer). Despite the fact that remission of prostate cancer can be achieved by using (ADT), treatment resistance and becoming CRPC is inevitable (194,195).

## **4.2 Aim of the study**

The aim of this chapter is to evaluate the effect of dmrFABP5 in combination with docetaxel or enzalutamide treatments on the malignant characteristics of prostate cancer cells. Specifically, the chapter focuses on examining the influence of the combination treatment on motility, invasion, and colony formation abilities of prostate cancer cells.

This chapter aims to address the importance of targeting dmrFABP5 in prostate cancer treatment, as well as explore the potential synergistic effects when combined with docetaxel or enzalutamide. By investigating the impact of these combination therapies on the malignant traits of prostate cancer cells, we can gain insights into their efficacy and potential therapeutic benefits.

The chapter will provide a comprehensive evaluation of the effects of the combination treatment on various cellular behaviours, including motility, invasion, and colony formation. Experimental methods involving cell culture, drug treatments, and functional assays will be employed to assess these parameters. The results obtained from this study will contribute to a better understanding of the molecular mechanisms underlying prostate cancer progression and may uncover novel strategies for combating the disease.



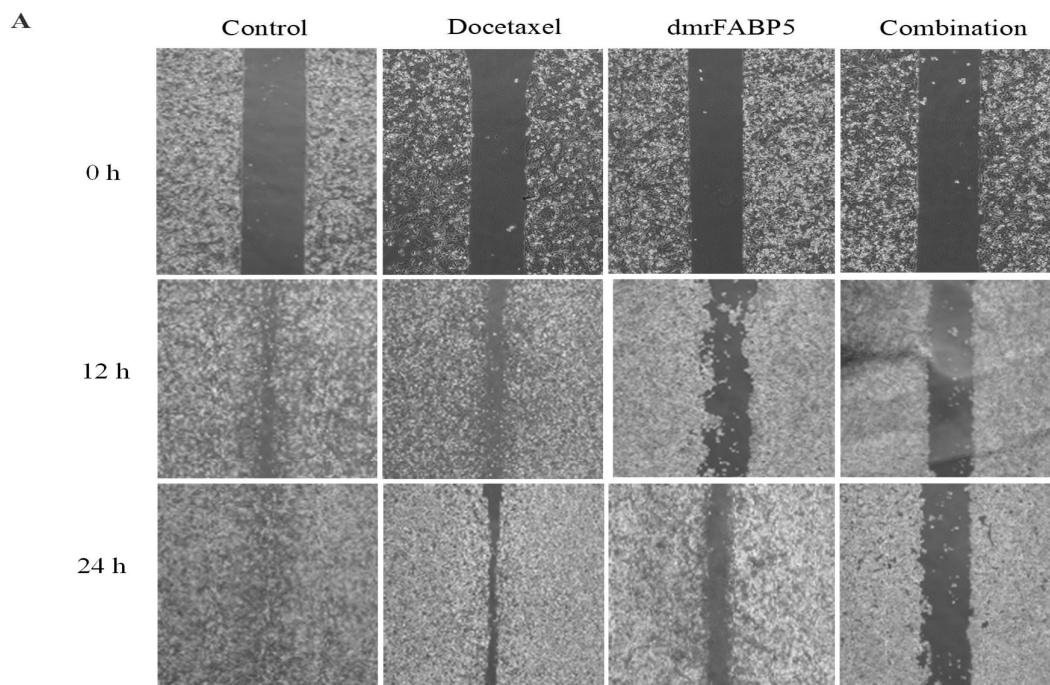
### **4.3 Synergistic action of dmrFABP5 to the treatment drug effect on motility of prostate cancer cells**

In order to evaluate the possible enhancement effect produced by dmrFABP5 to current treatment drugs on the tumorigenicity of prostate cancer cells, dmrFABP5 was used alone or in combination with either docetaxel or enzalutamide to assess its action to the effect of these agents on suppressing cancer cell migration. The high ability to migrate is a reliable indicator of the metastatic characteristic of cancer cells (196). In this section of the study, motility assay, also known as scratching or wound healing assay, was conducted to assess the effect of dmrFABP5 and other agents on the migration behaviour of the cancer cells. The assay was performed with a special culture insert (Ibidi™, Germany). DmrFABP5, docetaxel and enzalutamide were used as either a single agent or in combination.

#### **4.3.1 Synergistic action of dmrFABP5 to the effect of docetaxel on motility of DU145 cells**

DU145 cells growing to 60-80% confluence and harvested, seeded and in Ibidi inserts in triplicate for each treatment group, and incubated for 24h. Next day, old medium was removed, DMSO was used to treat the control group. The docetaxel concentration that used to treat DU145 was 3 nM. For dmrFABP5 treatment group, 5 μM was added to cells. The dmrFABP5 (5 μM) combined with docetaxel (3 nM) were used to treat the combination group. The wound areas were measured and normalised to measure the effect of the combination treatment group and each of other groups. Images were taken at three different experimental time points (0h, 12h, 24h) to assess the wound closure spaces. Results were shown in Figure 4.1. After the treatment with dmrFABP5 combined with docetaxel for 24h, the wound closure space remained to be the largest among the different treatment groups (Figure 4.1A). While the wound in the control group was almost

completely healed, docetaxel produced a larger wound clouser healing than dmrFABP5. Quantitative analysis of the wound closure spaces (Figure 4.1B) showed that after 12 h, 63%% of the wound space was closed in the control, whereas 70% and 82% were still not closed in the groups treated with docetaxel and dmrFABP5 respectively. But in the combined treatment group more than 96%of the wound space was not closed. After 24 h treatment, while the wound space was completely healed in the control, 37%, 51% (Student's *t*-test  $P<0.01^{**}$ ) and 93% ( $P<0.0001^{****}$ ) of the wound spaces were not closed in docetaxel-, dmrFABP5- and both jointly-treated groups respectively. Thus, dmrFABP5 exhibited a greater suppression than docetaxel on wound healing. When cells were treated with docetaxel and dmrFABP5 separately, they produced 88% suppression in wound healing, wherea when they were combined used to treat the cells, the wound healing suppression effect on cells was increased to 93%, that is 5% higher than the sum of the effect produced by the 2 treatments with docetaxel and dmrFABP5 separately.



**B**

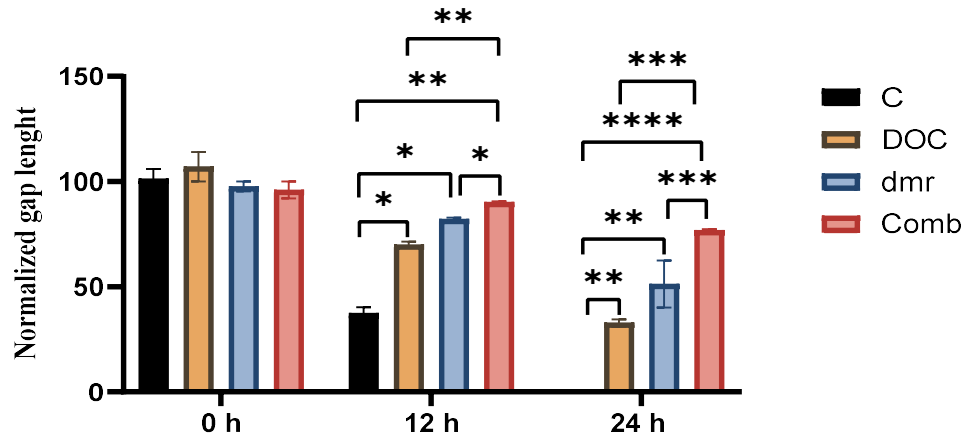


**Figure 4.1** The synergistic action of dmrFABP5 to the effect of docetaxel on the migration of DU145 cells. A), the effect on migration of DU145 cells produced by treatments of dmrFABP5 and docetaxel either singly or in combination at different experimental time points. B), The quantitative assessment as a normalized gap length against time (hours) of different treatments. The results (Mean  $\pm$  SE) was obtained from the measurements of triplicates independent data (n=3). The means were compared with Student *t*-test.  $P < 0.05$  was regarded as significant.

#### **4.3.2 Synergistic action of dmrFABP5 to the effect of docetaxel on motility of**

##### **22RV1 cells**

The control group was treated with DMSO. Docetaxel at a dose of 4 nM and dmrFABP5 at the dose of 10  $\mu$ M were utilized to treat 22RV1 cells, either respectively, or in combination. The wound space gaps were measured and normalised to assess the effectiveness of the different treatments. Images of the wound space gaps obtained at four separate experimental time periods (0h, 24h, 48h and 72h) were displayed in Figure 4.2A. The results of quantitative assessments of the wound space gaps were shown in Figure 4.2B. After 24h, 66% of the wound in control group remained not closed whereas 77%,

79%, 96% of wounds were not healed for docetaxel-, dmrFABP5- and the combination treatments, respectively. After 48h, the unclosed wound space gaps in the control cells, and in cells treated with docetaxel, dmrFABP5 and the combination of both were 49%, 70%, 69% and 92%, respectively. The wound gap in cells treated with dmrFABP5 combined with docetaxel (Figure 4.2A) remained to be larger than that in either cells treated with a single agent. After 72h (Figure 4.2B), the control gap was 20%, whereas either docetaxel or dmrFABP5 treatment produced very similar inhibitions in wound closure by 37% and 40% ( $P < 0.01^{**}$ ) respectively. The synergistic effect produced by the combined treatment inhibited the wound closure space by 89% ( $P < 0.0001^{****}$ ). Thus, the synergistic activity of dmrFABP5 to docetaxel induced 12% more suppressive effect on the migration ability of 22RV1 cells than the sum of the effect produced by each single agent treatment alone.

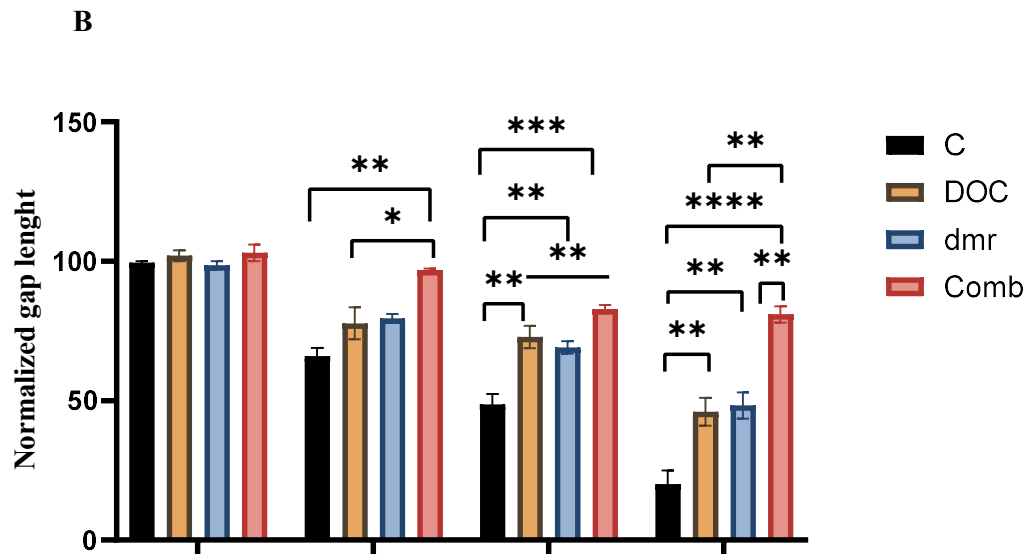
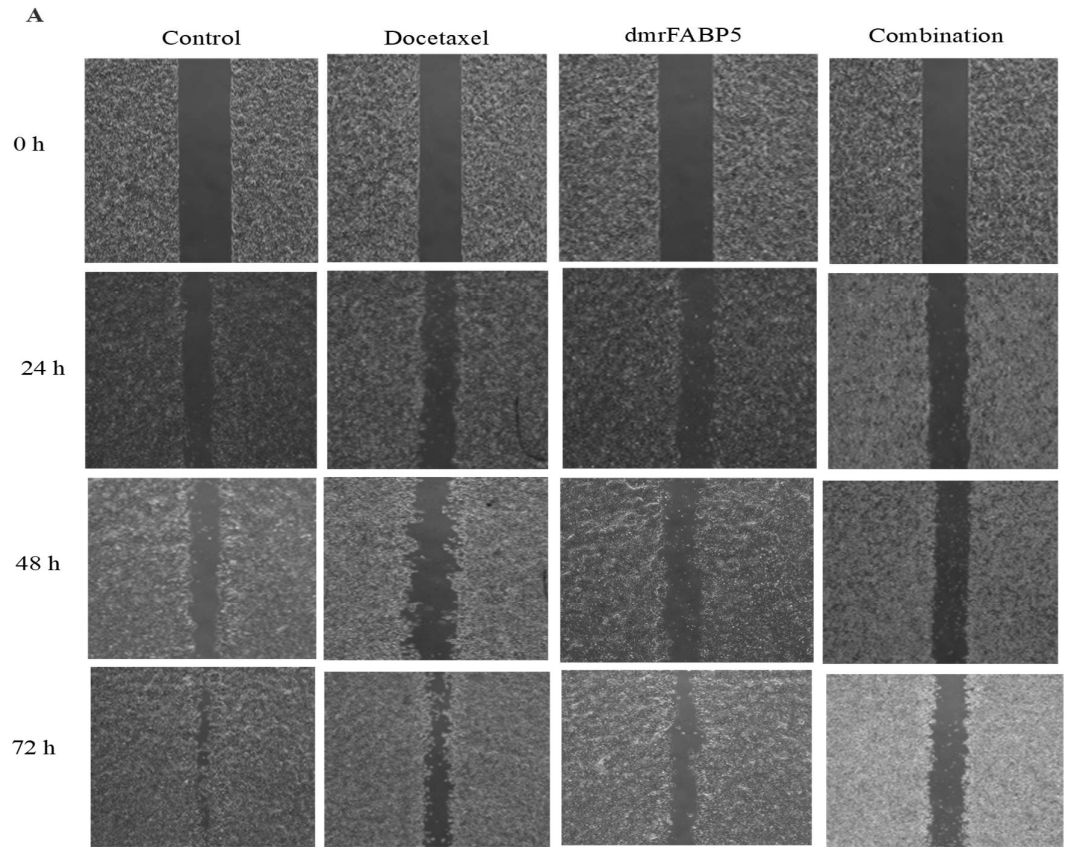


**Figure 4.2** The synergistic action of dmrFABP5 to the effect of docetaxel on the migration of 22RV1 cells. **A)**, the effect on migration of 22RV1 cells produced by treatments

of dmrFABP5 and docetaxel either singly or in combination at different experimental time points. **B)**, Quantitative assessment of normalized gap length against time (hours) of different treatments. The result (Mean  $\pm$  SE) was obtained from the measurements of triplicates independent experiments data (n=3). The means were compared with Student *t*-test.  $P < 0.05$  was regarded as significant.

### **4.3.3 The effect of dmrFABP5 combined with docetaxel in motility on LNCaP**

The results of the wound healing assay on the effect of dmrFABP5 along or combined with docetaxel on motility of LNCaP cells were shown in Figure 4.3. Images of the wound space gaps taken at four separate experimental time periods (0h, 24h, 48h and 72h) were shown in Figure 4.3A. The concentration of docetaxel that was used to treat LNCaP was 2nM, whereas 20 $\mu$ M dmrFABP5 was used to treat the cells. The combination group was treated with dmrFABP5 (20 $\mu$ M) combined with docetaxel (2 nM). Quantitative analysis of wound closure spaces (Figure 4.3B) showed that after 24h, 72% of control wound space was not closed while the unclosed spaces for docetaxel, dmrFABP5 and combination were 91% ,69% and 87% respectively. The wound space gaps in control and in dmrFABP5 treated cells were almost the same after 48h at 53% and 50% respectively, while those remained 81% and 79% for docetaxel treated cells and both jointly-treated cells, respectively. At the end of experiment (after 72h), the wound was almost completely healed in the control cells and dmrFABP5 treated cells with space gaps of only 3% and 4% ( $P > 0.05$ ) respectively. The wound space gap in docetaxel treated cells was 69%, and that in the cells treated by the combination of docetaxel and dmrFABP5 was 65%, very similar to that in docetaxel treated cells ( $P < 0.0001$ \*\*\*\*). Thus, dmrFABP5 did not enhance the effect of docetaxel since the wound space gap in combinedly treated

cells was not significantly (student *t*-test,  $P>0.05$ ) different from that in cells treated with docetaxel alone.

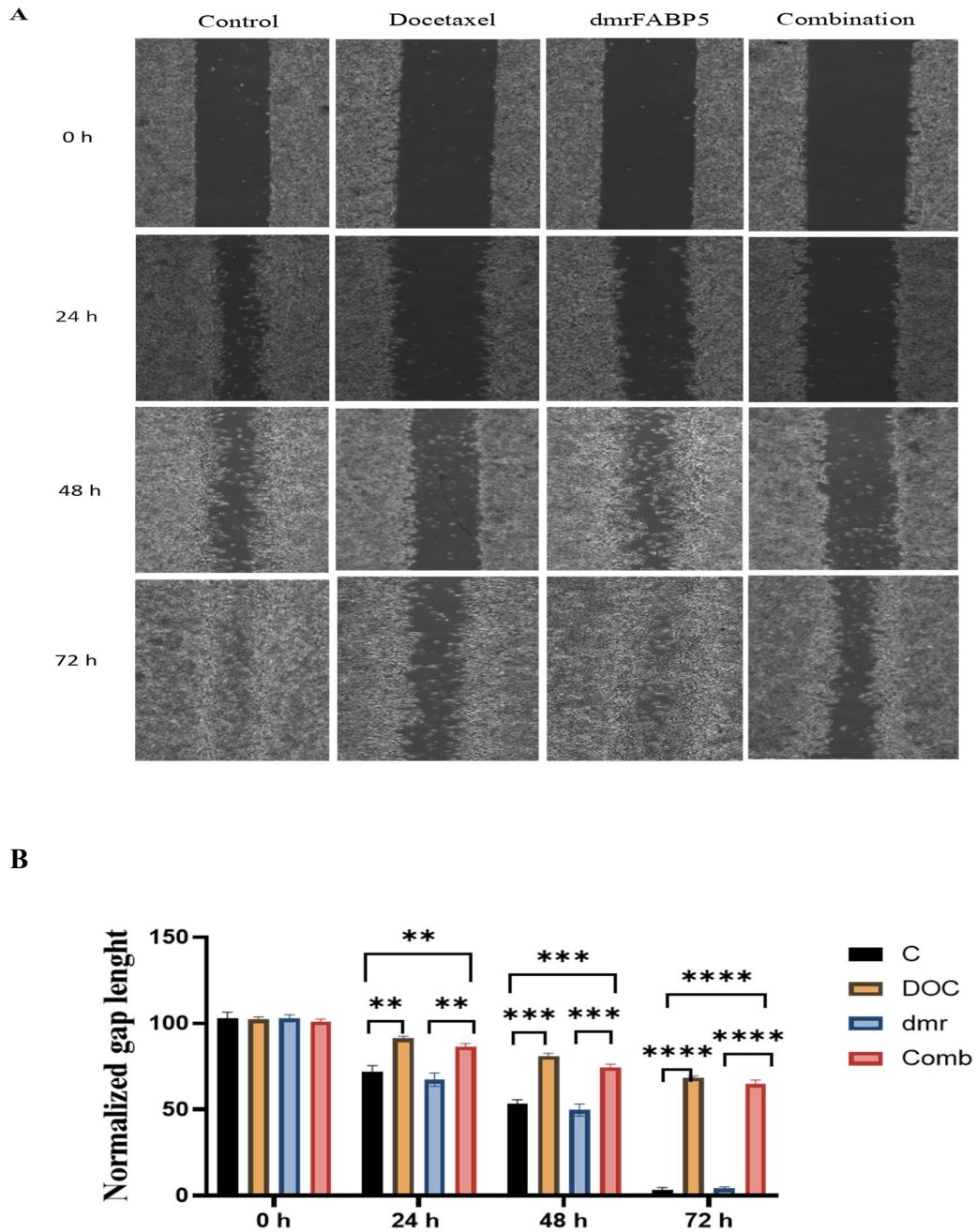


**Figure 4.3** The activity of dmrFABP5 to the effect of docetaxel on the migration of LNCaP cells. **A)** Images of the wound healing space gaps in LNCaP cells produced by

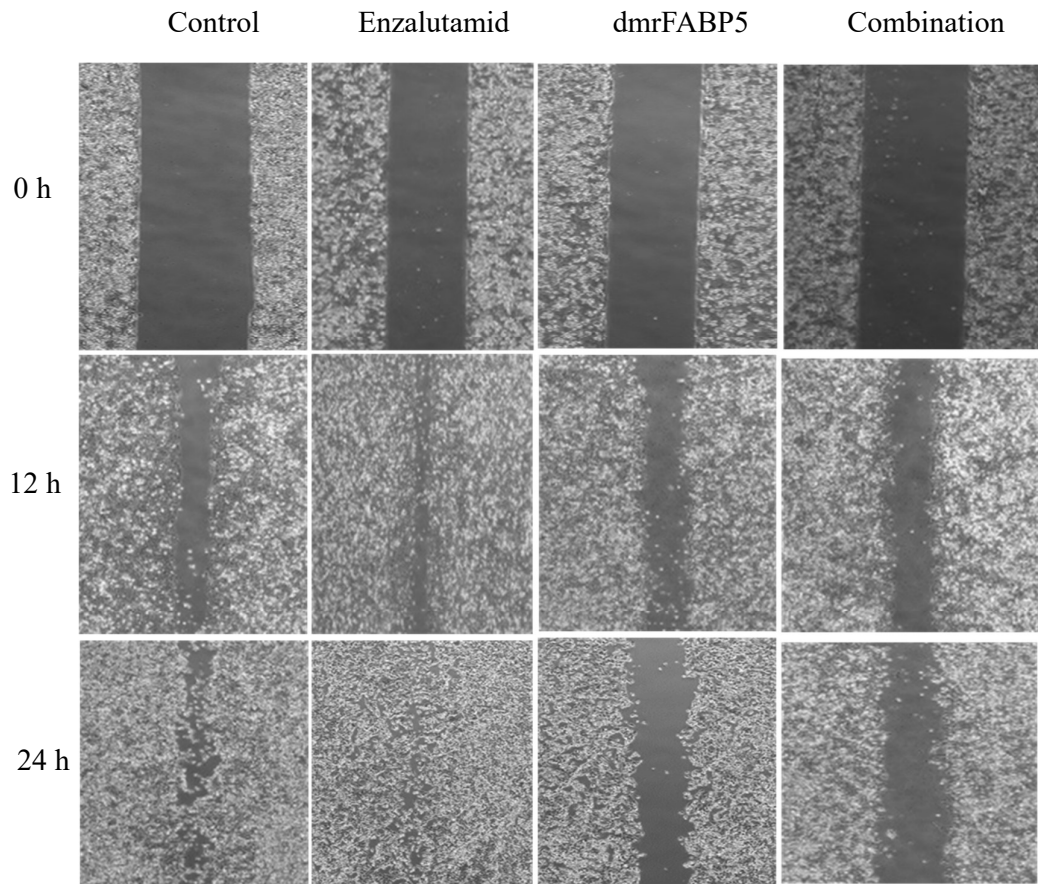
treatments of dmrFABP5 and docetaxel either singly or in combination at different experimental time points. **B**). The quantitative assessment as a normalized gap length against time (hours) of the different treatments. The result (Mean  $\pm$  SE) was obtained from the three independent measurements of triplicates data (n=3). The means were compared with Student *t*-test.  $P < 0.05$  was regarded as significant.

#### **4.3.4 The action of dmrFABP5 to the effect of enzalutamide on motility of DU145 cells**

The results of the wound healing assay on DU145 cells were shown in Figure 4.4. DMSO was used to treat the control cells. The concentration of the anti-androgen drug enzalutamide used to treat DU145 cells was 100  $\mu$ M. The concentration of dmrFABP5 used to treat the DU145 cells was 5  $\mu$ M. The cells were also treated by dmrFABP5 (5  $\mu$ M) combined with enzalutamide (100  $\mu$ M). Images of the wound space gaps taken at three different experimental time points (0h, 12h, 24h) were shown in Figure 4.4A. Quantitative analysis of the wound closure spaces (Figure 4.4B) showed that after 12 h, the space gaps in control cells and cells treated with enzalutamide were 46% and 47% respectively; those in cells treated with dmrFABP5 and with the combination of both agents were 89% and 90% respectively. After 24h, the space gaps in the control cells and cells treated with enzalutamide were completely closed ( $P > 0.05$ ), those in cells treated with dmrFABP5 and in cells treated with a combination of both agents were 78% and 76% ( $P < 0.0001$ \*\*\*\*), respectively. Thus enzalutamide did not have suppression on the size of the wound gaps and dmrFABP5 did not exhibit any additional effect on the activity of enzalutamide ( $P > 0.05$ ).



A



B

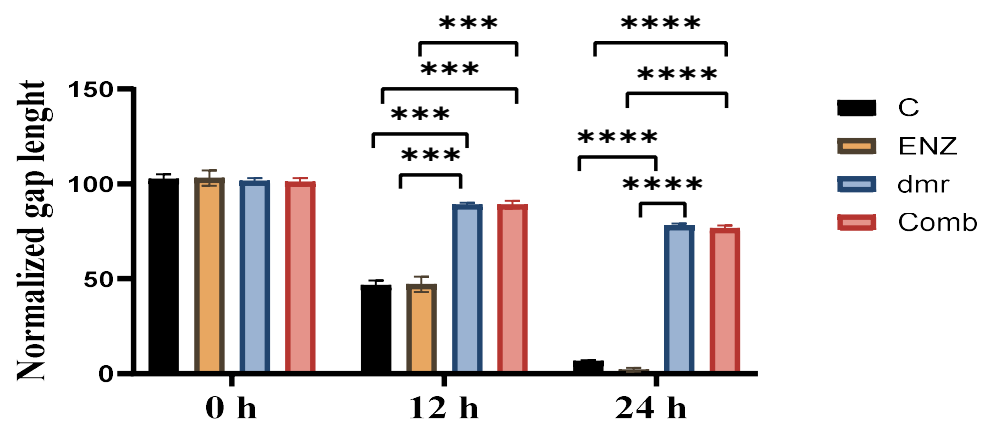


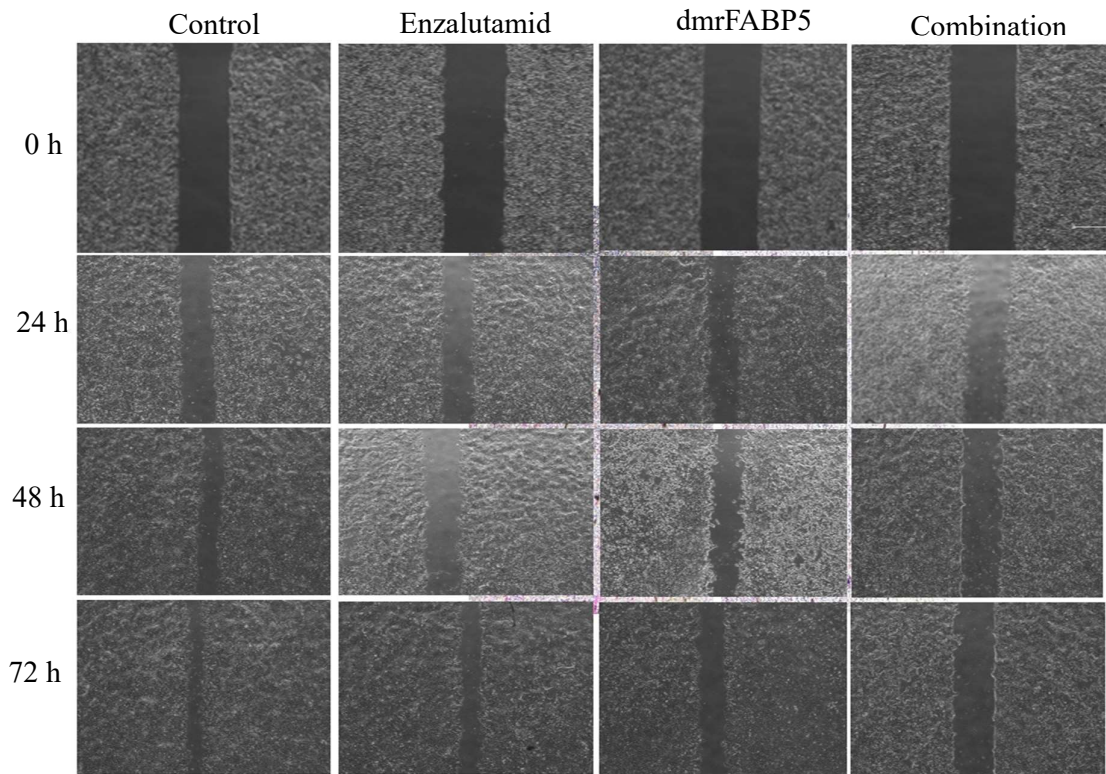
**Figure 4.4** The effect of dmrFABP5 alone or combined with enzalutamide on the migration of DU145 cells. **A).** Images of the wound healing space gaps in DU145 cells with different treatments at different experimental time points. **B).** Quantitative assessment as a

normalized gap length against time (hours). The result (Mean  $\pm$  SE) was obtained from the measurements of triplicates independent experiments data (n=3). The means were compared with Student *t*-test.  $P < 0.05$  was regarded as significant.

#### **4.3.5 Synergistic action of dmrFABP5 to the effect of enzalutamide on motility of 22RV1 cells**

The results of the wound healing assay of testing the synergistic action of dmrFABP5 to the effect of enzalutamide on motility of 22RV1 cells were shown in Figure 4.5. The cells in the control were treated with DMSO. The concentrations of Enzalutamide and dmrFABP5 used to treat the cells were 10  $\mu$ M and 10 $\mu$ M, respectively. The wound healing gap images (figure 4.5A) from cells treated with Enzalutamide, dmrFABP5 or a combination of both were taken at four separate experimental time periods (0h, 24h, 48h and 72h). Quantitative analysis (Figure 4.5B) showed that after 24h of the treatment, the wound gaps in control cells and the cells treated with enzalutamide were 74% and 76% respectively. Those in cells treated with dmrFABP5 and with a combination of both agents were 88% and 97%, respectively. At the end of the experiment (after 72h), the sizes of wound gaps in control cells and in enzalutamide-treated cells remained to be very similar, at 33% and 37%, respectively. Those in cells treated with dmrFABP5 and with a combination of both agents were 69% ( $P < 0.01^{**}$ ) and 91%, respectively. Thus, enzalutamide did not produce significantly more suppression compared with the control ( $P > 0.05$ ). But dmrFABP5 combined with enzalutamide produced the highest suppression by 91% ( $P < 0.001^{***}$ ).

**A**



**B**

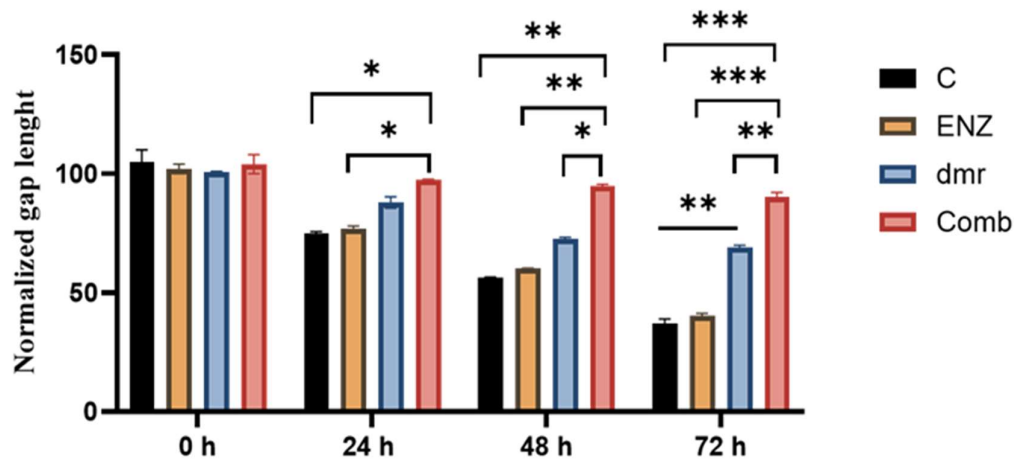


**Figure 4.5** The action of dmrFABP5 to the effect of enzalutamide on the migration of 22RV1 cells. **A).** The images of the wound space gaps in 22RV1 cells with different treatments at different experimental time points. **B).** Quantitative assessment as a normalized gap length

against time (hours) of different treatments. The result (mean  $\pm$  SE) was obtained from the measurements of three independent experiments data (n=3). The means were compared with Student t-test.  $P < 0.05$  was regarded as significant.

#### **4.3.6 The effect of dmrFABP5 combined with enzalutamide in motility on LNCaP**

The results of the wound healing assay in LNCaP cells were shown in Figure 4.6. The control cells were treated with DMSO. The concentrations of enzalutamide and dmrFABP5 used to treat the cells were 100 nM and 20  $\mu$ M, respectively. The images of the wound healing gaps (figure 4.6A) were taken at 4 different experimental time points (0h, 24h, 48h and 72h) after the different treatments of the cells. Quantitative analysis of wound space gaps (Figure 4.6B) showed that after 24h, the space gaps in control cells and in cells treated with dmrFABP5 were 74% and 71%, respectively. The cells treated with enzalutamide, or enzalutamide combined with dmrFABP5 produced significant suppressions on migration of the LNCaP cells with gaps of 91% and 86%, respectively. At the end of experiment (after 72h), the gaps in control and dmrFABP5-treated cells were 7% and 9% ( $P > 0.05$ ), respectively, nearly closed. The gaps in cells treated with enzalutamide with a combination of both agents were 65% and 63% ( $P < 0.0001^{***}$ ), respectively. Thus, dmrFABP5 did not suppress the migration ability of LNCaP cells. The effect in cells jointly treated with the 2 agents was due to the suppression activity of enzalutamide.

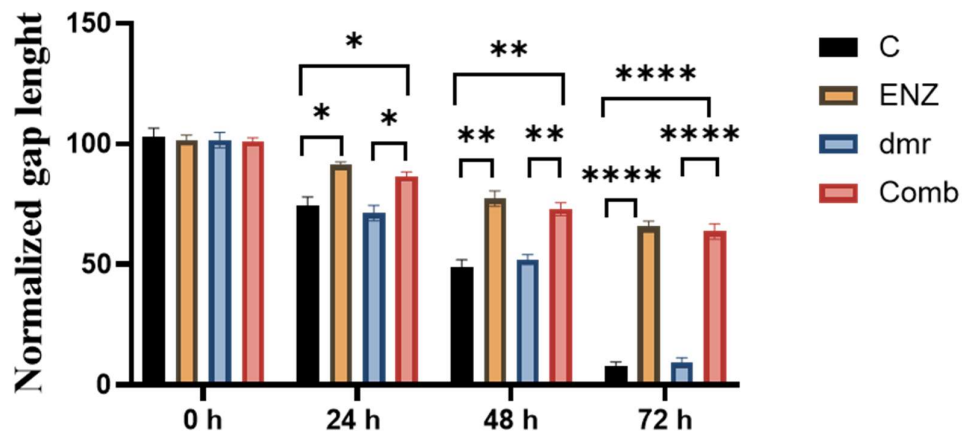
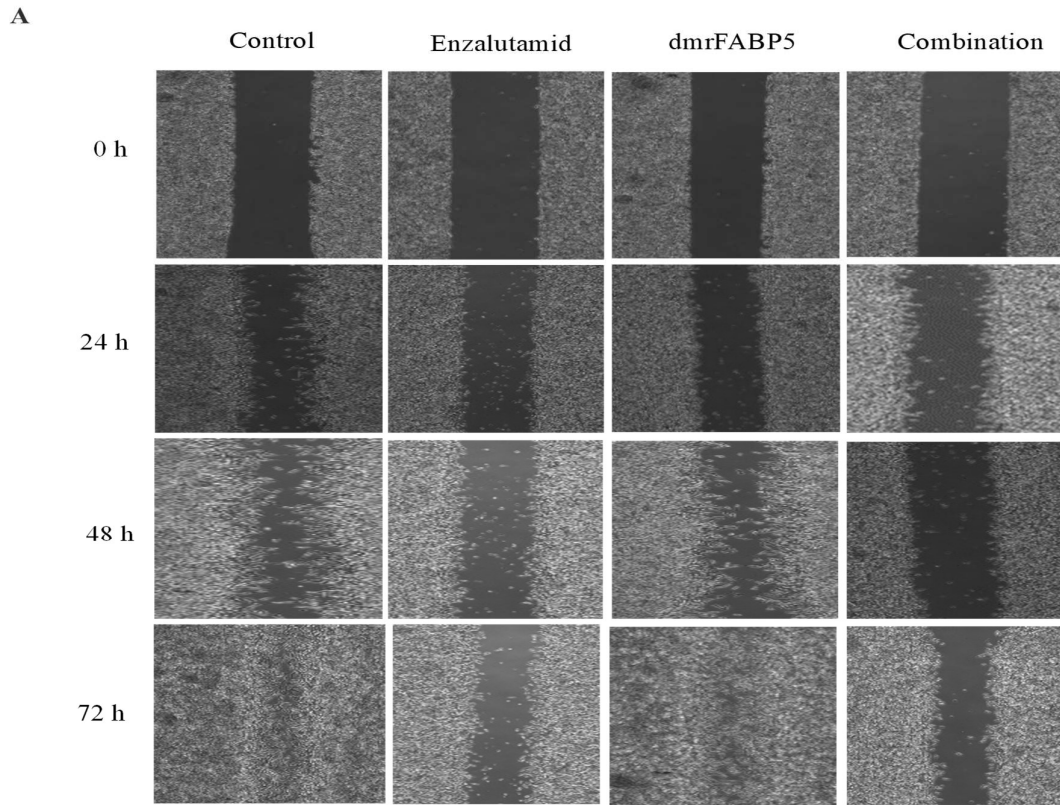


**Figure 4.6** The effect of dmrFABP5 alone or combined with enzalutamide on the migration of LNCaP cells. **A**). The wound space gap images taken at different experimental time points after the LNCaP cells were subjected to different treatments. **B**). The quantitative assessment as a normalized gap length against time (hours) of different treatments. The result

(Mean  $\pm$  SE) was obtained from the measurements of triplicates different experiments data (n=3). The means were compared with Student *t*-test.  $P < 0.5$  was regarded as significant.

#### **4.4 Invasion assay**

To evaluate the possible enhancement effect produced by dmrFABP5 to current treatment drugs on tumorigenicity of prostate cancer cells, dmrFABP5 was used alone or in combination with either docetaxel or enzalutamide to assess its action to the effect of these agents on suppressing the invasion of the cancer cells.

##### **4.4.1 The enhancement effect of dmrFABP5 to docetaxel on DU145**

###### **invasion**

Different treatments were given to DU145 cells to study the effect on cellular invasive ability. The control cells were treated with DMSO. The concentrations of docetaxel and dmrFABP5 used to treat DU145 cells were 3 nM and 5  $\mu$ M, respectively. The results of the invasion assay were shown in Figure 4.7. The microscopic images of the invaded cells from control cells treated with DMSO and from testing cells treated with docetaxel, dmrFABP5 and docetaxel plus dmrFABP5, respectively, were shown in Figure 4.7A. Quantitative analysis (Figure 4.7B) showed that the average number of invaded cells from the control was  $449 \pm 14$ . The average numbers of invaded cells treated with Docetaxel-, dmrFABP5-, and Docetaxel plus dmrFABP5, respectively, were  $89 \pm 3.2$ ,  $68 \pm 2.64$ , and  $9 \pm 1.2$ , respectively, therefore the average invaded cells of the combination were less than the difference between docetaxel and dmrFABP5 together table 4.1. Thus, in comparison with the control, treatments docetaxel, dmrFABP5 and their combination significantly suppressed the invasiveness of DU145 cells (results of statistical analysis were shown in table 4.2) by 77%, 79%, and 98%, respectively. Thus, the combination



induced greater suppression effect than each compound alone. These data showed that the action of dmrFABP5 combined with docetaxel had an enhancement suppression effect on suppressing the invasiveness of the DU145 cells (student t-test  $P < 0.0001$  \*\*\*\*).

**Table 4.1** Number of invaded cells from different treatment on DU145 invasion

Treatment groups (DU145)	Average number of invaded cells (Mean $\pm$ SE)
<b>Control</b>	<b>449 <math>\pm</math> 14</b>
<b>Docetaxel</b>	<b>89 <math>\pm</math> 3.2</b>
<b>dmrFABP5</b>	<b>68 <math>\pm</math> 2.6</b>
<b>Combination</b>	<b>9 <math>\pm</math> 1.2</b>

The average cell numbers were taken randomly from nine different locations. The combination invaded cells were less than the difference of docetaxel and dmrFABP5.

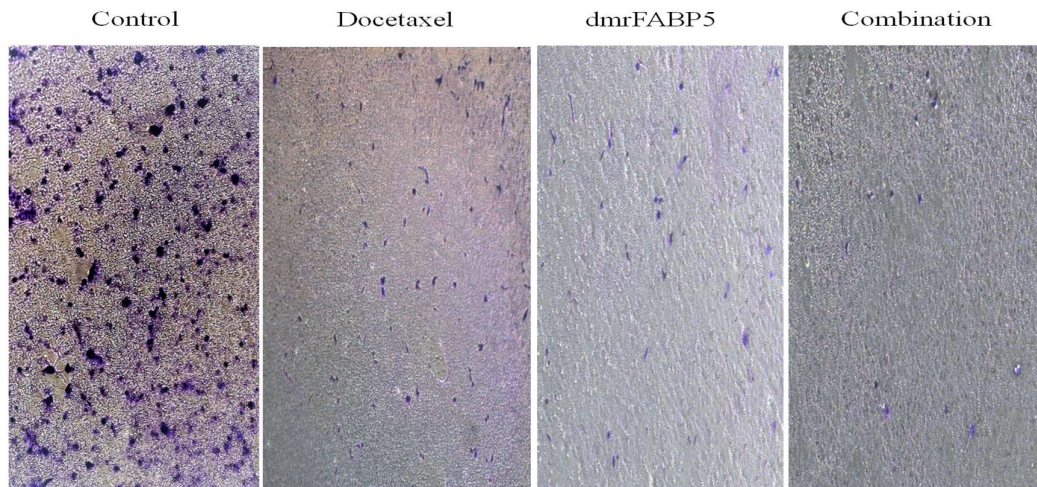
**Table 4.2** Student *t*-test used to compare the means of the invaded cell numbers obtained from different treatments to DU145 cells<sup>+</sup>

Treatment comparison	<i>P</i> value
C to DOC	$P = 0.0002$ ***
C to dmr	$P = 0.0001$ ***
C to Comb	$P < 0.0001$ ****
DOC to dmr	$P > 0.05$
DOC to Comb	$P = 0.0091$ **
Dmr to Comb	$P = 0.0008$ ***

<sup>+</sup> Each experiment was performed in triplicates and the data were presented as Mean  $\pm$  SE; a Student *t*-test was used to compare the means.

The number of invaded cells for each treatment (control, docetaxel, dmrFABP5 and combination) was  $449 \pm 14$ ,  $89 \pm 3.28$ ,  $68 \pm 2.64$  and  $9 \pm 1.2$ , respectively. C= Control, Docetaxel= DOC, dmrFABP5= dmr and Combination= Comb.

**A**



**B**

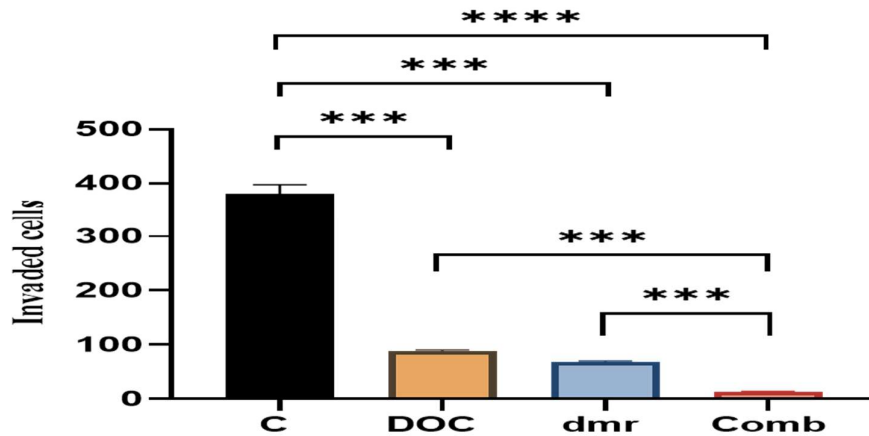


**Figure 4.7** The enhancement interaction of dmrFABP5 to docetaxel on cell invasion ability in DU145. A), the effect on invasion of DU145 cells produced by control and different treatments



with dmrFABP5 and docetaxel either singly or in combination. **B**), The quantitative assessments of the invaded cell numbers. The results (Mean  $\pm$  SE) were obtained from the measurements of triplicates independent experiments data (n=3). The means were compared with the Student *t*-test.  $P < 0.05$  was regarded as significant.

#### **4.4.2 The enhancement effect of dmrFABP5 to docetaxel on invasion of 22RV1**

22RV1 cells were treated with DMSO as control and treated with Docetaxel (4 nM), dmrFABP5 (10  $\mu$ M) and a combination of docetaxel and dmrFABP5 to study the effect of dmrFABP5 on the suppressing activity of docetaxel. The results were shown in Figure 4.8. Microscopic images of the invaded cells were shown in Figure 4.8A. Quantitative analysis (Figure 4.8B) showed that the average invaded cell number of the control was  $306 \pm 6.88$ . Both docetaxel and dmrFABP5 significantly inhibited the cell invasion with average numbers of invaded cells of  $88 \pm 3.2$ ,  $110 \pm 2.6$ , and with suppression rates of 71% and 64%, respectively. The combination treatment induced a greater effect than each treatment singly with only  $14 \pm 1.7$  invaded cells and a 93% suppression rate. Thus, the combination average invaded cell numbers were lower than the difference of both docetaxel and dmrFABP5 table 4.3. The Student *t*-test comparison of means from different treatments was shown in table 4.4. The enhancement suppression effect student *t*-test  $P < 0.0001$ \*\*\*\*

**Table 4.3** Number of invaded cells from different treatment on 22RV1\*

Treatment groups (22RV1)	Average number of invaded cells (Mean $\pm$ SE)
<b>Control</b>	<b>306 <math>\pm</math> 6.8</b>
<b>Docetaxel</b>	<b>88 <math>\pm</math>3.2</b>
<b>dmrFABP5</b>	<b>110 <math>\pm</math> 2.6</b>
<b>Combination</b>	<b>14 <math>\pm</math> 1.7</b>

\*The average invaded cell numbers were taken randomly from nine different locations. The effect of combination treatment on invaded cells were less than the difference of docetaxel and dmrFABP5.

**Table 4.4** Different treatment groups comparisons by Student-test on 22RV1 cells+

Treatment comparison	<i>P value</i>
C to DOC	<i>P=0.0001</i> ***
C to dmr	<i>P=0.0003</i> ***
C to Comb	<i>P&lt;0.0001</i> ****
DOC to dmr	<i>P&gt;0.05</i>
DOC to Comb	<i>P=0.0011</i> **
Dmr to Comb	<i>P=0.0045</i> **

+The average numbers of invaded cells from each treatment (control, docetaxel, dmrFABP5 and combination) were (306.66  $\pm$  6.88, 94  $\pm$  3.21, 89.66  $\pm$  2.6 and 22  $\pm$  1.73, respectively) from triplicate data presented as mean  $\pm$ SE; Student *t*-test was used to compare the means. C= Control, Docetaxel= DOC, dmrFABP5= dmr and Combination= Comb.

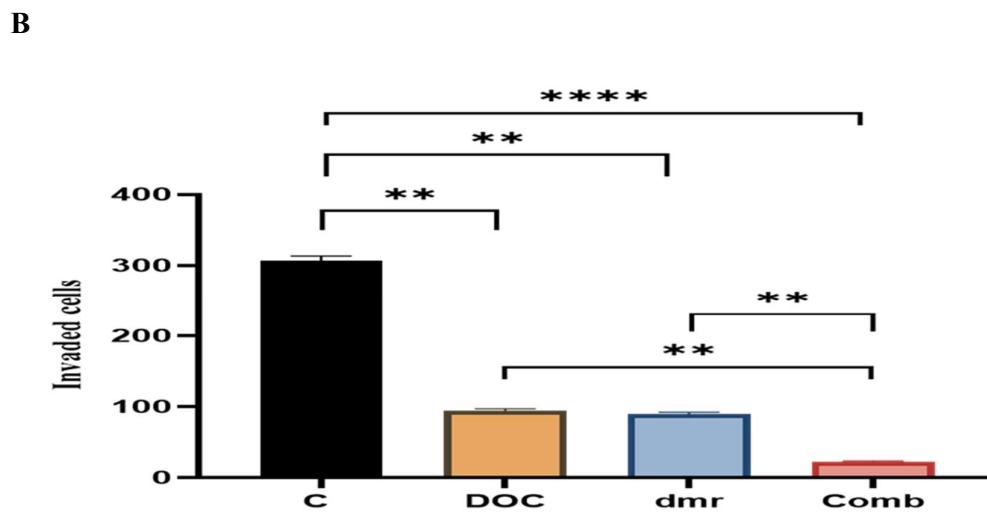
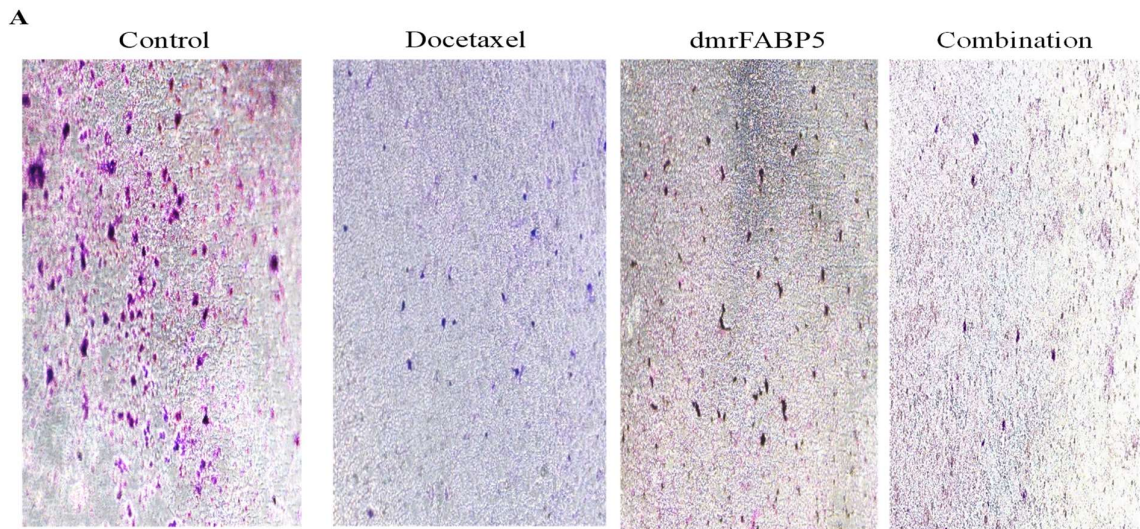


**Figure 4.8** The suppressive effect of dmrFABP5 to docetaxel on the invasion ability of 22RV1 cells. **A)** The microscopic images of the invaded cells of control 22RV1 cells and cells treated with dmrFABP5, docetaxel, or in a combination of both. **B)** The quantitative assessment of the average numbers of the invaded cells obtained from control cells and cells with different treatments. The results (Mean ± SE) were obtained from the measurements of triplicates

independent experiments data (n=3). The means were compared with the Student *t*-test.  $P < 0.05$  was regarded as significant.

#### **4.4.3 The activity of dmrFABP5 to the effect of docetaxel on the invasion of LNCaP**

The effect of dmrFABP5 on the suppression activity of docetaxel to LNCaP cells was tested with a cell invasion assay. The results of the test were shown in figure 4.9. DMSO was used to treat the control. Docetaxel (2 nM) and dmrFABP5 (20  $\mu$ M) were used to treat the cells either individually or in combination. The microscopic images of the invaded cells (shown in figure 4.9A) were taken at the end of the assay (24h). Quantitative analysis (Figure 4.9B) showed that the average number ( $294 \pm 8.55$ ) of the invaded cells after dmrFABP5 treatment was similar to that of the control ( $292 \pm 4.2$ ), with no significant difference (Student *t*-test,  $P > 0.05$ ). Docetaxel treatment significantly suppressed the invasion ability of LNCaP by 87% with an average number of ( $29 \pm 4$ ) cells invaded. A similar average number ( $37 \pm 5$ ) of invaded cells was found from the combination treatment which suppressed the invasion ability of the LNCaP cells by 85% Table 4.5. The average number of invaded cells by docetaxel treatment was not significantly different from that by the combination treatment (Student *t*-test,  $p > 0.05$ ). Thus, dmrFABP5 did not suppress the invasion of LNCaP cells and did not enhance the suppression effect of docetaxel. The treatment effect was assessed and shown in table 4.6.

**Table 4.5** Number of invaded cells from different treatment on LNCaP\*

Treatment groups (LNCaP)	Average number of invaded cells (Mean $\pm$ SE)
<b>Control</b>	<b>292 <math>\pm</math> 4.2</b>
<b>Docetaxel</b>	<b>29 <math>\pm</math> 4</b>
<b>dmrFABP5</b>	<b>294 <math>\pm</math>8.5</b>
<b>Combination</b>	<b>37 <math>\pm</math> 5</b>

\*Invaded cell numbers were calculated by taking the averaged of random nine different locations.

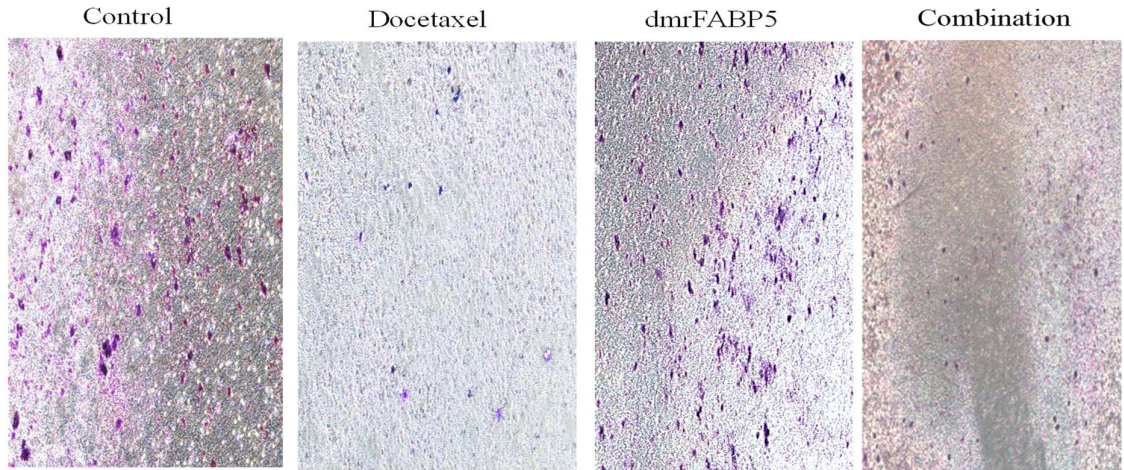
**Table 4.6** The Student-test comparison of different treatment groups on LNCaP cells+

Treatment comparison	<i>P value</i>
C to DOC	<i>P</i> <0.0001 ****
C to dmr	<i>P</i> >0.05
C to Comb	<i>P</i> <0.0001 ****
DOC to dmr	<i>P</i> <0.0001 ****
DOC to Comb	<i>P</i> >0.05
Dmr to Comb	<i>P</i> <0.0001 ***

+The table showed average numbers (292 $\pm$  11, 29  $\pm$  4, 294  $\pm$  21 and 37  $\pm$  5) of invaded cells by different treatments (control, docetaxel, dmrFABP5 and combination), respectively. Each experiment was performed in triplicates and the data were presented as Mean  $\pm$ SE; a Student *t*-test was used to compare the means. \**P* < 0.05, \*\**P* < 0.01,

\*\*\* $P < 0.001$ , \*\*\*\* $P < 0.0001$ . C= Control, Docetaxel= DOC, dmrFABP5= dmr and Combination= Comb.

**A**



**B**

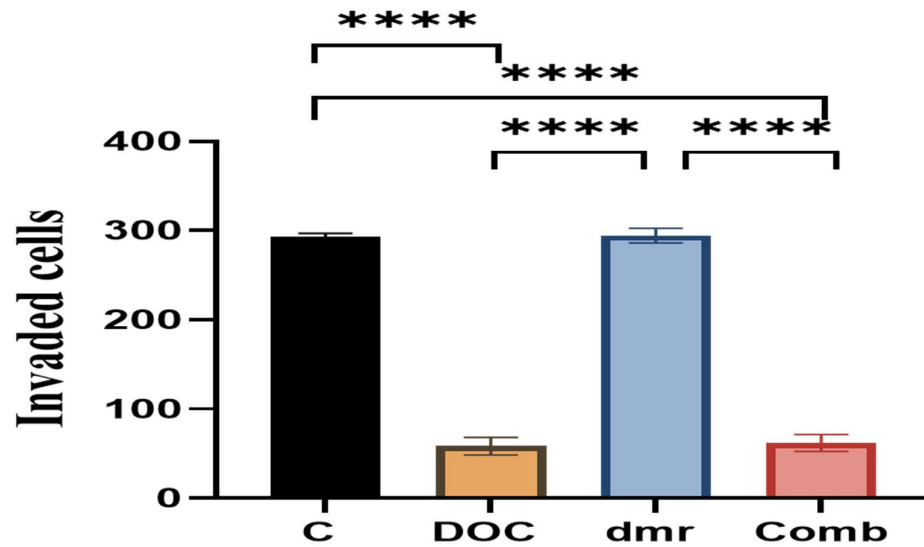


**Figure 4.9.** The action of dmrFABP5 to the effect of docetaxel on LNCaP cell invasion ability. **A)** the microscopic images of the invaded LNCaP cells 24 h after the different treatments. **B)** the quantitative assessment of invaded cell numbers. Each result (Mean ±

SE) was obtained from the measurements of triplicates independent experiments data (n=3). The means were compared with the Student *t*-test.  $P < 0.05$  was regarded as significant.

#### **4.5 The effect of dmrFABP5 on the suppressive activity of enzalutamide to DU145 invasion**

The androgen-independent DU145 cells were treated with DMSO for control. Enzalutamide and dmrFABP5 were used at a concentration of 100  $\mu\text{M}$  and 5  $\mu\text{M}$  respectively either alone or in combination. The results of invasion assay were shown in Figure 4.10. The microscopic images of invaded cells from control cells treated with DMSO and from treated cells with Enzalutamide, dmrFABP5 and combination of both respectively, were shown in Figure 4.10A. Quantitative analysis (Figure 4.10B) showed that the average number ( $425 \pm 25.8$ ) of the invaded cells after Enzalutamide treatment was almost similar to that of control ( $413 \pm 20.9$ ) with no significant difference (Student *t*-test  $P > 0.05$ ). Nearly similar suppression of dmrFABP5 and combination of both agents by 80% and 82% respectively, with average invaded cell numbers ( $27 \pm 2.4$ ) and ( $43 \pm 9.8$ ) respectively (Table 4.7), with no significant difference (Student *t*-test  $P > 0.05$ ). The treatment effect assessments were shown in Table 4.8

**Table 4.7** Numbers of cells different treatments in DU145\*

Treatment groups (Du145)	Average number of invaded cells (Mean±SEM)
Control	413 ± 20.9
Enzalutamide	425 ± 25.8
dmrFABP5	27 ± 2.4
Combination	43 ± 9.8

\*The table showed the average invaded cell numbers of DU145 after each treatment. They were calculated by taking the average of nine random locations of each experiment.

**Table 4.8** The Student *t*-test on the means of the invaded cell numbers after different treatments on DU145 cells+

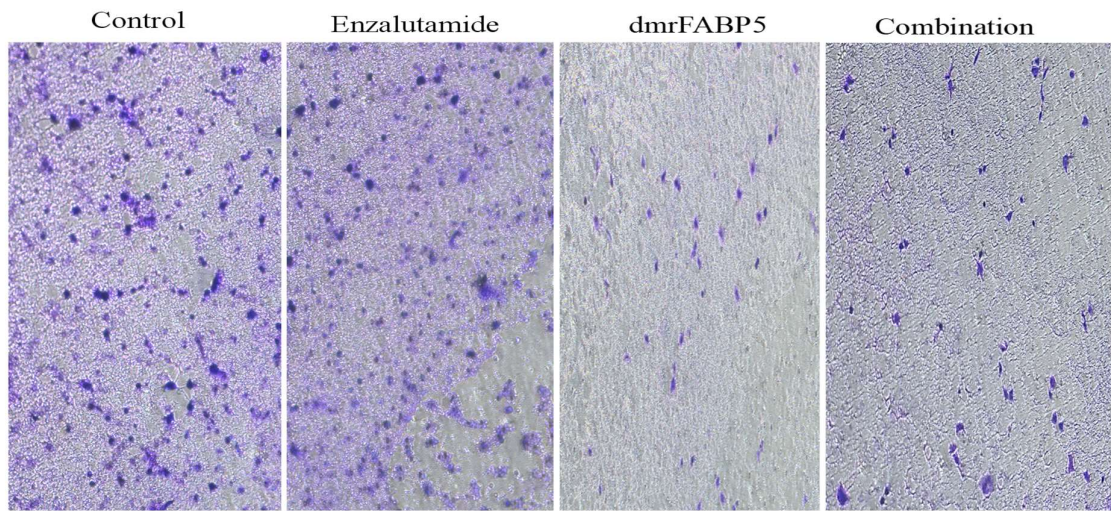
Treatment comparison	<i>P</i> value
C to ENZ	$P > 0.05$
C to dmr	$P = 0.0001$ ***
C to Comb	$P = 0.0001$ ***
ENZ to dmr	$P = 0.0005$ ***
ENZ to Comb	$P = 0.0006$ ***
Dmr to Comb	$P > 0.05$

+Each experiment was performed in triplicates and the data were presented as Mean ± SEM; Student *t*-test was used to compare the means.  $P < 0.05$  was regarded as significant.



Degree of significance was presented as number of stars as following: \* $P < 0.05$ , \*\* $P < 0.01$ , \*\*\* $P < 0.001$ , \*\*\*\* $P < 0.0001$ . The number of invaded cells from each treatment (control or C, Enzalutamide or ENZ, dmrFABP5 or dmr, and combination or Com) was  $413 \pm 20.9$ ,  $425 \pm 25.8$ ,  $27 \pm 2.4$  and  $43 \pm 9.8$ , respectively.

A



B

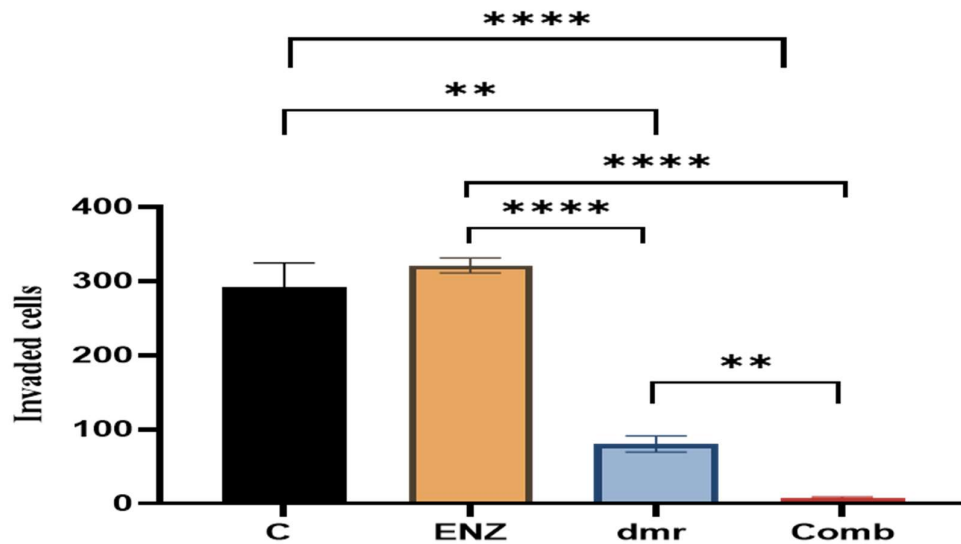


**Figure 4.10** The action of dmrFABP5 to enzalutamide on the invasion ability of DU145

**A)** The microscopic images of invaded DU145 cells after treatments of dmrFABP5 and enzalutamide either singly or in combination. **B)** Quantitative assessment of the number of cells invaded. The results (Mean  $\pm$  SEM) was obtained from calculations of triplicates independent experiments data (n=3). The means were compared with the Student *t*-test.  $P < 0.05$  was regarded as significant.

#### **4.5.1 The enhancement activity of dmrFABP5 to the effect of enzalutamide on the invasiveness of 22RV1 cells**

The control 22RV1 cells were treated with DMSO. Concentrations of both Enzalutamide and dmrFABP5 used to treat the cells were at 10  $\mu$ M, respectively, either singly or in combination. The result of the invasion assay were shown in Figure 4.11. Microscopic images exhibiting different treatment effects on the numbers of invaded cells were shown in Figure 4.11A. A quantitative assessment of the invaded cell numbers was shown in Figure 4.11B. The number of invaded cells from the control was  $292 \pm 33$ . The number of invaded cells from Enzalutamide treatment ( $321 \pm 10$ ) was not significantly different from the control (Student *t*-test  $P > 0.05$ ), indicating that Enzalutamide did not have an effect on cell invasiveness. The number of invaded cells from DmrFABP5 treatment was  $80 \pm 11$  cells, a significant reduction from that from the control by 72% (Student *t*-test  $P < 0.01^{**}$ ). The number of cells from the combination treatment was  $8 \pm 1.3$ , a highly significant reduction from that of the control by more than 97% (Student *t*-test  $P < 0.0001^{***}$ ) (Table 4.9). Table 4.10 showed the number of invaded cells for each different treatment.

**Table 4.9** The average numbers of invaded cells from different treatment\*

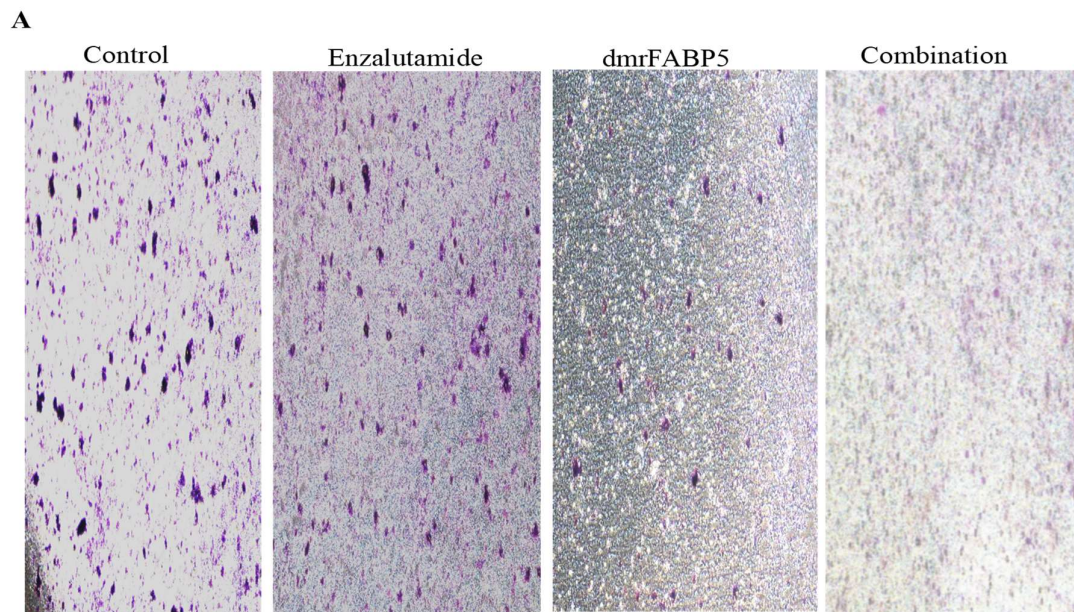
Treatment groups (22RV1)	Average number of invaded cells (mean $\pm$ SE)
<b>Control</b>	<b>292 <math>\pm</math> 33</b>
<b>Enzalumide</b>	<b>321 <math>\pm</math> 10</b>
<b>dmrFABP5</b>	<b>80 <math>\pm</math> 11</b>
<b>Combination</b>	<b>14 <math>\pm</math> 1.3</b>

**Table 4.10** The Student *t*-test on the means of the colonies formation numbers after different treatments on 22RV1 cells\*

Treatment comparison	<i>P</i> value
C to ENZ	<i>P</i> >0.05
C to dmr	<i>P</i> =0.0037 **
C to Comb	<i>P</i> <0.0001 ****
ENZ to dmr	<i>P</i> <0.0001 ****
ENZ to Comb	<i>P</i> <0.0001 ****
Dmr to Comb	<i>P</i> =0.0028 **

\*Each experiment was performed in triplicates and the data were presented as mean  $\pm$ SE; Student *t*-test was used to compare the means. *P*<0.05 was regarded as significant. Degree

of significance was presented as number of stars as following:  $*P < 0.05$ ,  $**P < 0.01$ ,  $***P < 0.001$ ,  $****P < 0.0001$ . The number of invaded cells from each treatment (control or C, Enzalutamide or ENZ, dmrFABP5 or Dmr, and combination or Com) was  $292 \pm 33$ ,  $321 \pm 10$ ,  $80 \pm 11$  and  $8 \pm 1.3$ , respectively.



**B**

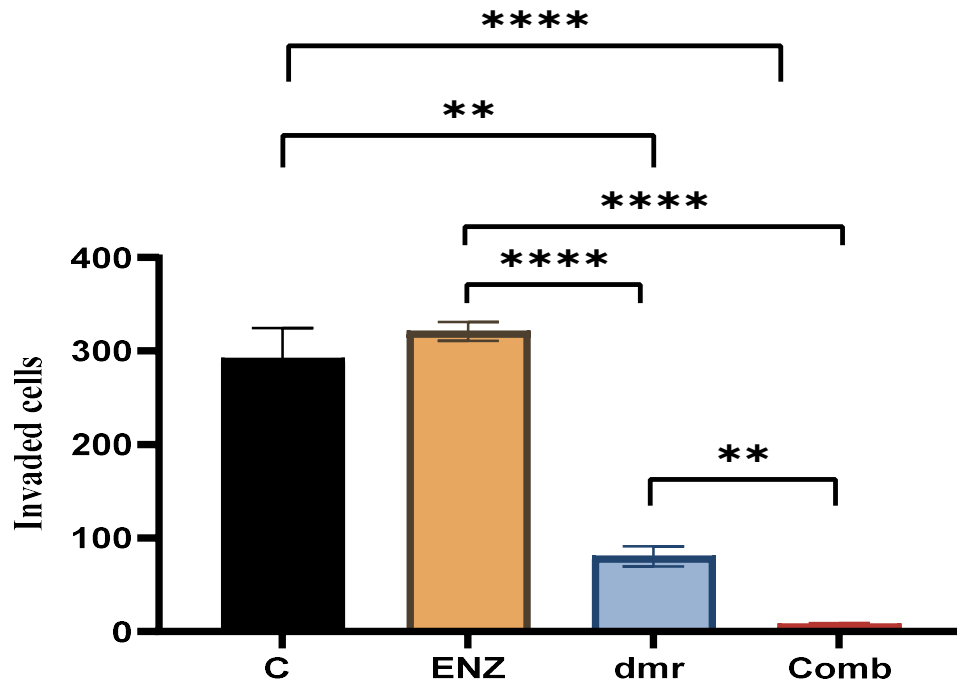


**Figure 4.11** The enhansive activity of dmrFABP5 to the effect of enzalutamide on the invasive ability of 22RV1 cells. **A)**, the effect on invasion of 22RV1 cells by treatments of dmrFABP5 and enzalutamide either singly or in combination. **B)**, the quantitative assessment of invaded cell numbers by the treatments. The results (Mean  $\pm$  SE) were obtained from the assessments of triplicates independent expermint data. The means were compared with the Student *t*-test.  $P < 0.05$  was regarded as significant.

#### **4.5.2 The treatment effect of dmrFABP5 to enzalutamide on the invasion of LNCaP**

The androgen-dependent LNCAP cells were treated with DMSO and used as a control. Enzalutamide (100 nM) and dmrFABP5 (20  $\mu$ M) were used to treat the cells either singly or in combination and the results on cell invasion were shown in Figure 4.12. The microscopic images of invaded cells from different treatments were taken at the end of

the experiment and were shown in Figure 4.12A. Quantitative analysis results (Figure 4.12B) showed that the average number of invaded cells from the control was  $315 \pm 22$  cells. The average number of the invaded cells from enzalutamide treatment was  $60 \pm 3$ , a significant reduction (Student *t*-test \*\*\* $P < 0.001$ ) from that of the control by 81%. No significant suppression was found in dmrFABP5 treated group and invaded cell number was  $310 \pm 42$  (Student *t*-test  $P > 0.05$ ). The combination treatment ended up with  $73 \pm 9$  invaded cells, a highly significant reduction from that of the control by 77% (Table 4.11). Statistical analysis of mean numbers of the invaded cells from different treatments was shown in Table 4.12.

**Table 4.11** Average invaded cell numbers of different treatment on LNCaP\*

Treatment groups (LNCaP)	Average number of invaded cells (Mean $\pm$ SE)
<b>Control</b>	<b>315 <math>\pm</math> 22</b>
<b>Enzalutamide</b>	<b>60 <math>\pm</math> 3</b>
<b>dmrFABP5</b>	<b>310 <math>\pm</math> 42</b>
<b>Combination</b>	<b>73 <math>\pm</math> 9</b>

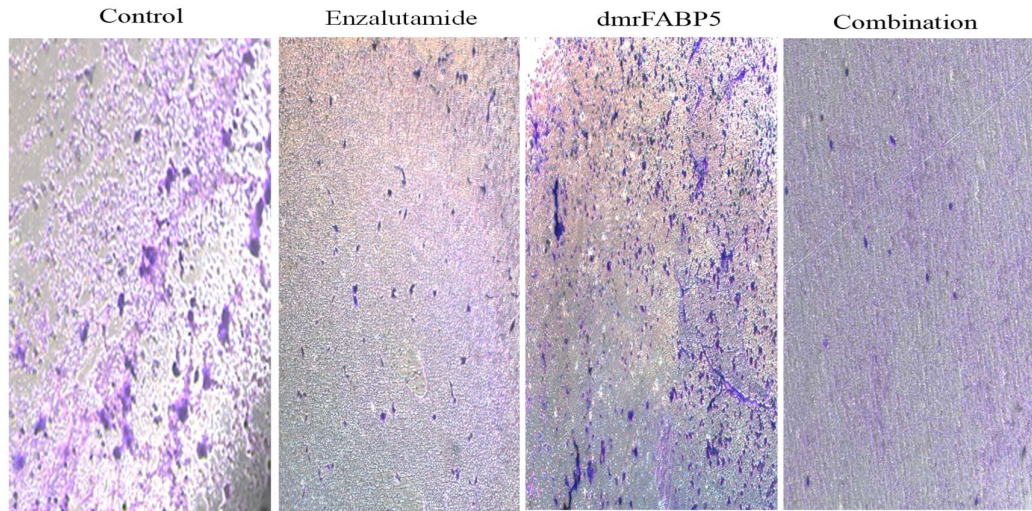
**Table 4.12** The Student *t*-test on mean numbers of invaded LNCaP cells after different treatments\*

Treatment comparison	<i>P</i> value
C to ENZ	$P=0.0010$ ***
C to dmr	$P>0.05$
C to Comb	$P=0.0010$ ***
ENZ to dmr	$P=0.0008$ ***
ENZ to Comb	$P>0.05$
Dmr to Comb	$P=0.0008$ ***

\*Each experiment was performed in triplicates and the data were presented as mean  $\pm$ SE; a Student *t*-test was used to compare the means.  $P<0.05$  was regarded as significant. Degree of significance was presented as number of stars as following: \* $P < 0.05$ , \*\* $P < 0.01$ , \*\*\* $P < 0.001$ , \*\*\*\* $P < 0.0001$ . The number of invaded cells from each treatment (control or C, Enzalutamide or ENZ, dmrFABP5 or Dmr, and combination or Com) was  $315 \pm 22$ ,  $60 \pm 3$ ,  $310 \pm 42$  and  $73 \pm 9$ , respectively.

A





**B**

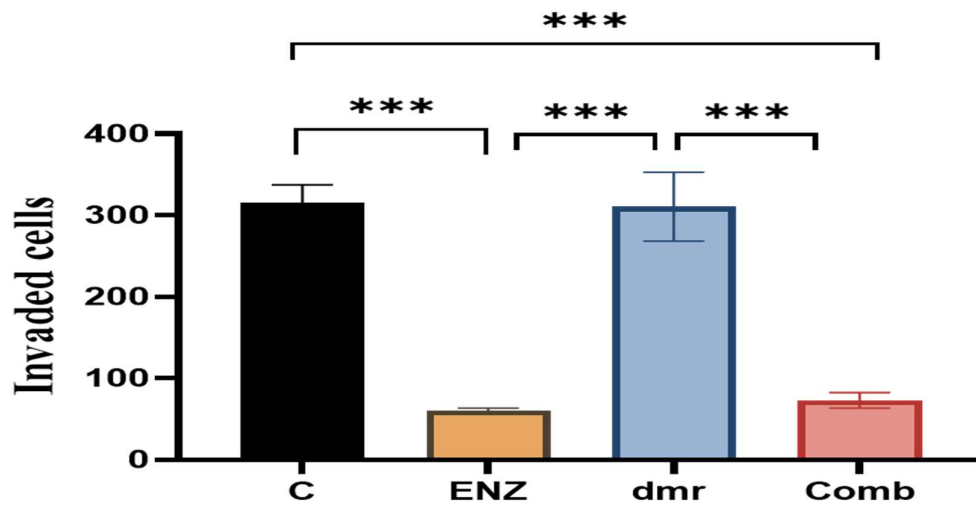


**Figure 4.11** The activity of dmrFABP5 to the effect of enzalutamide on the invasive ability of LNCaP cells. **A)** the effect on invasion of LNCaP cells by respective treatments of dmrFABP5 and enzalutamide either singly or in combination. **B)** The quantitative assessment of average invaded cell numbers and the result (Mean  $\pm$  SE) was obtained from the accounts of triplicates independent experiments data (n=3). The means were compared with the Student *t*-test.  $P < 0.05$  was regarded as significant.



## **4.6 Anchorage independent cell growth (soft agar assay)**

Soft agar assay was employed to assess the effect of dmrFABP5 singly or in combination with either docetaxel or enzalutamide on prostate cancer cell colony formation abilities which is an indication of tumorigenicity.

### **4.6.1 The effect of dmrFABP5 combined with docetaxel on the colony formation of DU145**

The soft agar assay experiment was performed to test the enhancement effect of the dmrFABP5 to docetaxel on the colony formation ability and the results were shown in Figure 4.12. The control DU145 were treated with DMSO. Doses of docetaxel and dmrFABP5 used in this assay were 3 nM and 5  $\mu$ M, respectively. For the combined treatment, 5  $\mu$ M of dmrFABP5 combined with 3 nM of docetaxel were jointly used. Images of soft agar plates were shown in Figure 4.12A. Quantitative analysis in (Figure 4.12B) showed that the average number of colonies form in the control were  $880 \pm 44$ . Average colony numbers in the plates treated with Docetaxel and dmrFABP5 were significantly to  $144 \pm 37$ ,  $217 \pm 33$ , respectively (Student *t*-test  $P < 0.001$  \*\*\*). The number of colonies form by the cells treated by the combination of docetaxel and dmrFABP5 was high significantly reduced to  $16 \pm 4$ , as shown in Table 4.13. Thus, dmrFABP5 significantly enhanced the suppressive effect of docetaxel on DU145 colonies formation (Student *t*-test  $P < 0.0001$  \*\*\*\*) (Table 4.14).

**Table 4.13** The average numbers of colony formed by Du145 cells after different treatments\*

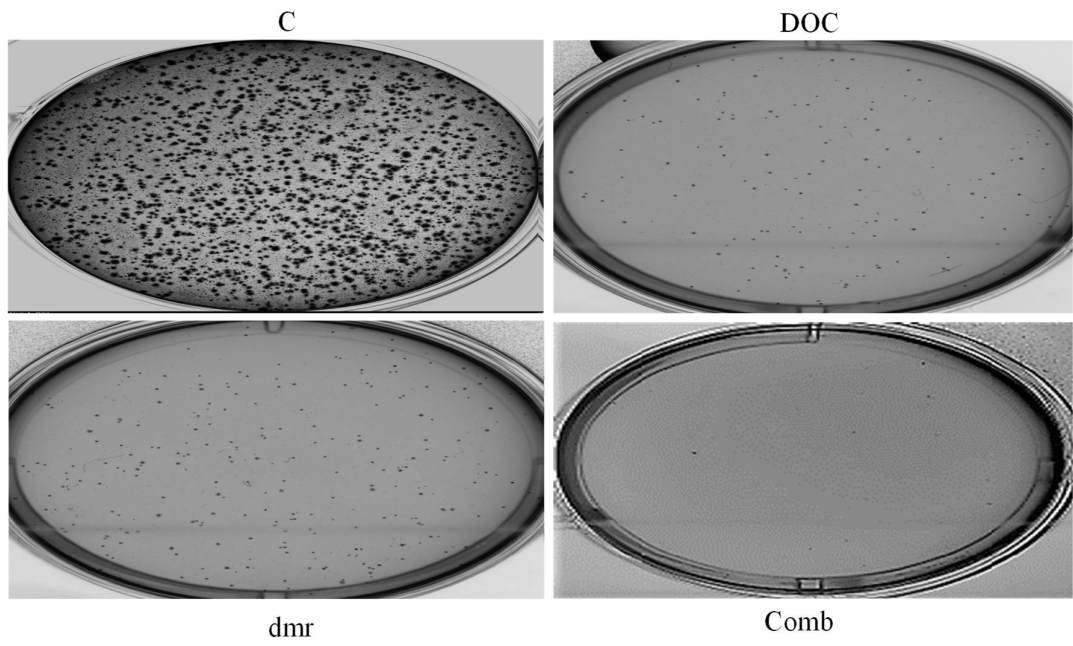
Treatment groups	Average number of colonies (Mean $\pm$ SE)
<b>Control</b>	<b>880 <math>\pm</math> 44</b>
<b>Docetaxel</b>	<b>144 <math>\pm</math> 37</b>
<b>dmrFABP5</b>	<b>217 <math>\pm</math> 33</b>
<b>Combination</b>	<b>16 <math>\pm</math> 4</b>

**Table 4.14** Student *t*-test on mean numbers of colonies formed by DU145 after different treatments\*

Treatment comparison	<i>P value</i>
C to DOC	<i>P</i> =0.0002***
C to dmr	<i>P</i> =0.0003***
C to Comb	<i>P</i> <0.0001****
DOC to dmr	<i>P</i> >0.05
DOC to Comb	<i>P</i> =0.0278*
Dmr to Comb	<i>P</i> =0.0041**

\*Each experiment was performed in triplicates and the data were presented as mean  $\pm$ SE; *P*<0.05 was regarded as significant. Degree of significance was presented as number of stars as following: \**P* < 0.05, \*\**P* < 0.01, \*\*\**P* < 0.001, \*\*\*\**P*<0.0001. C = control, DOC = docetaxel, dmr = dmrFABP5 and Comb = combination. The colony numbers for C, DOC, dmr and Comb were 880.66 $\pm$ 44.3, 144.66 $\pm$ 37.7, 217 $\pm$ 33.6, 16.33 $\pm$ 4.37, respectively.

A



B

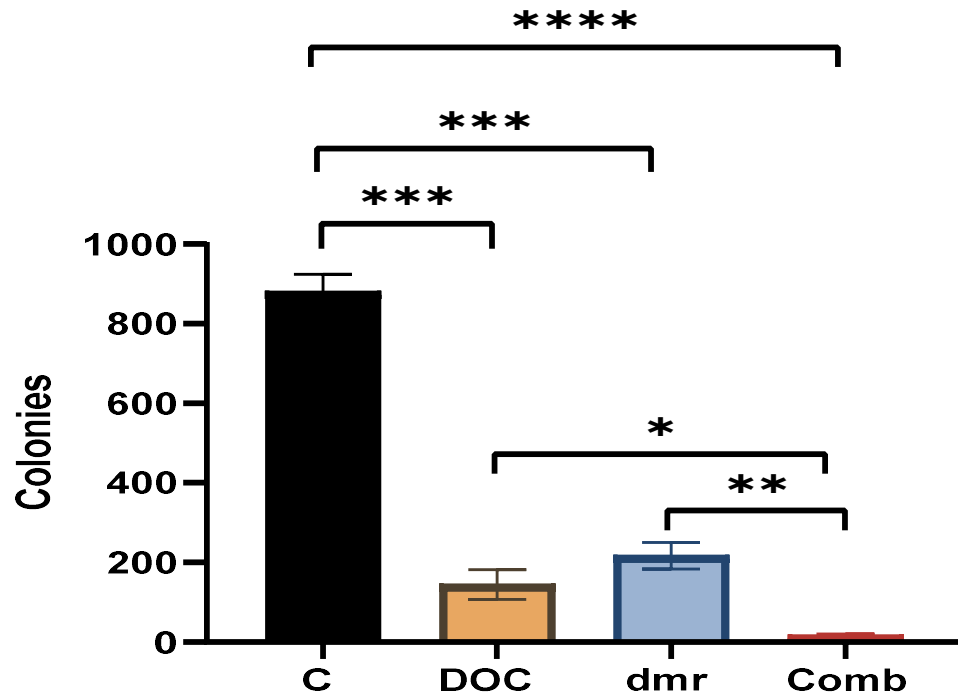


**Figure 4.12** The effect of treatments with dmrFABP5 and docetaxel either singly or in combination on number of colonies formed by DU145 cells. **A)**, representative soft agar plates showing images of the colonies form by DU145 cells after treatments of dmrFABP5 and docetaxel either alone or in combination. **B)**, The quantitative assessment of numbers of colonies formed by DU145 cells after different treatments. Results from each treatment were obtained by calculating triplicate independent expermint (n=3) data and presented as Mean  $\pm$  SE.

#### **4.6.2 The activity of dmrFABP5 to the effect of docetaxel on the colony formation by 22RV1**

DMSO was used to treat the control. Doses of docetaxel and dmrFABP5 used to treat the 22RV1 cells were 4 nM and 10  $\mu$ M, respectively. The doses were used in dmrFABP5 and docetaxel combination treatment. The results of the soft agar assay were shown in Figure 4.13. Images of the cell colonies formed in representative agar plates after different treatments were shown in Figure 4.13A. Quantitative analysis (Figure 4.13B) showed that  $621 \pm 30$  colonies were formed in the control. Docetaxel treatment produced a significantly greater suppression (Student *t*-test  $***P < 0.001$ ) on colony formation than dmrFABP5 with  $119 \pm 11$  and  $354 \pm 28$  colonies, respectively. DmrFABP5 combined with docetaxel produced significantly more suppression (Student *t*-test  $P < 0.0001****$ ) on colony formation with colony number of  $18 \pm 5$  (Table 4.15). Therefore, dmrFABP5 enhanced the suppressive effect of docetaxel significantly (Table 4.16).

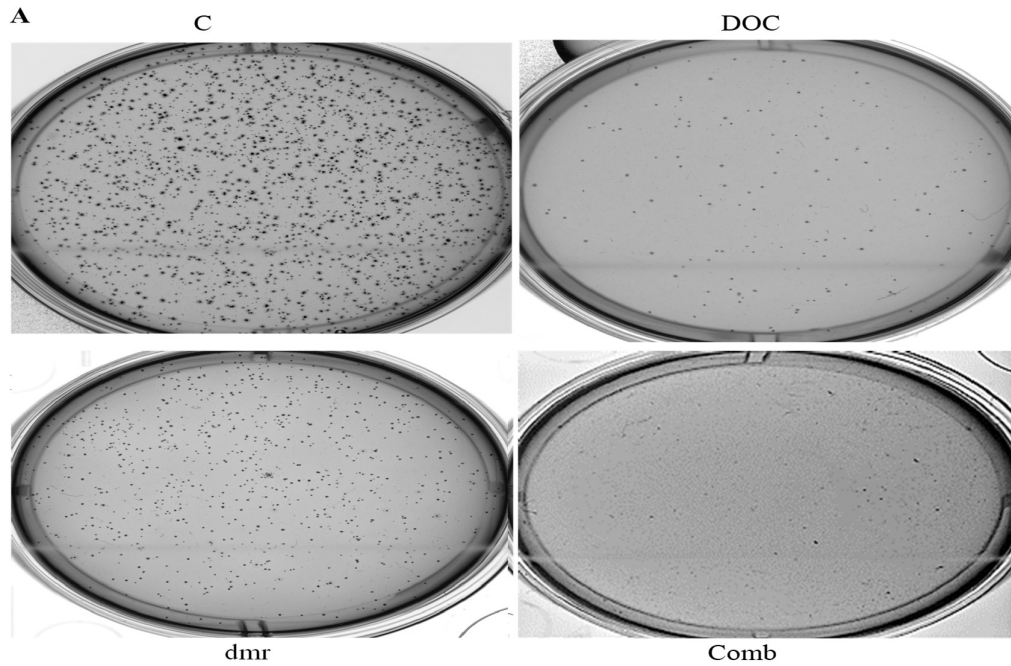
**Table 4.15** The average number of colonies formed by 22RV1 cells after different treatments\*

Treatment groups	Average number of colonies (Mean $\pm$ SE)
<b>Control</b>	<b>621 <math>\pm</math> 30</b>
<b>Docetaxel</b>	<b>119 <math>\pm</math> 11</b>
<b>dmrFABP5</b>	<b>354 <math>\pm</math> 28</b>
<b>Combination</b>	<b>18 <math>\pm</math> 5</b>

**Table 4.16** The Student *t*-test on the mean colony numbers after different treatments+

Treatment comparison	<i>P value</i>
C to DOC	$P = 0.0001^{***}$
C to dmr	$P=0.0030^{**}$
C to Comb	$P<0.0001^{****}$
DOC to dmr	$P=0.0015^{**}$
DOC to Comb	$P=0.0010^{**}$
Dmr to Comb	$P =0.0003^{***}$

+Each experiment was performed in triplicates and the data were presented as mean  $\pm$ SE;  $P<0.05$  was regarded as significant. Degree of significance was presented as number of stars as following: \* $P < 0.05$ , \*\* $P < 0.01$ , \*\*\* $P < 0.001$ , \*\*\*\* $P<0.0001$ . C = control, DOC = docetaxel, dmr = dmrFABP5 and Comb = combination. The colony numbers for C, DOC, dmr and Comb were, 621.66 $\pm$ 30.75, 119.66 $\pm$  10.75, 354 $\pm$ 28, 18 $\pm$ 5, respectively.



**B**

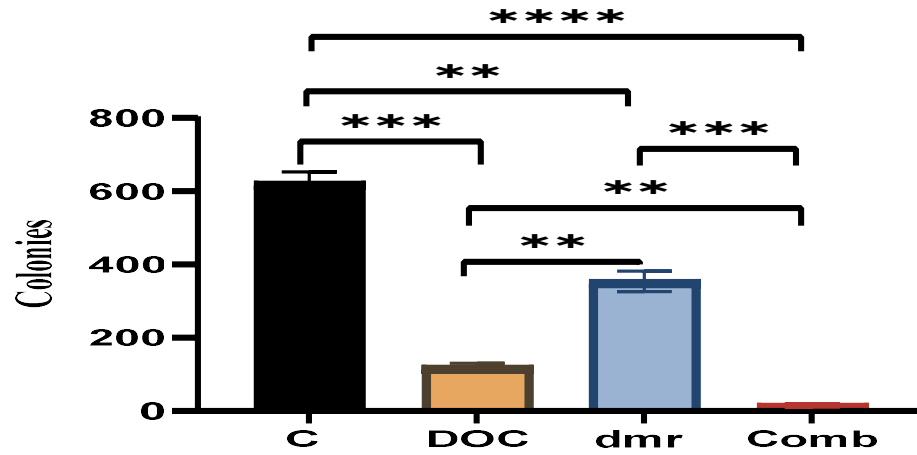


**Figure 4.13** The suppressive activity of dmrFABP5 to effect of docetaxel on 22RV1 cell colony formation. **A)** Images of the colonies formed in each representative plate after different treatment. **B)** Quantitative assessments of the number of colonies formed by 22RV1 cells after

different treatments. All results were obtained by calculating triplicate independent experiments (n=3) assays and presented as mean  $\pm$  SE.

#### 4.6.3 The effect of dmrFABP5 alone, or combined with docetaxel on the colony formation of LNCaP cell

The androgen-dependent growth assay was conducted to test effect of different treatments and the results were shown in Figure 4.14. DMSO was used to treat the control LNCaP cells, 2 nM docetaxel and 20  $\mu$ M dmrFABP5 and a combination of both at these concentrations were used to treat the cells respectively. Images of cell colonies from a representative plate of each treatment were shown in Figure 4.14A. Quantification results (Figure 4.14B) showed that dmrFABP5 had no significant suppression effect (Student *t*-test  $P > 0.05$ ), and the average colonies number obtained after dmrFABP5 treatment was similar to the control as  $290 \pm 12$  and  $299 \pm 45$  respectively. Both docetaxel and combination induced the same suppression effect with  $62 \pm 9$  and  $69 \pm 10$  colonies respectively, as shown in Table 4.17. Thus, as shown in Table 4.18, dmrFABP5 did not significantly enhance the suppressive effect of docetaxel (student *t*-test  $P > 0.05$ ).

**Table 4.17** The average number of colonies formed by LNCaP cells after each treatment\*

Treatment groups	Average number of colonies (Mean $\pm$ SE)
Control	290 $\pm$ 12
Docetaxel	62 $\pm$ 9
dmrFABP5	299 $\pm$ 12
Combination	69 $\pm$ 10

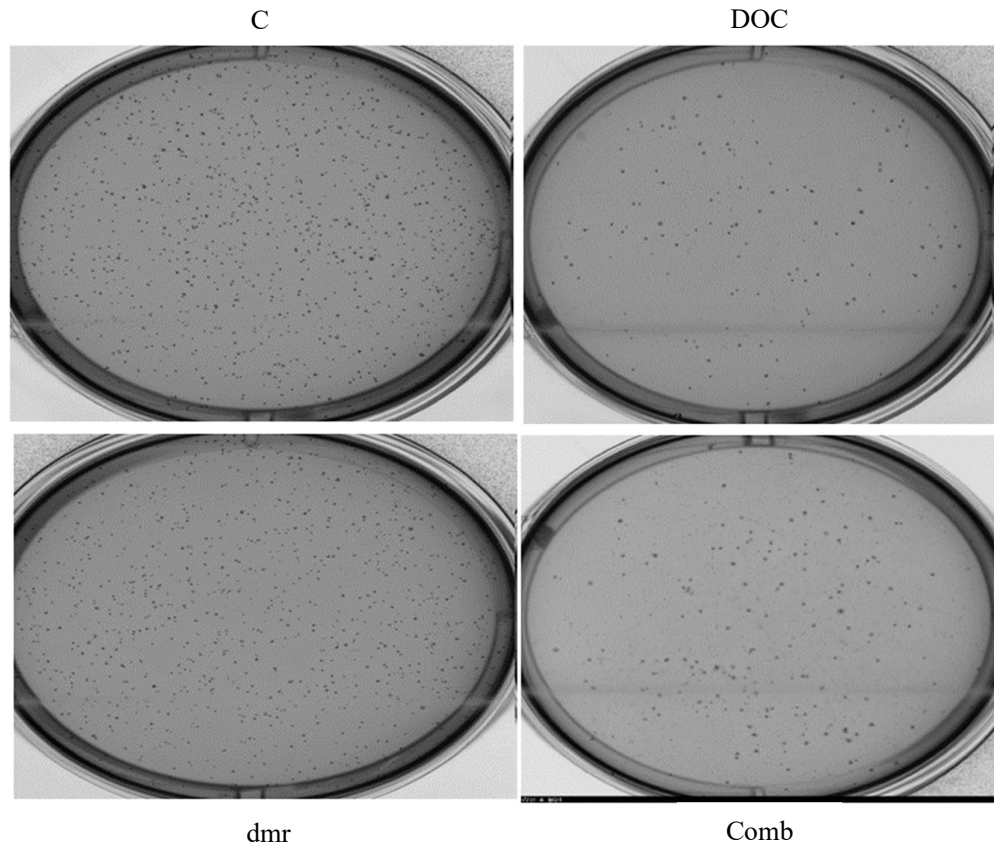
**Table 4.18** The Student *t*-test on the mean numbers of colonies formed by LNCaP cells after different treatments \*

Treatment comparison	<i>P</i> value
C to DOC	<i>P</i> =0.0001***
C to dmr	<i>P</i> >0.05
C to Comb	<i>P</i> =0.0002***
DOC to dmr	<i>P</i> =0.0006***
DOC to Comb	<i>P</i> >0.05
Dmr to Comb	<i>P</i> =0.0008***

\*Each experiment was performed in triplicates and the data were presented as mean  $\pm$ SE; *P*<0.05 was regarded as significant. Degree of significance was presented as number of stars as following: \**P* < 0.05, \*\**P* < 0.01, \*\*\**P* < 0.001, \*\*\*\**P*<0.0001. C = control, DOC = docetaxel, dmr = dmrFABP5 and Comb = combination. The colony numbers for C, DOC, dmr and Comb were, 290  $\pm$ 12, 62  $\pm$  9, 299  $\pm$  45, and 69  $\pm$  10, respectively.



A



B

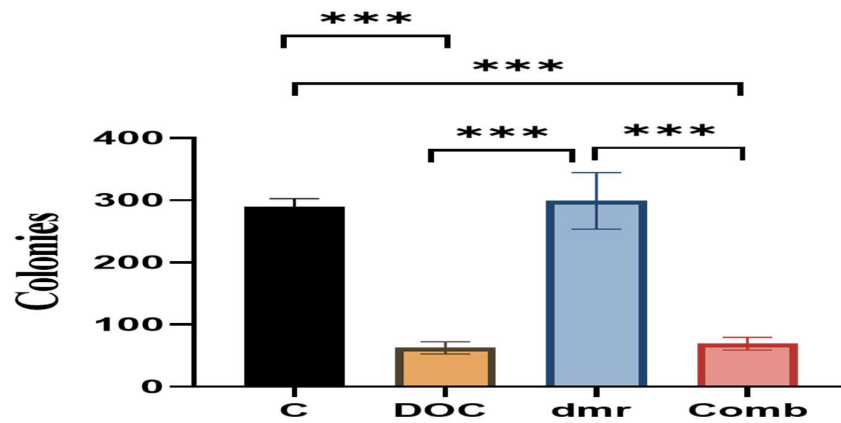


**Figure 4.14** The combined effect of dmrFABP5 with docetaxel on LNCaP cell colony formation. A), images of cell colonies form in the representative plates after treatemnts

with dmrFABP5, docetaxel, or a combination of both. **B**), the quantitative assessment of the colony numbers formed by LNCaP cells after each different treatment. All results were obtained from calculating triplicate independent experiments data (n=3) and presented as (Mean  $\pm$  SE).

#### **4.6.4 The activity of dmrFABP5 combined with enzalutamide on the colony formation of DU145**

DU145 (control) was treated with DMSO. High dose of enzalutamide at 100  $\mu$ M was used to treat androgen-independent DU145. DmrFABP5 at a concentration of 5  $\mu$ M was utilised for this group. For the combination group, 5  $\mu$ M of dmrFABP5 combined with 100  $\mu$ M of enzalutamide were used. Plates were visualized and shown in Figure 4.15A. Quantitative analysis Figure 4.15B showed that, colonies in both control and enzalutamide were  $743 \pm 81$  and  $778 \pm 66$  respectively as enzalutamide did not suppress the DU145 colony formation (Student *t*-test  $P > 0.05$ ) Table 20. DmrFABP5 significantly inhibited the colony formation of DU145 with  $113 \pm 9$  colonies (Student *t*-test  $P < 0.001$ \*\*\*). Slight higher colonies were found in the combination with  $159 \pm 12$  Table 4.19. Thus, dmrFABP5 did not potentiate enzalutamide.

**Table 4.19** DU145 average colonies number after received different treatemnt<sup>+</sup>

Treatment groups	Average number of colonies (Mean±SE)
<b>Control</b>	<b>743 ± 81</b>
<b>Enzalutamide</b>	<b>778 ±66</b>
<b>dmrFABP5</b>	<b>113 ± 9</b>
<b>Combination</b>	<b>159 ± 12</b>

**Table 4.20** Student *t*-test analysis of the means of colons numer of DU145 after different treatments \*

Treatment comparison	<i>P</i> value
C to ENZ	<i>P</i> >0.05
C to dmr	<i>P</i> =0.0005***
C to Comb	<i>P</i> =0.0003***
ENZ to dmr	<i>P</i> =0.0002***
ENZ to Comb	<i>P</i> =0.0008***
Dmr to Comb	<i>P</i> >0.05

\*Each experiment was performed in triplicates and the data were presented as Mean ±SE; a Student *t*-test was used to compare the means. *P*<0.05 was reagrded as significant. Degree of significance was presented as number of stars as following: \**P* < 0.05, \*\**P* < 0.01, \*\*\**P* < 0.001, \*\*\*\**P*<0.0001. Data was assessed as (control, enzalutamide, dmrFABP5 and combination) and evaluated as (743.66±80.68), (778.66±66.11), (113.66±9.14) and (159±12.49) respectevily. Treatment comparisons appointed as C= Control, Enzalutamide= ENZ, dmrFABP5= dmr and Combination= C

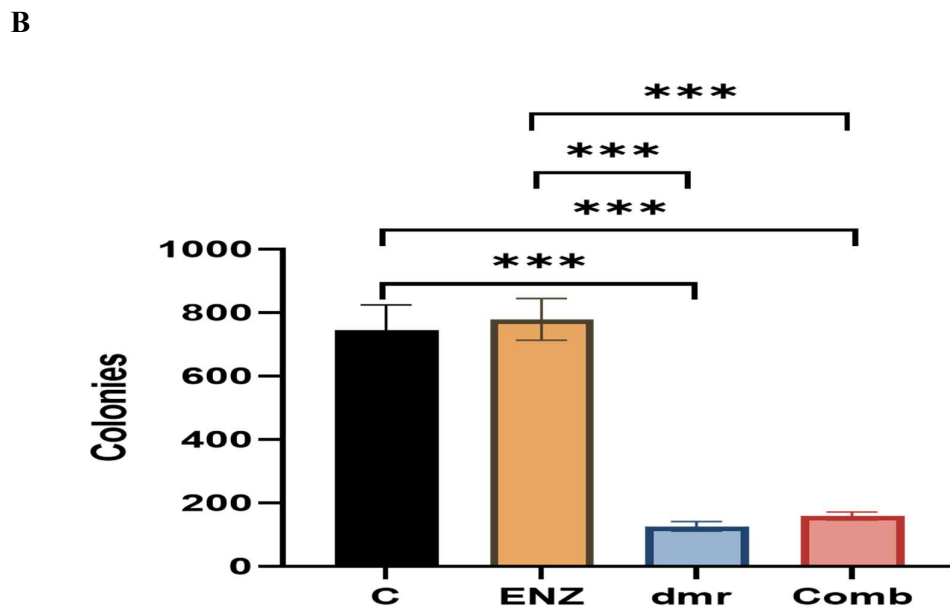
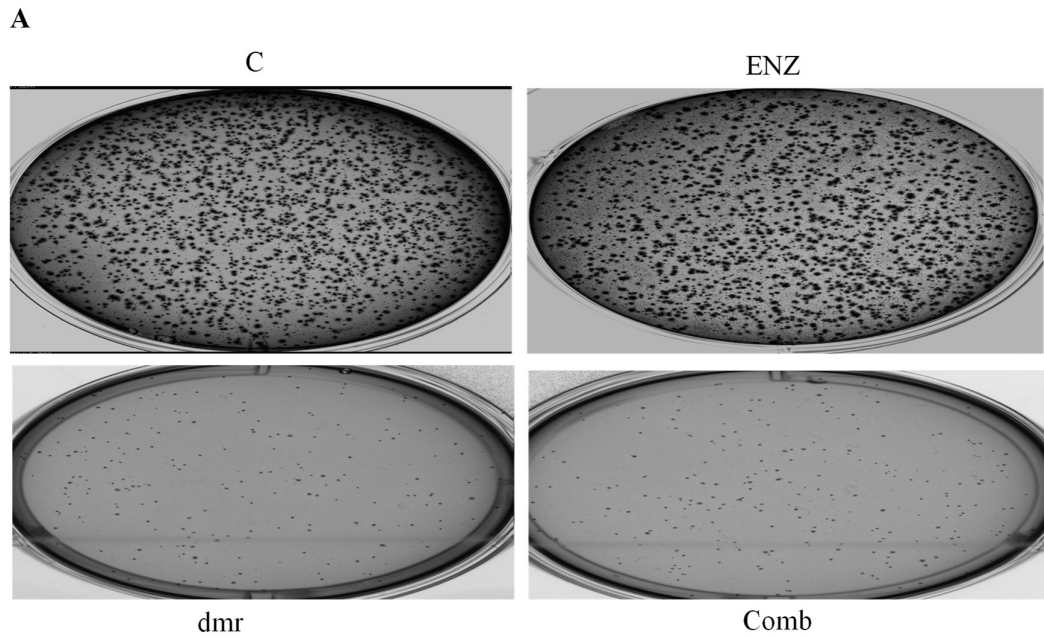


**Figure 4.15** The treatment action of dmrFABP5 plus enzalutamide on colony formation in DU145. A), Coloney formation of DU145 produced by either dmrFABP5 or enzalutamide alone or in combintion. B), The quantitave assessment illustrated the colonies

numbers of each treatment group. All results were performed in triplicate independent experiments (n=3) and presented as (Mean  $\pm$  SE).

#### **4.6.5 The treatment action of dmrFABP5 to enzalutamide on the colony formation abilities of 22RV1**

DMSO was used to treat the control. Enzalutamide was used to treat the cells with 10  $\mu$ M, and dmrFABP5 was utilised at a dose of 10  $\mu$ M. DmrFABP5 at 10  $\mu$ M combined with 10  $\mu$ M of enzalutamide were utilized for the combination. Colonies shown in (Figure 4.16A). Quantitative analysis (Figure 4.16B) showed that the average colonies of control was  $614 \pm 54$  whereas enzalutamide did not significantly effect the tumor growth with  $599 \pm 6.75$  (Student *t*-test  $P > 0.05$ ). DmrFABP5 induced potential suppression on average colonies formation number with  $219 \pm 19$  colonies (Student *t*-test  $P < 0.01^{**}$ ). DmrFABP5 significantly enhanced and induced more potent suppression on the growth and the average colonies number was  $23 \pm 6$  colonies (Student *t*-test  $P < 0.0001^{****}$ ) Table 4.21. Student *t*-test comparisons of the means shown in Table 4.22. Each experiment was performed in triplicates and the data was presented as mean  $\pm$  SE; Student *t*-test was used to compare the means.  $*P < 0.05$ ,  $**P < 0.01$ ,  $***P < 0.001$ ,  $****P < 0.0001$ . Table 4.8 showed an illustration of a comparison for all treatment groups.

**Table 4.21** Average colony formation numbers of 22RV1 after different treatment<sup>†</sup>

Treatment groups	Average number of colonies (mean ± SE)
<b>Control</b>	<b>614 ± 54</b>
<b>Enzalutamide</b>	<b>599 ± 6</b>
<b>dmrFABP5</b>	<b>219 ± 19</b>
<b>Combination</b>	<b>23 ± 6</b>

**Table 4.22** Student *t*-test of the mean of different treatments on the colony formation (22RV1)<sup>†</sup>

Treatment comparison	<i>P</i> value
C to ENZ	<i>P</i> >0.05
C to dmr	<i>P</i> =0.0041**
C to Comb	<i>P</i> <0.0001****
ENZ to dmr	<i>P</i> =0.0032**
ENZ to Comb	<i>P</i> <0.0001****
Dmr to Comb	<i>P</i> =0.0018**

<sup>†</sup>Each experiment was performed in triplicates and the data were presented as mean ±SE; a Student *t*-test was used to compare the means. *P*<0.05 was regarded as significant. Degree of significance was presented as number of stars as following: \**P* < 0.05, \*\**P* < 0.01, \*\*\**P* < 0.001, \*\*\*\**P*<0.0001. Data was assessed as (control, enzalutamide, dmrFABP5 and combination) and evaluated as (614.33±54.13), (599 ± 6.75), (219± 19) and (23.66±5.8) respectively. Treatment comparisons appointed as C=Control, enzalutamide=ENZ, dmrFABP5= dmr and Combination= Comb.

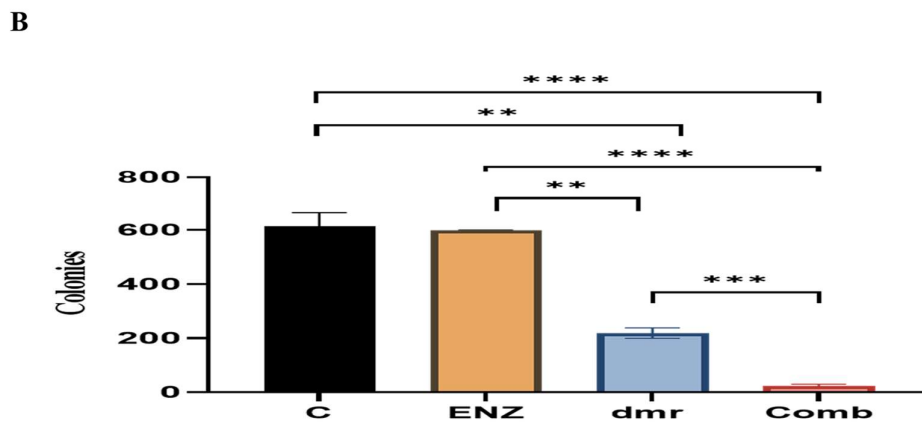
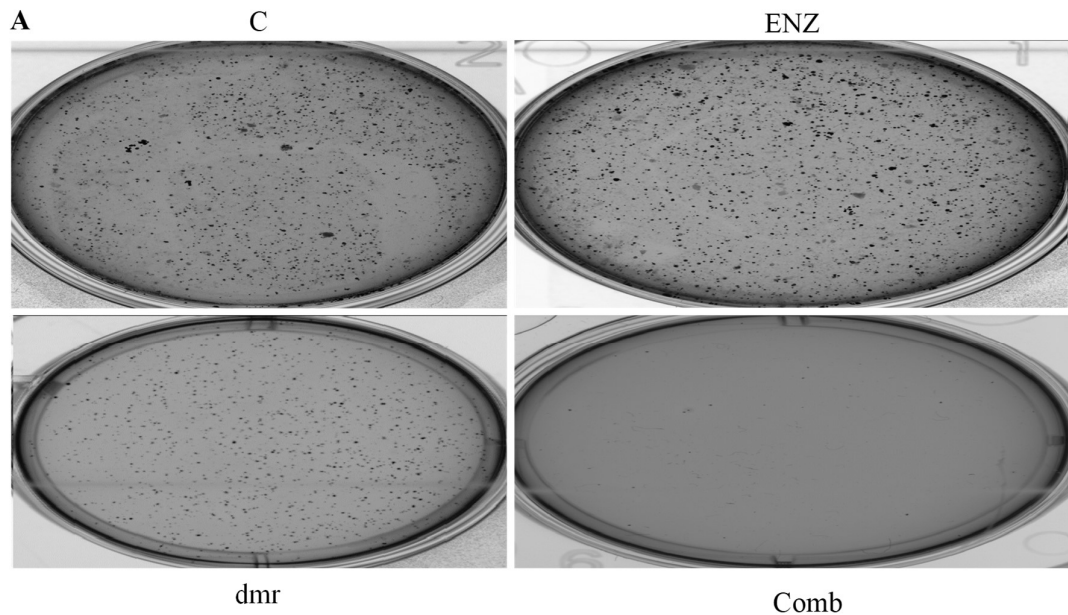


**Figure 4.16** The enhancement effect of dmrFABP5 to enzalutamide on colony formation in 22RV1. A), The effect on colony formation of 22RV1 either dmrFABP5 or enzalutamide alone or in combination. B), The quantitative assessment illustrated the colonies numbers of each treatment group. All results were performed in triplicate independent experiments (n=3) and presented as (Mean ± SE).

#### 4.6.6 The effect of dmrFABP5 to the suppressive effect of enzalutamide on the colony formation of LNCaP

LNCaP was treated with DMSO for control, 100 nM for enzalutamide, 20  $\mu$ M for dmrFABP5 and combining of both with same concentrations mentioned. Different plates contained different treatments were shown in Figure 4.17A. Quantification results (Figure 4.17B) showed that both control and dmrFABP5 colonies number were similar  $380 \pm 21$  and  $394 \pm 26$  respectively and no significant suppression was found from dmrFABP5. Both enzalutamide and combination induced same suppression effect with  $67 \pm 6$  and  $68 \pm 7$  colonies respectively ( $P < 0.001^{***}$ ) Table 4.23. Thus, dmrFABP5 did not enhance the suppressive effect of enzalutamide student *t*-test  $P > 0.05$  Table 4.24

**Table 4.23** The average colons number of LNCaP\*

Treatment groups	Average number of colonies (Mean $\pm$ SE)
Control	$380 \pm 21$
Enzalutamide	$67 \pm 6$
dmrFABP5	$394 \pm 26$
Combination	$68 \pm 7$



**Table 4.24** Illustration of Student *t*-test of the means different treatment on LNCaP in soft agar assay\*

Treatment comparison	<i>P</i> value
C to ENZ	<i>P</i> =0.0001***
C to dmr	<i>P</i> >0.05
C to Comb	<i>P</i> =0.0002***
ENZ to dmr	<i>P</i> =0.0003***
ENZ to Comb	<i>P</i> >0.05
Dmr to Comb	<i>P</i> =0.0003***

\*Each experiment was performed in triplicates and the data were presented as mean  $\pm$ SE; a Student *t*-test was used to compare the means. *P*<0.05 was regarded as significant. Degree of significance was presented as number of stars as following: \**P* < 0.05, \*\**P* < 0.01, \*\*\**P* < 0.001, \*\*\*\**P*<0.0001. Data was assessed as (control, enzalutamide, dmrFABP5 and combination) and evaluated as (380 $\pm$ 21.16), (67 $\pm$ 6.6), (394 $\pm$ 26.96) and (68 $\pm$ 7.211) respectively. Treatment comparisons appointed as C= Control, Enzalutamide=ENZ, dmrFABP5= dmr and Combination= Comb.

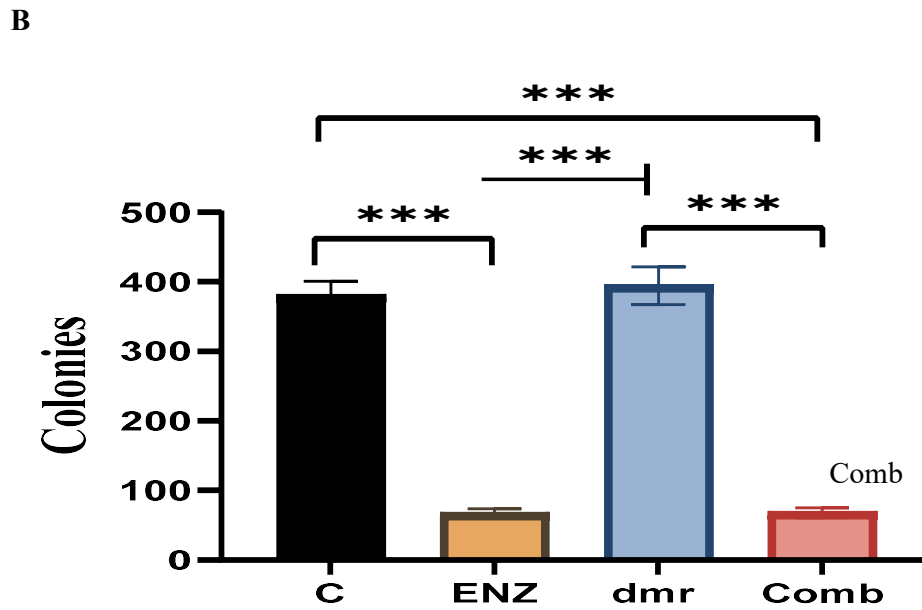
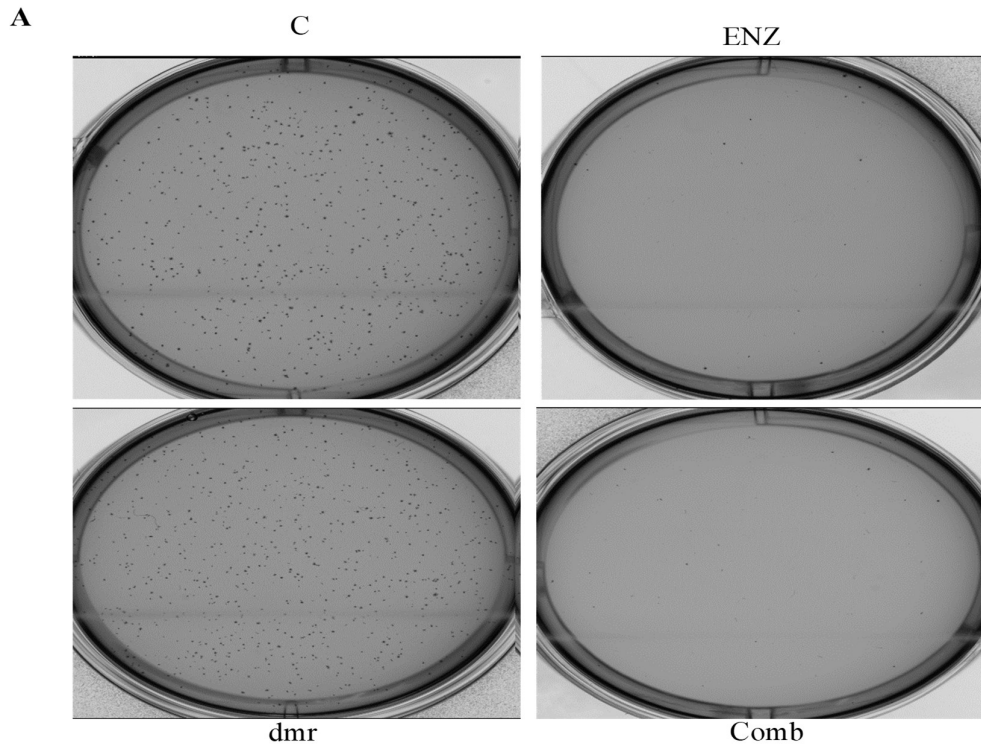


**Figure 4.17** The effect of dmrFABP5 combined with enzalutamide on colony formation in LNCaP. A), The effect on colony formation of LNCaP either dmrFABP5 or enzalutamide alone or in combinatio. B), The quantitive assessment illustrated the colonies numbers of each

treatment group. All results were performed in triplicate independent experiments (n=3) and presented as (Mean  $\pm$  SE).

## **4.7 Discussion**

The study conducted by Wassem et al. demonstrated that dmrFABP5 effectively inhibited the biological characteristics associated with prostate cancer PCa (175). The study investigated the effects of dmrFABP5, docetaxel, and enzalutamide on various prostate cancer cell lines. In DU145 cells, the combination of dmrFABP5 and docetaxel significantly suppressed cell motility by 93%, which was greater than the sum of the effects of each compound alone. However, combining dmrFABP5 with enzalutamide did not produce a significant additional reduction in cell motility compared to dmrFABP5 treatment alone. This suggests that enzalutamide did not affect the migration of AR-negative DU145 cells. In 22RV1 cells, combining dmrFABP5 with docetaxel resulted in a significant suppression of cell migration, while combining it with enzalutamide showed an even greater inhibitory effect. In LNCaP cells, neither the combination of dmrFABP5 with docetaxel nor with enzalutamide enhanced their suppressive effects on cell migration.

Regarding cell invasion, dmrFABP5 enhanced the suppressive effect of docetaxel on DU145 cells but did not show additional suppression when combined with enzalutamide. In 22RV1 cells, the combination of dmrFABP5 and enzalutamide resulted in a greater inhibition of cell invasion compared to either compound alone. However, in LNCaP cells, dmrFABP5 did not enhance the suppressive effects of either docetaxel or enzalutamide on cell invasion.

The anchorage-independent growth, dmrFABP5 enhanced the inhibitory effect of docetaxel on DU145 colony formation, but there was no significant enhancement when combined with enzalutamide. In 22RV1 cells, combining dmrFABP5 with either docetaxel or enzalutamide showed synergistic effects and greater suppression of colony formation. However, in LNCaP cells, dmrFABP5 did not significantly enhance the suppressive effects of docetaxel or enzalutamide on colony formation.

Overall, dmrFABP5 showed variable effects when combined with docetaxel or enzalutamide in different prostate cancer cell lines, suggesting its effectiveness may depend on the specific cellular context and AR expression.

## **Chapter 5**

**Result-3: The molecular mechanism involved in the interactions of the compounds in prostate cancer cells**

## 5.1 Introduction

The elevated expression of FABP5 has been linked to higher proliferation in prostate cancer as well as a poor prognosis in patients with the disease due to the dysregulation of lipid signalling (161,197). It was recently demonstrated that increased expression of oncogenic cytoplasmic FABP5 and nuclear PPAR $\gamma$  in CRPC cells is significantly associated. The elevated levels of both proteins were related to an increase in GS and were correlated with decreased patient survival (143). It has been established that fatty acids transported by FABP5 stimulate PPAR $\gamma$ , resulting in the activation of the FABP5-PPAR $\gamma$ -VEGF signaling transduction axis, which is a major signaling transduction axis pathway in promoting the malignant progression of CRPC cells (156). Previous research also demonstrated that inhibition of FABP5 or PPAR $\gamma$  expression by RNA interference in CRPC cells decreased in vitro invasiveness and suppressed mouse model tumorigenicity (157,159,160). Additionally, our previous group showed that dmrFABP5 significantly suppressed the protein levels of PPAR $\gamma$ , p-PPAR $\gamma$  and VEGF (160,175). The anti-neoplastic agent docetaxel play a significant role in treating prostate cancer by blocking the growth of the tumor and help to suppress the cancer proliferation. This drug used as a chemotherapy for hormone-refractory metastatic prostate cancer. It,s main molecular mechanism role is hyperstabilisation of microtubules by binding to beta-tubuline subunit of microtubulie which lead to cell cycle arrest and eventually apoptosis (198-200). The anti-androgen drug enzalutamide on the other hand works by blocking the androgen supply leading to treating prostate cancer. It is a hormone therapy that treat the cancer in advance level when the cancer spread to other parts of the body(188,201). It can be given for CRPC patients as a part of ADT to treat metastasis CRPC and for patients who recently received docetaxel (202). Androgen splice variant 7 has been linked to enzalutamide resistance (203). However, over the course of time, it is inevitable that every

patient will acquire resistance to the therapy, and their illness will continue to worsen (204).

## **5.2 Aim of the study**

The primary objective of this chapter is to investigate the molecular mechanisms involved in the potent synergistic interaction observed when dmrFABP5 is combined with docetaxel or enzalutamide in prostate cancer cells. Prostate cancer is a prevalent malignancy, and despite recent advancements in treatment strategies, there is a critical need to develop innovative therapeutic approaches to enhance patient outcomes. The findings from this study will provide valuable insights into the specific molecular pathways modulated by dmrFABP5 in conjunction with docetaxel or enzalutamide, leading to a better understanding of their combined therapeutic effects. Ultimately, our research aims to pave the way for the development of more effective and personalized treatment strategies for prostate cancer patients, with the potential to improve clinical outcomes and quality of life.

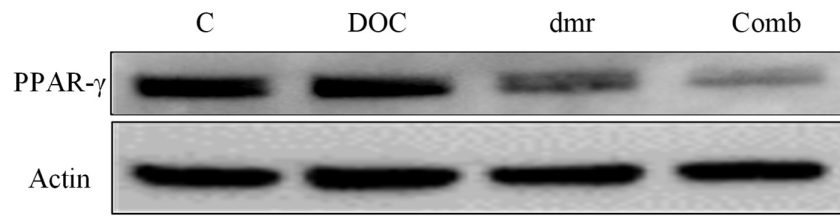
### **5.3 Investigating the molecular mechanism involved in the biological activity of dmrFABP5 on the effect of docetaxel on DU145**

#### **5.3.1 The effect of dmrFABP5 alone, or combined with docetaxel on PPAR $\gamma$ and p-PPAR $\gamma$ levels on DU145**

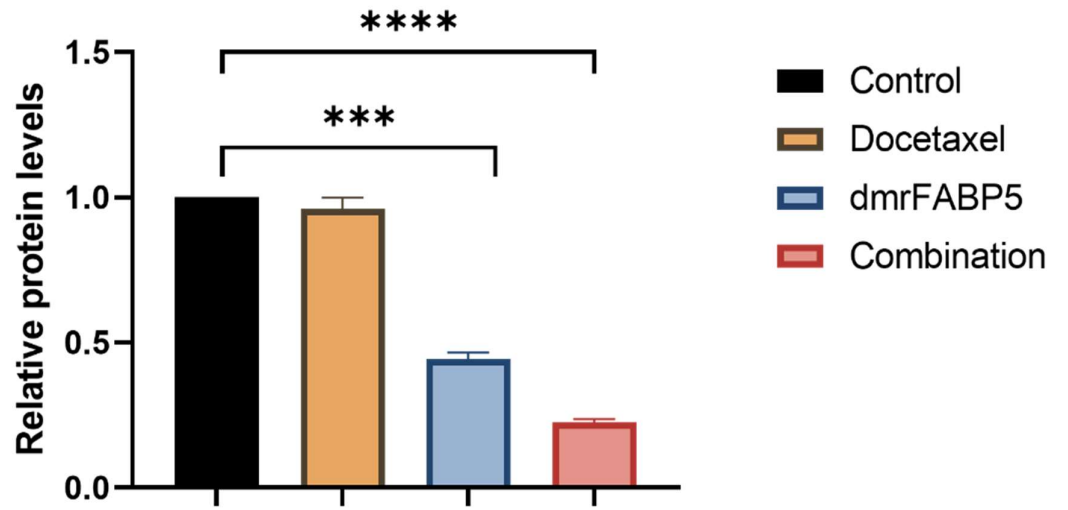
The potential effect of dmrFABP5 and docetaxel on PPAR $\gamma$  or phosphorylated PPAR $\gamma$  (p- PPAR $\gamma$ ) levels in DU145 cells were shown in Figure 5.1. Western blot analyses of the expressions of PPAR $\gamma$  and p-PPAR $\gamma$  in the cells treated with docetaxel, dmrFABP5, and the combination of both were shown in Figure 5.1A and 1C. The results of quantitative analysis were shown in Figure 5.1B and D. When the levels in the control were set at 1, respectively, the level of PPAR $\gamma$  ( $0.96 \pm 0.02$ ) was not significantly changed by docetaxel treatment ( $P > 0.05$ ), but docetaxel treatment significantly ( $P < 0.01^{**}$ ) decreased the level ( $0.75 \pm 0.005$ ) of p- PPAR $\gamma$  by 25%. As expected, dmrFABP5 significantly (Student t-test  $P < 0.001^{***}$ ) decreased the levels of both PPAR $\gamma$  and p- PPAR $\gamma$  by 56% and 35% to  $0.44 \pm 0.01$  and  $0.65 \pm 0.01$ , respectively. The combination treatment induced greater suppressions on levels of both PPAR $\gamma$  and p- PPAR $\gamma$  by 78% and 74%, with reduced expression levels  $0.22 \pm 0.007$  and  $0.26 \pm 0.01$  respectively. Thus, dmrFABP5 plus docetaxel produced higher downregulation effect on both PPAR $\gamma$  and p-PPAR $\gamma$  than those produced by each of the agents used separately ( $P < 0.0001^{****}$ ).



A



B



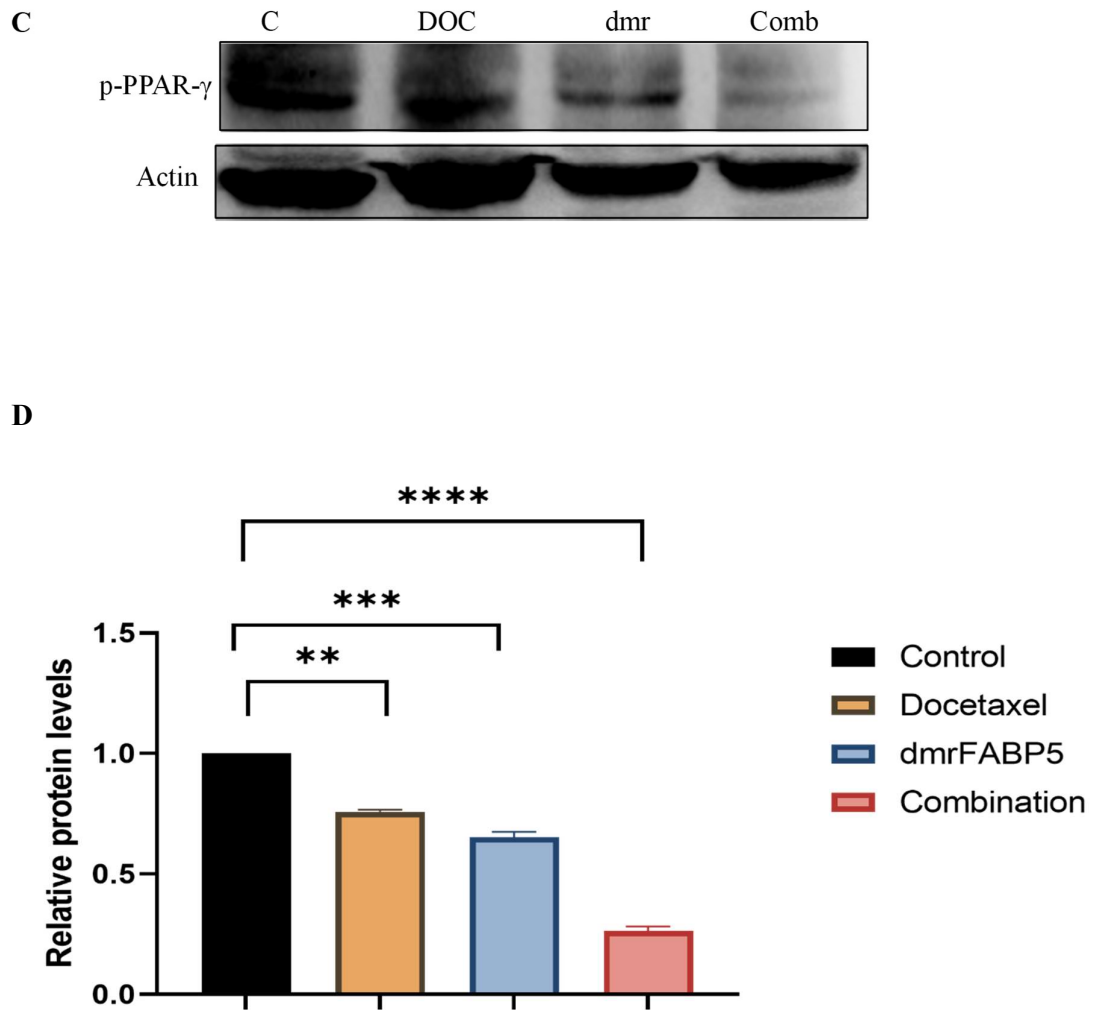
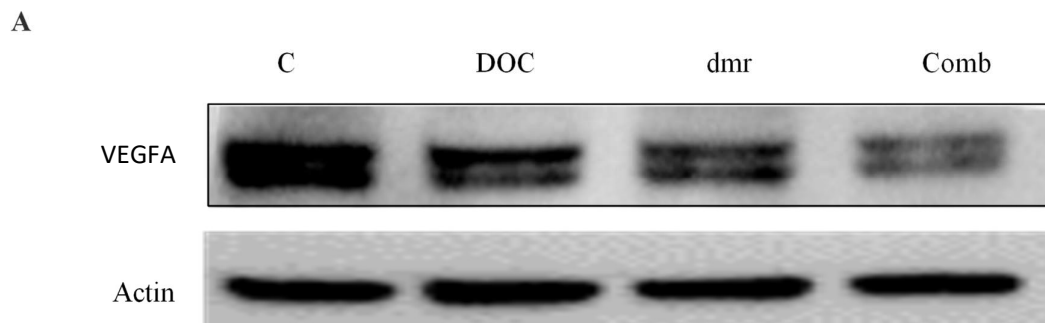


**Figure 5.1** The effect of dmrFABP5 and docetaxel on expression levels of PPAR $\gamma$  and p-PPAR $\gamma$  in DU145 cells. **A)** PPAR $\gamma$  expression in DU145 cells after each of the different treatments. **B)** Relative PPAR $\gamma$  levels in DU145 cells after each of the different treatments. **C)** p-PPAR $\gamma$  expression in DU145 cells after each of the different treatments. **D)** Relative p-PPAR $\gamma$  levels in DU145 cells after each of the different treatments. To normalize possible loading errors, anti- $\beta$ -actin was used to hybridize the blot. The intensities of the bands on the blot were subjected to densitometrical scanning and analysed with the Image-J software. Each experiment (Mean  $\pm$  SE) was performed in triplicate, the error of the mean values were calculated and data was obtained from three independent experiments (n=3).

### 5.3.2 The enhancement effect of dmrFABP5 to docetaxel on suppressing VEGFA expression in DU145

The bioactivity of dmrFABP5 on the effect of docetaxel on the expression of VEGFA in DU145 was measured by Western blot and the results were shown in Figure 5.2. Western blot analysis showed (Figure 5.2A) that in comparison with the control (treated with DMSO), treatments of the cells with either docetaxel (3nM), dmrFABP5 (5  $\mu$ M) separately or in combination of both reduced the VEGFA expression. As shown in Figure 5.2B, when the level of VEGF was set at 1, docetaxel treatment significantly reduced (Student *t*-test  $P < 0.01^{**}$ ), VEGF level by 34% to  $0.64 \pm 0.025$ , while dmrFABP5 produced similar suppressive effect with a relative VEGFA level of  $0.6 \pm 0.06$  which was significantly reduced by 40% from that of the control (Student *t*-test  $P < 0.01^{**}$ ). The combination treatment produced a highly significant suppression on VEGFA level by 65% to  $0.35 \pm 0.01$  ( $P < 0.001^{***}$ ).



**B**

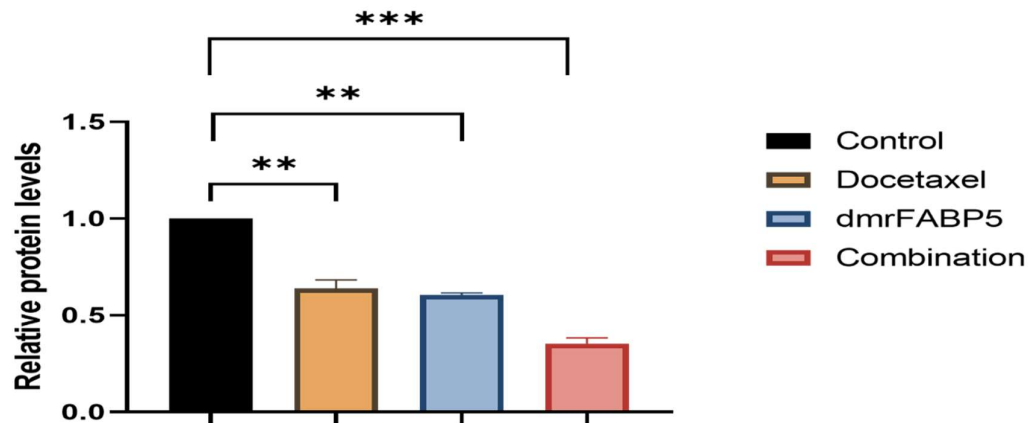


**Figure 5.2** The activity of dmrFABP5 to the effect docetaxel on VEGFA. **A)** Western blot analysis of VEGFA expression in DU145 cells after different treatments. **B)** Relevant levels of VEGFA after different treatments. To normalize possible loading errors, anti- $\beta$ -actin was used to hybridize the blot. The intensities of the bands on the blot were subjected to densitometrical scanning and analysed with the Image-J software. Each experiment (Mean  $\pm$  SE) was performed in triplicate, the error of the mean values were calculated and data was obtained from three independent experiments (n=3).

### **5.3.3 The effect of dmrFABP5 combined with docetaxel on Sp1 expression in DU145**

The control (DU145) was treated with DMSO. Doses of docetaxel and dmrFABP5 used to treat the cells were 3 nM and 5  $\mu$ M, respectively. The effect of treating the cells with docetaxel, dmrFABP5, or the combination of both on Sp1 expression was shown in Figure 5.3. Western blot analysis of Sp1 expression in DU145 cells after each different treatment was shown in Figure 5.3A. When the level of Sp1 in the control cells was set at 1 (Figure 5.3B), docetaxel inhibited the expression of Sp1 significantly by 54% to a relative level of  $0.46 \pm 0.07$  (Student *t*-test  $P < 0.001$ \*\*\*), whereas the dmrFABP5 treatment reduced Sp1 level slightly more by 43% to  $0.57 \pm 0.02$  ( $P < 0.01$ \*\*). The combination treatment with both agents high significantly reduced the level of Sp1 by 88%% to  $0.12 \pm 0.03$  ( $P < 0.0001$ \*\*\*\*). This scale of suppression was more than sum of the those obtained by 2 separate treatments, each with one agent.

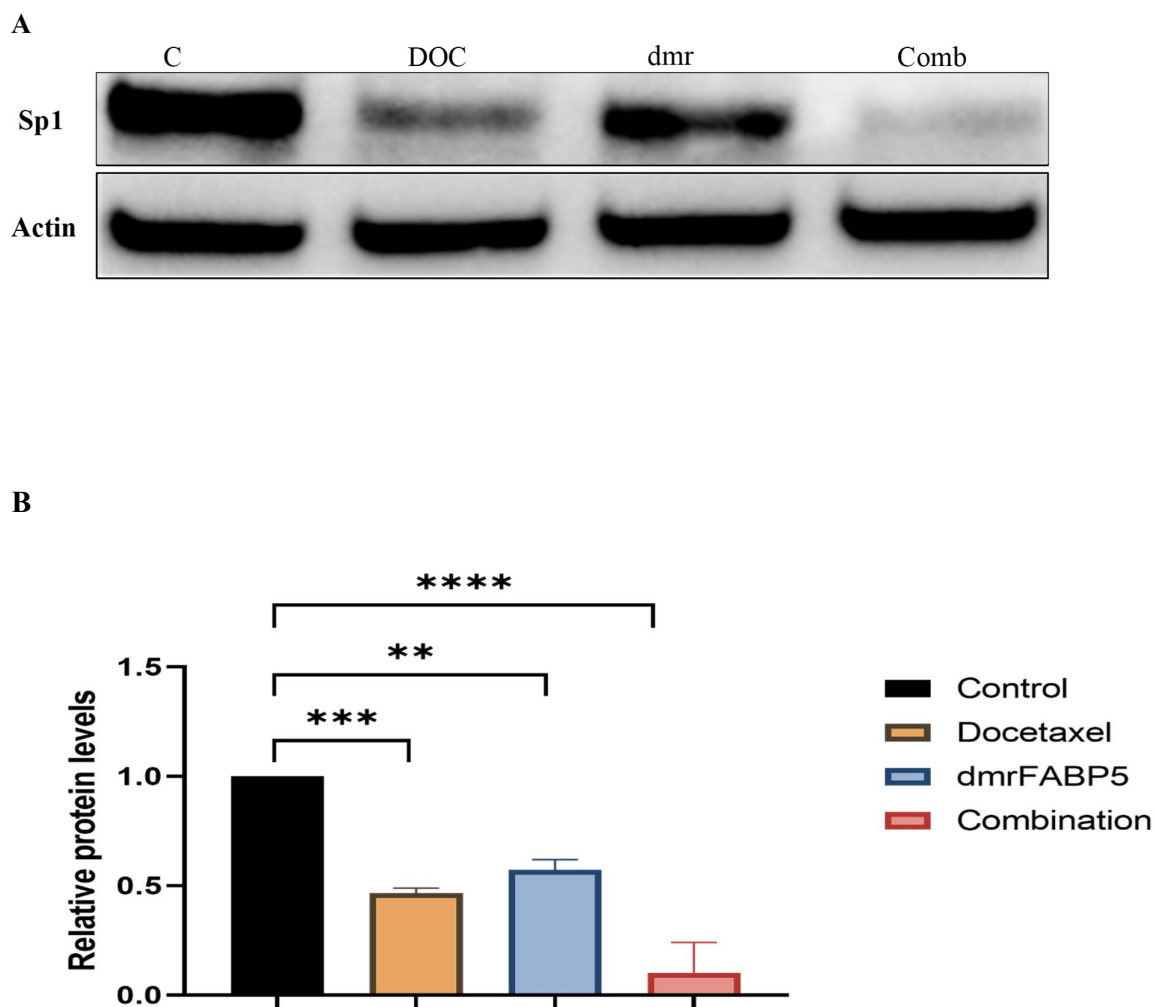
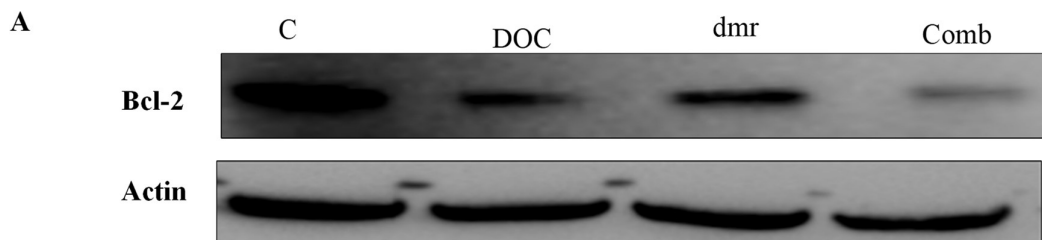


**Figure 5.3** The suppressive effect of dmrFABP5 and docetaxel on Sp1 expression in DU145 cells. **A)** Western blot detection of Sp1 expression in DU145 cells after different treatments. **B)** Relative levels of Sp1 expression in DU145 cells after different treatments. Anti- $\beta$ -actin was used to hybridise the blot to normalize for possible loading errors. The intensities of the bands on the blot were subjected to densitometry scanning and analysed by Image-J software. Each experiment (Mean  $\pm$  SE) was performed in triplicate, the error of the mean values were calculated and data was obtained from three independent experiments (n=3).

### 5.3.4 The effect of dmrFABP5 alone, or combined with docetaxel on Bcl-2 expression in DU145 cells

DU145 was treated with DMSO as control. The effect on Bcl-2 expression produced by treatment with docetaxel at 3nM, dmrFABP5 at 5  $\mu$ M, or combination of both, was tested and the results were shown in Figure 5.4. Western blot detection of Bcl-2 expression in DU145 cells after different treatments was shown in Figure 5.4A. When the level of Bcl-2 expression in the control was set at 1(Figure 5.4B), the relative level of Bcl-2 after docetaxel treatment significantly reduced by 63% to a relative level of  $0.37 \pm 0.02$  ( $P < 0.001$ \*\*\*); while dmrFABP5 treatment produced a significant reduction in Bcl-2 level by 51% to  $0.49 \pm 0.04$  ( $P < 0.01$ \*\*). The joint treatment of both compounds reduced the Bcl-2 level high significantly ( $P < 0.0001$ \*\*\*\*) by 87% to  $0.13 \pm 0.3$ , which was similar to the sum of each agent alone.



**B**

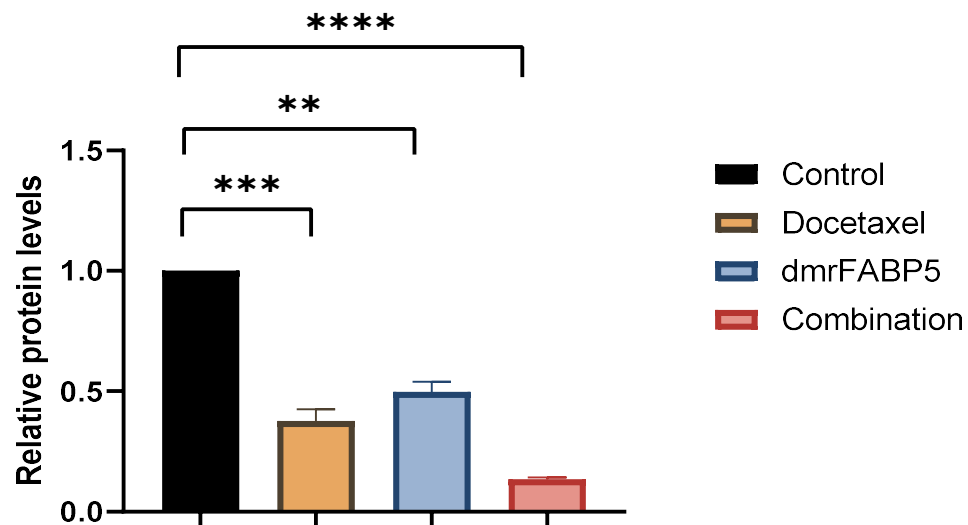


**Figure 5.4** The effect of dmrFABP5 and docetaxel on Bcl-2 expression in DU145 cells.

**A)** Western blot detection of Bcl-2 expression in DU145 cells after treatment with dmrFABP5, docetaxel and combination of both. **B)** Relative levels of Bcl-2 expression in DU145 cells after different treatments. To normalize possible loading errors, anti- $\beta$ -actin was used to hybridize the blot. The intensities of the bands on the blot were subjected to densitometrical scanning and were analysed by Image-J software. Each experiment (Mean  $\pm$  SE) was performed in triplicate, the error of the mean values were calculated and data was obtained from three independent experiments (n=3).

### **5.3.5 The effect of dmrFABP5 and docetaxel on BAX expression in DU145 cells**

DU145 was treated with DMSO as control. The effect of treating DU145 with docetaxel (3nM), dmrFABP5 (5  $\mu$ M), or the combination of both on BAX expression was tested and the results were shown in Figure 5.5B. Western blot detection of BAX expression in



DU145 cells after different treatments was shown in Figure 5.5A. When the level of BAX expressed in the control was set at 1 (Figure 5.5B), the BAX level after the docetaxel treatment was significantly increased ( $P < 0.01^{**}$ ) by 183% to  $1.83 \pm 0.0595$ ; while dmrFABP5 treatment produced even a greater increase ( $P < 0.001^{***}$ ) in BAX level by 263% to  $2.63 \pm 0.047$ . The combination treatment increased significantly ( $P < 0.0001^{****}$ ) the level of BAX more than the sum of each agent alone by 330% to a relative level of  $3.3 \pm 0.09$ .

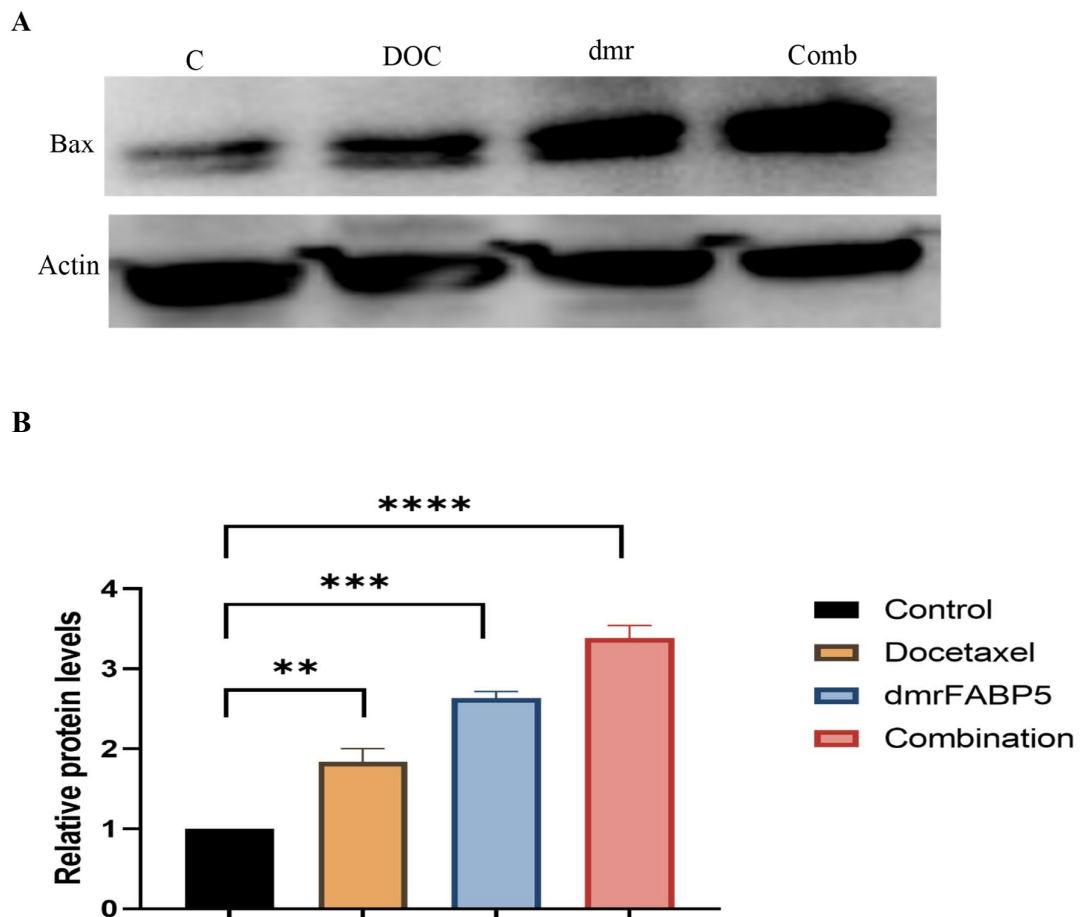


**Figure 5.5** The effect of dmrFABP5 and docetaxel on BAX expression in DU145 cells.

**A)** Western blot detection of BAX expression in DU145 cells after the treatment with dmrFABP5 and docetaxel either individually or in combination. **B)** The relative levels of

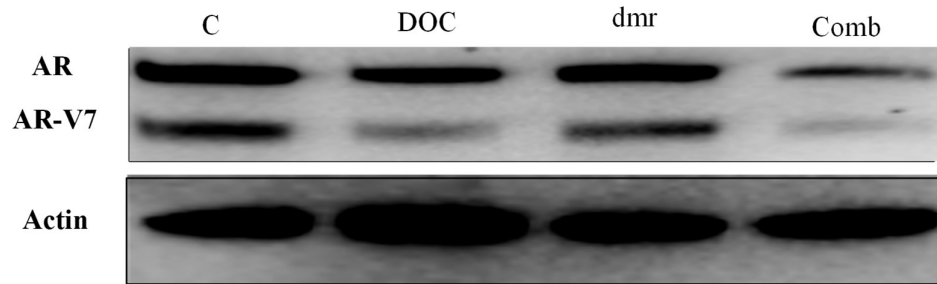
BAX expressed in DU145 cells after each of the different treatments. Anti- $\beta$ -actin was used to hybridise the blot to normalize possible loading errors. The intensities of the bands on the blot were subjected to densitometry scanning and were analysed by Image-J software. Each experiment (Mean  $\pm$  SE) was performed in triplicate, the error of the mean values were calculated and data was obtained from three independent experiments (n=3).

#### **5.4 Investigating the molecular mechanism involved in the biological activity of dmrFABP5 to the effect of docetaxel on 22RV1 cells**

#### **5.5 The effect of dmrFABP5 alone, or in combination with docetaxel on AR or AR-V7 expression in 22RV1 cells**

The androgen-responsive 22RV1 cells were treated with DMSO as a control. Docetaxel and dmrFABP5 were used respectively at 4nM and 10 $\mu$ M either singly or in combination to treat the 22RV1 cells to assess the effect on AR or AR-V7 expression. The results were shown in Figure 5.6. The effect of different treatments was detected by Western blot as shown in Figure 5.6A. The relative levels of the AR or AR-V7 expression were shown in Figure 5.6B. When the level of AR and AR-V7 in the control was respectively set at 1, both docetaxel (DOC) ( $P<0.05^*$ ) and dmrFABP5 (dmr) ( $P<0.05^*$ ) significantly reduced the level of AR expression by 32% and 22% to  $0.68\pm 0.027$  and  $0.78\pm 0.018$  respectively. Whereas docetaxel ( $P<0.001^{***}$ ) and dmrFABP5 ( $P<0.01^{**}$ ) downregulated the levels of AR-V7 by 66%% and 43% to  $0.34\pm 0.017$  and  $0.57\pm 0.030$  respectively. The combination (Comb) treatment of both compounds promoted a greater suppressive effect on both AR and AR-V7 levels by 75% and 92% to  $0.25\pm 0.039$  and  $0.089\pm 0.006$  respectively ( $P<0.0001^{***}$ ).

A



B

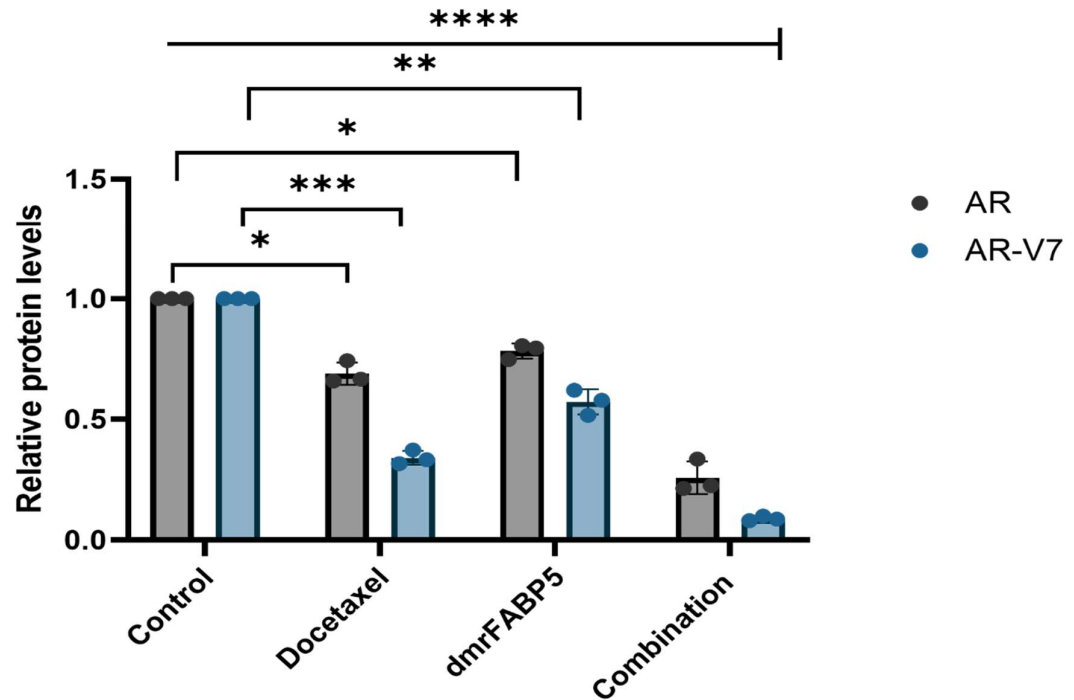


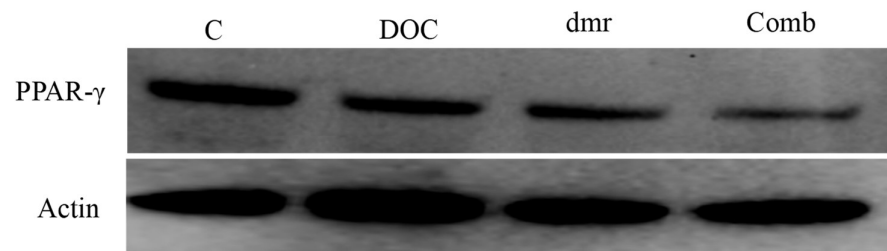
**Figure 5.6** The effect of dmrFABP5 alone, or in combination with docetaxel on expression levels of AR and AR-V7. **A)** Western blot detection of AR and AR-V7 expression in 22RV1 cells after different treatments. **B)** Relevant levels of AR and AR-V7 after different treatments. To normalize possible loading errors, anti- $\beta$ -actin was used to hybridize the blot. The bands on the blot were subjected to densitometry scanning and

analysed by Image-J software. Each experiment (Mean  $\pm$  SE) was performed in triplicate, the error of the mean values were calculated and data was obtained from three independent experiments (n=3).

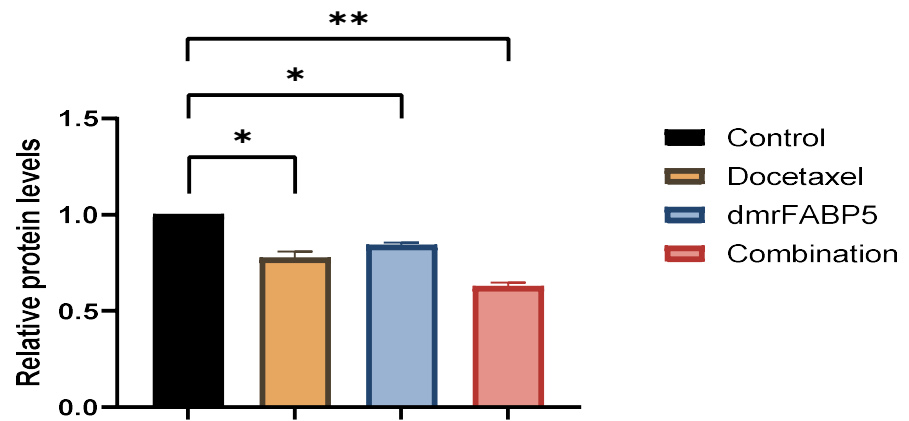
### **5.5.1 The effect of treatments with dmrFABP5 alone, or in combination with docetaxel on levels of PPAR $\gamma$ and p-PPAR $\gamma$ expressed in 22RV1 cells**

22RV1 (control) was treated with DMSO, either docetaxel at 4 nM, or dmrFABP5 at 10 $\mu$ M and a combination of both, and their effect on levels PPAR $\gamma$  and p-PPAR $\gamma$  was detected with Western blot and the results were shown in Figure 5.7. Images of the blot after different treatments were shown in Figures 5.7A and C. The results of western blot (Figure 5.7B and D) showed that, when the relative levels of PPAR $\gamma$  and p-PPAR $\gamma$  in the control were set at 1, docetaxel (DOC) significantly reduced the level of PPAR $\gamma$  by 23% to 0.774 $\pm$ 0.024 student *t*-test ( $P > 0.05^*$ ) and slightly downregulated p-PPAR $\gamma$  by 19% to 0.75 $\pm$ 0.045 ( $P < 0.05^*$ ), whereas dmrFABP5 (dmr) reduced the expression levels of both protein regulators PPAR $\gamma$  ( $P < 0.05^*$ ) and p-PPAR $\gamma$  ( $P < 0.001^{***}$ ) by 16% and 61% to 0.84 $\pm$ 0.010 and 0.38 $\pm$ 0.055 respectively. The combination (Comb) treatment produced greater reductions ( $P < 0.0001^{****}$ ) both on PPAR $\gamma$  and p-PPAR $\gamma$  levels, which are greater than the total reduction produced by the sum of each agent by 37% and 82% to 0.62 $\pm$  0.015 and 0.18 $\pm$ 0.037 respectively.

A



B



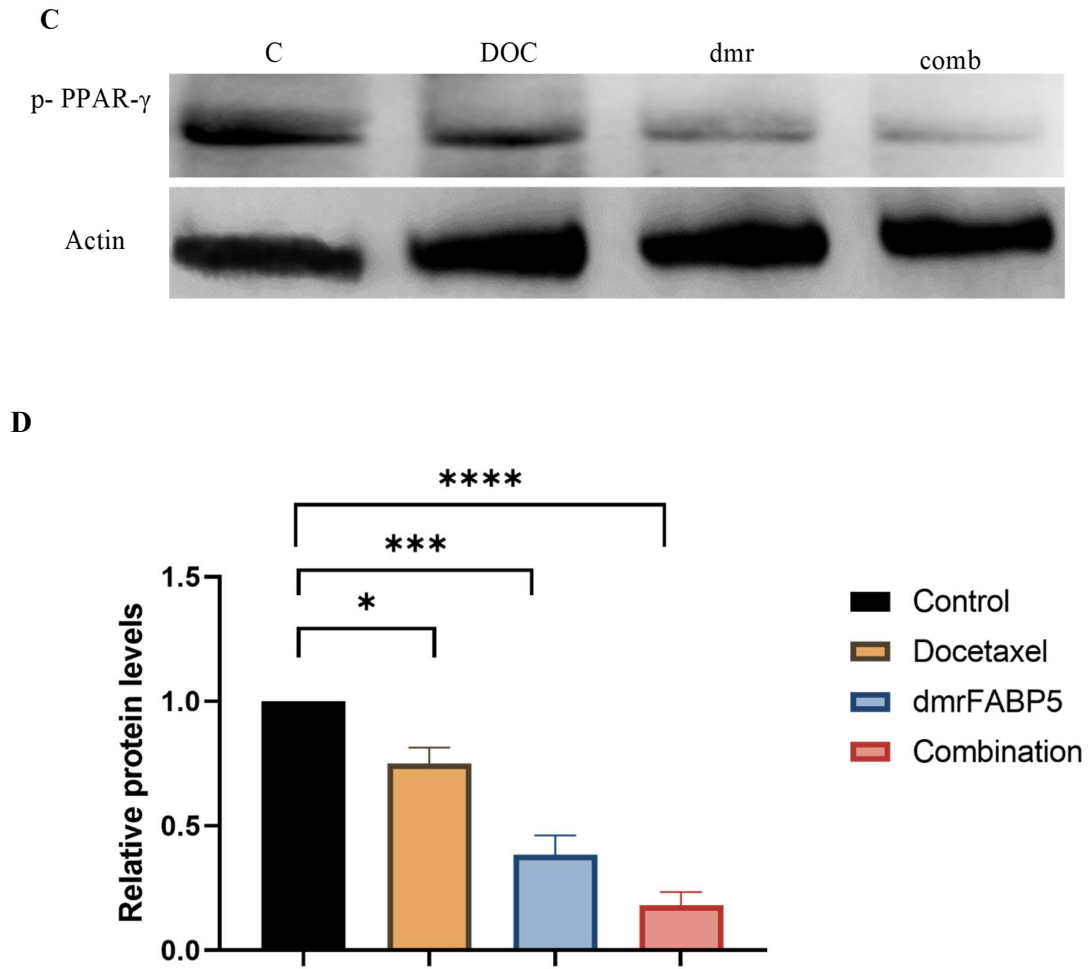


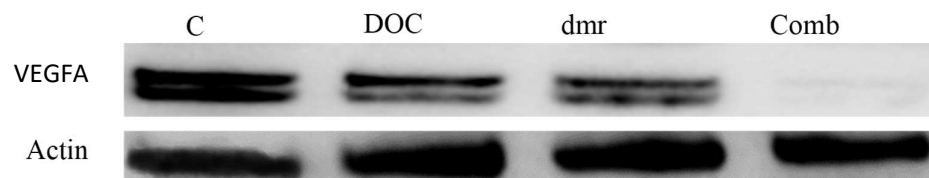
**Figure 5.7** The suppressive effect of dmrFABP5 and docetaxel on expression levels of PPAR $\gamma$  and p-PPAR $\gamma$  in 22RV1 cells. **A)** Western blot detection of PPAR $\gamma$  expressed in 22RV1 cells after different treatments. **B)** Relative levels of PPAR $\gamma$  in 22RV1 cells after different treatments. **C)** Western blot analysis of p-PPAR $\gamma$  expressed in 22RV1 cells after different treatments. **D)** Relative levels of p-PPAR $\gamma$  in 22RV1 cells after different treatments. To normalize possible loading errors, anti- $\beta$ -actin was used to hybridize the blot. The intensities of the bands on the blot were subjected to densitometrical scanning and analysed by Image-J software. Each experiment (Mean  $\pm$  SE) was performed in

triplicate, the error of the mean values were calculated and data was obtained from three independent experiments (n=3).

### 5.5.2 The effect of dmrFABP5 alone, or combined with docetaxel on VEGFA expression in 22RV1 cells

The bioactivity of dmrFABP5 to the effect of docetaxel on VEGFA expression in 22RV1 cells was measured by Western blot and the results were shown in Figure 5.8. Western blot analysis showed (Figure 5.8A) that in comparison with the control (treated with DMSO), treatments of 22RV1 cells with either 3nM of docetaxel (DOC), 10  $\mu$ M of dmrFABP5 (dmr) separately or in combination reduced the VEGFA expression. Quantitative analysis (Figure 5.8B) showed that both docetaxel and dmrFABP5 singly had a potent suppressive effect on VEGFA level by 51% and 59% to  $0.49\pm 0.077$  and  $0.41\pm 0.028$ , respectively (Student's *t*-test  $P<0.01^{**}$ ). The combination treatment produced an almost complete suppression on VEGFA expression by 99.9 % to  $0.035\pm 0.015$  ( $P<0.0001^{****}$ ). Thus, dmrFABP5 promoted the suppressive effect of docetaxel.

A



B

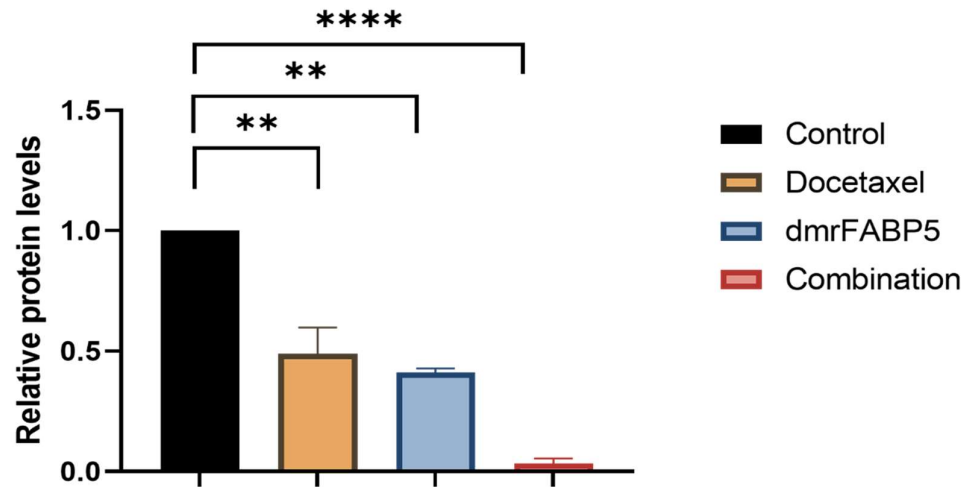


**Figure 5.8** The action of dmrFABP5 to the effect docetaxel on VEGFA expression in 22RV1 cells. **A)** Western blot detection of VEGFA expression in 22RV1 cells after different treatments. **B)** Relevant levels of VEGFA in 22RV1 cells after different treatments. To normalize possible loading errors, anti-  $\beta$ -actin was used to hybridize the blot. The intensities of the bands on the blot were subjected to densitometry scanning and the data was analysed with the Image-J software. Each result (Mean  $\pm$  SD) was obtained by 3 separate measurements. Each experiment was performed in triplicate and data was calculated from three independent experiments (n=3).

### 5.5.3 The action of dmrFABP5 alone, or in combination with docetaxel on Sp1 expression in 22RV1 cells

The suppressive effect of the treatments with dmrFABP5 and docetaxel, either singly or in combination, on Sp1 expression was shown in Figure 5.9. DMSO was used to treat 22RV1 cells as control. Docetaxel (DOC) at 3 nM and dmrFABP5 (dmr) at 10  $\mu$ M were used either individually or in combination and the effect was detected by western blot as



shown in Figure 5.9A. Quantitative assessments (Figure 5.9B) showed that, when the level of Sp1 in the control cells was set at 1, the level of Sp1 in 22RV1 cells after the docetaxel treatment was reduced by 82% to  $0.35 \pm 0.035$  ( $****P < 0.0001$ ). The level of Sp1 in 22RV1 cells treated with dmrFABP5 was reduced by 37% to  $0.6311 \pm 0.046$  ( $**P < 0.01$ ). The combination of both agents potently reduced Sp1 expression by 89% to  $0.109 \pm 0.009$ .

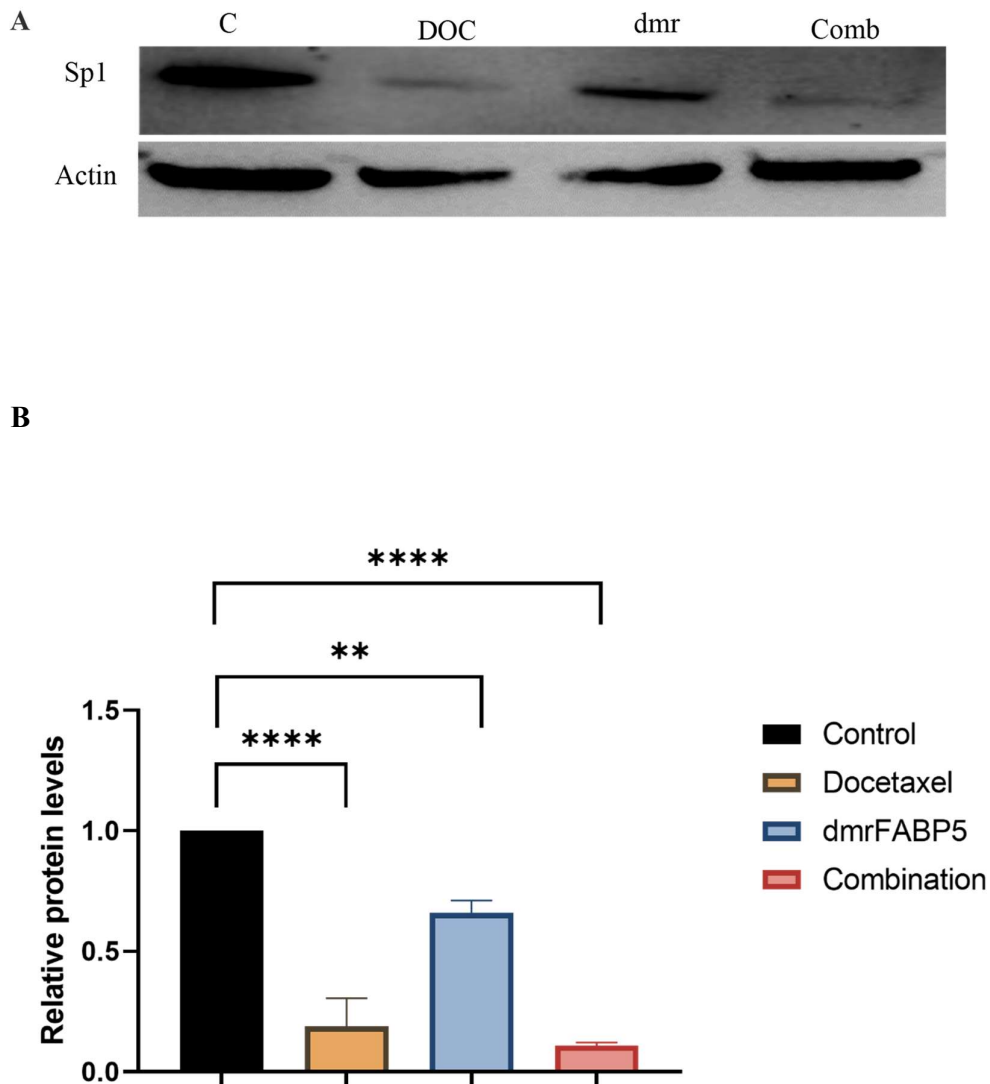


**Figure 5.9** The effect of dmrFABP5 combined with docetaxel on expression levels of protein regulators. **A)** Western blot of Sp1 expression level in 22RV1 after different

treatments. **B)** Relative levels of Sp1 in 22RV1 cells after different treatments. Anti- $\beta$ -actin was used to hybridise the blot to normalize the possible loading errors. The intensities of the bands on the blot was densitometrical scanned and the data was analysed with Image-J and Prism 9 software. Each experiment (Mean  $\pm$  SE) was performed in triplicate, the error of the mean values were calculated and data was obtained from three independent experiments (n=3).

#### **5.5.4 The action of dmrFABP5 singly or in combined with docetaxel on Bcl-2 expression in 22RV1 cells**

22RV1 as control (C) was treated with DMSO. The effect on Bcl-2 expression in 22RV1 cells treated with 4 nM of docetaxel (DOC), 10  $\mu$ M of dmrFABP5 (dmr), and a combination of both agents was assessed and the results were shown in Figure 5.10. Images of Western blot detection of Bcl-2 expression in 22RV1 cells after different treatments were shown in Figure 5.10A. When the 22RV1 control level was set at 1 (Figure 5.10B), the relative level of Bcl-2 after docetaxel treatment significantly (\*\* $P < 0.01$ ) reduced by 55% to  $0.45 \pm 0.049$ . Whereas treatment with dmrFABP5 reduced Bcl-2 ( $*P < 0.05$ ) by 39% to  $0.612 \pm 0.044$ . Both compounds in combination (dmrFABP5 with docetaxel) reduced the Bcl-2 expression by 86% to  $0.138 \pm 0.005$  (\*\*\*\* $P < 0.0001$ ) which was a higher suppression than any of those obtained by treatment with each agent separately.

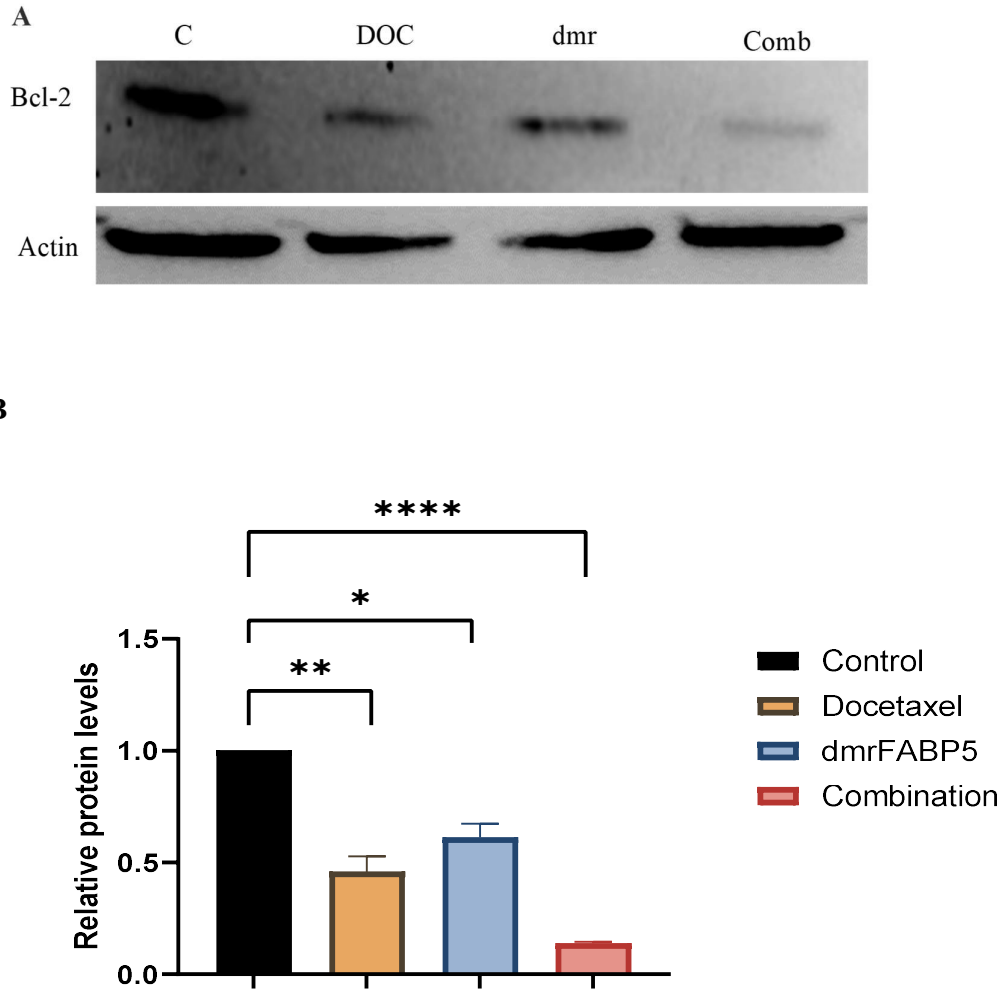
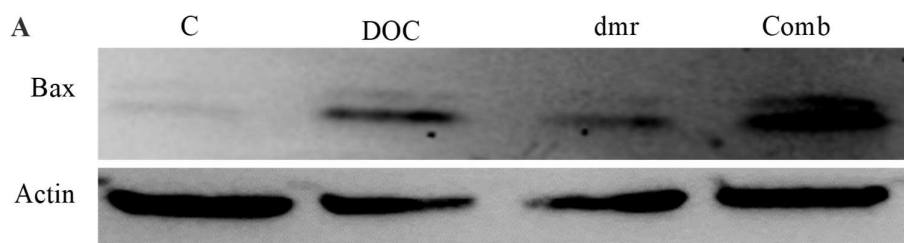


**Figure 5.10** The effect of dmrFABP5 combined with docetaxel on expression level of anti-apoptotic Bcl-2 in 22RV1 cells. A) Western blot of Bcl-2 expression in 22RV1 after different treatments. B) The quantitative assessment (relative levels of Bcl-2). To normalize possible loading errors, anti-  $\beta$ -actin was used to hybridize the blot. The intensities of the bands on the blot were subjected to densitometry scanning and analysed by Image-J software. Each experiment (Mean  $\pm$  SE) was performed in triplicate, the error of the mean values were calculated and data was obtained from three independent experiments (n=3).

### 5.5.5 The effect of dmrFABP5 alone, or combined with docetaxel on BAX expression in 22RV1

22RV1 was treated with DMSO as control. The effect of treating 22RV1 with docetaxel (DOC) at 3nM, dmrFABP5 (dmr) at 10  $\mu$ M, or the combination of both of them on Bax expression was investigated and the results were shown in Figure 5.11. The detection of Bax in 22RV1 by Western blot after different treatments was shown in Figure 5.11A. The level of BAX in 22RV1 as control was set at 1 (Figure 5.11B), the BAX level after docetaxel treatment was significantly increased (\*\* $P < 0.01$ ) by 184% to  $1.84 \pm 0.051$ , while dmrFABP5 treatment increased ( $*P < 0.05$ ) the level of BAX by 140% to  $1.4 \pm 0.051$ . The treatment with a combination of both compounds produced even increase on the level of BAX expression (\*\* $*P < 0.001$ ) by 314% to  $3.146 \pm 0.254$ .



**B**

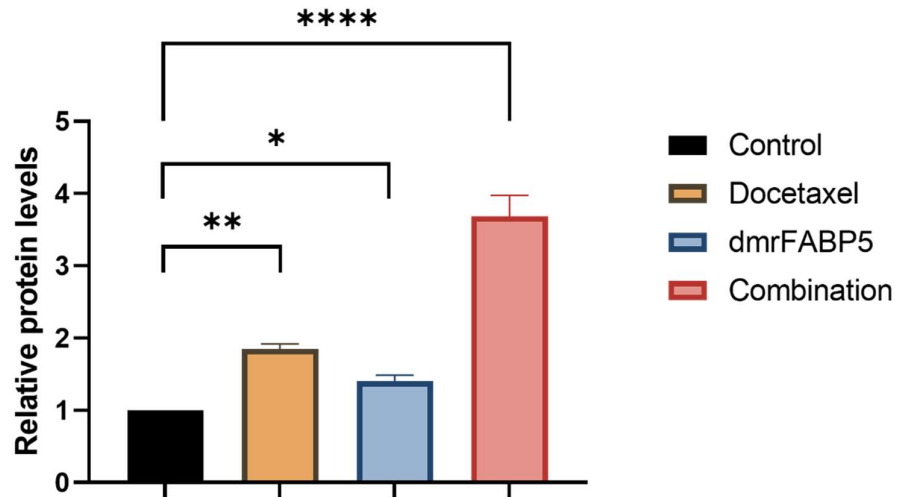


**Figure 5.11** The effect of dmrFABP5 combined with docetaxel on expression levels of protein regulator. **A)** Western blot detection of Bax expression in 22RV1 cells after different treatments. **B)** Relative levels of Bax in 22Rv1 cells after different treatments. Anti- $\beta$ -actin was used to hybridise the blot to normalize the possible loading errors. The intensities of the bands on the blot were subjected to densitometry scanning and the data was analysed by Image-J software. Each experiment (Mean  $\pm$  SE) was performed in triplicate, the error of the mean values were calculated and data was obtained from three independent experiments (n=3).

## **5.6 Investigating the molecular mechanism of the biological activity of dmrFABP5 to the effect of enzalutamide on 22RV1 cells**

### **5.6.1 The effect of dmrFABP5 alone, or combined with enzalutamide on AR or AR-V7 expression in 22RV1 cells**

The enhancement effect of dmrFABP5 singly or in combined with enzalutamide on AR or AR-V7 expression and results were investigated as shown in Figure 5.12. The androgen responsive 22RV1 cell was treated with DMSO as control (C), 10  $\mu$ M of enzalutamide (ENZ), 10 $\mu$ M of dmrFABP5 (dmr), or in combination of both treatments. The detection of AR and AR-V7 expression by Western blot was shown in Figure 5.12A. The level of AR and AR-V7 in 22RV1 cells as a control was set at 1 (Figure 5.12B), the treatment of enzalutamide did not significantly suppress AR nor AR-V7 (Student *t*-test  $P > 0.05$ ). DmrFABP5 significantly downregulated the expression of both AR ( $*P < 0.05$ ) and AR-V7 ( $**P < 0.01$ ) proteins by 26% and 59% to  $0.743 \pm 0.013$  and  $0.41 \pm 0.063$  respectively. The combination treatment with both compounds produced more downregulation effect of both AR and AR-V7 ( $****P < 0.0001$ ) and more than each agent alone by 72% and 99.5% to  $0.28 \pm 0.017$  and  $0.0057 \pm 0.0009$  respectively. Thus, dmrFABP5 significantly enhanced enzalutamide suppressive effect.

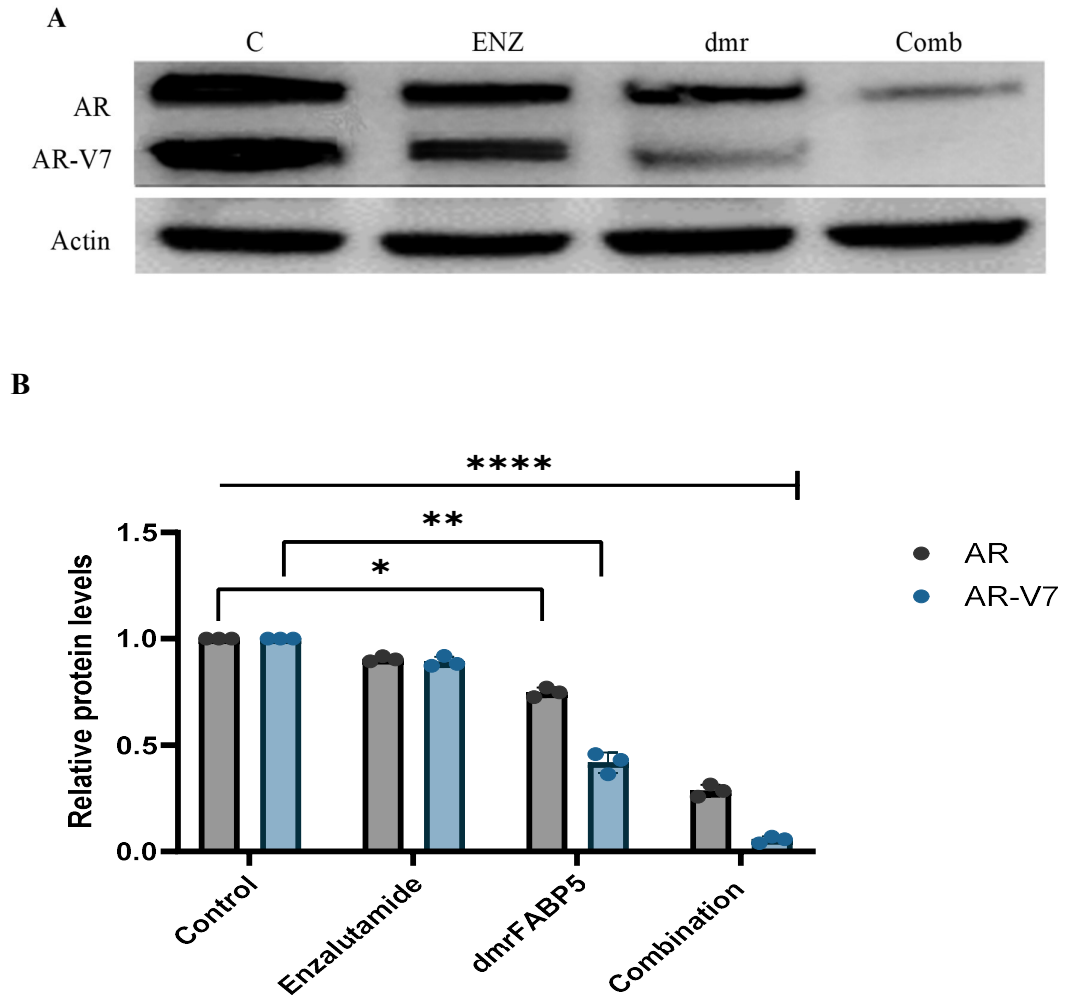
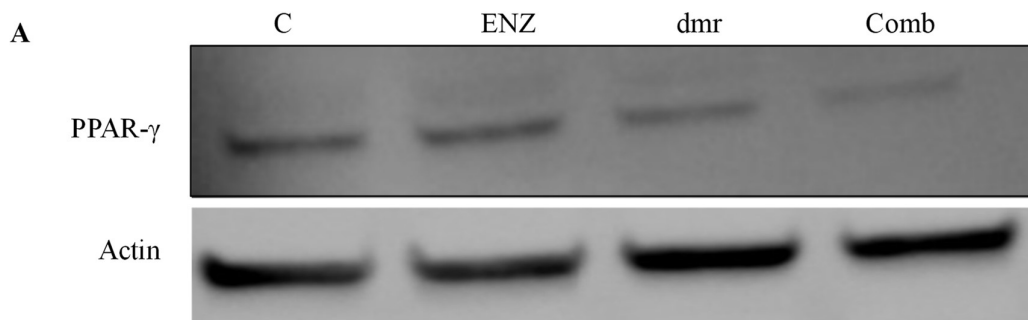


**Figure 5.12** The effect of dmrFABP5 either alone, or combined with enzalutamide on expression levels of AR and AR-V7. A) Western blot detection of AR and AR-V7 expression level in 22RV1 cells after different treatments. B) The relevant levels of AR and AR-V7 after utilized of different treatments. To normalize possible loading errors, anti-  $\beta$  -actin was used to hybridize the blot. The bands on the blot were subjected to densitometry scanning and analysed by Image-J software. Each experiment (Mean  $\pm$  SE) was performed in triplicate, the error of the mean values were calculated and data was obtained from three independent experiments (n=3).

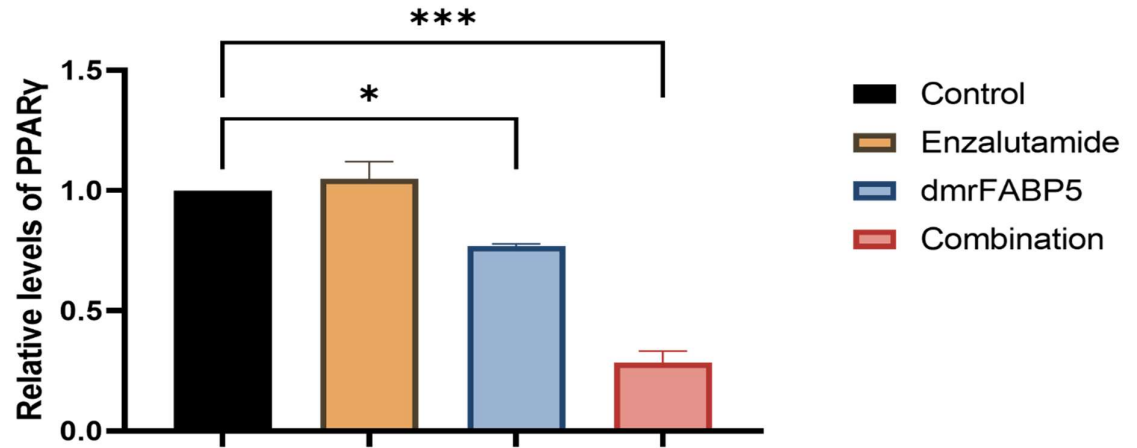
### 5.6.2 The effect of treatments with dmrFABP5 alone, combined with enzalutamide on levels of PPAR $\gamma$ and p-PPAR $\gamma$ in 22RV1 cells

22RV1 (control) was treated with DMSO, dmrFABP5 (dmr) at 10  $\mu$ M, or enzalutamide (ENZ) at 10  $\mu$ M, and a combination (Comb) of both. PPAR $\gamma$  and p-PPAR $\gamma$  expression after different treatments were assessed by using Western blot (Figure 5.13). The images of Western blot were shown in Figure 5.13A and C. The relative levels of PPAR $\gamma$  and p-PPAR $\gamma$  were shown in Figure 5.13B and D. When relative levels of PPAR $\gamma$  and p-PPAR $\gamma$  in the 22RV1 control cells set at 1, enzalutamide produced some changes of the expression levels of PPAR $\gamma$  and p-PPAR $\gamma$  to  $1.049\pm 0.051$  and  $0.910\pm 0.018$  respectively, but these changes were not statistically significant ( $p>0.05$ ). DmrFABP5 significantly downregulated PPAR $\gamma$  ( $*P < 0.05$ ) by 23% to  $0.77\pm 0.006$ , and significantly ( $**P < 0.01$ ) downregulated the level of p-PPAR $\gamma$  by 42% to  $0.58\pm 0.017$ . DmrFABP5 combined with enzalutamide produced a more significant ( $***P < 0.001$ ) suppression effect on PPAR $\gamma$  and p-PPAR $\gamma$  expression levels by 72% and 73% to  $0.284\pm 0.040$  and  $0.293\pm 0.055$  respectively.

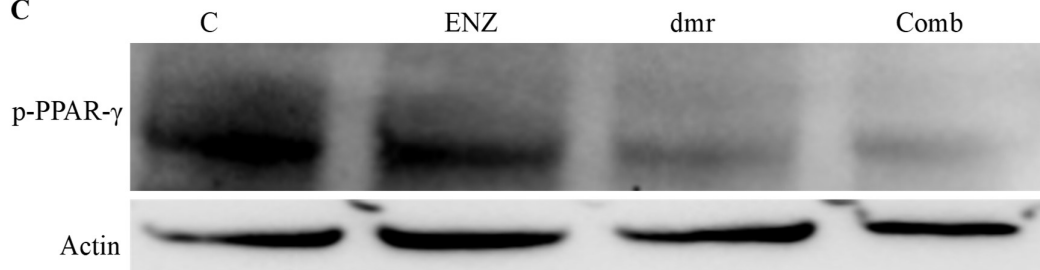




B



C



D

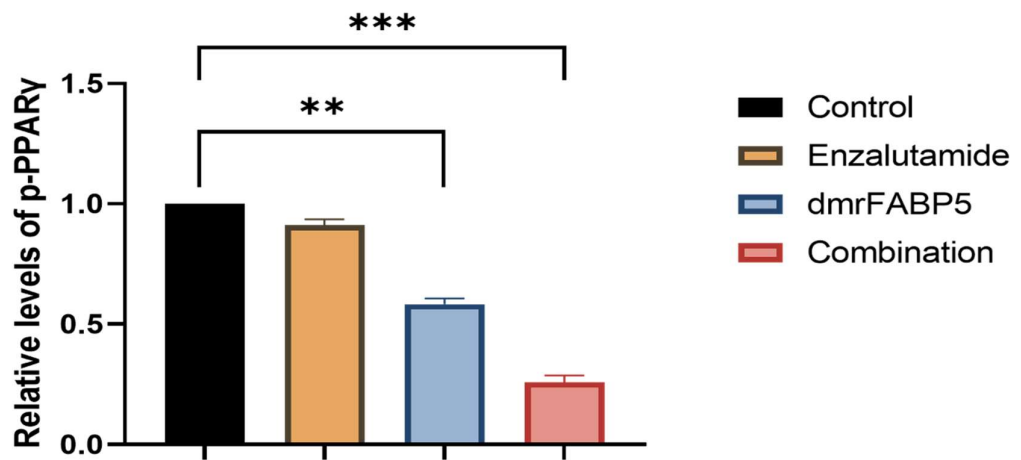
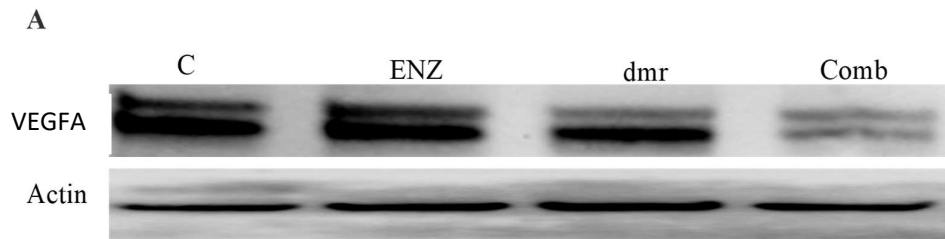


**Figure 5.13** The effect of dmrFABP5 singly or in combination with enzalutamide on expression levels of protein regulators. A) Western blot of PPAR $\gamma$  expression level in

22RV1 cells after different treatments. B) Relative quantitative levels of PPAR $\gamma$ . C) Western blot of p-PPAR $\gamma$  expression level in 22RV1 cells detected after different treatments. D) Relative quantitative levels of p-PPAR $\gamma$  expression. Anti- $\beta$ -actin was used to normalize for possible loading errors. Data analysis for western blot bands were analysed by Image-J and quantitative assessments were obtained by using Prism 9 software Each experiment (Mean  $\pm$  SE) was performed in triplicate, the error of the mean values were calculated and data was obtained from three independent experiments (n=3).

### 5.6.3 The action of dmrFABP5 singly or combined with enzalutamide on VEGFA expression in 22RV1 cells

DMSO was used to treat 22RV1 cells as control (C), dmrFABP5 (dmr) at 10  $\mu$ M or enzalutamide (ENZ) at 10  $\mu$ M were used alone or in combination (Comb) of both compounds, and results were shown in Figure 5.14. The images of western blot of VEGFA expression was shown in Figure 5.14A. When the androgen-responsive 22RV1 (control) was set at 1 (Figure 5.14B), the relative level of VEGFA after enzalutamide treatment was slightly ( $p>0.05$ ) reduced to  $0.95\pm 0.10$ . But the dmrFABP5 treatment significantly ( $**P < 0.01$ ) suppressed the expression level of VEGFA by 41% to  $0.59\pm 0.063$ . Both compounds in combination ( $***P < 0.001$ ) produced a greater reduction in VEGFA expression level by 77% to  $0.230\pm 0.032$ . Thus, dmrFABP5 promoted the enzalutamide activity.



B

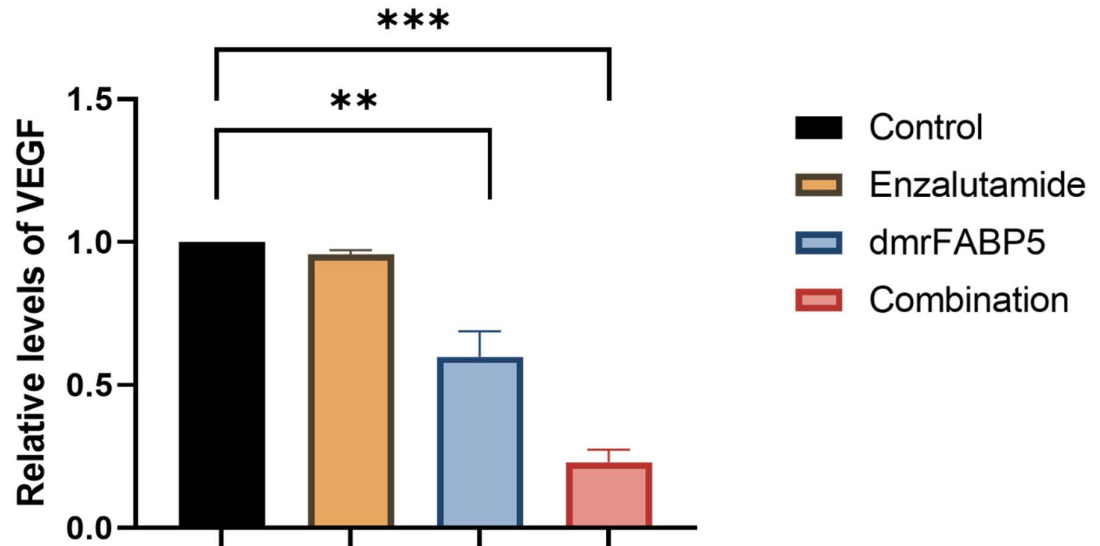
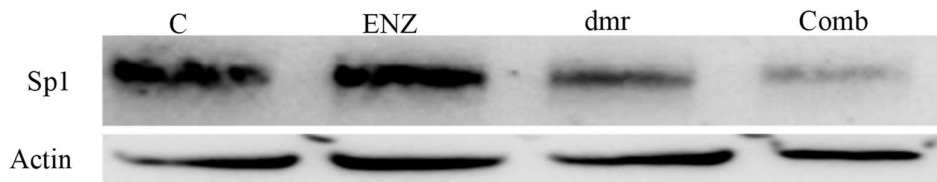


**Figure 5.14** The action of dmrFABP5 to the effect of enzalutamide on VEGFA expression in 22RV1 cells. **A)** Western blot of VEGFA expression level in 22RV1 cells after different treatments. **B)** Relevant levels of VEGFA in 22RV1. To normalize possible loading errors, anti-  $\beta$ -actin was used to hybridize the blot. The intensities of the bands on the blot were subjected to densitometrical scanning and the data was analysed with the Image-J software. Each experiment (Mean  $\pm$  SE) was performed in triplicate, the error of the mean values were calculated and data was obtained from three independent experiments (n=3).

### 5.6.4 The effect of the treatment of dmrFABP5 combined with enzalutamide on Sp1 level in 22RV1 cells

The androgen-responsive 22RV1 cells were treated with DMSO as control (C), enzalutamide (ENZ) at 10  $\mu$ M, dmrFABP5 (dmr) at 10  $\mu$ M, both compounds in combination (Comb), and the results were shown in Figure 5.15. The effect of different treatments was detected by western blot as shown in Figure 5.15A. Quantitative results (Figure 5.15B) showed that when control was set at 1, the relative level of Sp1 in 22RV1 after enzalutamide treatment reduced (but was not significantly) (Student *t*-test  $P > 0.05$ ) to  $0.943 \pm 0.024$ . The expression level of Sp1 was significantly ( $**P < 0.01$ ) reduced after dmrFABP5 treatment by 45% to  $0.56 \pm 0.62$ . The treatment with a combination of both compounds produced more significant ( $***P < 0.001$ ) reduction by 79% to  $0.2139 \pm 0.031$ .

A



B

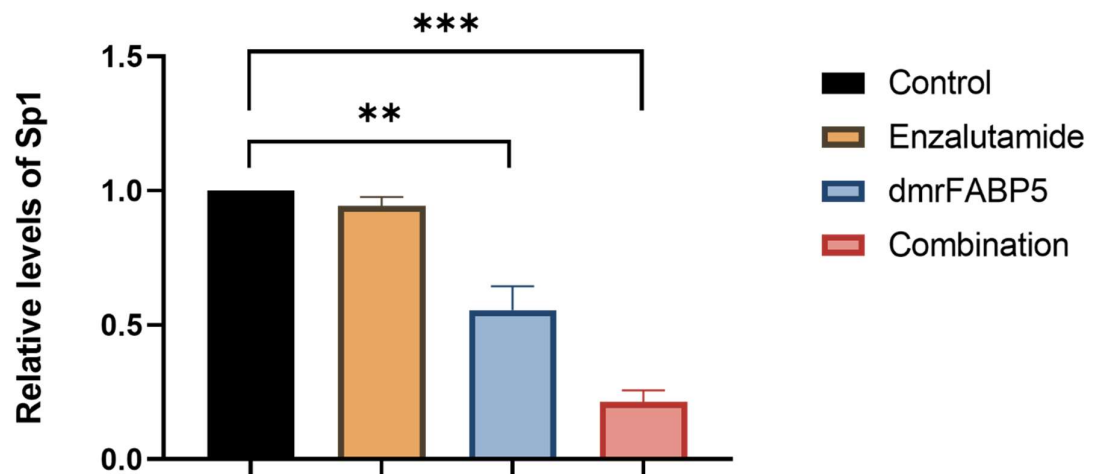


**Figure 5.15** The effect of dmrFABP5 alone, or in combination with enzalutamide, on the expression of Sp1 in 22RV1 cells. **A)** Western blot of Sp1 expression in 22RV1 cells after all different treatments. **B)** Relative levels of Sp1 expression in 22RV1 cells after different treatments. To normalize possible loading errors, anti- $\beta$ -actin was used to hybridize the blot. The intensities of the bands on the blot were densitometry scanning and the data was analysed with Image-J software. Each experiment (Mean  $\pm$  SE) was performed in triplicate, the error of the mean values were calculated and data was obtained from three independent experiments (n=3).

## **5.7 Further molecular mechanism investigations**

### **5.7.1 The effect of enzalutamide on AR and AR-V7 expression in**

#### **22RV1-FABP5- KO cells**

Both the parental 22RV1 and 22RV1-FABP5-KO cells were treated with DMSO as controls. Enzalutamide (ENZ), at a concentration of 10  $\mu$ M, was used to treat both cell lines, and the results were shown in Figure 5.16. Western blot detection of both AR and AR-V7 expression after enzalutamide treatment was shown in Figure 5.16A. The results of the quantitative analysis of the expression levels were shown in Figure 5.16B. When levels of AR and AR-V7 in parental 22RV1 was set at 1, the relative level of AR in 22RV1-FABP5-KO was not significantly different from that in the parental cells. But the relative level of AR-V7 was significantly ( $****P < 0.0001$ ) reduced by 91% to  $0.095 \pm 0.005$ . Interestingly, while enzalutamide did not significantly change the expression levels of AR and AR-V7 in the parental 22RV1 cells, it significantly ( $****P < 0.0001$ ) decreased both AR and AR-V7 by 89% and 100% to  $0.12 \pm 0.01$  and  $0.0001 \pm 0.00004$ , respectively, in 22RV1-FABP5-KO cells.

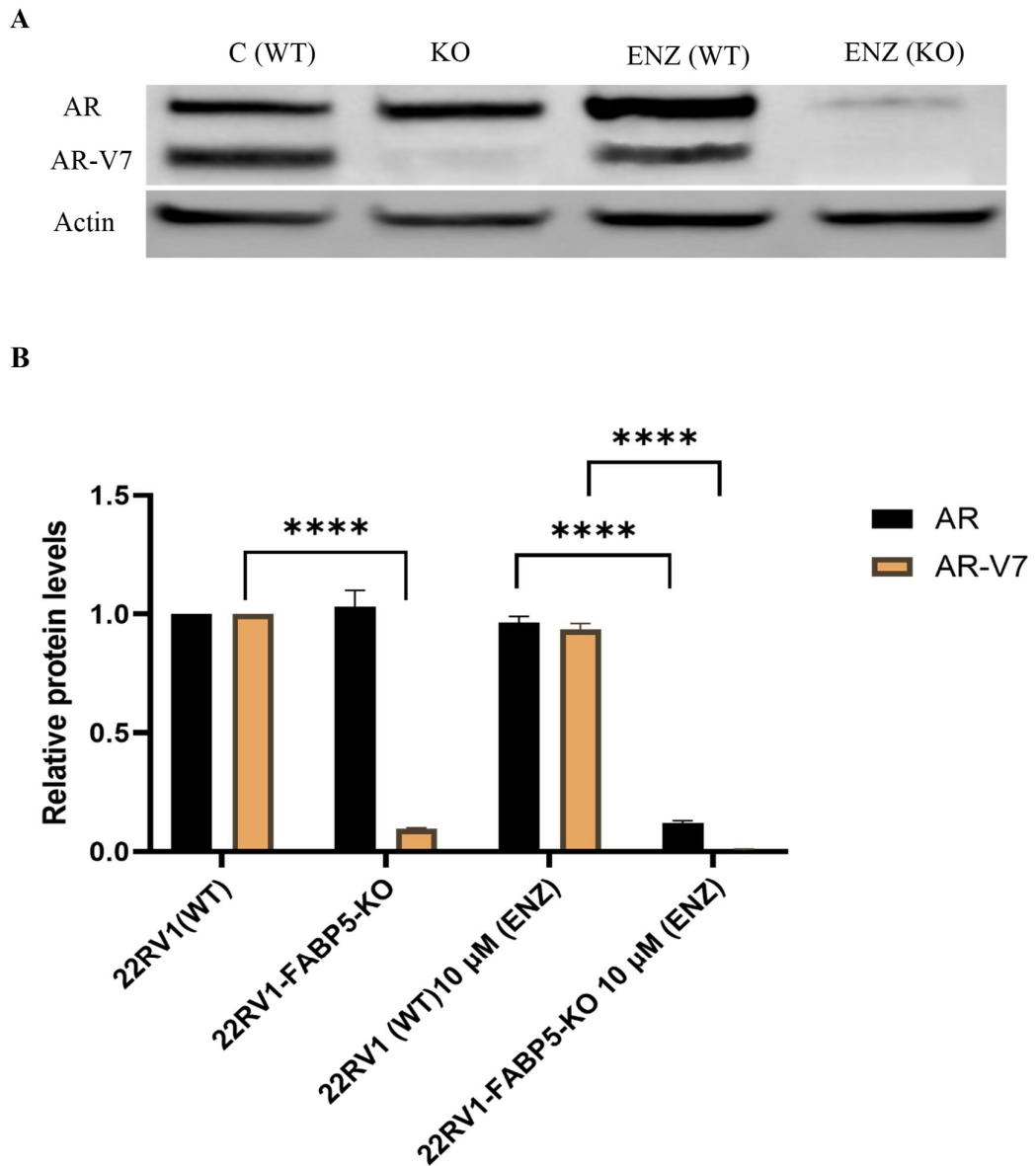
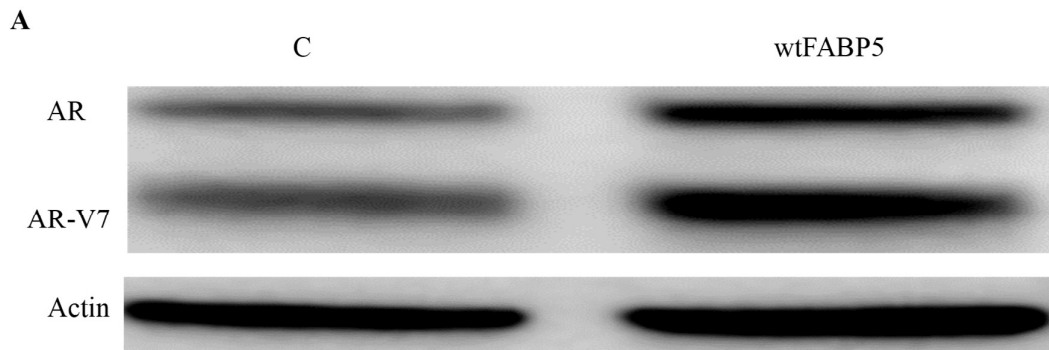


**Figure 5.16** The effect of enzalutamide on AR or AR-V7 expression in 22RV1 and 22RV1-FABP5-KO cells. **A)** Western blot detection of AR and AR-V7 expression after enzalutamide treatment in 22RV1 and 22RV1-FABP5-KO cells. **B)** Relevant levels of AR and AR-V7 in 22RV1 and FABP5-KO cells. To normalize possible loading errors, anti- $\beta$ -actin was used to hybridize the blot. The intensities of the bands on the blot were subjected to densitometrical scanning and the data was analysed with the Image-J

software. Each experiment was performed in triplicate and data was calculated from three independent experiments (n=3).

### 5.7.2 The effect of wtFABP5 treatment on levels of AR and AR-V7 in 22RV1 cells

The 22RV1 cells were treated with DMSO as control. The cells were also treated with 5  $\mu$ M wtFABP5, and the results were shown in Figure 5.17. Western blot image was shown in Figure 5.17A. Relative levels of AR and AR-V7 were shown in Figure 5.17B. When levels of AR and AR-V7 in 22RV1 were respectively set at 1, the relative levels of AR and AR-V7 after the wtFABP5 treatment were significantly (Student *t*-test  $***P < 0.001$ , and  $***P < 0.001$ ) increased by 80% and 84% to  $1.8 \pm 0.15$  and  $1.84 \pm 0.08$ , respectively.



**B**

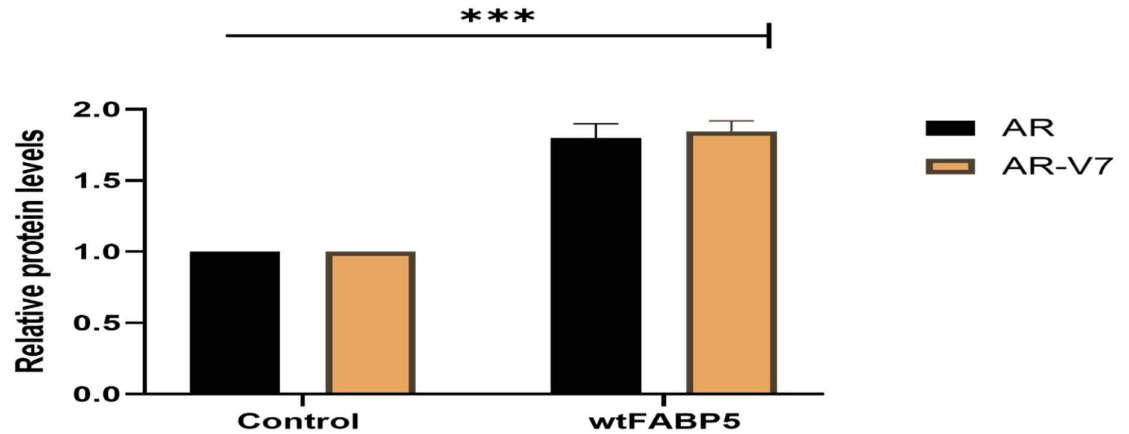
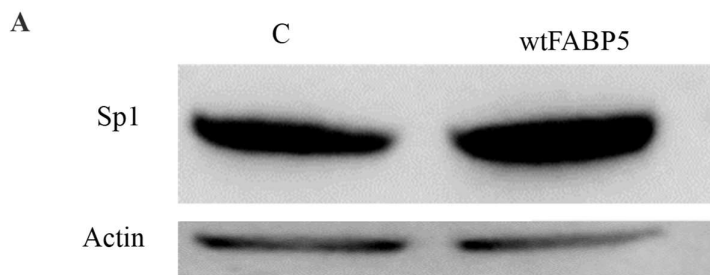


**Figure 5.17** The effect of wtFABP5 on AR or AR-V7 expression in 22RV1 cells. **A)** Western blot detection of AR and AR-V7 expression before and after the recombinant wtFABP5 treatment in 22RV1 cells. **B)** Relevant levels of AR and AR-V7 in 22RV1. Anti- $\beta$ -actin was used to hybridise the blot to normalize the possible loading errors. The intensities of the bands on the blot were subjected to densitometrical scanning and the data was analysed with the Image-J software. Each experiment was performed in triplicate  $n=3$  from three independent measurements.

### 5.7.3 The effect of wtFABP5 on Sp1 expression in 22RV1 cells

The 22RV1 cells were treated with DMSO (as control), 5  $\mu$ M wtFABP5, and results were shown in Figure 5.18. Western blot image was shown in Figure 5.18A. Quantitative assessments of the relative levels were shown in Figure 5.18B. When the level of Sp1 in





the control was set at 1, wtFABP5 treatment significantly (Student *t*-test  $**P < 0.001$ ) increased the Sp1 expression level in 22RV1 cells by 58% to  $1.58 \pm 0.09$ .

**B**

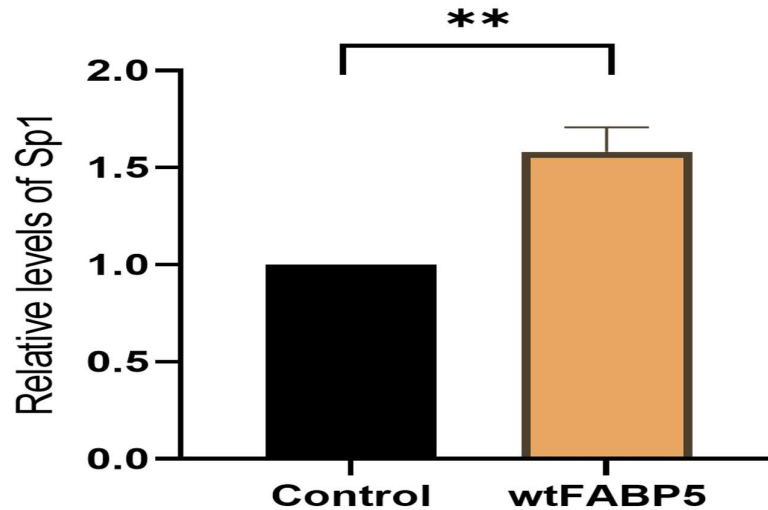


**Figure 5.18** The effect of wtFABP5 on Sp1 expressions in 22RV cells A) Western blot detection of Sp1 expression after wtFABP5 treatment in 22RV1 cells. B) Relevant levels of Sp1 in 22RV1 cells. To normalize possible loading errors, anti-  $\beta$ -actin was used to hybridize the blot. The intensities of the bands on the blot were subjected to densitometrical scanning and the data was analysed with the Image-J software. Each result data (Mean  $\pm$  SE) was obtained from 3 separate independent measurements. Each experiment was performed in triplicate  $n=3$ .

#### **5.7.4 Sp1 expression in 22RV1-FABP5-KO**

The expression of Sp1 was measured and the results were shown in Figure 5.19. Images of the Western blot detection of Sp1 in 22RV1 and 22RV1-FABP5-KO cells were shown in Figure 5.19A. When the level of Sp1 in 22RV1 (Figure 5.19B) was set at 1, the relative

level of Sp1 in 22RV1-FABP5-KO cells was significantly (Student *t*-test \*\*\* $P < 0.001$ ) reduced by 63% to  $0.37 \pm 0.04$ .

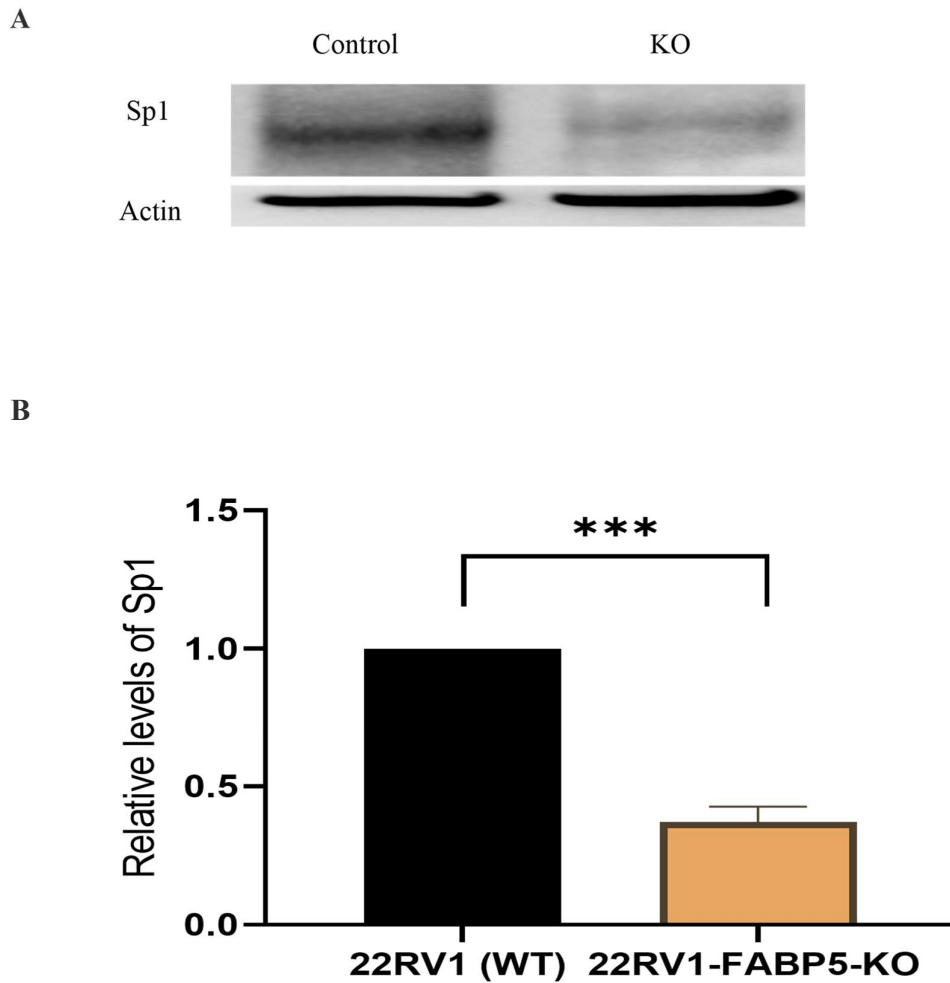


**Figure 5.19** The effect of wtFABP5 on Sp1 expressions in 22RV1 and 22RV1-FABP5-KO cells. **A)** Western blot detection of Sp1 expression after the wtFABP5 treatment in 22RV1 cells. **B)** Relative levels of Sp1 in 22RV1 and 22RV1-FABP5-KO cells. To normalize possible loading errors, anti- $\beta$ -actin was used to hybridize the blot. The intensities of the bands on the blot were subjected to densitometrical scanning and the data was analysed with the Image-J software. Each result data (Mean  $\pm$  SE) was obtained

from 3 separate independent measurements. Each experiment was performed in triplicate n=3.

### 5.7.5 The effect of Sp1 inhibitor (Plicamycin) on AR and AR-V7 expression in 22RV1 cells

The expression of AR and AR-V7 in the androgen-responsive 22RV1 cells treated with DMSO (C), and in 22RV1 cells treated with 1  $\mu$ M of Plicamycin (Pli) were shown in Figure 5.20. Western blot images were shown in Figure 5.20A. When levels of AR and AR-V7 (Figure 5.20B) in 22RV1 (C) was respectively set at 1, the relative levels of AR and AR-V7 were significantly reduced in 22RV1-FABP5-KO cells (\*\*\*\* $P$ <0.0001) by 95% and 99% to  $0.052 \pm 0.011$  and  $0.006 \pm 0.002$ , respectively.

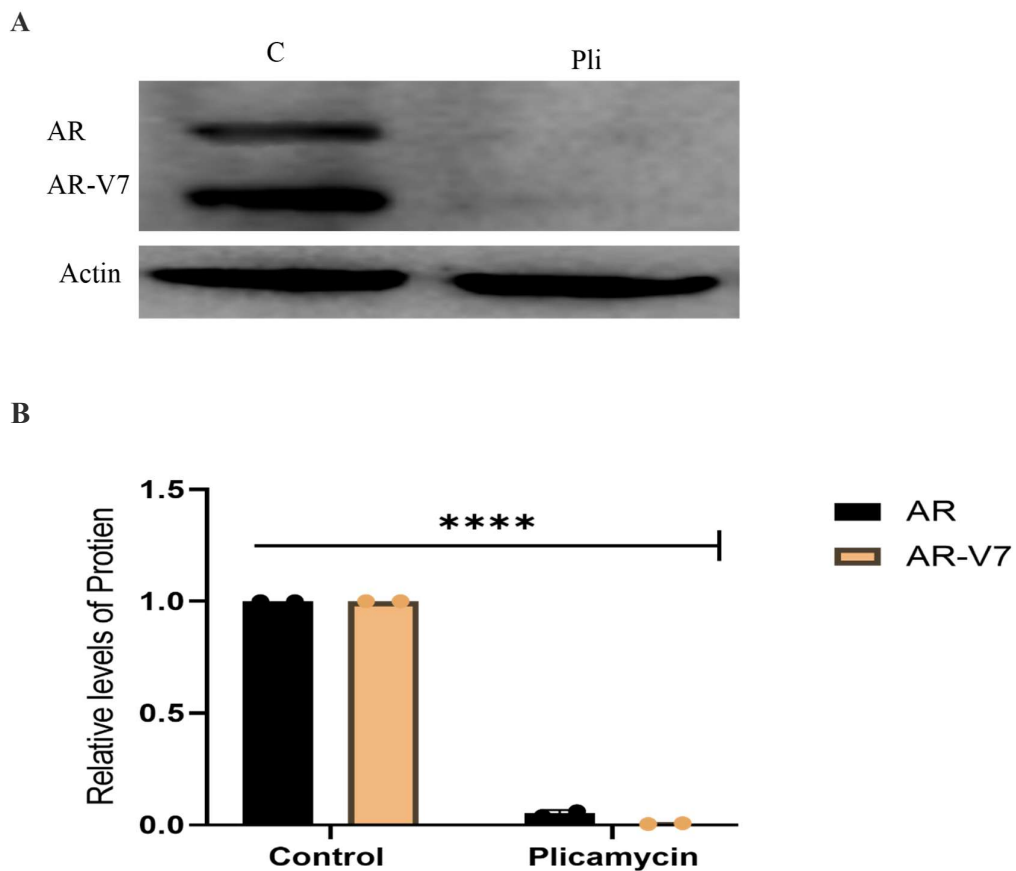


**Figure 5.20** The effect of Plicamycin on AR and AR-V7 expression in 22RV cells. A) Western blot detection of AR and AR-V7 expression after Sp1 inhibitor (Plicamycin)

treatment in 22RV1 cells. **B)** Relative levels AR and AR-V7 in 22RV1 cells. To normalize possible loading errors, anti-  $\beta$ -actin was used to hybridize the blot. The intensities of the bands on the blot were subjected to densitometrical scanning and the data was analysed with the Image-J software. Each result data (Mean  $\pm$  SE) was obtained from 3 separate independent measurements. Each experiment was performed in triplicate n=3.

### 5.7.6 The effect of Plicamycin on FABP5 expression in 22RV1 cells

DMSO (Control) and 1  $\mu$ M of Plicamycin were used to treat 22RV1 and the results were shown in Figure 5.21. Western blot images were shown in Figure 5.21A. The level of FABP5 in the control 22RV1 cells (Figure 5.21B) was set at 1, the relative FABP5 level after the Plicamycin treatment was significant ( $****P<0.0001$ ) decreased by 96% to  $0.037 \pm 0.016$ . Thus, the Sp1 inhibitor had a highly suppressive effect on FABP5 expression.

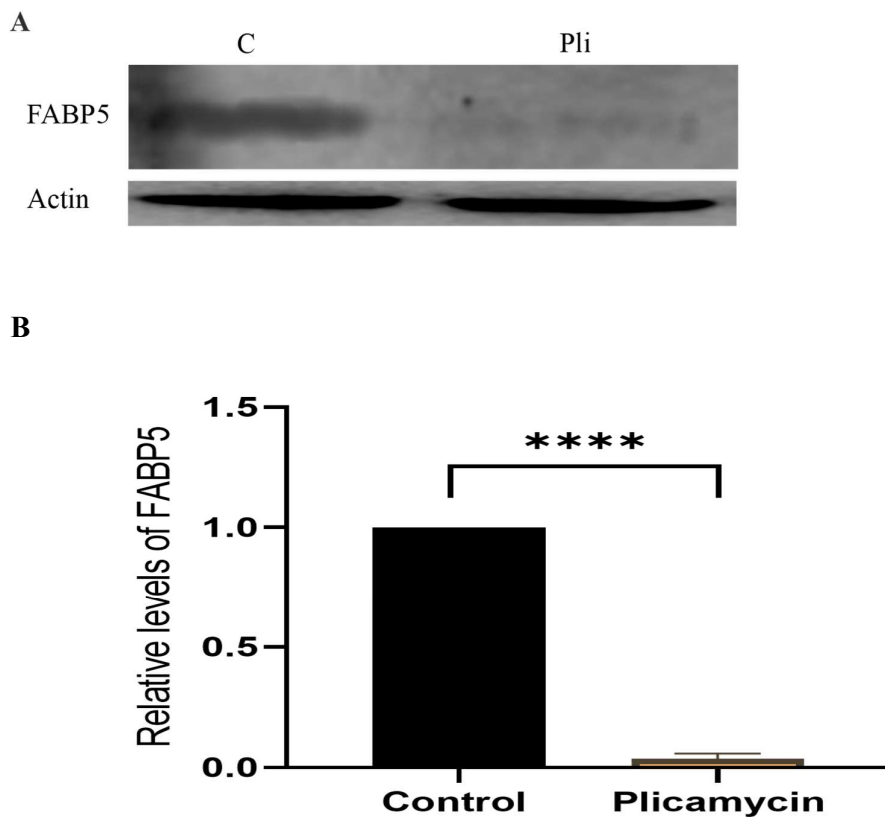
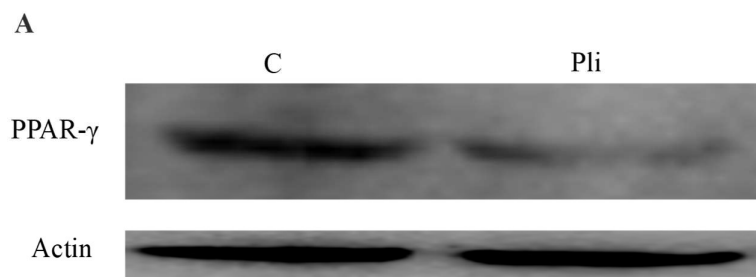


**Figure 5.21** The effect of Plicamycin on FABP5 expressions in 22RV cells. **A)** Western blot detection of the expression of FABP5 after Plicamycin treatment in 22RV1 cells. **B)** Relevant level of FABP5 in 22RV1 cells. To normalize possible loading errors, anti- $\beta$ -actin was used to hybridize the blot. The intensities of the bands on the blot were subjected to densitometrical scanning and the data was analysed with the Image-J software. Each result data (Mean  $\pm$  SE) was obtained from 3 separate independent measurements. Each experiment was performed in triplicate  $n=3$ .

### 5.7.7 The effect of Plicamycin on PPAR $\gamma$ expression in 22RV1 cells

The 22RV1 cells were treated with DMSO (C), or 1  $\mu$ M of Plicamycin (Pli), and the effect of these treatments on PPAR $\gamma$  expression was shown in Figure 5.22. The western blot images were shown in Figure 5.22A. Relative levels of PPAR $\gamma$  were shown in Figure 5.22B. When the level of PPAR $\gamma$  in the control was set at 1, the relative PPAR $\gamma$  level in 22RV1 cells treated with Plicamycin was significantly (\*\* $P<0.01$ ) reduced by 41% to  $0.59 \pm 0.075$ .



**B**

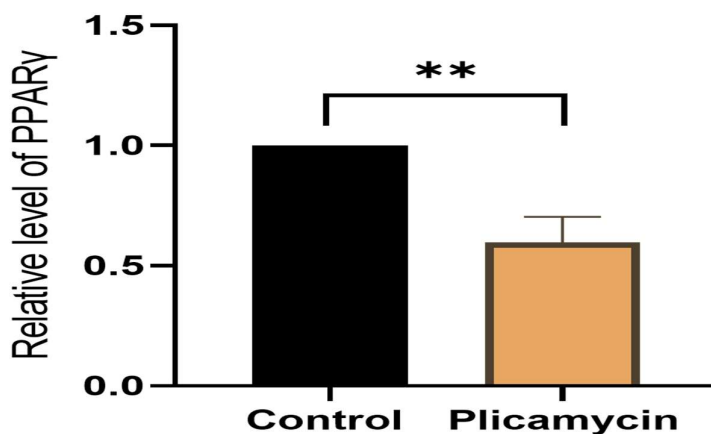


**Figure 5.22** The effect of Plicamycin on PPAR $\gamma$  expressions in 22RV cells. **A)** The image of a Western blot of the expression of PPAR $\gamma$  after Plicamycin treatment in 22RV1 cells. **B)** Relevant level of PPAR $\gamma$  in 22RV1 cells. To normalize possible loading errors, anti- $\beta$ -actin was used to hybridize the blot. The intensities of the bands on the blot were subjected to densitometrical scanning and the data was analysed with the Image-J software. Each result data (Mean  $\pm$  SE) was obtained from 3 separate measurements. Each experiment was performed in triplicate n=3.

### **5.7.8 The effect of Plicamycin on p-PPAR $\gamma$ in 22RV1 cells**

The 22RV1 cells were treated with DMSO (C), 1  $\mu$ M of Plicamycin (Pli), and the results were shown in Figure 5.23. The images of the Western blot on p-PPAR $\gamma$  were shown in Figure 5.23A. Relative levels of p-PPAR $\gamma$  were shown in Figure 5.23B. When the level of p-PPAR $\gamma$  in 22RV1 cells was set at 1, the relative level of p-PPAR $\gamma$  after the treatment with Plicamycin was significantly (\*\* $P < 0.01$ ) reduced by 38% to  $0.62 \pm 0.035$ .

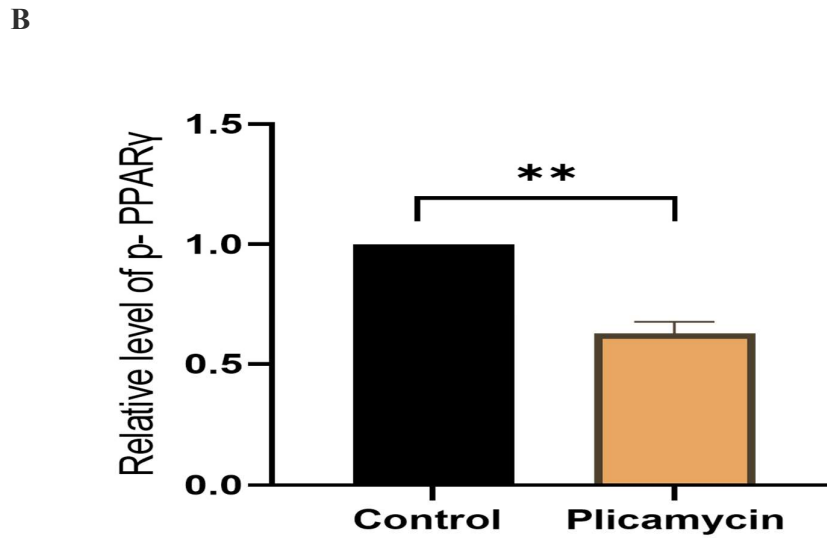
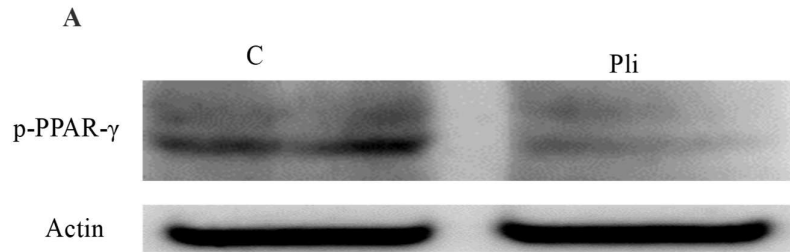


**Figure 5.23** The effect of Plicamycin on p-PPAR $\gamma$  expression in 22RV cells. **A)** The image of Western blot of the expression of p-PPAR $\gamma$  after Plicamycin treatment in 22RV1 cells. **B)** Relative level of p-PPAR $\gamma$  in 22RV1 cells. To normalize possible loading errors, anti- $\beta$ -actin was used to hybridize the blot. The intensities of the bands on the blot were subjected to densitometrical scanning and the data was analysed with the Image-J software. p-PPAR $\gamma$ . Each experiment was performed in triplicate n=3.

### 5.7.9 The effect of Sp1 expression in DU145-FABP5-KO cells

The Sp1 expression in DU145 (WT) and DU145-FABP5-KO were shown in Figure 5.24. The images of western blot were shown in Figure 5.24A. Relative results showed that

when Du145 (WT) level was set at 1, complete reduction of the level of Sp1 in Du145-FABP5-KO (\*\*\*\* $P < 0.0001$ ) by 100% to  $0.003 \pm 0.002$ .

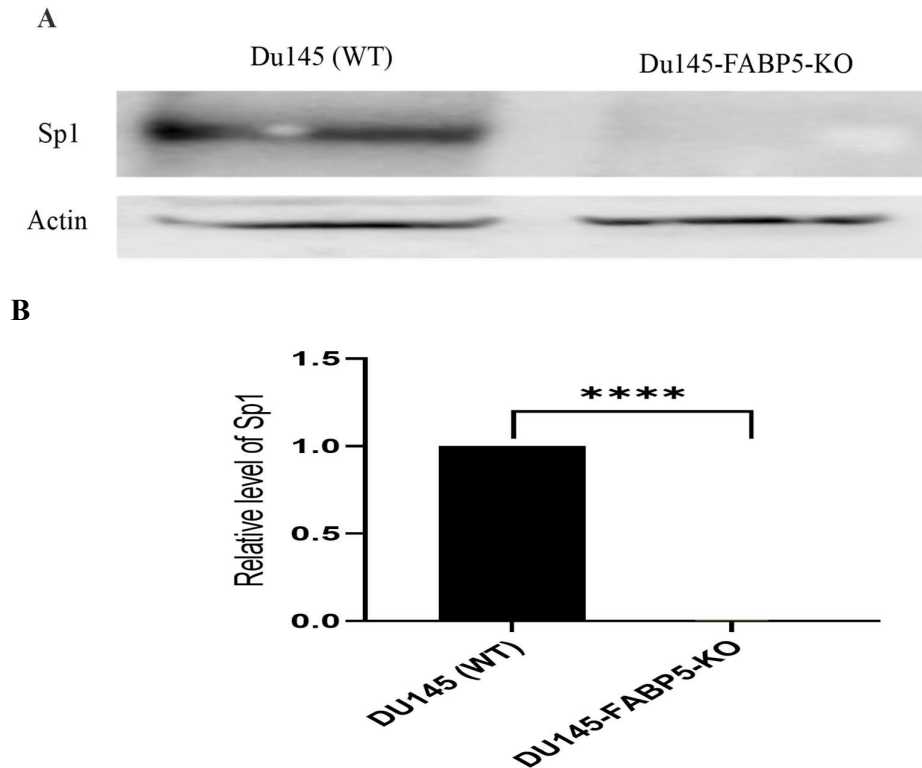


**Figure 5.24** The effect of DU145-FABP5-KO on Sp1 expressions A) The image of Western blot of the expression level of Sp1 in DU145-FABP5-KO. B) Relevant level of Sp1 in DU145-FABP5-KO cells. To normalize possible loading errors, anti- $\beta$ -actin was used to hybridize the blot. The intensities of the bands on the blot were subjected to densitometrical scanning and the data was analysed with the Image-J software. Each result data (Mean  $\pm$  SE) was obtained from 3 separate measurements.

### 5.7.10 The effect of Plicamycin on FABP5 expression in DU145 cells

DU145 cells were treated with DMSO (control), 1  $\mu$ M of Plicamycin (Pli) to study the effect on FABP5 expression and the results were shown in Figure 5.25. Images of Western blot were shown in Figure 5.25A. As shown in Figure 5.25B, when the level of



FABP5 in DU145 control cells was set at 1, the relative FABP5 level in the DU145 cells treated with the Sp1 inhibitor was significantly ( $***P<0.001$ ) reduced by 47% to  $0.53 \pm 0.045$ .

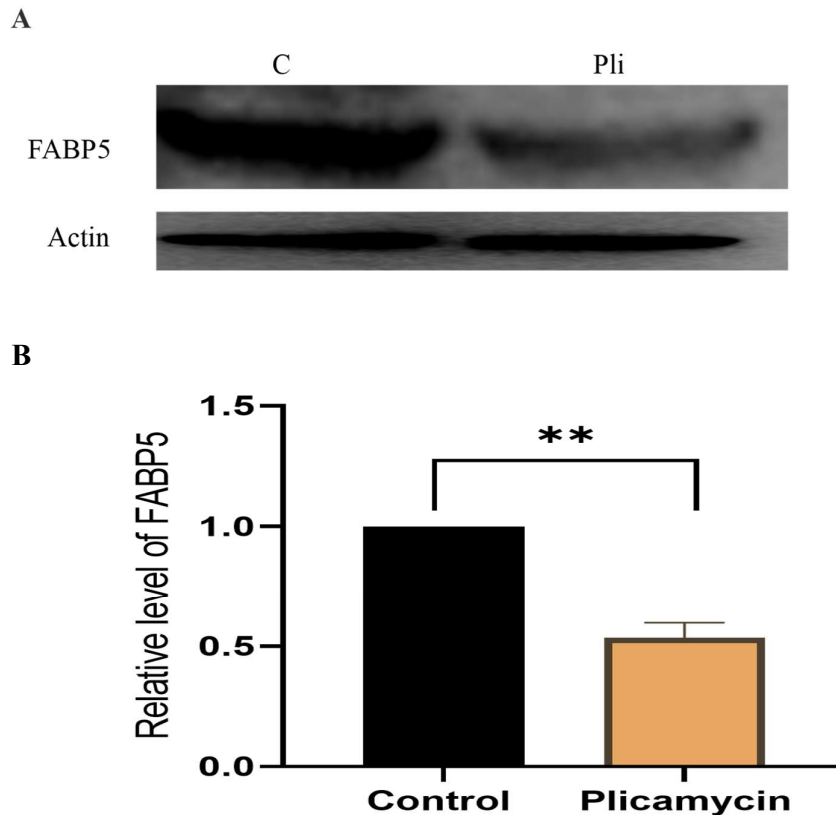
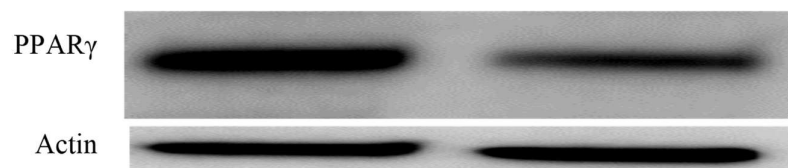


**Figure 5.25** The effect of Plicamycin on FABP5 expression in DU145 cells. **A)** Western blot detection of FABP5 expression in DU145 cells. **B)** Relative levels of FABP5 in DU145 cells. Anti- $\beta$ -actin was used to hybridise the blot to normalize the possible loading errors. The intensities of the bands on the blot were subjected to densitometrical scanning and the data was analysed with the Image-J software. Each result data (Mean  $\pm$  SE) was obtained from 3 separate measurements. Each experiment was performed in triplicate  $n=3$ .

### 5.7.11 The effect of Plicamycin on PPAR $\gamma$ expression in DU145 cells

The androgen-independent DU145 cells were treated with DMSO as control and 1  $\mu$ M of Plicamycin to study the effect on PPAR $\gamma$  expression. The results were shown in Figure 5.26. The images of Western blot detection were shown in Figure 5.26A. Relative PPAR $\gamma$  levels were shown in Figure 5.26B. When the level of PPAR $\gamma$  in the control was set at 1, the relative level of PPAR $\gamma$  in cells treated with Plicamycin was significantly (\*\*\*) reduced by 63% to  $0.37 \pm 0.033$ .

A



B

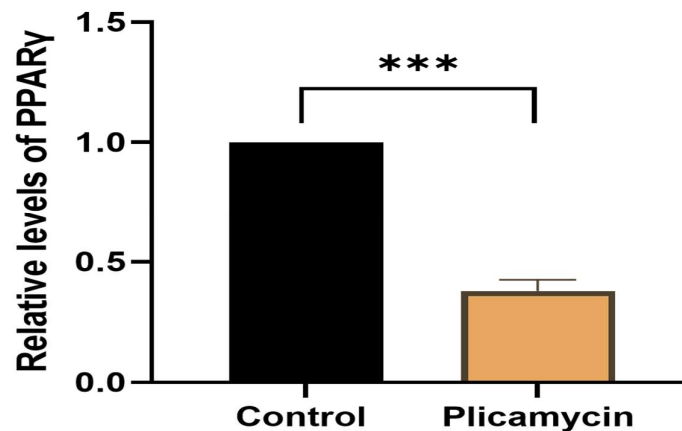


**Figure 5.26** The Effect of Plicamycin on PPAR $\gamma$  expression in Du145 cells. **A)** Western blot images of PPAR $\gamma$  expression in DU145 cells. **B)** Relative levels of PPAR $\gamma$  in DU145 cells. To normalize possible loading errors, anti- $\beta$ -actin was used to hybridize the blot. The intensities of the bands on the blot were subjected to densitometrical scanning and the data was analysed with the Image-J software. Each result data (Mean  $\pm$  SE) was

obtained from 3 separate measurements. Each experiment was performed in triplicate n=3.

### 5.7.12 The effect of Plicamycin on p-PPAR $\gamma$ expression in DU145 cells

To study the effect on p-PPAR $\gamma$  expression, Plicamycin was used at 1  $\mu$ M to treat DU145 cells and DMSO was used as control. The results were shown in Figure 5.27. The images of the Western blots were shown in Figure 5.26A. The relative levels of p-PPAR $\gamma$  were shown in figure 5.27B. When the level of PPAR $\gamma$  in the control was set at 1, the relative level of p-PPAR $\gamma$  in the cells treated with plicamycin was significant ( $*P<0.05$ ) reduced by 21% to  $0.79 \pm 0.04$ .

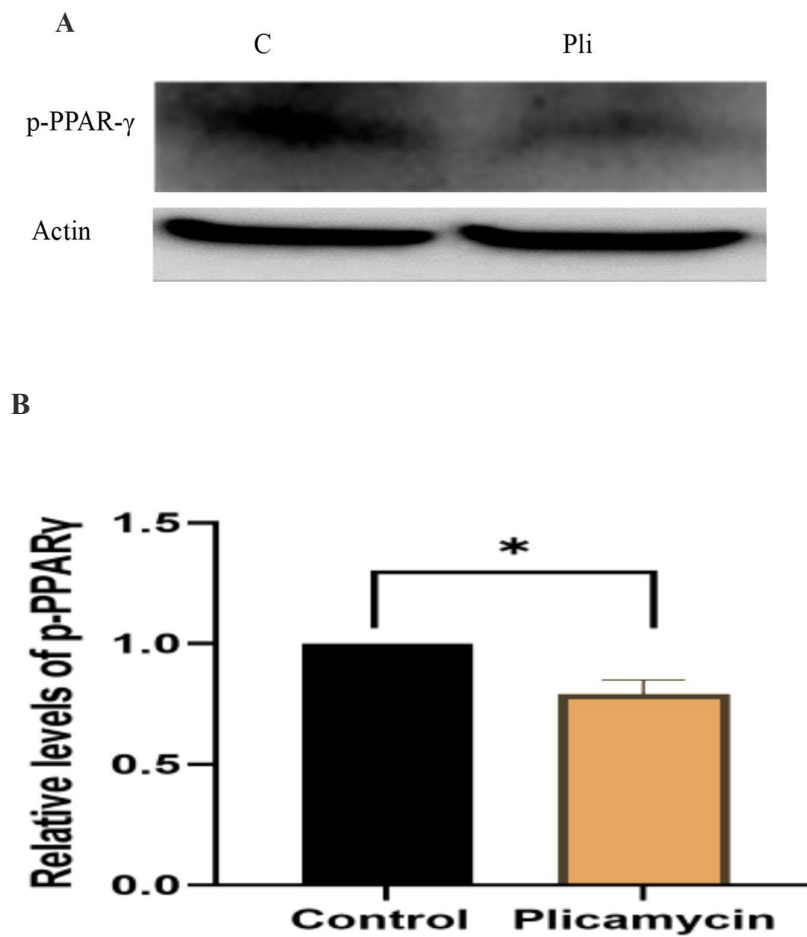


**Figure 5.27** The effect of Plicamycin on p-PPAR $\gamma$  expression in DU145 cells. **A)** Western blot images of p-PPAR $\gamma$  expression in DU145 cells. **B)** Relative levels of p-PPAR $\gamma$  in DU145 cells. Anti- $\beta$ -actin was used to hybridise the blot to normalize the possible loading errors. The intensities of the bands on the blot were subjected to densitometrical scanning and the data was analysed with the Image-J software. Each result data (Mean  $\pm$  SE) was obtained from 3 separate measurements. Each experiment was performed in triplicate n=3.

## 5.8 Discussion

The molecule FABP5 is important in various cellular metabolic processes, particularly lipid metabolism. It has been found to play a role in promoting cancer by transporting fatty acids to the nucleus, where they stimulate a receptor called PPAR $\gamma$ , leading to the up- or down-regulation of genes that promote cancer progression. Inhibitors of FABP5 have been shown to effectively suppress tumor growth and metastasis. A recent study compared a bio-inhibitor called dmrFABP5 with a chemical inhibitor called SB-FI-26. While both inhibitors targeted FABP5, dmrFABP5 did not block the uptake of fatty acids by cancer cells like SB-FI-26 did. Instead, dmrFABP5 promoted apoptosis (programmed cell death) in prostate cancer cells by disrupting the balance between pro- and anti-apoptotic proteins. The researchers investigated the treatment effect of dmrFABP5, along with the drugs docetaxel and enzalutamide, in prostate cancer. They found that dmrFABP5 suppressed FABP5-positive cancer cells, while docetaxel inhibited all cell lines and enzalutamide specifically targeted AR-positive cells. When dmrFABP5 was combined with docetaxel, it synergistically suppressed FABP5-positive cells. Similarly, the combination of dmrFABP5 with enzalutamide restored sensitivity to enzalutamide in AR-V7-expressing cells. The researchers used western blot analysis to study the molecular mechanisms involved in the synergistic effects of the combination treatments. They observed downregulation of various factors related to the FABP5 signalling pathway, such as p-PPAR $\gamma$ , VEGF, Sp1, and Bcl-2, as well as upregulation of the pro-apoptotic protein Bax. The combination treatment of dmrFABP5 with docetaxel also significantly inhibited the expression of AR and AR-V7, while dmrFABP5 treatment alone increased the expression of these proteins. The researchers further demonstrated a correlation between FABP5 and the co-regulator protein Sp1. They found that FABP5 overexpression increased Sp1 expression, while inhibition of Sp1 reduced AR and AR-

V7 expressions. Similarly, inhibition of Sp1 also reduced the expression of FABP5 and PPAR $\gamma$ . Overall, the study revealed that FABP5 overexpression is associated with the progression of prostate cancer by inhibiting apoptosis and upregulating the cancer-promoting protein Sp1. It also showed that FABP5 regulates AR and its variant AR-V7, as well as related signalling pathways. Suppression of FABP5 can restore sensitivity to enzalutamide treatment by reducing AR-V7 levels, which is responsible for treatment resistance. These findings provide insights into the synergistic effects observed when combining dmrFABP5 with other drugs, as they involve signalling pathways related to AR activity, apoptosis factors, and angiogenesis factors.

## **Chapter 6**

**Result -4: Identification of the genes regulated by dmrFABP5 and the investigation of the molecular mechanisms involved in its tumour-suppressing activity in DU145 cells**

## **6.1 Introduction**

Prostate cancer is a prevalent malignancy that affects a significant number of men worldwide. Despite advancements in treatment options, there is a need for novel therapeutic approaches to improve patient outcomes. Understanding the molecular mechanisms underlying prostate cancer development and progression is crucial for identifying potential targets for intervention. In this chapter, we delve into the investigation of the direct effects of dmrFABP5, a novel molecular entity, on prostate cancer cells at the transcriptome level.

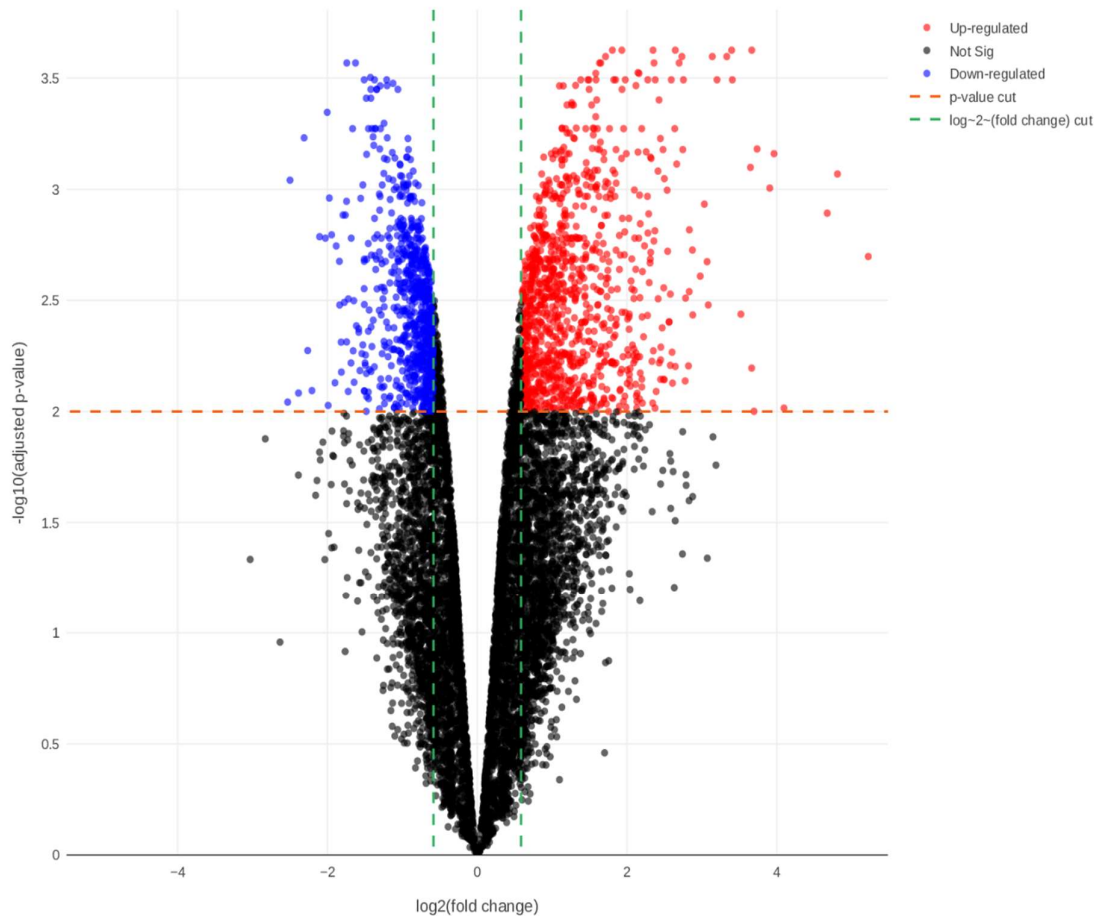
To begin our exploration, we compared the gene expression profiles between parental DU145 cells and dmrFABP5-treated cells, aiming to identify genes that are differentially expressed upon dmrFABP5 treatment. Our analysis revealed a substantial number of differentially expressed genes (DEGs), among which the most notable were FABP5, GRPR, CAV1, BMF, CRIP2, and EGR1. These genes exhibited significant up- or down-regulation in response to dmrFABP5 treatment, indicating their potential involvement in the molecular cascade triggered by dmrFABP5. In the subsequent sections of this chapter, we will delve further into the specific genes affected by dmrFABP5, their functional roles, and their implications for prostate cancer development and treatment. By unraveling the intricate molecular landscape influenced by dmrFABP5, we hope to pave the way for novel targeted therapies and improve patient outcomes in prostate cancer management.



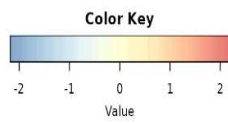
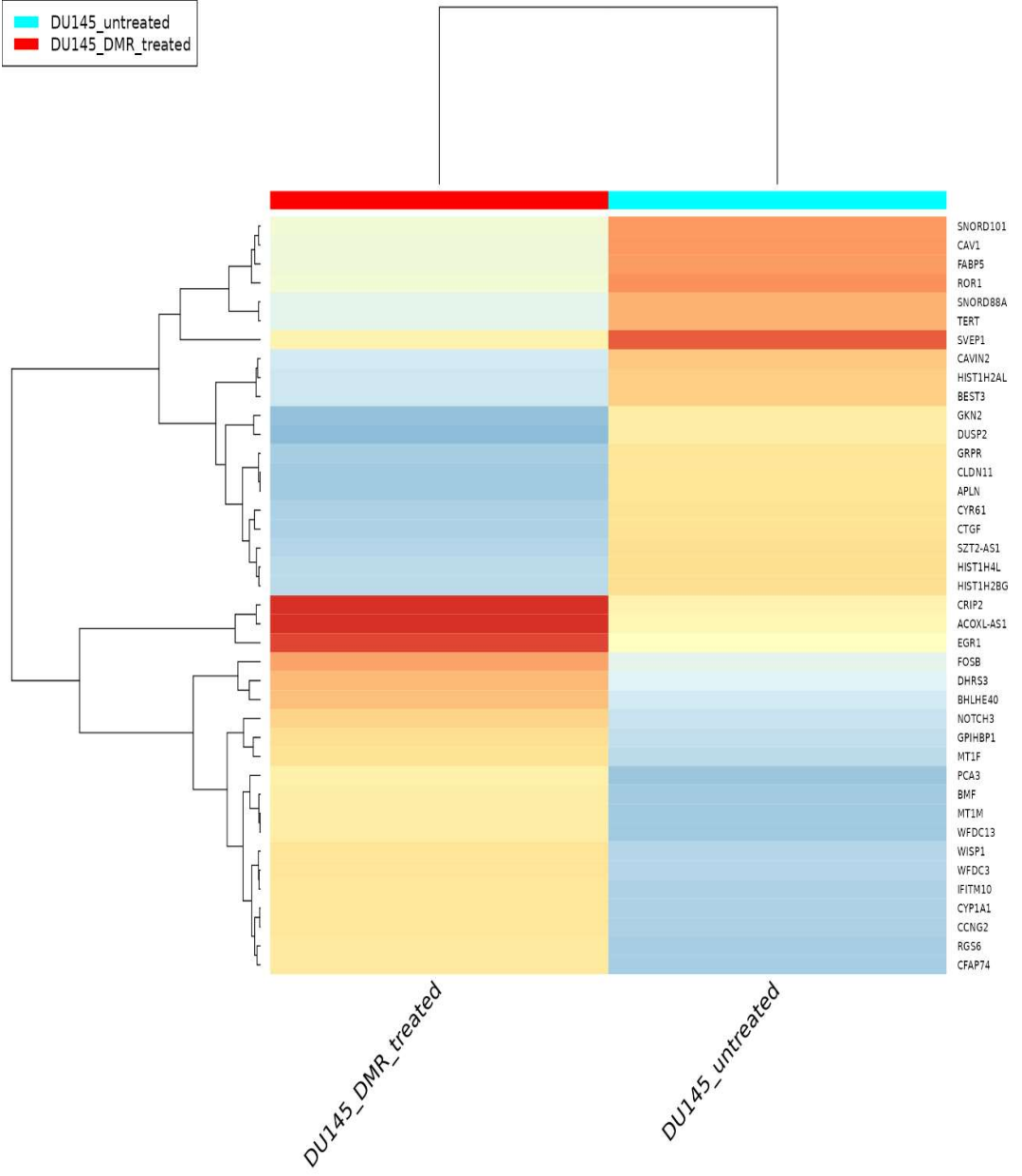
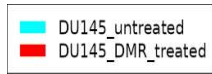
## **6.2 Identification of the DEGs between DU145 cells treated and untreated with dmrFABP5.**

The identified DEGs were shown in Figure 6.1. The upregulated genes were represented by a red colour and the downregulated genes were represented by a blue colour. A volcano plot (A) showed DEGs represented by different dots selected by the significance of the differences. Some gene responded to dmrFABP5 treatment to such an extent that their levels of mRNA were significantly changed, as shown in the heat map (B). Through analysing the heat map, 40 genes, including 20 up-regulated and 20 downregulated (Table 6.1) were identified as the most pronounced DEGs, and from which, six genes were picked up (C). These 6 genes appeared to be important factors that involved in pathways related to our hypothesised tumour-suppression network (C). The cut-off of  $p < 0.05$  were used to determine the DEGs.

A



**B**



C

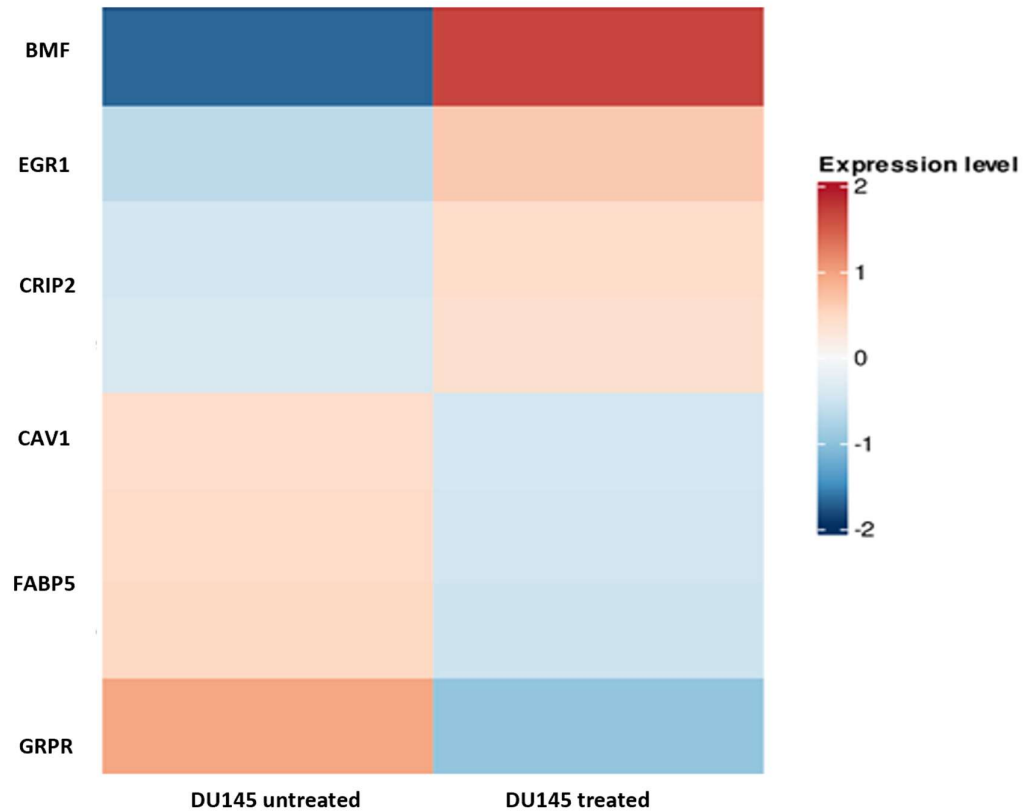


**Figure 6.1** The effect of dmrFABP5 treatment on gene expression profiles in DU145 cells. **A)** Volcano plots illustrating differential gene expression profiles between untreated and treated DU145 cells with dmrFABP5. Each scattered dot represented a gene with at least  $\log_2$  fold significant change ( $P < 0.01$ ). DEGs were shown as red (upregulated) or blue (downregulated) dots. **B)** Heat map showing high DEGs between untreated and treated DU145 cells with dmrFABP5. **C)** Heat map of six most pronounced DEGs obtained by dmrFABP5 treatment in DU145 cells, including the upregulated *EGR1*, *CRIP2*, *BMF*, and the downregulated *FABP5*, *GRPR*, *CAV1* genes.

**Table 6.1.** The significance and the fold change of each of the DEGs.

<b>Gene ID</b>	<b>Gene Name</b>	<b>Log<sub>2</sub>FoldChange (FC)</b>	<b><i>P</i>-Value</b>
ENSG00000205364	MT1M	3.665	2.63e-8
ENSG00000104081	BMF	3.396	2.69e-8
ENSG00000204581	ACOXL-AS1	1.002261	0.063314
ENSG00000104415	WISP1	2.554496	0.00119
ENSG00000277494	GPIHBP1	2.540369	2.60E-06
ENSG00000182809	CRIP2	1.038684	1.40E-05
ENSG00000120738	EGR1	1.026054	5.20E-08
ENSG00000140465	CYP1A1	2.732	1.09e-7
ENSG00000134107	BHLHE40	1.658877	1.49E-21
ENSG00000074181	NOTCH3	1.868493	4.28E-24
ENSG00000162496	DHRS3	1.619311	4.56E-18
ENSG00000138764	CCNG2	2.696	1.75e-7
ENSG00000244242	IFITM10	2.339934	8.25E-11
ENSG00000125740	FOSB	2.521	9.11E-06
ENSG00000198417	MT1F	2.593177	1.71E-09
ENSG00000225937	PCA3	2.769972	0.003697
ENSG00000182732	RGS6	2.763466	2.48E-08

ENSG00000124116	WFDC3	2.591	3.51e-7
ENSG00000142609	CFAP74	2.740678	0.0017
ENSG00000165124	SVEP1	-1.16828	0.05355
ENSG00000221241	H2AC16	-1.626	1.88e-7
ENSG00000196747	SNORD88A	-1.52187	0.01247
ENSG00000127325	BEST3	-1.63469	0.00382
ENSG00000206754	SNORD101	-1.52451	0.00177
ENSG00000275126	HIST1H4L	-1.81328	5.65E-06
ENSG00000185483	ROR1	-1.21269	0.00164
ENSG00000105974	CAV1	-1.02518	0.00227
ENSG00000142871	CYR61	-1.62259	0.00054
ENSG00000013297	CLDN11	-1.7681	0.00099
ENSG00000276903	HIST1H2AL	-1.62706	6.71E-26
ENSG00000168497	CAVIN2	-1.3422	9.64E-05
ENSG00000164362	TERT	-1.97505	0.00026
ENSG00000118523	CTGF	-1.99983	1.50E-23
ENSG00000164687	FABP5	-1.06314	4.55E-11
ENSG00000273802	HIST1H2BG	-1.61887	1.22e-6
ENSG00000126010	GRPR	-1.96129	5.75E-09
ENSG00000171388	APLN	-2.04898	1.12E-09

ENSG00000183607	GKN2	-2.06176	0.00565
ENSG00000158050	DUSP2	-1.74836	0.03694
ENSG00000229372	SZT2-AS1	-2.0398	0.00716

### **6.3 The effect of dmrFABP5 on Gene Ontology (GO) of biological processes Enriched in DEGs by comparing untreated and treated Du145 cells**

In order to investigate the GO of Biological Process Enrichment term, 300 upregulated and 200 downregulated genes were analysed and top 40 pathways were identified at their statistical threshold as shown in Figure 6.2 and table 6.2. DmrFABP5 significantly impacted many pathways and biological processes and were indicated in bar chart. Those effected DEGs were negatively involved in regulation of many processes such as cell migration involved in sprouting angiogenesis, lipid transport, fatty acids metabolic process, cholesterol biosynthetic process and lymphocyte apoptotic process. These results suggested that dmrFABP5 could interfere with these pathways.

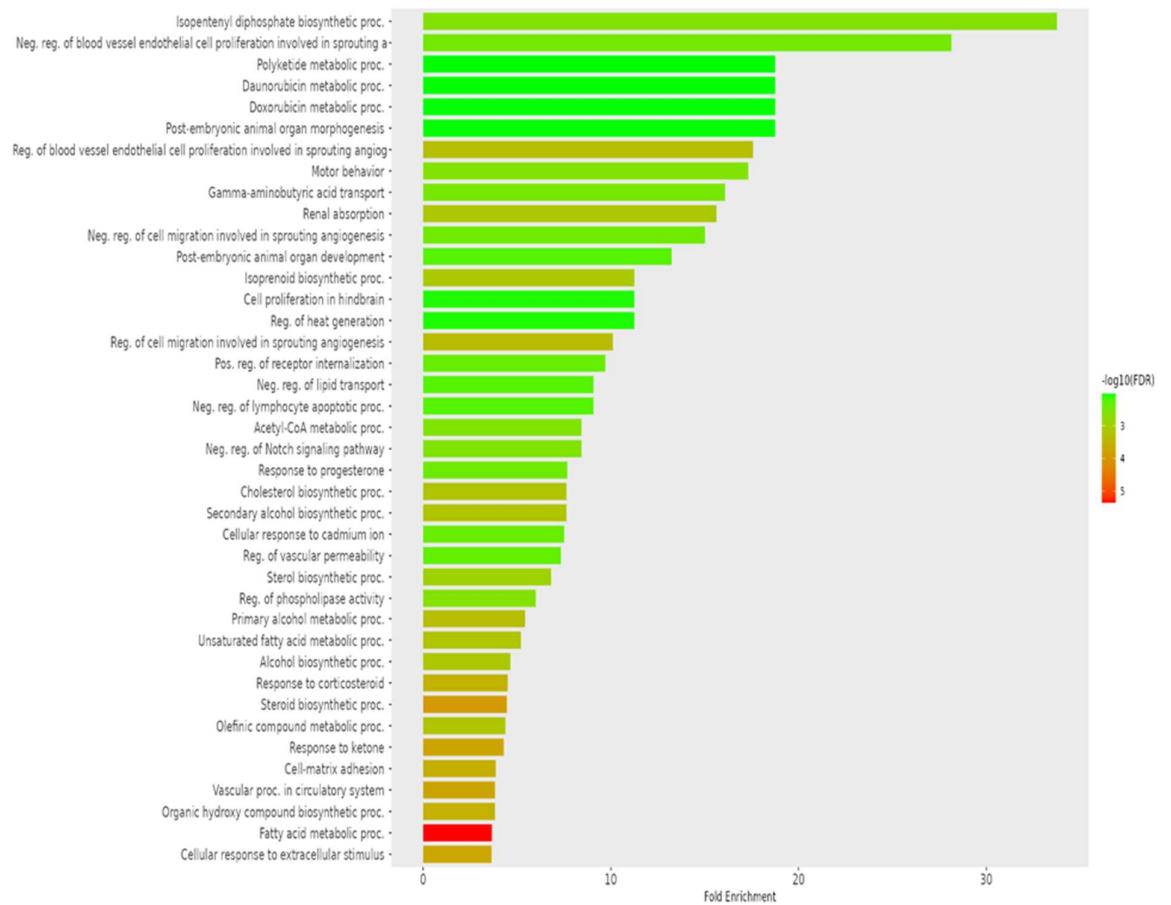


**Figure 6.2** Gene Ontology (GO) Biological Process Enrichment bar chart demonstrate the top 40 enriched pathways in DU145 cell line treated with dmrFABP5. Green represents the down-regulation whereas green represents up-regulation enriched pathway. Pathway changes were determined by log10 False Discovery Rate (FDR).



**Table 6.2** Enriched GO terms in up/down-regulated pathways in Du145 treated cells

<b>Enrichment FDR</b>	<b>Fold Enrichment</b>	<b>Pathway</b>
<b>0.000499</b>	17.58951	Reg. of blood vessel endothelial cell proliferation involved in sprouting angiogenesis
<b>0.000433</b>	10.10269	Reg. of cell migration involved in sprouting angiogenesis
<b>0.002329</b>	33.77185	Isopentenyl diphosphate biosynthetic proc.
<b>0.000734</b>	15.63512	Renal absorption
<b>0.000744</b>	11.25728	Isoprenoid biosynthetic proc.
<b>0.003468</b>	28.14321	Neg. reg. of blood vessel endothelial cell proliferation involved in sprouting a
<b>0.002474</b>	17.3189	Motor behavior
<b>0.000607</b>	7.632057	Cholesterol biosynthetic proc.
<b>0.000607</b>	7.632057	Secondary alcohol biosynthetic proc.
<b>0.003006</b>	16.08183	Gamma-aminobutyric acid transport
<b>0.003652</b>	15.00971	Neg. reg. of cell migration involved in sprouting angiogenesis
<b>0.001154</b>	6.822596	Sterol biosynthetic proc.
<b>0.000487</b>	5.431146	Primary alcohol metabolic proc.
<b>0.000109</b>	4.45833	Steroid biosynthetic proc.
<b>0.002615</b>	8.442963	Acetyl-CoA metabolic proc.
<b>0.002615</b>	8.442963	Neg. reg. of Notch signalling pathway
<b>0.005437</b>	13.24386	Post-embryonic animal organ development

<b>0.000607</b>	5.202946	Unsaturated fatty acid metabolic proc.
<b>0.00016</b>	4.288489	Response to ketone
<b>0.000295</b>	4.502914	Response to corticosteroid
<b>0.004332</b>	9.704555	Pos. reg. of receptor internalization
<b>4.50E-06</b>	3.670853	Fatty acid metabolic proc.
<b>0.002356</b>	6.003885	Reg. of phospholipase activity
<b>0.000705</b>	4.658186	Alcohol biosynthetic proc.
<b>0.003824</b>	7.675421	Response to progesterone
<b>0.000171</b>	3.83771	Vascular proc. in circulatory system
<b>0.009546</b>	18.76214	Polyketide metabolic proc.
<b>0.009546</b>	18.76214	Daunorubicin metabolic proc.
<b>0.009546</b>	18.76214	Doxorubicin metabolic proc.
<b>0.009546</b>	18.76214	Post-embryonic animal organ morphogenesis
<b>0.005547</b>	9.078455	Neg. reg. of lipid transport
<b>0.005547</b>	9.078455	Neg. reg. of lymphocyte apoptotic proc.
<b>0.004196</b>	7.504856	Cellular response to cadmium ion
<b>0.000247</b>	3.858343	Cell-matrix adhesion
<b>0.000618</b>	4.381578	Olefinic compound metabolic proc.
<b>0.000265</b>	3.827477	Organic hydroxy compound biosynthetic proc.
<b>0.008835</b>	11.25728	Cell proliferation in hindbrain
<b>0.008835</b>	11.25728	Reg. of heat generation
<b>0.004595</b>	7.341707	Reg. of vascular permeability
<b>0.000185</b>	3.637558	Cellular response to extracellular stimulus

#### **6.4 The effect of dmrFABP5 on expression of FABP5, GRPR, CAV1, EGR1, CRIP2, and BMF**

The 3 downregulated (*FABP5*, *GRPR* and *CAV1*) and 3 upregulated (*CRIP2*, *EGR1*, *BMF*) DEGs produced by dmrFABP5 treatment in Du145 cells were subjected to western blot verification and the results were shown in Figure 6.3. The expression of FABP5, GRPR and CAV1 were higher in the untreated DU145 (A). When relative levels of these proteins were set at 1, the relative levels of these proteins were significantly reduced by dmrFABP5 treatment to  $0.24 \pm 0.04$  ( $P < 0.0001$ \*\*\*\*),  $0.528 \pm 0.039$  ( $P < 0.01$ \*\*), and  $0.35 \pm 0.021$  ( $P < 0.001$ \*\*\*), which were reduced by 76%, 47% and 65%, respectively (C). The treatment with dmrFABP5 upregulated the EGR1, CRIP2 and BMF expression as shown in B. When levels in the untreated cells were set at 1, the relative levels of these proteins were high significantly (Student's *t*-test  $P < 0.0001$ \*\*\*\*) increased to  $1.73 \pm 0.085$ ,  $2.56 \pm 0.090$  and  $3.54 \pm 0.022$ , which were increased by 73%, 156% and 254%, respectively (C).

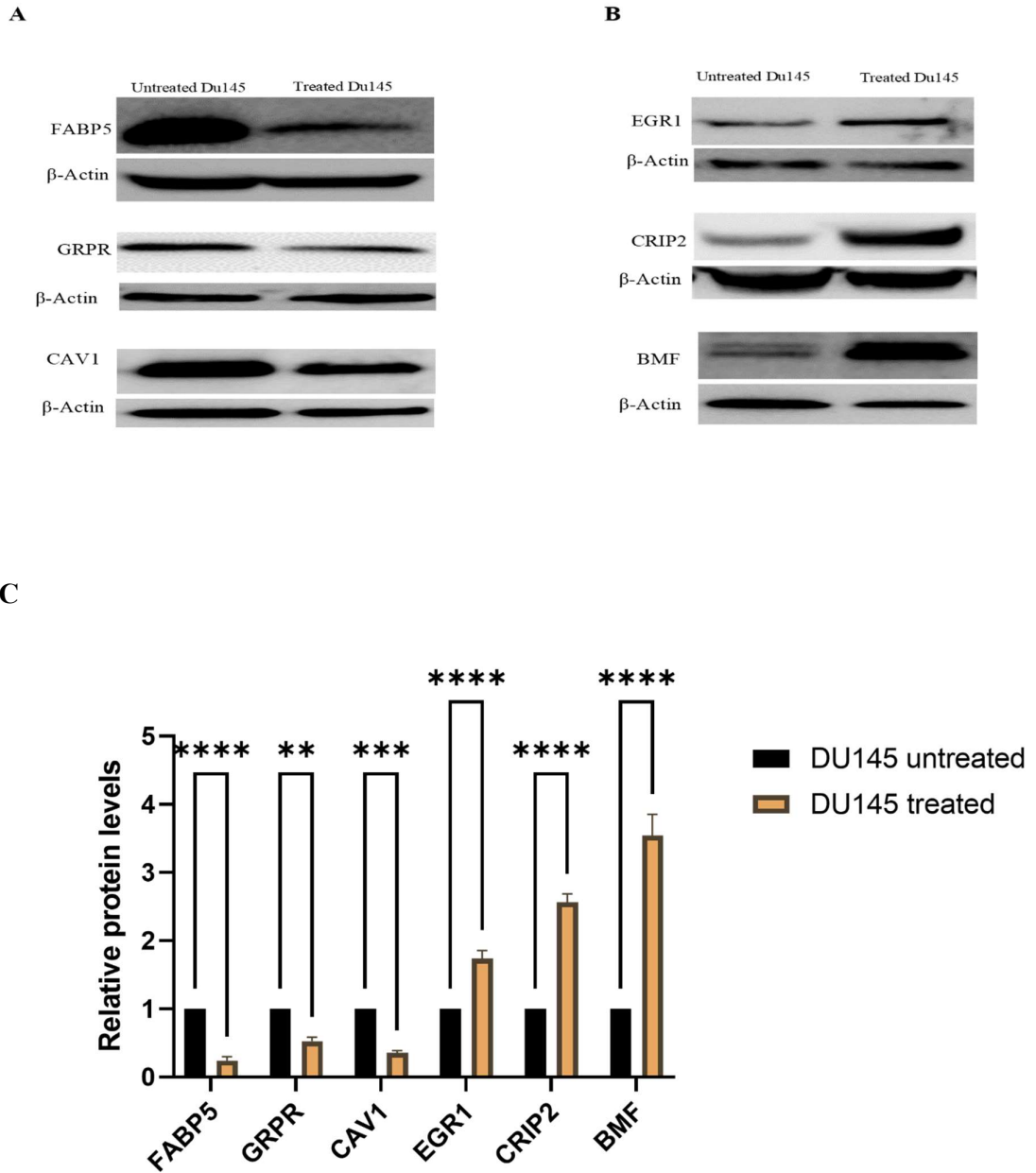


**Figure 6.3.** The effect of dmrFABP5 treatment on expression levels of FABP5, GRPR, CAV1, EGR1, CRIP2 and BMF in Du145 cells. **A)** Western blot detection of the expression status of FABP5, GRPR and CAV1. **B)** Western blots detection of the expression status of EGR1, CRIP2 and BMF. **C)** Relative protein levels of 6 DEGs in DU145 cells with or without dmrFABP5 treatments. All results (Mean  $\pm$  SD) were obtained from three separate measurements, the intensities of the bands were

densitometrically scanned and the data was analysed with Image J software. Each experiment was performed in triplicate n=3.

## **6.5 Discussion**

In this study, researchers investigated the effects of dmrFABP5 treatment on gene expression in prostate cancer cells. They found that dmrFABP5 downregulated FABP5, GRPR, and CAV1, while upregulating EGR1, CRIP2, and BMF. The upregulation of the FOSB gene by dmrFABP5 was particularly significant, as it suppressed cancer cell growth. The study also revealed that FABP5, GRPR, and CAV1 were involved in various cellular processes such as lipid metabolism, signal transduction, angiogenesis, and cell growth inhibition. Conversely, the upregulated genes EGR1, CRIP2, and BMF acted as tumor suppressors, promoting apoptosis.

The researchers demonstrated that dmrFABP5 had similar effects to FABP5 knockout in prostate cancer cells, indicating its potential as a therapeutic approach. The downregulation of genes involved in cell growth and anti-apoptotic processes, along with the upregulation of tumor suppressor genes, suggests that dmrFABP5 could be a promising treatment option for prostate cancer. The study emphasized the significance of FABP5 as a therapeutic target due to its involvement in various signalling pathways related to angiogenesis, apoptosis, and fatty acid transport.

**Chapter 7**  
**General Discussion, Conclusion and Future Work**

## 7.1 General discussion

Among the developed countries, prostate cancer is the most often documented male cancer and the second leading cause of cancer-related mortality in men (2). Androgen deprivation by physical or pharmacological castration and by suppressing the biological activity of AR have been the main treatment for prostate cancer patients since Higgins and colleagues found in 50 years ago that the development and expansion of prostate cancer depended on stimulations of male hormones (102,205). Generally speaking, ADT is a successful first-line therapy. However, the illness recurs over time in a more aggressive form known as CRPC, which is much less responsive to ADT due to the fact that CRPC cells no longer need circulating hormones to grow and spread. The molecular mechanisms underlying the transition from androgen-dependent cancer cells to CRPC cells were not well understood. Currently, there are several theories on the mechanisms of how androgen-dependent cells become androgen-independent cells. The main hypothesis is that after the initial round of ADT, the AR biological sensitivity is enhanced to the point that even very small or micro-quantities of residual hormone in peripheral blood can still accelerate the malignant development of CRPC cells (206,207). However, a recent counterargument to this technique suggested that ADT might result in a therapy dead end (208). Our earlier research indicated that there may be no link between AR and the progression of CRPC, but instead, the FABP5- PPAR $\gamma$ - VEGF axis is the possible underlying cause (160,209). In cancer cells, it was shown that fatty acids were signal molecules that could initiate signalling pathways which could have a significant impact on tumorigenicity and metastasis. Overexpression of FABP5 in PCa was reported as a cell growth and metastasis promoter (159,210,211). In prostate cancer cells, it has been demonstrated that FABP5 transported fatty acids from both intracellular and extracellular sources into the cells and delivered fatty acids to activate the nuclear receptor

PPAR $\gamma$  (159,209). Then the activated PPAR $\gamma$  might initiate a chain of molecular events that led to an enhanced malignant progression of the cancer cells. Thus, the biological function of FABP5 may be the target of a novel approach to CRPC treatment and the inhibitor of FABP5 may enhance the effect of drugs currently in use to treat prostate cancer. Previous study demonstrated that targeting the FABP5 and related signaling transduction through a FABP5 bio-inhibitor named dmrFABP5 (developed by our group) or a chemical inhibitor (SB-FI-26) inhibited the proliferation of the highly malignant PC3M cells *in vitro* and *in vivo* (175). Prostate cancer drug treatments such as anti-androgen (enzalutamide) or chemotherapeutic agent (docetaxel) are considered as a full treatment strategy. Despite the initial effectiveness of all these treatment regimes, prostate cancer eventually relapsed and eventually lost response to these treatments due to the resistance (125,212). One of the main factors causing enzalutamide resistance was AR-V7 due to the fact that it lacked the LBD which is the essential domain for the therapy to be effective (112,114,115,122). It was shown that knockdown of AR-V7 in cells resisted enzalutamide led to resensitize cells to anti-androgen treatments (213). Treatment with docetaxel is a well-known strategy which can reduce the levels of AR and AR-V7 in CRPC cells, but the resistance gradually developed and the mechanisms are not fully understood (125,214). Thus, it is important to develop a new treatment strategy such as finding a new combination treatment to treat CRPC. Combination therapy was used within a therapeutic drug treatment regime and benefited patients because different drugs can target different pathways or genes, drastically reducing the number of cancer cells that survive the treatment and significantly postponing or even completely preventing cancer recurrence (178,215). It was shown that FABP5 inhibitor, SB-FI-26 synergistically worked with docetaxel *in vitro* and *in vivo* (216), although how this was achieved was not known.



This current work is aimed to investigate the possible synergistic effect of dmrFABP5 in combination with current drugs docetaxel or enzalutamide used for PCa treatment. The relevant molecular mechanisms related to the synergistic effect was also investigated.

## **7.2 Half inhibitory concentration or IC<sub>50</sub> of different compounds in PCa cells**

IC<sub>50</sub> is a commonly used metric for the potency of a drug or a compound. The IC<sub>50</sub> value is defined as the concentration of the drug that results in 50% inhibition of the target biological process (213). In the present study, the IC<sub>50</sub> values of three compounds (dmrFABP5, docetaxel, and enzalutamide) were determined in three PCa cell lines (DU145, 22RV1, and LNCaP). The results showed that the IC<sub>50</sub> values of dmrFABP5 in DU145 and 22RV1 cells were 5 $\mu$ M and 12 $\mu$ M respectively (Figures 3.1, A and B), while no significant inhibition was observed in LNCaP cells (Figure 3.1C). The IC<sub>50</sub> values of docetaxel in DU145, 22RV1, and LNCaP cells were 3nM, 4 nM, and 2.2 nM, respectively (Figures 3.2A, B and C). The IC<sub>50</sub> of enzalutamide was not achieved in Du145 and 22RV1 cells, with no significant inhibition detected (Figures 3.3A and B). In LNCaP cells, the IC<sub>50</sub> value of enzalutamide was 97 nM (Figure 3.3C). These results suggested that dmrFABP5 only worked in FABP5-positive cells, no effect was observed in the FABP5-negative LNCaP cells. The results also suggested that the potent chemotherapy drug docetaxel suppressed all PCa cells. As showed in the results, the anti-androgen drug enzalutamide, did not suppress the androgen-independent DU145 cells. It did not suppress the androgen-responsive 22RV1 cells although these cells express AR. The resistance of 22RV1 cells to enzalutamide treatment was likely due to the expression of AR-V7 which lacked the LBD (120,123,212). Enzalutamide suppressed the growth of LNCaP cells as it expressed only AR-FL, did not express AR-V7 (217,218).

### **7.3 The effect of dmrFABP5 treatment combined with docetaxel in PCa cells**

The treatment effect of dmrFABP5 combined with docetaxel was assessed for its potential to enhance the suppression activity in DU145 cells. The results showed (Table 3.1, A and B) that a maximum suppression of 89% of the cells was achieved when dmrFABP5 (5  $\mu$ M) was combined with docetaxel (3 nM), with a CI of 0.00445, indicating a very strong synergistic effect of dmrFABP5 on docetaxel in Du145 cells. When the synergistic interaction between these two compounds in 22RV1 cells was assessed (Figures 3.5, A and B), it was found that a maximum suppression of 92% was achieved when dmrFABP5 and docetaxel were administered at suitable concentrations. With a CI of 0.06834 (Table 3.2), the synergistic effect of dmrFABP5 on the activity of docetaxel in 22RV1 cells is highly significant. However, the same combination did not result in a synergistic interactions in LNCaP, since the CI > 1 (Tables 3.3A and B), although docetaxel alone significantly suppressed cell growth. Treatment with dmrFABP5 alone did not exhibit suppression effect in LNCaP cells, which was expected since LNCaP cells did not express FABP5.

### **7.4 The effect of dmrFABP5 treatment combined with enzalutamide in PCa cells**

When the combination of dmrFABP5 with enzalutamide was assessed for their potential of an enhanced suppression effect in DU145 cells (Tables 3.4, A and B), it was found that there was no synergistic effect produced by the combination. Although dmrFABP5 was found to significantly suppress the growth of DU145 cells, enzalutamide did not exhibit any significant effect which was likely due to the fact that, enzalutamide was specifically designed to target AR, whereas DU145 cells did not express AR and were considered androgen-independent cells.

A significant enhancement was observed when dmrFABP5 was combined with enzalutamide in 22RV1 cells (Table 3.5, A and B). While the maximum suppression of

87% was achieved when dmrFABP5 and enzalutamide were jointly used, a CI of 0.14490 was achieved, indicating a highly synergistic effect on cell growth suppression. When the effect of dmrFABP5 and enzalutamide on LNCaP cells was assessed, it was found that (Tables 3.6, A and B), there was no synergistic interaction between the two compounds. Although dmrFABP5 did not suppress LNCaP cell growth, enzalutamide did produce a significant suppressive effect. The lack of dmrFABP5 action may be attributed to the AR-positive nature of LNCaP cells, as it was considered FABP5-negative, resulting in an enzalutamide suppression independently.

### **7.5 The action of dmrFABP5 to the effect of docetaxel or enzalutamide on PCa cell motility**

DmrFABP5 in combination with docetaxel significantly suppressed the motility of DU145 cells by 93% which was 5% greater than the sum of treatment with each compound alone (Figure 4.1). But when dmrFABP5 treatment was combined with enzalutamide to treat DU145 cells, it did not produce significantly more reduction on cell motility in comparison with dmrFABP5 treatment alone, as the suppressive effect produced by the combination treatment was similar to that produced by dmrFABP5 treatment alone (Figure 4.4). The result showed that enzalutamide did not suppress DU145 cells may due to the fact that enzalutamide was designed to target AR, it did not affect the migration of the AR-negative DU145 cells. Significant suppression on the migration of 22RV1 cells was observed when dmrFABP5 treatment was combined with docetaxel (Figure 4.2). This combination treatment prevented a maximum of 89% wound gap closure. The synergistic activity of dmrFABP5 to docetaxel induced greater suppressive effect on the migration ability of 22RV1 cells than each single agent treatment alone. When enhancement effect produced by combination treatment of

dmrFABP5 with enzalutamide (Figure 4.5) in 22RV1 cells, 91% cell motility inhibition was achieved, which was significantly more than enzalutamide or dmrFABP5 alone that produced 37% and 69%, respectively. When tested in LNCaP cells, dmrFABP5 treatment in combination with either docetaxel or enzalutamide (Figure 4.3 and 4.6) did not enhance docetaxel or enzalutamide, although both treatments inhibited the migration significantly by 69% or 65%, respectively. This result suggested again that dmrFABP5 did not suppress the FABP5-negative LNCaP cells.

### **7.6 The action of dmrFABP5 to the suppression effect of docetaxel or enzalutamide on invasiveness of PCa cells**

DmrFABP5 enhanced the suppressive effect of docetaxel (Figure 4.7) by suppressing 98% of the invaded DU145 cells. These combination produced more inhibition than each compound singly. Thus dmrFABP5 had synergistic action to the treatment effect of docetaxel. But when dmrFABP5 was combined with enzalutamide, no greater suppression was seen in DU145 cell invasion (Figure 4.10), although dmrFABP5 alone inhibited the invasion of DU145 by 80% compared to the combination of both by 82%. This result suggested that although dmrFABP5 can effectively suppress DU145 invasion, enzalutamide, as an ADT drug designed to target AR, did not exhibit suppressive effect on DU145 invasion. No synergistic effect was observed when dmrFABP5 and enzalutamide were used together.

When tested in AR-positive 22RV1 cells, enzalutamide alone did not significantly suppress the invasion while dmrFABP5 alone produced a significant 72% suppression in 22RV1 cell invasion (Figure 4. 11). When dmrFABP5 was combined with enzalutamide to treat the 22RV1 cells, the cell invasion was inhibited by 97%. This result showed that although enzalutamide did not produced suppression effect on 22RV1 invasion, probably

due to the ARV7 expression, the enzalutamide enhanced the effect produced by dmrFABP5 by 25%. More study is needed to understand the mechanisms on how this enhancement effect was produced. No enhancement was found when dmrFABP5 combined with either docetaxel or enzalutamide, on the invasion of LNCaP (Figure 4.9 and 4.11) although docetaxel or enzalutamide used separately significantly ( $P < 0.001$ ) inhibited the invasion of LNCaP cells by 87% (Figure 4.9A and B) and 81% (Figure 4.12, A and B), respectively, whereas dmrFABP5 combination with each of them produced similar suppressions on invasion by 85% and 77% respectively. This result showed that both enzalutamide and docetaxel were effective on LNCaP cells, dmrFABP5 was not effective in FABP5-negative LNCaP cells.

### **7.7 The effect of dmrFABP5 in combination with docetaxel or enzalutamide on PCa cell anchorage-independent growth**

Previously, it was shown that dmrFABP5 suppressed the colony formation of PC3-M (175). When dmrFABP5 were jointly used with either of the compounds to treat DU145 cells (Figure 4.12), dmrFABP5 significantly enhanced the inhibition effect of docetaxel on DU145 colony formation, but the treatment of dmrFABP5 combined with enzalutamide did not significantly inhibit the colony formation of DU145 compared to that obtained by dmrFABP5 treatment alone. This result showed that enzalutamide, an ADT drug in current use, did not have effect in AR-negative DU145 cells. In 22RV1 cells, treatment of dmrFABP5 combined with either docetaxel or enzalutamide, exhibited synergistic effect and produced greater suppressions on colony formation than the sum of each compound alone (Figure 4.13 and 4.16). Thus, dmrFABP5 enhanced docetaxel and enzalutamide suppressive effect in 22RV1 cells. No significant suppression of the colony formation in LNCaP cells was seen when the same combinations were used (Figure 4.14 and 4.17), as they produced same suppression effect as docetaxel or

enzalutamide alone. Thus, dmrFABP5 did not significantly enhance the suppressive effect of docetaxel or enzalutamide in LNCaP cells and it did not have suppressive effect on the colony formation ability of the FABP5-negative LNCaP cells.

### **7.8 The molecular mechanisms underlying the synergistic action of dmrFABP5 to the suppression effect of docetaxel or enzalutamide on the malignant characteristics of PCa cells**

FABP5 is an important molecule plays multiple roles in some cell motabolic processes, particularly the lipid motabolism process (134,219). Previous studies showed that cancer-promoting activity exerted by FABP5 was through transporting exssesive amount of fatty acids from intracellular and extracellular sources into cytoplasm and delivered to the nuclear fatty acid-receptor PPAR $\gamma$ . The fatty acids stimulated and activated their receptor PPAR $\gamma$  and the activated PPAR $\gamma$  triggered a series of molecular events that lead to the up- or down- regulations of the cancer-promoting- or suppressing- genes and thus, facilitating the malignant progression of the cancer cells (130,160). Both chemically and biologically sythsesised FABP5 inhibitors were shown to be very effective in suppressing tumorigenicity and metastatic ability of the cancer cells (175). Recent study showed that the bio- inhibitor dmrFABP5 was more potent than the chemical inhibitor SB-FI-26 in cancer-supression. It was showed that SB-FI-26 competitively binded to FABP5 to inhibit the fatty acids uptake by the cancer cells, thus prevented the exsessive signalling moleculs fatty acids to stimulate PPAR $\gamma$  and hence stopped cancer promoting signal transduction through FABP5-PPAR $\gamma$ -VEGF axis (175). But unlike the SB-FI-26, dmrFABP5 did not block the cell uptake of fatty acids. Recent studies showed that the cancer-suppression effect of dmrFABP5 might be achieved, at least partially, by promoting apoptosis in

prostate cancer cells through various mechanisms, including disrupting BAX-BCL-2 balance by downregulating the anti-apoptotic Bcl-2 and upregulating the pro-apoptotic Bax (130,220). Despite the recent progress, molecular mechanisms on how dmrFABP5 suppressed cancer cells were not fully known. A clear understanding on how dmrFABP5 played its functional role and whether it can enhance the treatment effect of the drug in current use are imperative tasks for establishment of FABP5-targeted therapy for prostate cancer.

In this work, we investigated the treatment effect of dmrFABP5, docetaxel and enzalutamide in prostate cancer and studied the synergistic effect of combination treatment of dmrFABP5 with either enzalutamide or docetaxel. Our results showed that dmrFABP5 exhibited suppression activity in FABP5-positive cells 22RV1 and DU145, but not in FABP5-negative LNCaP cells. Whereas docetaxel worked as an inhibitor in all cell lines used, enzalutamide played a suppressive role in AR-positive LNCaP cells, not in AR-negative DU145 and 22RV1 which expressed AR-V7, a drug resistant variant that lacked the LBD. DmrFABP5 treatment worked synergistically with docetaxel by suppressing the FABP5- positive DU145 and 22RV1 cells, but did not significantly suppress the FABP5- negative LNCaP cells. When dmrFABP5 combined with enzalutamide, it produced synergistic effect in 22RV1 cells whereas same combination treatment did not synergistically suppress DU145 and LNCaP cells. These results indicated that dmrFABP5's inhibiting role and its synergistic effect on enzalutamide and docetaxel were related to AR or other factors that were related to FABP5-initiated signal pathway, or the FABP5-PPAR $\gamma$ -VEGF axis.

To investigate the molecular mechanism involved in the synergistic interaction between dmrFABP5 combined with either docetaxel or enzalutamide, western blot were used to detect the changes in expression of the main factors related to FABP5-initiated signal

pathways. The combination treatment of dmrFABP5 with docetaxel in Du145 cells significantly downregulated the expression levels of p-PPAR $\gamma$ , VEGF, Sp1, Bcl-2 (Figures 5.1-5.5), and upregulated the expression level of Bax. In 22RV1 cells, this combination treatment suppressed the expression levels of AR, AR-V7, p-PPAR $\gamma$ , VEGF, Sp1, Bcl-2 (Figures 5.6-5.11), increased the expression of Bax (Figure 5.12). This result showed that the factors (p-PPAR $\gamma$ , VEGF, Sp1, Bcl-2, Bax) affected by the treatment were all related to the FABP5 in these cancer cells. While both docetaxel and dmrFABP5 targeted almost the same molecules, the enhancement could be partially caused by the double-strike effect.

The combination of dmrFABP5 with enzalutamide showed promising results in restoring sensitivity to enzalutamide in 22RV1 cells, which did not respond to enzalutamide treatment due to AR-V7 expression. Like the treatment effect on the malignant characteristics, the combination significantly suppressed AR and AR-V7 expressions, while enzalutamide alone did not (Figure 5.13). This inhibition effect could be due to the fact that dmrFABP5 suppressed the expression of Sp1 which act as a co-regulator of AR and VEGF (127,221). Moreover, same combination was shown to significantly reduced many protein regulators including PPAR $\gamma$ , p-PPAR $\gamma$ , VEGFA and Sp1 (Figures 5.14-5.16), with greater suppressive effect than each agent alone. To further evaluate the relationship between FABP5 and AR, or AR-V7, the expression of AR was analyzed in 22RV1-FABP5-KO cells. The results showed that the expression of AR did not decrease in 22RV1-FABP5-KO cells compared to the parental 22RV1 cells. However, AR-V7 expression was significantly decreased in 22RV1-FABP5-KO cells. The treatment of 22RV1-FABP5-KO cells with enzalutamide resulted in a significant suppression of both AR and AR-V7 expression (Figure 5.15). Subsequently, our results validated the hypothesized correlation between FABP5 and AR, revealing that the treatment with



wtFABP5 to 22RV1 cells resulted in a significant increase in the expression of both AR and AR-V7 (Figure 5.16). We further substantiated the correlation between FABP5 overexpression and its impact on Sp1 expression. Results indicated that treatment with wtFABP5 increased the expression of Sp1 significantly in 22RV1 cells (Figure 5.17). Further analysis was conducted to examine the relationship between FABP5 and Sp1 expression. The results indicated that Sp1 expression was reduced significantly in 22RV1-FABP5-KO cells, as shown in Figure 5.18. The experiment involved treating 22RV1 cells with Plicamycine, Sp1 inhibitor. The results showed significant suppression of AR and AR-V7 expressions (Figure 5.19). Subsequently, the efficacy of the Sp1 inhibitor in downregulating FABP5 expression was also verified, and it was found to be effective (Figure 5.20). Anti-Sp1 also reduced both PPAR $\gamma$ , p- PPAR $\gamma$  (Figure 5.21). The expression of Sp1 in DU145-FABP5-KO was evaluated and found to be significantly reduced (Figure 5.22). The effectiveness of Plicamycin was also tested in terms of its impact on FABP5, PPAR $\gamma$ , and p-PPAR $\gamma$  expressions. The results showed a significant reduction in all three expressions (Figure 5.23 and 5.24).

These results suggested that overexpression of FABP5 was associated with the progression of prostate cancer (PCa) cells through the inhibition of apoptosis and upregulation of the cancer promoter Sp1 in DU145. Additionally, FABP5 was found to regulate the androgen receptor (AR) and its variant AR-V7, as well as related signalling pathways. Suppression of FABP5 through either knockout or dmrFABP5 resulted in restored sensitivity to enzalutamide treatment by reducing the level of AR-V7, which is responsible for treatment resistance. These findings provide insight into the synergistic effects observed, as the results demonstrate the involvement of signalling transduction pathways related to AR activity, apoptosis factors, and angiogenesis factors.

## **7.9 Highlighted the possible interactions between dmrFABP5 and differentially expressed genes identified by comparing expression profile in DU145 cells.**

To investigate further on the genes directly affected by the dmrFABP5, we compared the gene expression profiles between the parental DU145 cells and the dmrFABP5-treated cells, and identified a large number of differential expressed genes (DEGs). From the top 20 DEGs (Figure 6.1B), six most pronounced DEGs: *FABP5*, *GRPR*, *CAV1*, *BMF*, *CRIP2*, and *EGR1*, were found to be down- or up- regulated by dmrFABP5 treatment. To validate these findings, Western blot was performed, which showed that dmrFABP5 treatment significantly downregulated FABP5, GRPR, and CAV1 by 76%, 47%, and 65%, respectively (Figure 6.3A), and upregulated EGR1, CRIP2, and BMF by 73%, 156%, and 254%, respectively. The dmrFABP5 treatment significantly upregulated the *FOSB* gene by 2.5 fold, as illustrated in Table 6.1. The same upregulation was seen in the DU145-FABP5-KO cells. The increased expression of the *FOSB* gene had a significant effect in suppressing the growth of cancer cells, acting as a tumour suppressor (222). These finding suggested that dmrFABP5 had a similar effect as that achieved in DU145-*FABP5*-KO. Thus dmrFABP5 suppressed the tumorigenicity by reversing the *FABP5* function. The gene ontology (GO) enriched pathway analysis revealed that FABP5, GRPR, and CAV1 were involved in several pathways, including lipid metabolism, signal transduction, angiogenesis, cell growth, and had an anti-apoptotic effect. In contrast, the three up-regulated genes by dmrFABP5 treatment, EGR1, CRIP2, and BMF, were tumour suppressors which promoted apoptosis. These results provide evidence for the complex molecular mechanism by which dmrFABP5 affects prostate cancer at the transcriptome level. While we showed that dmrFABP5 played a tumour-suppressor role by reversing the biological effect of wtrFABP5 in prostate cancer cells, the downregulation of genes

involved in cell growth and anti-apoptotic processes, combined with the upregulation of tumour suppressor genes, highlights the potential of dmrFABP5 as a promising therapeutic approach for prostate cancer.

FABP5 is a highly significant therapeutic target due to its association with multiple signalling transduction pathways, such as angiogenesis and apoptosis, in addition to its role in fatty acid transport. The treatment with dmrFABP5 was found to produce similar effects on the molecular mechanism and RNA profiling as observed with FABP5-KO in DU145 and 22RV1 cells, as evidenced by another separate study (Abdulghani Naeem, Submitted PhD. Thesis, Feb, 2023). This suggested that suppressing FABP5 through either dmrFABP5 or KO elicits similar outcomes and highlights the potential of dmrFABP5 as a promising treatment.

## **7.10 Six most pronounced DEGs between dmrFABP5- treated and untreated DU145 cells.**

### **7.10.1 FABP5**

FABP5, a fatty acid binding protein, has been identified as playing a crucial role in the development and progression of prostate cancer. In particular, FABP5 was shown to regulate the expression of PPAR $\gamma$ , which was involved in the regulation of cellular metabolism, as well as angiogenesis and apoptosis. The regulation of PPAR $\gamma$  by FABP5 was therefore of significant interest in the field of prostate cancer research, as it highlights the potential for targeting FABP5 as a therapeutic strategy for the treatment of this disease. By increasing the expression of PPAR $\gamma$ , FABP5 may modulate cellular metabolism, angiogenesis, and programmed cell death in prostate cancer cells, potentially leading to an enhancement in tumour growth and progression. The role of FABP5 in

regulating the expression of PPAR $\gamma$  highlighted the importance of this protein in the progression of prostate cancer (158,160,220). The dmrFABP5 treatment directly caused the suppressed in FABP5 expression was a direct evidence that dmrFABP5 suppressed prostate cancer by acting as an inhibitor of FABP5.

### **7.10.2 GRPR**

In the field of prostate cancer research, it has been observed that overexpression of GRPR and GRPR-mediated signalling may have a significant impact on the growth and progression of both androgen-dependent and androgen-independent prostate cancer cells. The overexpression of GRPR was shown to indirectly stimulate angiogenesis and increase the invasive potential of prostate cancer. This highlights the importance of GRPR and GRPR-mediated signalling as potential therapeutic targets for the treatment of prostate cancer. These findings suggest that the regulation of GRPR expression levels and GRPR-mediated signalling pathways could play a critical role in the management of prostate cancer. By targeting GRPR and its downstream signalling pathways, it may be possible to inhibit the growth and progression of prostate cancer, reduce angiogenesis, and prevent the spread of cancer cells to other parts of the body. Further study is needed to fully understand the roles of GRPR and GRPR-mediated signalling in prostate cancer, to develop targeted therapeutic approaches for this disease (223,224), and to study how dmrFABP5 suppressed the expression of GRPR.

### **7.10.3 CAV1**

CAV1 is a gene that was identified as playing a crucial role in several key cellular processes. These processes include lipid metabolism, signal transduction, and angiogenesis. The expression of CAV1 was therefore considered to be of significant importance in cellular biology and disease development (225). In the context of cellular

metabolism, CAV1 was shown to regulate lipid metabolism by controlling the transport of lipids into and out of cells. In addition, CAV1 was involved in signal transduction. Finally, CAV1 was also shown to be involved in angiogenesis, which was critical for tumour growth and progression (226,227). Results from these previous works highlighted the importance of CAV1 expression in maintaining the proper functioning of cells and tissues and suggested that targeting CAV1 expression may have therapeutic potential in the treatment of diseases related to lipid metabolism, signal transduction, and angiogenesis (228,229). More study is needed on the possible relationship between CAV1 and FABP5 and how dmrFABP5 suppressed CAV1.

#### **7.10.4 EGR1**

EGR1, also known as Early Growth Response 1, is a transcription factor that was shown to have tumour suppressor properties to promote apoptosis, or programmed cell death. This is an important aspect of maintaining the balance of cell growth and division and preventing the development of cancer. Research showed that EGR1 was commonly downregulated in various types of cancer, including breast, lung, and prostate cancer. This decrease in EGR1 expression was linked to increased cell proliferation and decreased apoptosis, allowing for the uncontrolled growth and spread of cancer cells.

In addition to its role in promoting apoptosis, EGR1 was also shown to have a role in regulating immune responses and angiogenesis, further highlighting its importance in the prevention and treatment of cancer.

Overall, the findings on EGR1 as a tumour suppressor and promoter of apoptosis suggest that it could potentially be used as a therapeutic target for the treatment of cancer. Further research is needed to fully understand the mechanisms by which EGR1 regulates tumour growth and cell death, and to develop treatments that effectively restore EGR1 expression

in cancer cells (230-232). Further study is also needed to investigate its possible link to FABP5 and how the suppressed expression of FABP5 by dmrFABP5 increased the level of EGR1 expression.

#### **7.10.5 CRIP2**

CRIP2, also known as Cysteine-rich intestinal protein, is a protein that has been shown to have important roles in angiogenesis and apoptosis. These processes play critical roles in the development and progression of cancer, making CRIP2 a potential target for therapeutic intervention. CRIP2 was shown to regulate angiogenesis. For example, CRIP2 was shown to regulate the expression of VEGF, a growth factor that is essential for angiogenesis. By regulating VEGF expression, CRIP2 can either promote or suppress angiogenesis, depending on the context (233). More study is required to understand how CRIP2 was increased by dmrFABP5 treatment.

#### **7.10.6 BMF**

BMF, also known as Bcl-2 Modifying Factor, is a protein that has been shown to play important roles in apoptosis and cancer. Apoptosis, or programmed cell death, is a critical mechanism that helps maintain the balance between cell growth and death, preventing the development of cancer. BMF was shown to play a key role in the regulation of apoptosis by promoting the activation of the intrinsic apoptosis pathway.

BMF is a pro-apoptotic protein that functions as a Bcl-2 homology 3 (BH3) domain-containing protein. BH3 domain-containing proteins play critical roles in the regulation of apoptosis by interacting with anti-apoptotic proteins, such as Bcl-2 and Bcl-xL, and promoting their activation. BMF was shown to interact with anti-apoptotic proteins and promote their activation, leading to the initiation of apoptosis. In addition to its role in promoting apoptosis, BMF was also shown to play a role in cancer. BMF expression was

found to be downregulated in various types of cancer, including breast, lung, and prostate cancer. This decrease in BMF expression was linked to increased cell survival and decreased apoptosis, allowing for the uncontrolled growth and spread of cancer cells (234-236). Like the other 5 genes, how BMF was increased by dmrFABP5 treatment requires more investigation.

### **7.11 Future Perspectives and Clinical Implications**

Combination therapy targeting FABP5, docetaxel, and enzalutamide holds promise for prostate cancer treatment, particularly in FABP5-positive cells.

Understanding the synergistic effects of dmrFABP5 with docetaxel or enzalutamide can guide the development of more effective combination treatment strategies.

Further research is needed to elucidate the molecular mechanisms underlying the synergistic interactions between dmrFABP5 and the other drugs.

The identification of specific factors related to FABP5-initiated signal pathways, such as p-PPAR $\gamma$ , VEGF, Sp1, Bcl-2, and Bax, can serve as potential therapeutic targets.

Targeting FABP5 in combination with enzalutamide may help restore sensitivity to enzalutamide in AR-V7-expressing prostate cancer cells.

The regulation of AR and AR-V7 by FABP5 suggests a potential therapeutic approach to overcome treatment resistance.

Inhibition of Sp1 expression may provide an effective strategy to suppress FABP5 and downstream signaling pathways associated with prostate cancer progression.

The findings highlight the importance of apoptosis factors and angiogenesis factors in prostate cancer development and suggest potential targets for therapeutic interventions.

By exploring the treatment effects, molecular mechanisms, and potential therapeutic implications, this study contributes to advancing our understanding of prostate cancer and provides valuable insights for future clinical approaches.

## **7.12 Conclusion**

According on the results achieved in this research, several significant discoveries have been made:

This research clearly revealed that the mutant FABP5 (dmrFABP5) suppresses prostate cancer cells (FABP5 positive) DU145 and 22RV1 alone and produce synergistic interaction when combining with current prostate cancer drugs in use such as docetaxel (chemotherapeutic agent) in DU145 and 22RV1 cells whereas it synergistically works with enzalutamide (anti-androgen agent) in 22RV1 but not DU145. DmrFABP5 did not produce any enhancement effect either with docetaxel or enzalutamide in FABP5-negative cells LNCaP.

The combination treatment can significantly suppress the malignant characteristics of prostate cancer cells (DU145 and 22RV1) including cell viability, migration, invasion and anchorage- independent colony formation of the CRPC cells, greater than the sum of both single agent alone on their  $IC_{50}$  concentrations.

The combination treatment significantly affected several protein regulators and disrupting FABP5-initiated signal transduction pathway. The treatment with dmrFABP5 may disrupting a number of cancer-related signal transduction pathways, including those leading to angiogenesis and apoptosis.



The identification of the six most pronounced DEGs between dmrFABP5 treated cells and the control provided novel targets for developing novel therapeutic strategies for prostate cancer. DmrFABP5 was shown to reverse FABP5 biological function with almost similar effect produced by DU145-FABP5-KO.

### **7.13 Future work**

In this study, several combination cycles were conducted to confirm the enhancement effect of dmrFABP5 with docetaxel or enzalutamide on the CRPC cells. As shown previously, the combination treatments of dmrFABP5 with docetaxel or enzalutamide produced greater effect than each compound alone (at  $IC_{50}$ ) when combined them at their  $IC_{50}$  values. Same combination revealed a significant reduction in pathological signs and important molecular mechanism involved in this work were studied. RNA-sequencing was also conducted for the effect of dmrFABP5 in DU145 cells.

To completely comprehend the intricate molecular processes behind dmrFABP5's inhibitory effect, further preclinical study in pharmacokinetics and toxicity are needed before the clinical trial is conducted. Also, further study is needed on the combination treatment of dmrFABP5 with docetaxel or enzalutamide using other model of studying such as animal model (in vivo) and primary culture of human tissue.

## References

1. Sung H, Ferlay J, Siegel RL, Laversanne M, Soerjomataram I, Jemal A, *et al.* Global cancer statistics 2020: GLOBOCAN estimates of incidence and mortality worldwide for 36 cancers in 185 countries. *CA: a cancer journal for clinicians* **2021**;71:209-49
2. The 10 Most Commonly Diagnosed Cancers, World. Cancer Research UK 2018.
3. Prostate cancer statistics. 2018 ed: Cancer Research UK (CRUK); 2018.
4. Cancer Registration Statistics, England. OSN.
5. Ferlay J, Soerjomataram I, Dikshit R, Eser S, Mathers C, Rebelo M, *et al.* Cancer incidence and mortality worldwide: sources, methods and major patterns in GLOBOCAN 2012. *International journal of cancer* **2015**;136:E359-E86
6. Brenner H, Stegmaier C, Ziegler H. Long-term survival of cancer patients in Germany achieved by the beginning of the third millenium. *Annals of oncology* **2005**;16:981-6
7. Hsing AW, Chokkalingam AP. Prostate cancer epidemiology. *Front Biosci* **2006**;11:1388-413
8. Lin DW, Porter M, Montgomery B. Treatment and survival outcomes in young men diagnosed with prostate cancer: A population-based cohort study. *Cancer* **2009**;115:2863-71
9. CRUK Prostate cancer survival rates (2016) [online] Available from : <https://www.cancerresearchuk.org/>. **2016**
10. Krieger N, Quesenberry C, Peng T, Horn-Ross P, Stewart S, Brown S, *et al.* Social class, race/ethnicity, and incidence of breast, cervix, colon, lung, and prostate cancer among Asian, Black, Hispanic, and White residents of the San Francisco Bay Area, 1988–92 (United States). *Cancer Causes & Control* **1999**;10:525-37
11. Woods VD, Montgomery SB, Belliard JC, Ramírez-Johnson J, Wilson CM. Culture, black men, and prostate cancer: what is reality? *Cancer control* **2004**;11:388-96
12. Crawford ED. Epidemiology of prostate cancer. *Urology* **2003**;62:3-12

13. Gann PH. Risk factors for prostate cancer. *Reviews in urology* **2002**;4:S3
14. McAllister BJ. The association between ethnic background and prostate cancer. *British Journal of Nursing* **2019**;28:S4-S10
15. Watkins Bruner D, Moore D, Parlanti A, Dorgan J, Engstrom P. Relative risk of prostate cancer for men with affected relatives: systematic review and meta-analysis. *International journal of cancer* **2003**;107:797-803
16. Kiciński M, Vangronsveld J, Nawrot TS. An epidemiological reappraisal of the familial aggregation of prostate cancer: a meta-analysis. *PloS one* **2011**;6:e27130
17. Johns LE, Houlston RS. A systematic review and meta-analysis of familial colorectal cancer risk. *The American journal of gastroenterology* **2001**;96:2992-3003
18. Hemminki K, Chen B. Familial association of prostate cancer with other cancers in the Swedish Family-Cancer Database. *The Prostate* **2005**;65:188-94
19. Chen YC, Page JH, Chen R, Giovannucci E. Family history of prostate and breast cancer and the risk of prostate cancer in the PSA era. *The Prostate* **2008**;68:1582-91
20. Hemminki K, Czene K. Age specific and attributable risks of familial prostate carcinoma from the family-cancer database. *Cancer* **2002**;95:1346-53
21. Wolk A. Diet, lifestyle and risk of prostate cancer. *Acta Oncologica* **2005**;44:277-81
22. Niclis C, Díaz MdP, Eynard AR, Román MD, Vecchia CL. Dietary habits and prostate cancer prevention: a review of observational studies by focusing on South America. *Nutrition and cancer* **2012**;64:23-33
23. Sonn GA, Aronson W, Litwin M. Impact of diet on prostate cancer: a review. *Prostate cancer and prostatic diseases* **2005**;8:304-10
24. Barnard RJ, Ngo TH, Leung PS, Aronson WJ, Golding LA. A low-fat diet and/or strenuous exercise alters the IGF axis in vivo and reduces prostate tumor cell growth in vitro. *The Prostate* **2003**;56:201-6

25. Pelser C, Mondul AM, Hollenbeck AR, Park Y. Dietary fat, fatty acids, and risk of prostate cancer in the NIH-AARP diet and health study. *Cancer Epidemiology and Prevention Biomarkers* **2013**;22:697-707
26. Rose DP, Connolly JM. Effects of fatty acids and eicosanoid synthesis inhibitors on the growth of two human prostate cancer cell lines. *The Prostate* **1991**;18:243-54
27. Hori S, Butler E, McLoughlin J. Prostate cancer and diet: food for thought? *BJU international* **2011**;107:1348-59
28. Hiatt RA, Anne Armstrong M, Klatsky AL, Sidney S. Alcohol consumption, smoking, and other risk factors and prostate cancer in a large health plan cohort in California (United States). *Cancer Causes & Control* **1994**;5:66-72
29. Wilson A. The prostate gland: a review of its anatomy, pathology, and treatment. *Jama* **2014**;312:562-
30. Bhavsar A, Verma S. Anatomic imaging of the prostate. *BioMed research international* **2014**;2014
31. Matthew Hoffman M. 2020 14/06/2022. Picture of the Prostate.   
<<https://www.webmd.com/men/picture-of-the-prostate> Accessed June 2022>.   
Accessed 2022 14/06/2022.
32. Cohen RJ, Shannon BA, Phillips M, Moorin RE, Wheeler TM, Garrett KL. Central zone carcinoma of the prostate gland: a distinct tumor type with poor prognostic features. *The Journal of urology* **2008**;179:1762-7
33. Kayhan A, Fan X, Oommen J, Oto A. Multi-parametric MR imaging of transition zone prostate cancer: Imaging features, detection and staging. *World journal of radiology* **2010**;2:180
34. McNeal JE. The zonal anatomy of the prostate. *The prostate* **1981**;2:35-49

35. Vargas HA, Akin O, Franiel T, Goldman DA, Udo K, Touijer KA, *et al.* Normal central zone of the prostate and central zone involvement by prostate cancer: clinical and MR imaging implications. *Radiology* **2012**;262:894
36. Wadhera P. An introduction to acinar pressures in BPH and prostate cancer. *Nature Reviews Urology* **2013**;10:358-66
37. Mawhinney M, Mariotti A. Physiology, pathology and pharmacology of the male reproductive system. *Periodontology 2000* **2013**;61:232-51
38. Abate-Shen C, Shen MM. Molecular genetics of prostate cancer. *Genes & development* **2000**;14:2410-34
39. Elterman DS, Barkin J, Kaplan SA. Optimizing the management of benign prostatic hyperplasia. *Therapeutic advances in urology* **2012**;4:77-83
40. Berry SJ, Coffey DS, Walsh PC, Ewing LL. The development of human benign prostatic hyperplasia with age. *The Journal of urology* **1984**;132:474-9
41. Dhingra N, Bhagwat D. Benign prostatic hyperplasia: An overview of existing treatment. *Indian journal of pharmacology* **2011**;43:6
42. Miah S, Catto J. BPH and prostate cancer risk. *Indian journal of urology: IJU: journal of the Urological Society of India* **2014**;30:214
43. Izumi K, Mizokami A, Lin W-J, Lai K-P, Chang C. Androgen receptor roles in the development of benign prostate hyperplasia. *The American journal of pathology* **2013**;182:1942-9
44. van der Sluis TM, Meuleman EJ, van Moorselaar RJA, Bui HN, Blankenstein MA, Heijboer AC, *et al.* Intraprostatic testosterone and dihydrotestosterone. Part II: concentrations after androgen hormonal manipulation in men with benign prostatic hyperplasia and prostate cancer. *BJU international* **2012**;109:183-8
45. Bostwick DG, Qian J. High-grade prostatic intraepithelial neoplasia. *Modern Pathol* **2004**;17:360-79

46. Bostwick DG, Brawer MK. Prostatic intra-epithelial neoplasia and early invasion in prostate cancer. *Cancer* **1987**;59:788-94
47. Zlotta A, Schulman C. Clinical evolution of prostatic intraepithelial neoplasia. *European urology* **1999**;35:498-503
48. Bonkhoff H, Stein U, Remberger K. The proliferative function of basal cells in the normal and hyperplastic human prostate. *The Prostate* **1994**;24:114-8
49. Sakr W, Grignon D, Crissman J, Heilbrun L, Cassin B, Pontes J, *et al.* High grade prostatic intraepithelial neoplasia (HGPIN) and prostatic adenocarcinoma between the ages of 20-69: an autopsy study of 249 cases. *In Vivo (Athens, Greece)* **1994**;8:439-43
50. Cheville JC, Reznicek MJ, Bostwick DG. The focus of "atypical glands, suspicious for malignancy" in prostatic needle biopsy specimens: incidence, histologic features, and clinical follow-up of cases diagnosed in a community practice. *American journal of clinical pathology* **1997**;108:633-40
51. Ayala AG, Ro JY. Prostatic intraepithelial neoplasia: recent advances. *Archives of pathology & laboratory medicine* **2007**;131:1257-66
52. Epstein JI, Allsbrook Jr WC, Amin MB, Egevad LL, Committee IG. The 2005 International Society of Urological Pathology (ISUP) consensus conference on Gleason grading of prostatic carcinoma. *The American journal of surgical pathology* **2005**;29:1228-42
53. NCI. 1977 MORPHOLOGY & GRADE National Cancer Institute  
<http://training.seer.cancer.gov/prostate/abstract-code-stage/morphology.html>  
Accessed June 2022. National Cancer Institute **1977**
54. Roehrborn CG. Clinical management of lower urinary tract symptoms with combined medical therapy. *BJU international* **2008**;102:13-7
55. Shah RB. Current perspectives on the Gleason grading of prostate cancer. *Archives of pathology & laboratory medicine* **2009**;133:1810-6

56. Humphrey PA. Gleason grading and prognostic factors in carcinoma of the prostate. *Modern Pathol* **2004**;17:292-306
57. Epstein JI, Zelefsky MJ, Sjoberg DD, Nelson JB, Egevad L, Magi-Galluzzi C, *et al.* A contemporary prostate cancer grading system: a validated alternative to the Gleason score. *European urology* **2016**;69:428-35
58. Bostwick DG. The pathology of early prostate cancer. *CA: a cancer journal for clinicians* **1989**;39:376-93
59. Naeem AA, Abdulsamad SA, Al-Bayati A, Zhang J, Malki MI, Ma H, *et al.* Prostate Cell Lines. *Journal of Oncology and Medicine* **2022**
60. Cussenot O, Berthon P, Berger R, Mowszowicz I, Faille A, Hojman F, *et al.* Immortalization of human adult normal prostatic epithelial cells by liposomes containing large T-SV40 gene. *The Journal of urology* **1991**;146:881-6
61. BERTHON P, CUSSENOT O, HOPWOOD L, LEDUC A, MAITLAND NJ. Functional expression of sv40 in normal human prostatic epithelial and fibroblastic cells- differentiation pattern of nontumorigenic cell-lines. *Int J Oncol* **1995**;6:333-43
62. Horoszewicz J. The LNCaP cell line-a new model for studies on human prostatic carcinoma. *Prog Clin Biol Res* **1980**;37:115-32
63. Castanares MA, Copeland BT, Chowdhury WH, Liu MM, Rodriguez R, Pomper MG, *et al.* Characterization of a novel metastatic prostate cancer cell line of LNCaP origin. *The Prostate* **2016**;76:215-25
64. Horoszewicz JS, Leong SS, Kawinski E, Karr JP, Rosenthal H, Chu TM, *et al.* LNCaP model of human prostatic carcinoma. *Cancer research* **1983**;43:1809-18
65. Namekawa T, Ikeda K, Horie-Inoue K, Inoue S. Application of prostate cancer models for preclinical study: advantages and limitations of cell lines, patient-derived xenografts, and three-dimensional culture of patient-derived cells. *Cells* **2019**;8:74

66. Sramkoski RM, Pretlow TG, Giaconia JM, Pretlow TP, Schwartz S, Sy M-S, *et al.* A new human prostate carcinoma cell line, 22Rv1. *In Vitro Cellular & Developmental Biology-Animal* **1999**;35:403-9
67. Stone KR, Mickey DD, Wunderli H, Mickey GH, Paulson DF. Isolation of a human prostate carcinoma cell line (DU 145). *International journal of cancer* **1978**;21:274-81
68. Pulukuri SM, Gondi CS, Lakka SS, Jutla A, Estes N, Gujrati M, *et al.* RNA interference-directed knockdown of urokinase plasminogen activator and urokinase plasminogen activator receptor inhibits prostate cancer cell invasion, survival, and tumorigenicity in vivo. *Journal of biological chemistry* **2005**;280:36529-40
69. Kozlowski JM, Fidler IJ, Campbell D, Xu Z-I, Kaighn ME, Hart IR. Metastatic behavior of human tumor cell lines grown in the nude mouse. *Cancer research* **1984**;44:3522-9
70. Tai S, Sun Y, Squires JM, Zhang H, Oh WK, Liang CZ, *et al.* PC3 is a cell line characteristic of prostatic small cell carcinoma. *The Prostate* **2011**;71:1668-79
71. Kaighn M, Narayan KS, Ohnuki Y, Lechner JF, Jones L. Establishment and characterization of a human prostatic carcinoma cell line (PC-3). *Investigative urology* **1979**;17:16-23
72. Mickey DD, Stone KR, Wunderli H, Mickey GH, Vollmer RT, Paulson DF. Heterotransplantation of a human prostatic adenocarcinoma cell line in nude mice. *Cancer research* **1977**;37:4049-58
73. Taplin ME, Ho S-M. The endocrinology of prostate cancer. *The Journal of Clinical Endocrinology & Metabolism* **2001**;86:3467-77
74. Attar RM, Takimoto CH, Gottardis MM. Castration-resistant prostate cancer: locking up the molecular escape routes. *Clinical Cancer Research* **2009**;15:3251-5
75. Heinlein CA, Chang C. Androgen receptor in prostate cancer. *Endocrine reviews* **2004**;25:276-308



76. Heinlein CA, Chang C. Androgen receptor (AR) coregulators: an overview. *Endocrine reviews* **2002**;23:175-200
77. Fujita K, Nonomura N. Role of androgen receptor in prostate cancer: a review. *The world journal of men's health* **2019**;37:288-95
78. Buchanan G, Irvine RA, Coetzee GA, Tilley WD. Contribution of the androgen receptor to prostate cancer predisposition and progression. *Prostate Cancer: New Horizons in Research and Treatment* **2002**:71-87
79. Knudsen KE, Penning TM. Partners in crime: deregulation of AR activity and androgen synthesis in prostate cancer. *Trends in Endocrinology & Metabolism* **2010**;21:315-24
80. Jenster G. The role of the androgen receptor in the development and progression of prostate cancer. 1999. p 407-21.
81. Quigley CA, De Bellis A, Marschke KB, El-Awady MK, Wilson EM, French FS. Androgen receptor defects: historical, clinical, and molecular perspectives. *Endocrine reviews* **1995**;16:271-321
82. Taplin M-E, Rajeshkumar B, Halabi S, Werner CP, Woda BA, Picus J, *et al.* Androgen receptor mutations in androgen-independent prostate cancer: Cancer and Leukemia Group B Study 9663. *Journal of clinical oncology* **2003**;21:2673-8
83. Taplin M-E, Bubley GJ, Ko Y-J, Small EJ, Upton M, Rajeshkumar B, *et al.* Selection for androgen receptor mutations in prostate cancers treated with androgen antagonist. *Cancer research* **1999**;59:2511-5
84. Dehm SM, Schmidt LJ, Heemers HV, Vessella RL, Tindall DJ. Splicing of a novel androgen receptor exon generates a constitutively active androgen receptor that mediates prostate cancer therapy resistance. *Cancer research* **2008**;68:5469-77
85. Bergerat JP, Céraline J. Pleiotropic functional properties of androgen receptor mutants in prostate cancer. *Human mutation* **2009**;30:145-57

86. Culig Z, Hobisch A, Cronauer MV, Cato A, Hittmair A, Radmayr C, *et al.* Mutant androgen receptor detected in an advanced-stage prostatic carcinoma is activated by adrenal androgens and progesterone. *Molecular endocrinology* **1993**;7:1541-50
87. Koivisto P, Kolmer M, Visakorpi T, Kallioniemi O-P. Androgen receptor gene and hormonal therapy failure of prostate cancer. *The American journal of pathology* **1998**;152:1
88. Koivisto P, Kononen J, Palmberg C, Tammela T, Hyytinen E, Isola J, *et al.* Androgen receptor gene amplification: a possible molecular mechanism for androgen deprivation therapy failure in prostate cancer. *Cancer research* **1997**;57:314-9
89. Visakorpi T, Hyytinen E, Koivisto P, Tanner M, Keinänen R, Palmberg C, *et al.* In vivo amplification of the androgen receptor gene and progression of human prostate cancer. *Nature genetics* **1995**;9:401-6
90. Linja MJ, Savinainen KJ, Saramäki OR, Tammela TL, Vessella RL, Visakorpi T. Amplification and overexpression of androgen receptor gene in hormone-refractory prostate cancer. *Cancer research* **2001**;61:3550-5
91. Wang W, Chen Z-X, Guo D-Y, Tao Y-X. Regulation of prostate cancer by hormone-responsive G protein-coupled receptors. *Pharmacology & Therapeutics* **2018**;191:135-47
92. Freedland SJ, Humphreys EB, Mangold LA, Eisenberger M, Dorey FJ, Walsh PC, *et al.* Death in patients with recurrent prostate cancer after radical prostatectomy: prostate-specific antigen doubling time subgroups and their associated contributions to all-cause mortality. *Journal of Clinical Oncology* **2007**;25:1765-71
93. Feng Q, He B. Androgen receptor signaling in the development of castration-resistant prostate cancer. *Frontiers in oncology* **2019**;9:858

94. Magnan S, Zarychanski R, Pilote L, Bernier L, Shemilt M, Vigneault E, *et al.* Intermittent vs continuous androgen deprivation therapy for prostate cancer: a systematic review and meta-analysis. *JAMA oncology* **2015**;1:1261-9
95. Miyamoto H, Messing EM, Chang C. Androgen deprivation therapy for prostate cancer: current status and future prospects. *The Prostate* **2004**;61:332-53
96. Higano CS, Beer TM, Taplin M-E, Efstathiou E, Hirmand M, Forer D, *et al.* Long-term safety and antitumor activity in the Phase 1–2 study of enzalutamide in pre-and post-docetaxel castration-resistant prostate cancer. *European urology* **2015**;68:795-801
97. Tran C, Ouk S, Clegg NJ, Chen Y, Watson PA, Arora V, *et al.* Development of a second-generation antiandrogen for treatment of advanced prostate cancer. *Science* **2009**;324:787-90
98. Tannock IF, De Wit R, Berry WR, Horti J, Pluzanska A, Chi KN, *et al.* Docetaxel plus prednisone or mitoxantrone plus prednisone for advanced prostate cancer. *New England Journal of Medicine* **2004**;351:1502-12
99. Galletti G, Leach BI, Lam L, Tagawa ST. Mechanisms of resistance to systemic therapy in metastatic castration-resistant prostate cancer. *Cancer treatment reviews* **2017**;57:16-27
100. Zhu M-L, Horbinski CM, Garzotto M, Qian DZ, Beer TM, Kyprianou N. Tubulin-targeting chemotherapy impairs androgen receptor activity in prostate cancer. *Cancer research* **2010**;70:7992-8002
101. Waltering KK, Urbanucci A, Visakorpi T. Androgen receptor (AR) aberrations in castration-resistant prostate cancer. *Molecular and cellular endocrinology* **2012**;360:38-43
102. Huggins C, Hodges CV. Studies on prostatic cancer. *Cancer Res* **1941**;1:293-7
103. Robinson D, Van Allen EM, Wu Y-M, Schultz N, Lonigro RJ, Mosquera J-M, *et al.* Integrative clinical genomics of advanced prostate cancer. *Cell* **2015**;161:1215-28

104. Ross RW, Xie W, Regan MM, Pomerantz M, Nakabayashi M, Daskivich TJ, *et al.* Efficacy of androgen deprivation therapy (ADT) in patients with advanced prostate cancer: association between Gleason score, prostate-specific antigen level, and prior ADT exposure with duration of ADT effect. *Cancer: Interdisciplinary International Journal of the American Cancer Society* **2008**;112:1247-53
105. Kuiper G, Faber P, Van Rooij H, Van der Korput J, Ris-Stalpers C, Klaassen P, *et al.* Structural organization of the human androgen receptor gene. *Journal of Molecular Endocrinology* **1989**;2:R1-R4
106. Attard G, Swennenhuis JF, Olmos D, Reid AH, Vickers E, A'Hern R, *et al.* Characterization of ERG, AR and PTEN gene status in circulating tumor cells from patients with castration-resistant prostate cancer. *Cancer research* **2009**;69:2912-8
107. Griffiths K. The regulation of prostatic growth. *Molecular Biology of Prostate Cancer* Berlin, New York, NY: Walter de Gruyter **1998**:9-22
108. Tsao CK, Galsky MD, Small AC, Yee T, Oh WK. Targeting the androgen receptor signalling axis in castration-resistant prostate cancer (CRPC). *BJU international* **2012**;110:1580-8
109. Harris WP, Mostaghel EA, Nelson PS, Montgomery B. Androgen deprivation therapy: progress in understanding mechanisms of resistance and optimizing androgen depletion. *Nature clinical practice Urology* **2009**;6:76-85
110. Watson PA, Chen YF, Balbas MD, Wongvipat J, Succi ND, Viale A, *et al.* Constitutively active androgen receptor splice variants expressed in castration-resistant prostate cancer require full-length androgen receptor. *Proceedings of the national academy of sciences* **2010**;107:16759-65
111. Zhang X, Morrissey C, Sun S, Ketchandji M, Nelson PS, True LD, *et al.* Androgen receptor variants occur frequently in castration resistant prostate cancer metastases. *PloS one* **2011**;6:e27970

112. Hörnberg E, Ylitalo EB, Crnalic S, Antti H, Stattin P, Widmark A, *et al.* Expression of androgen receptor splice variants in prostate cancer bone metastases is associated with castration-resistance and short survival. *PloS one* **2011**;6:e19059
113. Li Y, Alsagabi M, Fan D, Bova GS, Tewfik AH, Dehm SM. Intragenic rearrangement and altered RNA splicing of the androgen receptor in a cell-based model of prostate cancer progression. *Cancer research* **2011**;71:2108-17
114. Welti J, Rodrigues DN, Sharp A, Sun S, Lorente D, Riisnaes R, *et al.* Analytical validation and clinical qualification of a new immunohistochemical assay for androgen receptor splice variant-7 protein expression in metastatic castration-resistant prostate cancer. *European urology* **2016**;70:599-608
115. Guo Z, Yang X, Sun F, Jiang R, Linn DE, Chen H, *et al.* A novel androgen receptor splice variant is up-regulated during prostate cancer progression and promotes androgen depletion-resistant growth. *Cancer research* **2009**;69:2305-13
116. Mostaghel EA, Marck BT, Plymate SR, Vessella RL, Balk S, Matsumoto AM, *et al.* Resistance to CYP17A1 inhibition with abiraterone in castration-resistant prostate cancer: induction of steroidogenesis and androgen receptor splice variants. *Clinical cancer research* **2011**;17:5913-25
117. Hu R, Dunn TA, Wei S, Isharwal S, Veltri RW, Humphreys E, *et al.* Ligand-independent androgen receptor variants derived from splicing of cryptic exons signify hormone-refractory prostate cancer. *Cancer research* **2009**;69:16-22
118. Hu R, Isaacs WB, Luo J. A snapshot of the expression signature of androgen receptor splicing variants and their distinctive transcriptional activities. *The Prostate* **2011**;71:1656-67
119. Li Y, Hwang TH, Oseth L, Hauge A, Vessella RL, Schmechel SC, *et al.* AR intragenic deletions linked to androgen receptor splice variant expression and activity in models of prostate cancer progression. *Oncogene* **2012**;31:4759-67

120. Antonarakis ES, Lu C, Wang H, Lubner B, Nakazawa M, Roeser JC, *et al.* AR-V7 and resistance to enzalutamide and abiraterone in prostate cancer. *New England Journal of Medicine* **2014**;371:1028-38
121. Maughan BL, Antonarakis ES. Clinical relevance of androgen receptor splice variants in castration-resistant prostate cancer. *Current treatment options in oncology* **2015**;16:1-14
122. Smith R, Liu M, Liby T, Bayani N, Bucher E, Chiotti K, *et al.* Enzalutamide response in a panel of prostate cancer cell lines reveals a role for glucocorticoid receptor in enzalutamide resistant disease. *Scientific reports* **2020**;10:1-13
123. Li Y, Chan SC, Brand LJ, Hwang TH, Silverstein KA, Dehm SM. Androgen Receptor Splice Variants Mediate Enzalutamide Resistance in Castration-Resistant Prostate Cancer Cell Lines Truncated AR Splice Variants and Enzalutamide Resistance. *Cancer research* **2013**;73:483-9
124. Masoodi KZ, Eisermann K, Yang Z, Dar JA, Pascal LE, Nguyen M, *et al.* Inhibition of androgen receptor function and level in castration-resistant prostate cancer cells by 2-[[isoxazol-4-ylmethyl]thio]-1-(4-phenylpiperazin-1-yl) ethanone. *Endocrinology* **2017**;158:3152-61
125. Zhou W, Su Y, Zhang Y, Han B, Liu H, Wang X. Endothelial Cells Promote Docetaxel Resistance of Prostate Cancer Cells by Inducing ERG Expression and Activating Akt/mTOR Signaling Pathway. *Frontiers in Oncology* **2020**;10:584505
126. Shi S, Zhang ZG. Role of Sp1 expression in gastric cancer: A meta-analysis and bioinformatics analysis. *Oncology Letters* **2019**;18:4126-35
127. Eisermann K, Broderick CJ, Bazarov A, Moazam MM, Fraizer GC. Androgen up-regulates vascular endothelial growth factor expression in prostate cancer cells via an Sp1 binding site. *Molecular cancer* **2013**;12:1-12

128. McDonnell TJ, Navone NM, Troncoso P, Pisters LL, Conti C, Von Eschenbach AC, *et al.* Expression of bcl-2 oncoprotein and p53 protein accumulation in bone marrow metastases of androgen independent prostate cancer. *The Journal of urology* **1997**;157:569-74
129. Gleave M, Tolcher A, Miyake H, Nelson C, Brown B, Beraldi E, *et al.* Progression to androgen independence is delayed by adjuvant treatment with antisense Bcl-2 oligodeoxynucleotides after castration in the LNCaP prostate tumor model. *Clinical Cancer Research* **1999**;5:2891-8
130. Bao Z, Malki MI, Forootan SS, Adamson J, Forootan FS, Chen D, *et al.* A novel cutaneous fatty acid-binding protein-related signaling pathway leading to malignant progression in prostate cancer cells. *Genes & cancer* **2013**;4:297-314
131. Calamandrei G, Alleva E. Neuronal growth factors, neurotrophins and memory deficiency. *Behavioural brain research* **1995**;66:129-32
132. Luo J, Miller MW. Growth factor-mediated neural proliferation: target of ethanol toxicity. *Brain Research Reviews* **1998**;27:157-67
133. Randle P, Garland P, Hales C, Newsholme E. The glucose fatty-acid cycle its role in insulin sensitivity and the metabolic disturbances of diabetes mellitus. *The Lancet* **1963**;281:785-9
134. Furuhashi M, Hotamisligil GS. Fatty acid-binding proteins: role in metabolic diseases and potential as drug targets. *Nature reviews Drug discovery* **2008**;7:489-503
135. Di Sebastiano KM, Mourtzakis M. The role of dietary fat throughout the prostate cancer trajectory. *Nutrients* **2014**;6:6095-109
136. McArthur MJ, Atshaves BP, Frolov A, Foxworth WD, Kier AB, Schroeder F. Cellular uptake and intracellular trafficking of long chain fatty acids. *Journal of lipid research* **1999**;40:1371-83

137. Chmurzyńska A. The multigene family of fatty acid-binding proteins (FABPs): function, structure and polymorphism. *Journal of applied genetics* **2006**;47:39-48
138. Ockner RK, Manning JA, Poppenhausen RB, Ho WK. A binding protein for fatty acids in cytosol of intestinal mucosa, liver, myocardium, and other tissues. *Science* **1972**;177:56-8
139. Smathers RL, Petersen DR. The human fatty acid-binding protein family: evolutionary divergences and functions. *Human genomics* **2011**;5:1-22
140. Haunerland NH, Spener F. Fatty acid-binding proteins—insights from genetic manipulations. *Progress in lipid research* **2004**;43:328-49
141. Crovetto CA, Córdoba OL. Structural and biochemical characterization and evolutionary relationships of the fatty acid-binding protein 10 (Fabp10) of hake (*Merluccius hubbsi*). *Fish physiology and biochemistry* **2016**;42:149-65
142. Storch J, Thumser AE. The fatty acid transport function of fatty acid-binding proteins. *Biochimica et Biophysica Acta (BBA)-Molecular and Cell Biology of Lipids* **2000**;1486:28-44
143. Storch J, McDermott L. Structural and functional analysis of fatty acid-binding proteins. *Journal of lipid research* **2009**;50:S126-S31
144. Schachtrup C, Emmler T, Bleck B, Sandqvist A, Spener F. Functional analysis of peroxisome-proliferator-responsive element motifs in genes of fatty acid-binding proteins. *Biochemical journal* **2004**;382:239-45
145. Tan N-S, Shaw NS, Vinckenbosch N, Liu P, Yasmin R, Desvergne B, *et al.* Selective cooperation between fatty acid binding proteins and peroxisome proliferator-activated receptors in regulating transcription. *Molecular and cellular biology* **2002**;22:5114-27
146. Michalik L, Wahli W. PPARs mediate lipid signaling in inflammation and cancer. *PPAR research* **2008**;2008



147. Forootan FS, Forootan SS, Malki MI, Chen DQ, Li GD, Lin K, *et al.* The expression of C-FABP and PPAR gamma and their prognostic significance in prostate cancer. *Int J Oncol* **2014**;44:265-75
148. Zimmerman A, Veerkamp J. New insights into the structure and function of fatty acid-binding proteins. *Cellular and Molecular Life Sciences CMLS* **2002**;59:1096-116
149. Balendiran GK, Schnütgen F, Scapin G, Börchers T, Xhong N, Lim K, *et al.* Crystal structure and thermodynamic analysis of human brain fatty acid-binding protein. *Journal of Biological Chemistry* **2000**;275:27045-54
150. Coe NR, Bernlohr DA. Physiological properties and functions of intracellular fatty acid-binding proteins. *Biochimica Et Biophysica Acta-Lipids and Lipid Metabolism* **1998**;1391:287-306
151. Madsen P, Rasmussen HH, Leffers H, Honoré B, Celis JE. Molecular cloning and expression of a novel keratinocyte protein (psoriasis-associated fatty acid-binding protein [PA-FABP]) that is highly up-regulated in psoriatic skin and that shares similarity to fatty acid-binding proteins. *Journal of Investigative Dermatology* **1992**;99:299-305
152. Masouyé I, Saurat J-H, Siegenthaler G. Epidermal fatty-acid-binding protein in psoriasis, basal and squamous cell carcinomas: an immunohistological study. *Dermatology* **1996**;192:208-13
153. Jing C, Beesley C, Foster CS, Chen H, Rudland PS, West DC, *et al.* Human cutaneous fatty acid-binding protein induces metastasis by up-regulating the expression of vascular endothelial growth factor gene in rat Rama 37 model cells. *Cancer research* **2001**;61:4357-64
154. Suojalehto H, Kinaret P, Kilpeläinen M, Toskala E, Ahonen N, Wolff H, *et al.* Level of fatty acid binding protein 5 (FABP5) is increased in sputum of allergic asthmatics and links to airway remodeling and inflammation. *PLoS One* **2015**;10:e0127003

155. Hu Z, Fan C, Livasy C, He X, Oh DS, Ewend MG, *et al.* A compact VEGF signature associated with distant metastases and poor outcomes. *BMC medicine* **2009**;7:1-14
156. Morgan EA, Forootan SS, Adamson J, Foster CS, Fujii H, Igarashi M, *et al.* Expression of cutaneous fatty acid-binding protein (C-FABP) in prostate cancer: potential prognostic marker and target for tumorigenicity-suppression. *Int J Oncol* **2008**;32:767-75
157. Forootan SS, Bao ZZ, Forootan FS, Kamalian L, Zhang Y, Bee A, *et al.* Atelocollagen-delivered siRNA targeting the FABP5 gene as an experimental therapy for prostate cancer in mouse xenografts. *Int J Oncol* **2010**;36:69-76
158. Naeem AA, Abdulsamad SA, Rudland PS, Malki MI, Ke Y. Fatty acid-binding protein 5 (FABP5)-related signal transduction pathway in castration-resistant prostate cancer cells: a potential therapeutic target. *Precision Clinical Medicine* **2019**;2:192-6
159. Adamson J, Morgan EA, Beesley C, Mei Y, Foster CS, Fujii H, *et al.* High-level expression of cutaneous fatty acid-binding protein in prostatic carcinomas and its effect on tumorigenicity. *Oncogene* **2003**;22:2739-49
160. Forootan FS, Forootan SS, Gou X, Yang J, Liu B, Chen D, *et al.* Fatty acid activated PPAR $\gamma$  promotes tumorigenicity of prostate cancer cells by up regulating VEGF via PPAR responsive elements of the promoter. *Oncotarget* **2016**;7:9322
161. Kawaguchi K, Kinameri A, Suzuki S, Senga S, Ke Y, Fujii H. The cancer-promoting gene fatty acid-binding protein 5 (FABP5) is epigenetically regulated during human prostate carcinogenesis. *Biochemical Journal* **2016**;473:449-61
162. Fang LY, Wong TY, Chiang WF, Chen YL. Fatty-acid-binding protein 5 promotes cell proliferation and invasion in oral squamous cell carcinoma. *Journal of oral pathology & medicine* **2010**;39:342-8
163. Morgan E, Kannan-Thulasiraman P, Noy N. Involvement of fatty acid binding protein 5 and PPAR/in prostate cancer cell growth. *PPAR research* **2010**;2010

164. Núñez NP, Liu H, Meadows GG. PPAR- $\gamma$  ligands and amino acid deprivation promote apoptosis of melanoma, prostate, and breast cancer cells. *Cancer letters* **2006**;236:133-41
165. Nwankwo J, Robbins M. Peroxisome proliferator-activated receptor- $\gamma$  expression in human malignant and normal brain, breast and prostate-derived cells. *Prostaglandins, Leukotrienes and Essential Fatty Acids (PLEFA)* **2001**;64:241-5
166. Segawa Y, Yoshimura R, Hase T, Nakatani T, Wada S, Kawahito Y, *et al.* Expression of peroxisome proliferator-activated receptor (PPAR) in human prostate cancer. *The Prostate* **2002**;51:108-16
167. Chaffer CL, Thomas DM, Thompson EW, Williams ED. PPAR $\gamma$ -independent induction of growth arrest and apoptosis in prostate and bladder carcinoma. *BMC cancer* **2006**;6:1-13
168. Kliewer SA, Umesono K, Noonan DJ, Heyman RA, Evans RM. Convergence of 9-cis retinoic acid and peroxisome proliferator signalling pathways through heterodimer formation of their receptors. *Nature* **1992**;358:771-4
169. Wolfrum C, Borrmann CM, Börchers T, Spener F. Fatty acids and hypolipidemic drugs regulate peroxisome proliferator-activated receptors  $\alpha$ -and  $\gamma$ -mediated gene expression via liver fatty acid binding protein: a signaling path to the nucleus. *Proceedings of the National Academy of Sciences* **2001**;98:2323-8
170. Seargent JM, Yates EA, Gill JH. GW9662, a potent antagonist of PPAR $\gamma$ , inhibits growth of breast tumour cells and promotes the anticancer effects of the PPAR $\gamma$  agonist rosiglitazone, independently of PPAR $\gamma$  activation. *British journal of pharmacology* **2004**;143:933-7
171. Zhang J. Molecular mechanisms of the apoptosis-promoting activity of FABP5 inhibitors in prostate cancer cells: University of Liverpool; February 2019.

172. Balcom E, Liu R-Z, Poon S, Godbout R. FABP5 (fatty acid binding protein 5 (psoriasis-associated)). *Atlas of Genetics and Cytogenetics in Oncology and Haematology* **2015**
173. Levine AJ, Oren M. The first 30 years of p53: growing ever more complex. *Nature reviews cancer* **2009**;9:749-58
174. Hohoff C, Borchers T, Rüstow B, Spener F, van Tilbeurgh H. Expression, purification, and crystal structure determination of recombinant human epidermal-type fatty acid binding protein. *Biochemistry* **1999**;38:12229-39
175. Al-Jameel W, Gou X, Jin X, Zhang J, Wei Q, Ai J, *et al.* Inactivated FABP5 suppresses malignant progression of prostate cancer cells by inhibiting the activation of nuclear fatty acid receptor PPAR $\gamma$ . *Genes & cancer* **2019**;10:80
176. Ashton JC. Drug combination studies and their synergy quantification using the Chou–Talalay method. *Cancer research* **2015**;75:2400-
177. Cheng B, Xu P. Nanoparticle-based formulation for drug repurposing in cancer treatment. *Drug Repurposing in Cancer Therapy*: Elsevier; 2020. p 335-51.
178. Mansoori B, Mohammadi A, Davudian S, Shirjang S, Baradaran B. The different mechanisms of cancer drug resistance: a brief review. *Advanced pharmaceutical bulletin* **2017**;7:339
179. Nam J, Son S, Park KS, Zou W, Shea LD, Moon JJ. Cancer nanomedicine for combination cancer immunotherapy. *Nature Reviews Materials* **2019**;4:398-414
180. He F. Bradford protein assay. *Bio-protocol* **2011**:e45-e
181. Chou T-C. Drug Combination Studies and Their Synergy Quantification Using the Chou-Talalay Method Synergy Quantification Method. *Cancer research* **2010**;70:440-6
182. Report GR-SA, 2022 fCUAODtc-GR-SARhA. GENEWIZ. RNA-Seq Analysis Report  
<file:///C:/Users/Abdul/OneDrive/Desktop/thesis%20correction/40-546310215\_GENEWIZ\_RNA-Seq\_Analysis\_Report.html>. Accessed 2022.

183. Clarke SJ, Rivory LP. Clinical pharmacokinetics of docetaxel. *Clinical pharmacokinetics* **1999**;36:99-114
184. Crown J. Docetaxel: overview of an active drug for breast cancer. *The Oncologist* **2001**;6:1-4
185. Qi C, Zhu YJ, Zhao XY, Lu BQ, Tang QL, Zhao J, *et al.* Highly stable amorphous calcium phosphate porous nanospheres: microwave-assisted rapid synthesis using ATP as phosphorus source and stabilizer, and their application in anticancer drug delivery. *Chemistry—A European Journal* **2013**;19:981-7
186. Yvon A-MC, Wadsworth P, Jordan MA. Taxol suppresses dynamics of individual microtubules in living human tumor cells. *Molecular biology of the cell* **1999**;10:947-59
187. Golshayan AR, Antonarakis ES. Enzalutamide: an evidence-based review of its use in the treatment of prostate cancer. *Core evidence* **2013**;8:27
188. Guerrero J, Alfaro IE, Gómez F, Protter AA, Bernales S. Enzalutamide, an androgen receptor signaling inhibitor, induces tumor regression in a mouse model of castration-resistant prostate cancer. *The Prostate* **2013**;73:1291-305
189. Kim W, Ryan CJ. Androgen receptor directed therapies in castration-resistant metastatic prostate cancer. *Current treatment options in oncology* **2012**;13:189-200
190. Swinney DC. Molecular mechanism of action (MMoA) in drug discovery. *Annual Reports in Medicinal Chemistry: Elsevier*; 2011. p 301-17.
191. Chou T-C. Drug combination studies and their synergy quantification using the Chou-Talalay method. *Cancer research* **2010**;70:440-6
192. Du Q, Jiang G, Li S, Liu Y, Huang Z. Docetaxel increases the risk of severe infections in the treatment of non-small cell lung cancer: a meta-analysis. *Oncoscience* **2018**;5:220
193. Antonarakis E, Armstrong A. Evolving standards in the treatment of docetaxel-refractory castration-resistant prostate cancer. *Prostate cancer and prostatic diseases* **2011**;14:192-205

194. FDA Approved Drug Products: Xtandi (enzalutamide) capsules/tablets for oral use  
hwafgddls, 213674s005lbl.pdf. FDA Approved Drug Products: Xtandi (enzalutamide)  
capsules/tablets for oral use,  
[https://www.accessdata.fda.gov/drugsatfda\\_docs/label/2022/203415s018,213674s005lbl.pdf](https://www.accessdata.fda.gov/drugsatfda_docs/label/2022/203415s018,213674s005lbl.pdf)

**2012**

195. Menon MP, Higano CS. Enzalutamide, a second generation androgen receptor antagonist: development and clinical applications in prostate cancer. *Current oncology reports* **2013**;15:69-75
196. Justus CR, Leffler N, Ruiz-Echevarria M, Yang LV. In vitro cell migration and invasion assays. *JoVE (Journal of Visualized Experiments)* **2014**:e51046
197. Carbonetti G, Wilpshaar T, Kroonen J, Studholme K, Converso C, d'Oelsnitz S, *et al.* FABP5 coordinates lipid signaling that promotes prostate cancer metastasis. *Scientific reports* **2019**;9:1-16
198. Bionews Prostate cancer news today hpcd. Bionews Prostate cancer news today,  
<https://prostatecancernewstoday.com/docetaxel/>
199. Imran M, Saleem S, Chaudhuri A, Ali J, Baboota S. Docetaxel: An update on its molecular mechanisms, therapeutic trajectory and nanotechnology in the treatment of breast, lung and prostate cancer. *Journal of Drug Delivery Science and Technology* **2020**;60:101959
200. Ramaswamy B, Puhalla S. Docetaxel: A tubulin-stabilizing agent approved for the management of several solid tumor. *Drugs of today* **2006**;42:265
201. Prostate cancer Uhpop-ite. Enzalutamide. **Updated 2022**

202. Sternberg CN. Enzalutamide, an oral androgen receptor inhibitor for treatment of castration-resistant prostate cancer. *Future Oncology* **2019**;15:1437-57
203. Zheng Z, Li J, Liu Y, Shi Z, Xuan Z, Yang K, *et al.* The Crucial Role of AR-V7 in Enzalutamide-Resistance of Castration-Resistant Prostate Cancer. *Cancers* **2022**;14:4877
204. Armstrong CM, Gao AC. Drug resistance in castration resistant prostate cancer: resistance mechanisms and emerging treatment strategies. *American journal of clinical and experimental urology* **2015**;3:64
205. Sharifi N, Gulley JL, Dahut WL. Androgen deprivation therapy for prostate cancer. *Jama* **2005**;294:238-44
206. Forootan S, Hussain S, Aachi V, Foster C, Ke Y. Molecular mechanisms involved in the transition of prostate cancer cells from androgen dependant to castration resistant state. *J Androl Gynaecol* **2014**;2
207. Karantanos T, Corn PG, Thompson TC. Prostate cancer progression after androgen deprivation therapy: mechanisms of castrate resistance and novel therapeutic approaches. *Oncogene* **2013**;32:5501-11
208. Katzenwadel A, Wolf P. Androgen deprivation of prostate cancer: Leading to a therapeutic dead end. *Cancer letters* **2015**;367:12-7
209. Forootan FS, Forootan SS, Malki MI, Chen D, Li G, Lin K, *et al.* The expression of C-FABP and PPAR $\gamma$  and their prognostic significance in prostate cancer. *Int J Oncol* **2014**;44:265-75
210. Currie E, Schulze A, Zechner R, Walther TC, Farese Jr RV. Cellular fatty acid metabolism and cancer. *Cell metabolism* **2013**;18:153-61
211. Pascual G, Avgustinova A, Mejetta S, Martín M, Castellanos A, Attolini CS-O, *et al.* Targeting metastasis-initiating cells through the fatty acid receptor CD36. *Nature* **2017**;541:41-5

212. Antonarakis ES. Current understanding of resistance to abiraterone and enzalutamide in advanced prostate cancer. *Clinical Advances in Hematology and Oncology* **2016**;14:316-9
213. Zhao J, Ning S, Lou W, Yang JC, Armstrong CM, Lombard AP, *et al.* Cross-Resistance Among Next-Generation Antiandrogen Drugs Through the AKR1C3/AR-V7 Axis in Advanced Prostate Cancer. *Molecular cancer therapeutics* **2020**;19:1708-18
214. Park SE, Kim H-G, Kim DE, Jung YJ, Kim Y, Jeong S-Y, *et al.* Combination treatment with docetaxel and histone deacetylase inhibitors downregulates androgen receptor signaling in castration-resistant prostate cancer. *Investigational New Drugs* **2018**;36:195-205
215. Root A, Ebhardt HA. A two-drug combination simulation study for metastatic castrate resistant prostate cancer. *Prostate* **2018**;78:1196-200
216. Carbonetti G, Converso C, Clement T, Wang C, Trotman LC, Ojima I, *et al.* Docetaxel/cabazitaxel and fatty acid binding protein 5 inhibitors produce synergistic inhibition of prostate cancer growth. *The Prostate* **2020**;80:88-98
217. Khurana N, Kim H, Chandra PK, Talwar S, Sharma P, Abdel-Mageed AB, *et al.* Multimodal actions of the phytochemical sulforaphane suppress both AR and AR-V7 in 22Rv1 cells: Advocating a potent pharmaceutical combination against castration-resistant prostate cancer. *Oncology Reports* **2017**;38:2774-86
218. Weber H, Ruoff R, Garabedian MJ. MED19 alters AR occupancy and gene expression in prostate cancer cells, driving MAOA expression and growth under low androgen. *PLoS Genetics* **2021**;17:e1008540
219. Xu B, Chen L, Zhan Y, Marquez KNS, Zhuo L, Qi S, *et al.* The Biological Functions and Regulatory Mechanisms of Fatty Acid Binding Protein 5 in Various Diseases. *Frontiers in Cell and Developmental Biology* **2022**;10



220. Zhang J, He G, Jin X, Alenezi BT, Naeem AA, Abdulsamad SA, *et al.* Molecular mechanisms on how FABP5 inhibitors promote apoptosis-induction sensitivity of prostate cancer cells. *Cell Biology International* **2023**
221. Shin T, Sumiyoshi H, Matsuo N, Satoh F, Nomura Y, Mimata H, *et al.* Sp1 and Sp3 transcription factors upregulate the proximal promoter of the human prostate-specific antigen gene in prostate cancer cells. *Archives of biochemistry and biophysics* **2005**;435:291-302
222. Liu S, Luan J, Ding Y. miR-144-3p targets FosB proto-oncogene, AP-1 transcription factor subunit (FOSB) to suppress proliferation, migration, and invasion of PANC-1 pancreatic cancer cells. *Oncology Research Featuring Preclinical and Clinical Cancer Therapeutics* **2018**;26:683-90
223. Rinne SS, Abouzayed A, Gagnon K, Tolmachev V, Orlova A. <sup>66</sup>Ga-PET-imaging of GRPR-expression in prostate cancer: Production and characterization of [<sup>66</sup>Ga] Ga-NOTA-PEG2-RM26. *Scientific Reports* **2021**;11:3631
224. Roesler R, Schwartzmann G. GRPR antagonists for prostate cancer—prospects and caveats. *Nature Reviews Urology* **2013**;10:424-
225. Díaz MI, Díaz P, Bennett JC, Urrea H, Ortiz R, Orellana PC, *et al.* Caveolin-1 suppresses tumor formation through the inhibition of the unfolded protein response. *Cell death & disease* **2020**;11:648
226. Huang Q, Zhong W, Hu Z, Tang X. A review of the role of cav-1 in neuropathology and neural recovery after ischemic stroke. *Journal of Neuroinflammation* **2018**;15:1-16
227. Xu H, Zhang L, Chen W, Xu J, Zhang R, Liu R, *et al.* Inhibitory effect of caveolin-1 in vascular endothelial cells, pericytes and smooth muscle cells. *Oncotarget* **2017**;8:76165

228. Vykoukal J, Fahrmann JF, Gregg JR, Tang Z, Basourakos S, Irajizad E, *et al.* Caveolin-1-mediated sphingolipid oncometabolism underlies a metabolic vulnerability of prostate cancer. *Nature communications* **2020**;11:4279
229. Pezeshkian W, Chevrot G, Khandelia H. The role of caveolin-1 in lipid droplets and their biogenesis. *Chemistry and physics of lipids* **2018**;211:93-9
230. Calogero A, Arcella A, De Gregorio G, Porcellini A, Mercola D, Liu C, *et al.* The early growth response gene EGR-1 behaves as a suppressor gene that is down-regulated independent of ARF/Mdm2 but not p53 alterations in fresh human gliomas. *Clinical Cancer Research* **2001**;7:2788-96
231. Schmidt K, Carroll JS, Yee E, Thomas DD, Wert-Lamas L, Neier SC, *et al.* The lncRNA SLNCR recruits the androgen receptor to EGR1-bound genes in melanoma and inhibits expression of tumor suppressor p21. *Cell reports* **2019**;27:2493-507. e4
232. Wang B, Guo H, Yu H, Chen Y, Xu H, Zhao G. The role of the transcription factor EGR1 in cancer. *Frontiers in Oncology* **2021**;11:642547
233. Cheung AKL, Ko JM, Lung HL, Chan KW, Stanbridge EJ, Zabarovsky E, *et al.* Cysteine-rich intestinal protein 2 (CRIP2) acts as a repressor of NF- $\kappa$ B-mediated proangiogenic cytokine transcription to suppress tumorigenesis and angiogenesis. *Proceedings of the National Academy of Sciences* **2011**;108:8390-5
234. Grespi F, Soratroi C, Krumschnabel G, Sohm B, Ploner C, Geley S, *et al.* BH3-only protein Bmf mediates apoptosis upon inhibition of CAP-dependent protein synthesis. *Cell Death & Differentiation* **2010**;17:1672-83
235. Schmelzle T, Mailleux AA, Overholtzer M, Carroll JS, Solimini NL, Lightcap ES, *et al.* Functional role and oncogene-regulated expression of the BH3-only factor Bmf in mammary epithelial anoikis and morphogenesis. *Proceedings of the National Academy of Sciences* **2007**;104:3787-92

236. VanBrocklin MW, Verhaegen M, Soengas MS, Holmen SL. Mitogen-activated protein kinase inhibition induces translocation of Bmf to promote apoptosis in melanoma. *Cancer research* **2009**;69:1985-94

## **Appendices**

## **A Reagents**

### **A 1. Cell culture and treatments reagents**

DMSO	Sigma-Aldrich, Germany
Docetaxel	MedChemExpress, UK
Enzalutamide	MedChemExpress, UK
Foetal bovine serum	Gibco, Invitrogen, UK
L-Glutamine	Lonza, Belgium
Penicillin/Streptomycin	Lonza, Belgium
Phosphate buffered saline	Gibco, Invitrogen, UK
Phosphate buffered saline (tablets)	Gibco, Invitrogen, UK
RPMI 1640	Gibco, Invitrogen, UK
Sodium pyruvate	Sigma, USA
TrypleE	Gibco, Invitrogen, UK

### **A 2. Routine cell culture medium**

500ml of 1640 RPMI medium+ 50ml of Foetal bovine serum (10%)+ 5ml of Penicillin-Streptomycin (5000U/ml)+ 5ml L-Glutamine 20mM+ 5ml Sodium pyruvate 100mM

### **A 3. Freezing medium**

Routine cell culture medium 95%(v/v)+ 5% of DMSO (v/v)

### **A 4. Reagents for molecular biology**

Absolute ethanol	BDH, England, UK
Ampicillin	Invitrogen, CA, USA
BL21 E.coli bacteria	Invitrogen, CA, USA
Glycerol	Sigma, USA
Isopropylthiogalactoside (IPTG)	Sigma, USA
LB agar	Sigma, USA
LB broth	Sigma, USA
QIAGEN Ni-NTA Fast Start Kit	QIAGEN, UK
SDS	Sigma, UK
Magnesium chloride	Sigma, USA
Magnesium sulphate	Sigma, USA

### **A 5. Reagents for western blot**

$\beta$ -mercaptoethanol	Sigma, USA
Ammonium persulfate (APS)	Sigma, USA
Bradford reagent	Sigma, USA
Bromophenole blue	Sigma, USA

CelLytic-M	Sigam, USA
Coomassie blue	Bio-Rad GmbH, UK
ECL detection kit	GE Healthcare, UK
Glycine	Melford, UK
Methanol	Fisher scientific, UK
PVDF membrane	Millipore, USA
Quick Start Bradford Protein assay	Bio-Rad, UK
Tris Base salt	Melford, UK
Tween-20	Sigma, UK
dH <sub>2</sub> O	

#### **A 6. Reagents for drug combinations**

Docetaxel	MedChemExpress, UK
Enzalutamide	MedChemExpress, UK

#### **A 7. Reagents for cell viability detection**

PrestoBlue HS	ThermoFisher, UK
---------------	------------------

#### **A 8. Reagents for invasion assay**

Crystal violet	Sigma, USA
----------------	------------

## **A 9. Reagent for soft agar assay**

Low melting point agarose

Thermofisher, UK

MTT

Sigma, USA

## **B . Buffers**

### **B 1. Bacterial culture**

#### **LB medium**

1 Lit (dH<sub>2</sub>O)

20g of LB broth

Autoclaved

#### **LB agar**

1 lit (dH<sub>2</sub>O)

35g of LB agar

Autoclaved

### **B 2. Bacterial Stock medium**

5ml of Glycerol

4ml of LB medium

3ml of Bacterial culture



### **B 3. 100Mm of IPTG**

238mg of IPTG

10ml of sterile distilled water

Sterilized filter

### **B 4. Ampicillin stock solution**

100µg/ml

PBS 2 tablets/ 1 Lit of dH<sub>2</sub>O

### **Routine cell culture**

RPMI medium 1640 (500ml)

Foetal bovine serum 10%(v/v)

Pen/Strep (5000U/ML) 5ml

LGlutamine (20Mm) 5ml

Sodium pyruvate (100mM) 5ml

TrypleE 5ML

MTT (5mg/ml)

PBS (10ml)

Autoclaved

## C. Western blot

**3.1 1M Tris pH 6.8** = (12.1g of Tris base + 100ml of dH<sub>2</sub>O). Ph adjusted with HCL

**10% of SDS solution** = ( 10g of Sodium Dodecyl Sulfate + 100ml of dH<sub>2</sub>O)

**10% of APS solution** = (100g of Ammonium persulfate + 1ml of dH<sub>2</sub>O)

**Sample loading buffer** = (2.5 ml of 1M of Tris-HCL, Ph 6.8 +4ml of Glycerol, 40%+ 0.8ml of Bromophenol blue, 0.5%+ 2ml of SDS, 10%+ 0.5ml of β-mercaptoethanol+ 4.7ml of dH<sub>2</sub>O)

**Transfer buffer (pH 8.3)** = (14.4g of Glycine, 192mM + 20% of Methanol, (v/v)+3.03g of Tris base, 25mM +up to 1 Lit of dH<sub>2</sub>O), HCL for pH adjustment

**10x TBS buffer (pH 7.6)**= (87.66g of Sodium chloride, 1500mM+ 60.58g of Tris base, 500mM+ up to 1Lit of dH<sub>2</sub>O) AUTOCLAVED

**1x TBS-TWEEN 1%**=(100ml of 10x TBS buffer+1ml of Tween20+ up to 1 Lit)

**(Washing buffer) TBS-T milk 5%** = ( 5g of Skimmed dried milk+ 100ml of 1x TBS-T buffer)

**Colonies formation detection stain 5%**=(0.5mg +10ml PBS)

**Cleaning recombinant protein (Dialysis)** =(2 tablets of PBS +1 Lit of dH<sub>2</sub>O)

AUTOCLAVED

#### **D. Equipment**

Corning™ BioCoat™ Matrigel™ Invasion Chamber: With GFR Matrigel  
Matrix

FisherScientific, UK

---

#### **CO<sub>2</sub> incubator**

Borolabs, Basingstoke, UK

---

#### **Cell culture filter cap flasks**

**Cell culture plates Cryogenic vial Nunc, Denmark**

---

#### **Carbon steel surgical blades**

Swann-Morton, Sheffield, UK

---

#### **Falcon tubes**

Becton, Dickinson, USA

#### **Gel electrophoresis**

Bio-Rad, UK

-----

**GelCount**

OXFORD OPTRONIX, Oxford, UK

-----

**Haemocytometer slide**

Weber Scientific International, NJ, USA

-----

**Hot plate**

Thermofisher, UK

-----

**Haemocytometer**

SLS LTD, Nottingham, UK

-----

**Immobilon, Transfer membrane**

Milipore, UK

**Microtubes**

Starlab, Milton Keynes, UK

-----

**Multiskan MS plate reader**

Labsystem, Finland

-----

**Needle**

**BD Microlance, Ireland**

-----

**NanoDrop spectrophotometer**

Labtech International, Ringmer, UK

-----

**Pipetter tips**

QIAGEN, UK

-----

**Syringes and filters**

Fisherscientific, UK

**Spectrophotometer**

BioTec, UK

-----

**Pipettes for cell culture**

Eppendorf, UK

-----

**Universal tube**

Greiner Bio-One, UK

-----

**Water bath**

Grant Instruments, UK

-----

**Whatman filter paper**

Whatman, England, UK

-----

**Tips for pipettes**

Eppendorf, UK

**E. DNA authentications for PCa cell lines and Publications**

### Laboratory Report

Test Requested Cell Line Authentication  
 Case Number C-25831d  
 Date Sample Received 01/06/2022  
 Date Sample Tested 08/06/2022  
 Date Sample Reported 24/06/2022

Sample Name	Sample/Comparison Profile Source	Sample Number	DNA Number
DU145	University of Liverpool	S-1059099	D-1059099
DU-145	DSMZ Database	N/A	N/A

### Table of Allelic Data

STR Locus	Genotypes		Match vs. Mis-Match
	DU145 (Test Sample)	DU-145 (Comparison Sample)	
D5	10   13	10   13	Match
D13	12   14	12   13   14	Mis-Match
D7	7   10   11	7   10   11	Match
D16	11   13	11   13	Match
vWA	17   18	17   18	Match
Amel	X   Y	X   Y	Match
TPOX	11   11	11   11	Match
CSF1PO	10   11	10   11	Match
THO1	7   7	7   7	Match

Matching Percentage: **97%**  
 Outcome: **Related**

The outcome percentage is calculated using a formulae which compares the number of alleles present against the number of alleles shared between the two DNA profiles. The outcome is designated one of the following statements based upon the outcome percentage:

Related (>80%) The Cell Lines are considered to be related.  
 Inconclusive (56-79%) Further profiling is required to determine whether the profiles are related.  
 No Match (55%>) It is considered that the two cell lines are unrelated.  
 Misidentified Cell Lines have been found to match a different donor within the database

Reported By: Mr. Callum Teeling (Laboratory Scientist) 

Authorised By: Ms. Eleanor Ralston (Senior Scientist) 

These test results should only be used in conjunction with a client's information. The results relate only to the items sampled, as received and

**Laboratory Report**

Test Requested Cell Line Authentication  
 Case Number C-25831c  
 Date Sample Received 01/06/2022  
 Date Sample Tested 08/06/2022, 10/06/2022  
 Date Sample Reported 24/06/2022

Sample Name	Sample/Comparison Profile Source	Sample Number	DNA Number
22RV1	University of Liverpool	S-1059097	D-1059097
22RV1	DSMZ Database	N/A	N/A

**Table of Allelic Data**

STR Locus	Genotypes		Match vs. Mis-Match
	22RV1 (Test Sample)	22RV1 (Comparison Sample)	
D5	11   13	11   12   13	Mis-Match
D13	9   12	9   12	Match
D7	9   10   11	9   10   11	Match
D16	12   12	12   12	Match
vWA	15   21	15   21	Match
Amel	X   Y	X   Y	Match
TPOX	8   8	8   8	Match
CSF1PO	10   11	10   11	Match
THO1	6   9.3	6   9.3	Match

Matching Percentage: **97%**  
 Outcome: **Related**

The outcome percentage is calculated using a formulae which compares the number of alleles present against the number of alleles shared between the two DNA profiles. The outcome is designated one of the following statements based upon the outcome percentage:

- Related (>80%) The Cell Lines are considered to be related.
- Inconclusive (56-79%) Further profiling is required to determine whether the profiles are related.
- No Match (55%>) It is considered that the two cell lines are unrelated.
- Misidentified Cell Lines have been found to match a different donor within the database

Reported By: Mr. Callum Teeling (Laboratory Scientist) 

Authorised By: Ms. Eleanor Ralston (Senior Scientist) 



### Laboratory Report

Test Requested Cell Line Authentication  
Case Number C-25831b  
Date Sample Received 01/06/2022  
Date Sample Tested 08/06/2022  
Date Sample Reported 24/06/2022

Sample Name	Sample/Comparison Profile Source	Sample Number	DNA Number
LnCap	University of Liverpool	S-1059096	D-1059096
LNCAP	DSMZ Database	N/A	N/A

### Table of Allelic Data

STR Locus	Genotypes		Match vs. Mis-Match
	LnCap (Test Sample)	LNCAP (Comparison Sample)	
D5	11   12	11   12	Match
D13	10   12	10   12	Match
D7	FAIL	9.1   10.3	FAIL
D16	11   11	11   11	Match
vWA	15   16   18   19	16   18	Mis-Match
Amel	X   Y	X   Y	Match
TPOX	8   9	8   9	Match
CSF1PO	10   11	10   11	Match
THO1	9   9	9   9	Match

Matching Percentage:

**88%**

Outcome:

**Related**

The outcome percentage is calculated using a formulae which compares the number of alleles present against the number of alleles shared between the two DNA profiles. The outcome is designated one of the following statements based upon the outcome percentage:

Related (>80%) The Cell Lines are considered to be related.  
Inconclusive (56-79%) Further profiling is required to determine whether the profiles are related.  
No Match (55%>) It is considered that the two cell lines are unrelated.  
Misidentified Cell Lines have been found to match a different donor within the database

Reported By: Mr. Callum Teeling (Laboratory Scientist)



Authorised By: Ms. Eleanor Ralston (Senior Scientist)



These test results should only be used in conjunction with a client's information. The results relate only to the items sampled, as received and tested at this time.

2  
2

### Laboratory Report

Test Requested Cell Line Authentication  
 Case Number C-25831d  
 Date Sample Received 28/06/2022  
 Date Sample Tested 28/06/2022  
 Date Sample Reported 11/07/2022

Sample Name	Sample/ Comparison Profile Source	Sample Number	DNA Number
PC3M Secondary Pellet	University of Liverpool	S-1059518	D-1059518
PC-3M	DSMZ Database	N/A	N/A

### Table of Allelic Data

STR Locus	Genotypes		Match vs. Mismatch
	PC3M Secondary Pellet (Test Sample)	PC-3M (Comparison Sample)	
D5	13   13	13   13	Match
D13	11   11	11   11	Match
D7	8   11	8   11	Match
D16	11   11	11   11	Match
vWA	17   17	17   17	Match
Amel	X   X	X   X	Match
TPOX	8   9	8   9	Match
CSF1PO	11   11	11   11	Match
THO1	6   7	6   7	Match

Matching Percentage: **100%**  
 Outcome: **Related**

The outcome percentage is calculated using a formulae which compares the number of alleles present against the number of alleles shared between the two DNA profiles. The outcome is designated one of the following statements based upon the outcome percentage:

- Related (>80%) The Cell Lines are considered to be related.
- Inconclusive (56-79%) Further profiling is required to determine whether the profiles are related.
- No Match (55%>) It is considered that the two cell lines are unrelated.
- Misidentified Cell Lines have been found to match a different donor within the database

Reported By: Mr. Benjamin Hickey (Laboratory Scientist) *B. Hickey*

Authorised By: Ms. Eleanor Ralston (Senior Scientist) *ER*

Date: 12/07/2022

These test results should only be used in conjunction with a client's information. The results relate only to the items sampled, as received and tested at this time.

### Laboratory Report

Test Requested Cell Line Authentication  
Case Number C-25831a  
Date Sample Received 28/06/2022  
Date Sample Tested 28/06/2022  
Date Sample Reported 11/07/2022

Sample Name	Sample/Comparison Profile Source	Sample Number	DNA Number
PNT2 Secondary Pellet	University of Liverpool	S-1059517	D-1059517
PNT2	DSMZ/HPACC Database	N/A	N/A

### Table of Allelic Data

STR Locus	Genotypes		Match vs. Mis-Match
	PNT2 Secondary Pellet (Test Sample)	PNT2 (Comparison Sample)	
D5	12   13	12   13	Match
D13	8   13	8   13	Match
D7	11   11	11   11	Match
D16	9   9	9   9	Match
vWA	17   17	17   17	Match
Amel	X   Y	X   Y	Match
TPOX	8   9	8   9	Match
CSF1PO	10   11   13	11   13	Mis-Match
THO1	6   9.3	6   9.3	Match

Matching Percentage: **97%**  
Outcome: **Related**

The outcome percentage is calculated using a formulae which compares the number of alleles present against the number of alleles shared between the two DNA profiles. The outcome is designated one of the following statements based upon the outcome percentage:

Related (>80%) The Cell Lines are considered to be related.  
Inconclusive (56-79%) Further profiling is required to determine whether the profiles are related.  
No Match (55%>) It is considered that the two cell lines are unrelated.  
Misidentified Cell Lines have been found to match a different donor within the database

Reported By: Mr. Benjamin Hickey (Laboratory Scientist) *B. Hickey*

Authorised By: Ms. Eleanor Ralston (Senior Scientist) *E. Ralston*

Date: 12/07/2022

## SHORT COMMUNICATION

## Fatty acid-binding protein 5 (FABP5)-related signal transduction pathway in castration-resistant prostate cancer cells: a potential therapeutic target

Abdulghani A. Naeem<sup>1,§</sup>, Saud A. Abdulsamad<sup>1,§</sup>, Philip S. Rudland<sup>2</sup>,  
Mohammed I. Malki<sup>3</sup> and Youqiang Ke<sup>1,\*</sup>

<sup>1</sup>The Molecular Pathology Laboratory, Department of Molecular and Clinical Cancer Medicine; <sup>2</sup>Department of Biochemistry, Liverpool University, Liverpool L69 3GA, UK; and <sup>3</sup>College of Medicine, Qatar University, Doha 2713, Qatar

\*Correspondence: Youqiang Ke, yqk@liverpool.ac.uk

### Abstract

In this short communication, a novel fatty acid-binding protein 5 (FABP5)-related signal transduction pathway in prostate cancer is reviewed. In castration-resistant prostate cancer (CRPC) cells, the FABP5-related signal transduction pathway plays an important role during transformation of the cancer cells from androgen-dependent state to androgen-independent state. The detailed route of this signal transduction pathway can be described as follows: when FABP5 expression is increased as the increasing malignancy, excessive amounts of fatty acids from intra- and extra-cellular sources are transported into the nucleus of the cancer cells where they act as signalling molecules to stimulate their nuclear receptor peroxisome proliferator-activated receptor gamma (PPAR $\gamma$ ). The phosphorylated or biologically activated PPAR $\gamma$  then modulates the expression of its downstream target regulatory genes to trigger a series of molecular events that eventually lead to enhanced tumour expansion and aggressiveness caused by an overgrowth of the cancer cells with a reduced apoptosis and an increased angiogenesis. Suppressing the FABP5-related pathway via RNA interference against FABP5 has produced a 63-fold reduction in the average size of the tumours developed from CRPC cells in nude mice, a seven-fold reduction of tumour incidence, and a 100% reduction of metastasis rate. Experimental treatments of CRPC with novel FABP5 inhibitors have successfully inhibited the malignant progression of CRPC cells both *in vitro* and in nude mouse. These studies suggest that FABP5-related signal transduction pathway is a novel target for therapeutic intervention of CRPC cells.

**Key words:** FABP5; CRPC; fatty acids; PPAR $\gamma$ ; tumorigenicity; metastasis

<sup>§</sup>These authors contributed equally to this work

Received: 18 June 2019; Revised: 19 July 2019; Accepted: 22 July 2019

© The Author(s) 2019. Published by Oxford University Press on behalf of West China School of Medicine & West China Hospital of Sichuan University. This is an Open Access article distributed under the terms of the Creative Commons Attribution Non-Commercial License (<http://creativecommons.org/licenses/by-nc/4.0/>), which permits non-commercial re-use, distribution, and reproduction in any medium, provided the original work is properly cited. For commercial re-use, please contact [journals.permissions@oup.com](mailto:journals.permissions@oup.com)



---

## Epidemiology of Prostate Cancer in Saudi Arabia

Abdulghani A. Naeem<sup>1</sup>, Saud A. Abdulsamad<sup>1</sup>, Xi Jin<sup>2</sup>, Gang He<sup>3</sup>,  
Jiachen Zhang<sup>1</sup>, Qiang Wei<sup>2\*</sup> and Youqiang Ke<sup>1,2\*</sup>

DOI: 10.9734/bpi/nfmmr/v14/12894D

---

### ABSTRACT

**Problem identification:** Prostate Cancer and its prevalence worldwide have increased over the past several years as the knowledge and methods for early detection of cancer have been improving. Prostate Cancer is also considered to be the second most common cancer in Middle Eastern countries, and is ranked as the sixth leading cause of mortality among men. This study aims to identify the role of genetics and environmental factors in the development and progression of Prostate Cancer among Middle Eastern countries, with focus on the prevalence and mortality of Prostate Cancer in Saudi Arabia. The study also aims to examine proposed risk factors for the development of Prostate Cancer among Middle Eastern men.

**Literature search:** Extensive literature search was made to find articles and studies regarding to the prevalence of Prostate Cancer in Saudi Arabia, and the potential reasons for its increased prevalence over the years. Studies about the established and proposed risk factors contributing to the development of Prostate Cancer was also included in the literature search.

**Conclusion:** Results of literature reviewed and studied in this paper showed that genetics and individual anatomy of Arab men are of importance in the development of Prostate Cancer. For environmental causes, it was identified that the changing lifestyle of Arab men, and becoming more open to Western influence also contributed to the prevalence of Prostate Cancer. It was also found out that with the improving status of the medical practices in Saudi Arabia, it is expected that more cases are to be detected, as more access will be rendered available to the citizens for the immediate detection of Prostate Cancer..

*Keywords: Prostate Cancer; Saudi Arabia; Epidemiology; Risk factors and prevention.*

### 1. INTRODUCTION

Prostate Cancer is considered to be one of the most common types of cancer in men and the second most common cancer in the Middle Eastern region (Table 1) and has been ranked 6<sup>th</sup> on the most significant number of deaths associated with the disease [1]. It has become an emerging disease among developed and developing countries and is mostly associated with men over 55 years (Fig. 3) of age [2-3]. Men affected by prostate cancer are on the rise and are expected to continuously rise [1]. Even though prostate cancer is far more common among African-American men [1] its incidence is considerably higher in the North American region and most European countries [4]. There has been continuous spike of reported cases of prostate cancer in the United States and Canadian region (Table 2), while the reports of prostate cancer as lower in the Asian region, specifically the Arabic region [5]. Though incidence rate of prostate cancer in Saudi Arabia does not match those with other American and European countries, Saudi nationals are still at risk and number of Saudi nationals affected each year is on the rise, a trend that has been observed from 2001 to 2008 (Fig. 1), as well as studies done in 2012 and 2018. It is expected that the number of affected in Middle Eastern countries in 2012 (29, 377) will increase to 38, 562 in 2020 [5,43]. This increase in affected persons will result in increased mortality associated with the disease from 15, 422 deaths in 2012 to 19, 681

---

<sup>1</sup>Department of Molecular & Clinical Cancer Medicine, Liverpool University, Liverpool, L69 3GA, United Kingdom.

<sup>2</sup>Institute of Urology, West China Hospital, Sichuan University, No.37 Guo Xue Xiang, Chengdu, Sichuan, 610041, China.

<sup>3</sup>Sichuan Antibiotics Industrial Institute, Chengdu University, Chengdu 610081, China.

\*Corresponding author: E-mail: yqk@liverpool.ac.uk, wq933@hotmail.com;

## Prostate Cell Lines

Abdulghani A Naeem<sup>1</sup>, Saud A Abdulsamad<sup>1</sup>, Asmaa Al Bayati<sup>1</sup>, Jiacheng Zhang<sup>1</sup>, Mohammed I Malki<sup>2</sup>, Hongwen Ma<sup>3</sup>, and Youqiang Ke<sup>1\*</sup>

<sup>1</sup>Department of Molecular & Clinical Cancer Medicine, Liverpool University, Liverpool, United Kingdom

<sup>2</sup>College of Medicine, QU Health, Qatar university, Doha, Qatar

<sup>3</sup>Department of Urology, Institute of Urology, West China Hospital, Sichuan University, China

\*Corresponding author: Youqiang Ke, Professor, Department of Molecular & Clinical Cancer Medicine, Liverpool University, L69 3GA, United Kingdom

Received:  February 11, 2022

Published:  February 25, 2022

### Abstract

When it comes to studying biological processes, cell lines are typically utilized in lieu of original cell samples. Like in the studies for other cancer types, researchers in prostate cancer can be constrained in their ability to discover new treatments because of a lack of cell lines to investigate pre-clinical status. There are various forms of prostate cancer cell lines that are reviewed in this work. A cautionary note is in need since cell lines may not always correctly mimic the original cells. Cancerous cells are immortal and using cell lines produced from cancer cells as a model to better understand cancer and to develop novel therapies are common in research. Apart from the prostate cancer cells, we also reviewed two cell lines PNT2 and RWPE-1 which were established from non-neoplastic male prostatic epithelial cells.

### Introduction


Cancers are known for their ability to prolong life indefinitely [1,2]. However, it remains a mystery how mortal somatic cells become the source of immortal malignancies. Cancerous cells are immortal, despite the fact that healthy somatic cells may develop into organs as well as creatures that include much more cells than lethal tumors [3-11]. By exceeding the Hayflick threshold, which is approximately 50 cycles in vitro, immortality is established operationally. Telomerase stimulation is now the most widely accepted explanation of immortality [4-6]. Cancers are supposed to gain immortality via the stimulation of telomerase, which is a gene that is normally shut off throughout development in somatic cells. To put it another way, cells that have maintained their telomeres by the acts of telomerase process are considered to be immortalized. All individual tumors seem to be governed by the process of cell immortalization.

It is these cells that serve as a starting point for tumor development and are known as the cancer cells of origin. Unlike cancer stem cells, which constitute the cellular subfractions capable of regenerating tumors, these cells are classified in a different way. It's been a major focus of cancer research to identify the cells that give rise to the disease. Since there is so much interest in testing

the concept that tumors are caused by various cell types, this has resulted in a lot of research being done in this area. This knowledge will aid in the early detection and precise prognosis of cancer, as well as in the development of new preventative treatments for people at high risk. Based on the histological appearance of malignancies, it was formerly considered that they had a cellular origin. We now know, based on our existing understanding, that tumor specimens may be deceiving when random as well as static observations are made. A direct genetic method should be used to test any hypotheses. Tumors may have gene expression patterns that are more like those of their own cells' ancestors than those of other cell types within the same tissue, which is a similar but much more elegant concept. The basal-like breast cancer may originate from luminal epithelial progenitors in the mammary gland luminal epithelium. Gene expression patterns may be used to classify brain tumors with similar histological characteristics into separate groups that represent the cellular genesis of the tumors. Molecular profiles don't always line up with tumor pathology, according to these findings. It is still necessary to do more direct genetic research in order to verify the findings drawn from these sorts of studies. Cell lines having diverse lineage features from human or mouse tissues may be established, transformed, and then analyzed



# Molecular mechanisms on how FABP5 inhibitors promote apoptosis-induction sensitivity of prostate cancer cells

Jiacheng Zhang<sup>1</sup> | Gang He<sup>2</sup> | Xi Jin<sup>3</sup> | Bandar T. Alenezi<sup>1</sup> |  
Abdulghani A. Naeem<sup>1</sup> | Saud A. Abdulsamad<sup>1</sup> | Youqiang Ke<sup>1,2,3</sup> 

<sup>1</sup>Department of Molecular and Clinical Cancer Medicine, Liverpool University, Liverpool, UK

<sup>2</sup>Sichuan Industrial Institute of Antibiotics, Chengdu University, Chengdu, Sichuan, China

<sup>3</sup>Institute of Urology, West China Hospital, Sichuan University, Chengdu, Sichuan, China

## Correspondence

Youqiang Ke and Jiacheng Zhang, Department of Molecular and Clinical Cancer Medicine, Liverpool University, the Cancer Research Centre Bldg, 200 London Rd, Liverpool L3 9TA, UK.  
Email: [yqk@liverpool.ac.uk](mailto:yqk@liverpool.ac.uk) and [aster65@163.com](mailto:aster65@163.com)

## Abstract

Previous work showed that FABP5 inhibitors suppressed the malignant progression of prostate cancer cells, and this suppression might be achieved partially by promoting apoptosis. But the mechanisms involved were not known. Here, we investigated the effect of inhibitors on apoptosis and studied the relevant mechanisms. WtrFABP5 significantly reduced apoptotic cells in 22Rv1 and PC3 by 18% and 42%, respectively. In contrast, the chemical inhibitor SB-FI-26 produced significant increases in percentages of apoptotic cells in 22Rv1 and PC3 by 18.8% ( $\pm 4.1$ ) and 4.6% ( $\pm 1.1$ ), respectively. The bio-inhibitor dmrFABP5 also did so by 23.1% ( $\pm 2.4$ ) and 15.8% ( $\pm 3.0$ ), respectively, in these cell lines. Both FABP5 inhibitors significantly reduced the levels of the phosphorylated nuclear fatty acid receptor PPAR $\gamma$ , indicating that these inhibitors promoted apoptosis-induction sensitivity of the cancer cells by suppressing the biological activity of PPAR $\gamma$ . Thus, the phosphorylated PPAR $\gamma$  levels were reduced by FABP5 inhibitors, the levels of the phosphorylated AKT and activated nuclear factor kappa B (NF $\kappa$ B) were coordinately altered by additions of the inhibitors. These changes eventually led to the increased levels of cleaved caspase-9 and cleaved caspase-3; and thus, increase in the percentage of cells undergoing apoptosis. In untreated prostate cancer cells, increased FABP5 suppressed the apoptosis by increasing the biological activity of PPAR $\gamma$ , which, in turn, led to a reduced apoptosis by interfering with the AKT or NF $\kappa$ B signaling pathway. Our results suggested that the FABP5 inhibitors enhanced the apoptosis-induction of prostate cancer cells by reversing the biological effect of FABP5 and its related pathway.

## KEYWORDS

AB-FI-26, apoptosis, dmrFABP5, FABP5, PPAR $\gamma$ , prostate cancer